Monitoring Climate for the Effects of Increasing Greenhouse Gas Concentrations

---

A Compendium of Papers
Presented at a Workshop Sponsored
August 26-28, 1987 by the

Cooperative Institute for Research in the Atmosphere

Roger A. Pielke
Timothy G.F. Kittel
Co-Editors

Colorado State University, Fort Collins, CO

1988

CIRA

PREFACE and SUMMARY

The influence of increasing concentrations of CO_2 and other greenhouse gases on climate has received considerable attention from scientists, policy makers, and the public during recent years. Claims of the potential for climate change due to greenhouse gases have been far-ranging and have been the basis for much controversy. The detection of such climatic impacts is of utmost importance, not only from a scientific point of view, but also to society. If a climatic change signal can be attributed to increases in greenhouse gases, then models can be validated and policy options may become clearer.

The Cooperative Institute for Research in the Atmosphere (CIRA) at Colorado State University held a workshop at the Pingree Park Campus on August 26-28, 1987, to focus on the level of scientific understanding regarding current and anticipated effects of greenhouse gases on climate. Invited participants included climate modelers and observational scientists. In this volume, we present their papers and summarize (below) workshop discussions on requirements for monitoring climate for change.

The volume begins with an overview of climate model simulations. Michael Schlesinger reviews predictions for elevated-CO_2 equilibrium and transient climates. He presents results for an OSU coupled atmosphere-ocean general circulation model (GCM). A run for the period 1850 (beginning of the Industrial Revolution) to 1980 shows a 0.5-0.7°C rise in global surface air temperatures, which is consistent with observed data. The warming given by the coupled model is roughly half that of an atmosphere-only GCM simulation. At the workshop, Sergej Lebedeff (Goddard Institute for Space Studies) presented transient climate simulations with the GISS GCM; this

work is published elsewhere [Hansen et al. 1988, Global climate changes as forecast by the GISS 3-D model, J. Geophys. Res. (Atmospheres), in press].

A second section covers observational studies. Hugh Ellsaesser suggests that abrupt global temperature changes in the geological and historic climatic record indicate that the earth climate system is capable of internal rearrangements resulting in new equilibrium states. He proposes that such a shift may be responsible for observed Northern Hemisphere temperature increases earlier this century, rather than CO_2-forcing. Henry Diaz and Thomas Karl examine historical U.S. and regional temperature trends by removing stations with potential urban heat island effects; they find no long-term (1901 to 1984) trends that are statistically significant. Also using U.S. data, Tom Karl concludes in the next paper that many multi-year (e.g., decadal scale) changes in the level and/or the variance of temperature and precipitation are likely due to stochastic processes. He discusses problems this causes for the detection of climate change.

Patrick Michaels et al. developed a proxy temperature data set independent of site effects and with little instrument bias based on 1000-500 mbar thickness. They extend the data set back to 1885 for the U.S. and southern Canada based on historical cyclone frequency data and find a trend of +1.0°C from 1899 to 1975, but with similar magnitude warming and cooling occurring during that period. For stations in the Colorado region with records back to the late 1800's, Nolan Doesken and John Kleist find strong linear increases in cloudiness, little change in precipitation, increases in mean temperatures and decreases in diurnal temperature range; however, causes of these trends are not evident. Robert Jarrett considers sources of error present in hydroclimatic data sets, including biases in the measurement of extreme events by precipitation and steamflow gauges.

Finally, two papers present methods to increase the resolution and applications of global climate model results. Roger Pielke discusses the use of mesoscale models in conjunction with GCMs to generate regional climate change scenarios, either by running mesoscale models on dominant weather patterns based on synoptic classification of GCM output or by nesting GCMs and mesoscale models. Tim Kittel and Michael Coughenour introduce a hierarchial approach for the simulation of ecological response to climate and CO_2 changes that will permit modeling the multiscale interactions of ecosystem, community, and physiological processes.

Workshop discussions focused on problems of monitoring climatic change. Two areas of needed effort were identified: climate simulations and observational data. Improved climate predictions are required for the establishment of monitoring protocols. Monitoring efforts can be guided by predictions that identify climatic measures and geographical regions with high signal (climate change) to noise ratios. However, improvements in GCMs are needed. The models currently lack parameterizations of several important physical processes. These include changes in colloidal cloud stability due to increased aerosol loading of the atmosphere by pollution, venting of such aerosol pollution to upper tropospheric/lower stratospheric levels by deep cumulonimbus systems, mesoscale circulations driven by land surface contrasts such as irregular land use patterns, and biospheric feedbacks to climate resulting from climate-induced changes in trace gas production (e.g., CH_4) and biome distribution. Another area of concern is whether the resolution of GCMs is adequate to faithfully reproduce synoptic scale wave-wave interactions. This could be determined by comparing GCM model physics and numerics to those of weather prediction models.

Developing regional level predictions is a priority for model validation and for monitoring. Regional predictions from GCMs are limited

not only by the models' coarse grid size, but also by the lack of simulated oceanic processes in many of the models. Increased spatial resolution can be accomplished by nesting GCM and mesoscale models for regions of interest. To incorporate oceanic processes, GCMs need to be coupled with ocean GCMs that simulate deep overturning and horizontal transport. Attention also needs to be given to designing GCM output that is consistent with regional monitoring strategies (e.g., output that can be compared to point station data and basin hydrological data) and output of variables of socio-economic and ecological importance (e.g., temperature extremes). Finally, tests of GCMs should continue to include simulation of the past 100+ years for validation with observed or proxy data with the goal of being able to resolve at least multi-decadal trends.

Climate data bases need to be improved and extended for model validation and monitoring climate change. The climate record can be upgraded by (1) improved documentation of climate station history and instrument biases, (2) maintaining the density of climate stations globally at current or increased levels, including ship stations, and (3) continued development and retrospective analysis of space-based remote sensing of the atmosphere, oceans, and land surface climate. An integrated regional approach in which multiple sources of observational and proxy climate data are combined may enhance climate trend signals. In addition to climate station data, such sources include stream flow data, tree rings, cave temperatures, and data from glaciers and permafrost soils. Finally, careful statistical analyses are called for to test the significance of trends in the climate record and their comparison with model simulations.

The papers and discussion from this workshop continue to raise scientific issues concerning modeling and detection of greenhouse gas-induced climate change: e.g., observational studies do not find

statistically significant trends because of low signal to noise ratios or are unable to attribute trends to increases in greenhouse gases because of the lack of credible regional predictions. We hope that this volume identifies areas where improvements in climate modeling and monitoring will be fruitful.

R. A. Pielke
Co-Organizer

T. Kittel
Co-Organizer

ACKNOWLEDGEMENTS

We wish to thank workshop participants for their presentations and contributions to discussions. We are grateful to Joanne Williams, Lisa Huss, Bobbie Schwinger and Judy Sorbie for their organizational support thus making the workshop and publication of its proceedings possible.

We would like to acknowledge the National Oceanic and Atmospheric Administration (thru Grant No. NA-85-RAH-05045) and Colorado State University for their continued support.

TABLE OF CONTENTS

I. Global Climate Simulations

M. Schlesinger

MODEL PROJECTIONS OF THE EQUILIBRIUM AND TRANSIENT CLIMATIC CHANGES INDUCED BY INCREASED ATMOSPHERIC CO_2

Michael E. Schlesinger

Department of Atmospheric Sciences
and
Climatic Research Institute
Oregon State University
Corvallis, Oregon 97331
USA

ABSTRACT

The simulations of CO_2-induced equilibrium climatic change by energy-balance models, radiative-convective models and general circulation models are reviewed and characterized in terms of the direct radiative forcing of the increased CO_2, the response of the climate system in the absence of feedback processes, and the feedbacks of the climate system.

The direct radiative forcing due to a doubling of the CO_2 concentration is about 4 Wm^{-2} for the surface-troposphere system. In the absence of feedbacks the gain (output/input) of the climate system is about $0.3°C/(Wm^{-2})$, and the change in the surface air temperature is therefore about 1.2°C. Surface energy-balance models (SEBMs) have given a warming induced by a CO_2 doubling of about 0.2 to 10°C. This wide range is the result of the inherent difficulty in specifying the behavior of the atmosphere in SEBMs. Radiative-convective models (RCMs) have given a warming of about 0.5 to 4.2°C for a CO_2 doubling. This range is the result of water vapor feedback, lapse rate feedback, surface albedo feedback, cloud altitude feedback, cloud cover feedback and cloud optical depth feedback. General circulation models (GCMs) have given a warming of about 1.3 to 5.2°C for a CO_2 doubling. This also is a result of the feedbacks listed above, except that due to cloud optical depth feedback which has not yet been included in the GCM simulations of CO_2-induced climatic change.

Five recent simulations of CO_2-induced climatic change by atmospheric GCM/mixed-layer ocean models are contrasted in terms of their surface air temperature and soil moisture changes. These comparisons reveal qualitative similarities but quantitative differences.

The simulations of CO_2-induced transient climatic change by planetary energy-balance models, radiative-convective models and general circulation models are reviewed in terms of the e-folding time τ_e of the response of the climate system. Simplified models have given an e-folding time of about 10-100 years for the response of the climate system to an abrupt increase in the CO_2 concentration. A simulation with a global coupled atmosphere/ocean general circulation model indicates that τ_e is about 50-100 years as a result of the transport of the CO_2-induced surface heating into the interior of the ocean. Theoretical studies for a time-dependent CO_2 increase between 1850 and 1890 indicate that this sequestering of heat into the ocean's interior is responsible for the concomitant warming being only about half that which would have occurred in the absence of the ocean. These studies also indicate that the climate system will continue to warm towards its as yet unrealized equilibrium temperature change, even if there is no further increase in the CO_2 concentration.

1. Introduction

If the Earth's atmosphere were composed of only its two major constituents, nitrogen (N_2, 78% by volume) and oxygen (O_2, 21%), the Earth's surface temperature would be close to the -18°C radiative-equilibrium value necessary to balance the approximately 240 Wm^{-2} of solar radiation absorbed by the Earth-atmosphere system. The fact that the Earth's global-mean surface temperature is a life-supporting 15°C is a consequence of the greenhouse effect of the atmosphere's minor constituents, mainly water vapor

(H_2O, 0.2%) and carbon dioxide (CO_2, 0.03%). Measurements taken at Mauna Loa, Hawaii show that the CO_2 concentration has increased from about 315 ppmv in 1958 to 346 ppmv in 1985 (Keeling and Boden, 1986), a 10% increase in 28 years. Measurements of the air entrapped within the ice sheet of Antarctica indicate that the pre-industrial CO_2 concentration increased from about 280 ppmv in 1750 to 290 ppmv in 1880 (Siegenthaler and Oeschger, 1987). Rotty and Masters (1985) report that, with the exception of the periods of the Depression and World Wars I and II, the CO_2 concentration increased from 1860 to 1949 due to a 4.2% yr^{-1} growth in the consumption of fossil fuels (gas, oil, coal). Subsequently, the growth rate of CO_2 emissions was a steady 4.4% yr^{-1} from 1950 to 1973, and then decreased to 1.5% yr^{-1} from 1973 to 1982 as a result of the rise in the price of oil. A probabilistic scenario analysis of the future usage of fossil fuels predicts about an 80% chance that the CO_2 concentration will reach twice the pre-industrial value by 2100 (Nordhaus and Yohe, 1983). Computer simulations of the equilibrium climatic change induced by a doubling of the CO_2 concentration have been made with a hierarchy of mathematical climate models, the most recent of which have given a warming as large as 5.2°C in the global-mean surface air temperature. Since such a global warming is comparable to that which is estimated to have occurred during the transition from the last ice age to the present interglacial (Gates, 1976a, b; Imbrie and Imbrie, 1979), there is considerable interest in the detection of a CO_2-induced climatic change, and in the potential impacts of such a change on the spectrum of human endeavors.

The majority of the simulations of CO_2-induced climatic change have been performed to determine the change in the equilibrium climate of the Earth resulting from an abrupt increase in CO_2 such as a doubling from 300 to 600 ppmv. The goal of these simulations has been to estimate the

magnitude of the eventual climatic change which may occur as a consequence of the doubled CO_2 concentration projected to occur in the next century. These equilibrium climatic-change simulations have not been concerned with the time required for the climatic change to reach its equilibrium and, in fact, have generally tried to minimize that time in an effort to economize on computer time. More recently, concern has been focussed on the detection of a CO_2-induced climatic change. A simple scaling of the equilibrium $2xCO_2$-induced warming to the increase in CO_2 from 1861 to 1984 indicates an increase in the global-mean surface temperature of about 1.0°C, this for a sensitivity of 4°C for a CO_2 doubling. However, the observed surface temperature increase over this period is only about half this value (Jones et al., 1986). This discrepancy suggests that either the equilibrium warming of our climate models is twice as large as that of nature, or that there is a lag in the response of the climate system. The latter possibility has been the focus of research on the transient response of climate to both abrupt and time-dependent increases in the CO_2 concentration. In the following, the studies of equilibrium and transient climatic change induced by increased CO_2 are reviewed in sections 2 and 3, respectively; a summary of these results is presented in section 4 and conclusions are given in section 5.

2. CO_2-Induced Equilibrium Climatic Change

Three different types of climate model have been used to simulate the change in the equilibrium climate resulting from an increase in the CO_2 concentration: energy-balance models (EBMs), radiative-convective models (RCMs), and general circulation models (GCMs). These models and their projections of CO_2-induced climatic change are described in turn below.

2.1. Energy-balance models

Energy-balance models predict the change in temperature at the Earth's surface, ΔT_s, from the requirement that $\Delta N = 0$, there N is the net energy flux expressed by $N = N(\mathbf{E}, T_s, \mathbf{I})$. Here **E** is a vector of quantities that can be regarded as "external" to the climate system, that is, quantities whose change can lead to a change in climate, but which are independent of climate. **I** is a vector of quantities that are internal to the climate system, that is, quantities that can change as the climate changes and, in so doing, feed back to modify the climatic change. The external quantities include, for example, the solar constant, the optically-active ejecta from volcanic eruptions and, for the present purpose, the CO_2 concentration (although eventually it may change as a result of climatic change). The internal quantities include all the variables of the climatic system other than T_s. Since T_s is the only dependent variable in an EBM, the internal quantities must be represented therein by functions of T_s, that is, by $\mathbf{I} = \mathbf{I}(T_s)$.

A small change in the energy flux, ΔN, can be expressed as

$$\Delta N = \Delta Q - (G_o^{-1} - F)\, \Delta T_s$$

where

$$\Delta Q = \sum_i \frac{\partial N}{\partial E_i}\, \Delta E_i$$

is the change in N due to a change in one or more external quantity, ΔE_i,

$$- G_o^{-1}\, \Delta T_s = \frac{\partial N}{\partial T_s}\, \Delta T_s$$

is the change in N due to the change in T_s alone, and

$$F\,\Delta T_s = \sum_j \frac{\partial N}{\partial I_j}\frac{dI_j}{dT_s}\,\Delta T_s$$

is the change in N due to the change in the internal variables I through their dependence on T_s. When the equilibrium ΔT_s is reached in response to the forcing ΔQ, $\Delta N = 0$ and

$$\Delta T_s = \frac{G_o}{1 - G_o F}\,\Delta Q = \frac{G_o}{1 - f}\,\Delta Q = G_f \Delta Q. \qquad (1)$$

This relation can be represented by a feedback block diagram for the climate system as shown in Fig. 1. It is seen that G_o is the gain (output/input) of the climate system when the feedback $f = G_o F = 0$. Thus G_o is the zero-feedback gain and $(\Delta T_s)_o = G_o \Delta Q$ is the zero-feedback temperature change; correspondingly, G_f and ΔT_s are the gain and the temperature change with feedback. Letting $R_f = \Delta T_s/(\Delta T_s)_o = G_f/G_o$, it can be seen from Fig. 2 that $0 < R_f < 1$ when the feedback is negative ($f < 0$) and $R_f > 1$ when the feedback is positive ($0 < f < 1$). Consequently, the sign of the response is always the same as the sign of the forcing, even when there is negative feedback, regardless of its magnitude. This is in contrast to what has sometimes been erroneously inferred for the outcome of negative feedback (for example, see Nature, 1987). On the other hand, for positive feedback $f > 1$, $R_f < 0$ and the sign of the response is opposite to that of the forcing. This outcome, while mathematically possible (and actually obtained

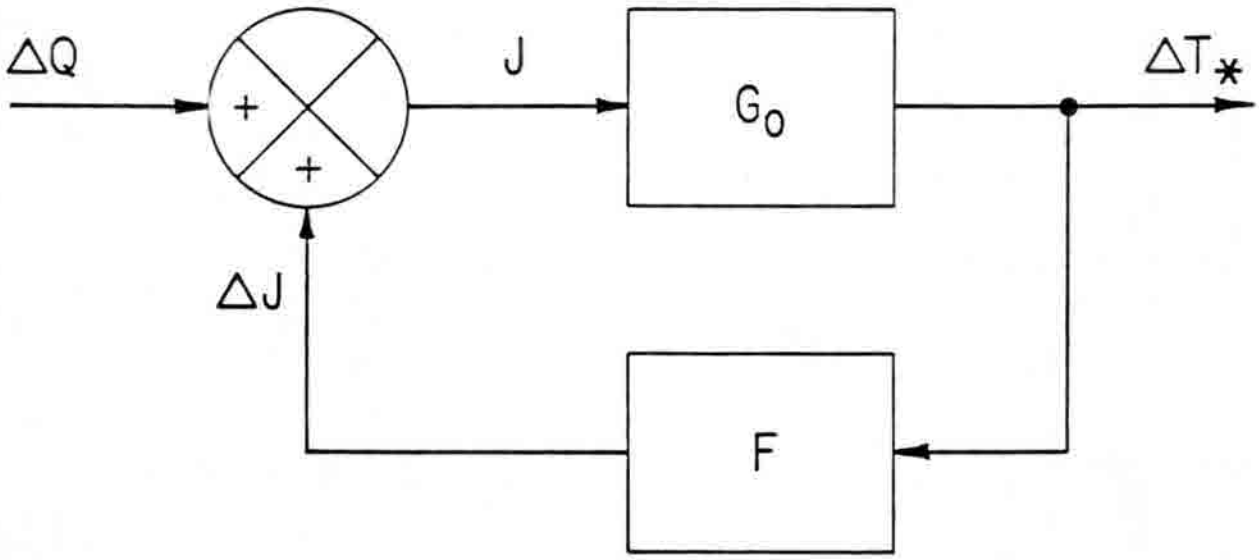

Fig. 1. Block diagram of the climate system with a feedback loop. (From Schlesinger, 1985.)

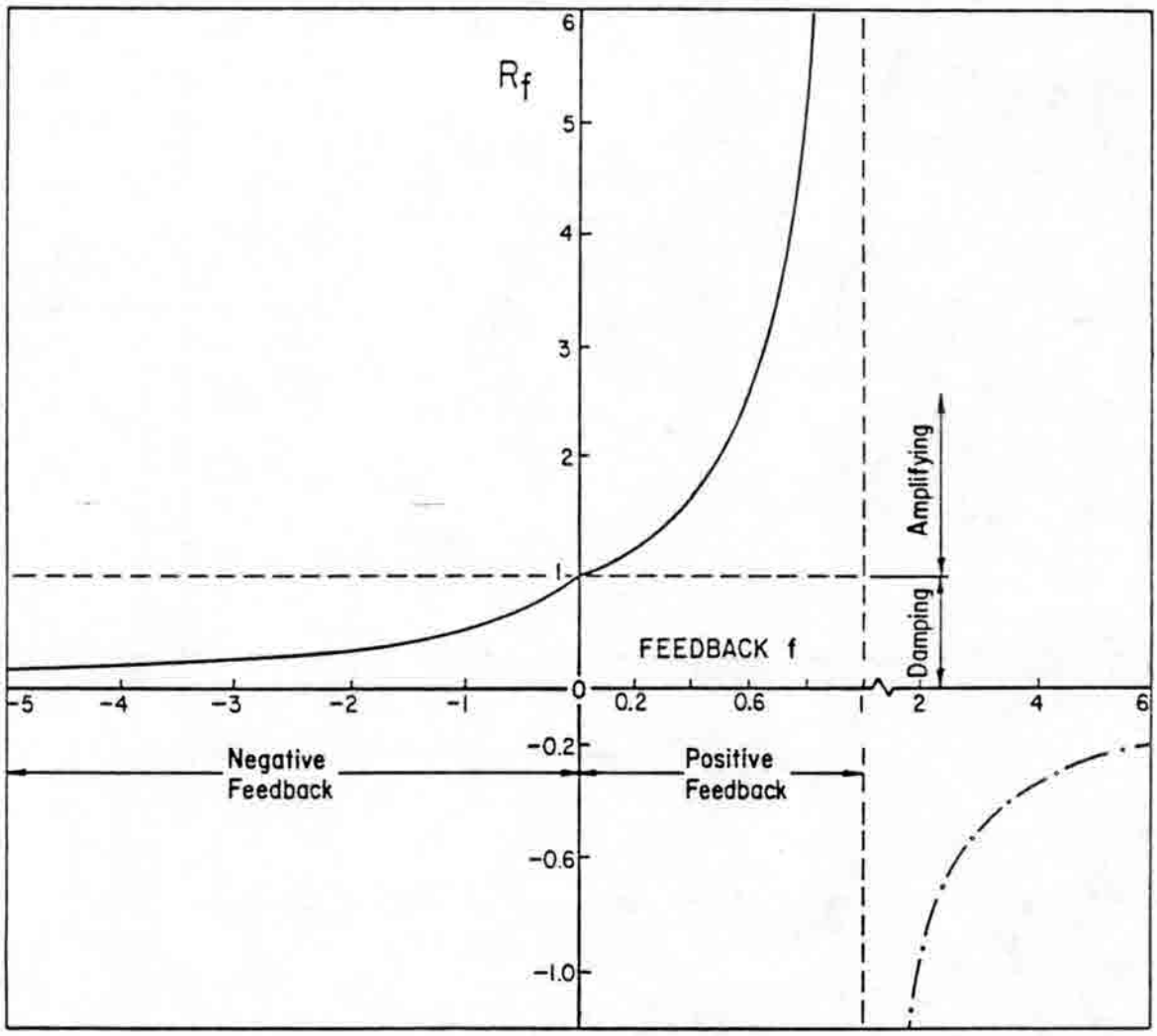

Fig. 2. The ratio of the surface temperature change ΔT_s to the zero-feedback value $(\Delta T_s)_o$, $R_f = \Delta T_s/(\Delta T_s)_o$, versus the feedback f. (From Schlesinger, 1985.)

by one improperly formulated EBM; see Schlesinger, 1985, 1988a), is not physically-consistent and must therefore be rejected.

Energy-balance models impose the condition $\Delta N = 0$ at either the Earth's surface or the top of the atmosphere. The former models may be called surface energy-balance models (SEBMs) and the latter planetary energy-balance models (PEBMs). SEBMs have given a warming induced by a CO_2 doubling of about 0.2 to 10°C. This wide range is due in part to the inherent difficulty in specifying the behavior of the atmosphere in terms of the surface temperature in SEBMs, that is $I(T_s)$, and to the large sensitivity of ΔT_s in SEBMs to this specification (Schlesinger, 1985, 1988a). Therefore, it is preferable to use models which calculate the atmosphere's behavior based on the fundamental laws of physics.

Before turning our attention to these physically-based models, it is useful to consider PEBMs for which

$$N = \frac{1 - \alpha_p}{4} S - \epsilon\sigma T_s^4 ,$$

where S is the solar constant, α_p the planetary albedo, ϵ the effective emissivity of the Earth-atmosphere system, and σ the Stefan-Boltzmann constant. From this equation we can estimate the zero-feedback gain as

$$G_o = - \left(\frac{\partial N}{\partial T_s}\right)^{-1} = \frac{T_s}{(1 - \alpha_p)S} , \qquad (2)$$

an expression which we will use subsequently. For a PEBM, ΔT_s is given by Eq. (1) with Eq. (2) and

$$f = G_o \sum_j \frac{\partial N}{\partial I_j} \frac{dI_j}{dT_s} ,$$

where I_j are again the internal variables of the climate system. This expression means that the feedback depends on the specification of the behavior of the atmosphere and the Earth's surface. Thus PEBMs also have the same problem as SEBMs, namely, the need to treat the behavior of the climate system away from the energy-balance level. In PEBMs this has been done semi-empirically following the initial studies by Budyko (1969) and Sellers (1969). The equilibrium surface temperature change for a CO_2 doubling given by PEBMs ranges from 0.6°C (Rasool and Schneider, 1971) to 3.3°C (Ramanathan et al., 1979).

2.2. Radiative-convective models

Radiative-convective models determine the equilibrium vertical temperature distribution for an atmospheric column and its underlying surface for given solar insolation and prescribed atmospheric composition and surface albedo. An RCM includes submodels for the transfer of solar and terrestrial (longwave) radiation, the turbulent heat transfer between the Earth's surface and atmosphere, the vertical redistribution of heat within the atmosphere by dry or moist convection, and the atmospheric water vapor content and clouds. The radiative transfer models used in RCMs are frequently identical to those used in GCMs. The surface heat exchange is treated either as an equivalent radiative exchange or is parameterized as a Newtonian exchange with a prescribed transfer coefficient. The vertical heat redistribution by convective atmospheric motions is modeled as an adjustment whereby the temperature lapse rate of the atmosphere is prevented from exceeding some given value. The amount of water vapor is determined in RCMs either by prescribing the absolute humidity or the relative humidity; in the latter case the amount of water vapor increases (decreases) with increasing (decreasing) temperature. Finally, the fractional cloudiness and

the altitude of the clouds are either prescribed or predicted, the latter by some assumption about the behavior of clouds.

The equilibrium change in temperature simulated by RCMs for an increase in the CO_2 concentration shows a cooling in the stratosphere and a warming in the troposphere and at the Earth's surface, the latter with a range of 0.48 to 4.2°C. As indicated by Eq. (1), the change in the surface temperature induced by a doubling of the CO_2 concentration can be understood in terms of the direct radiative forcing ΔQ due to the CO_2 increase; the response of the climate system if the surface temperature alone changed, as characterized by the zero-feedback gain G_o; and the negative and positive feedbacks f which occur to reduce and enhance the zero-feedback response, respectively. Each of these is discussed below.

About 95% of the direct radiative forcing due to the increase in the CO_2 concentration occurs in the longwave radiation emitted by the Earth and 5% in the shortwave solar radiation (Ramanathan et al., 1979). The direct radiative forcing of the troposphere-surface system ΔR_T has been found to be 4.0 Wm^{-2}, of which 2.7 Wm^{-2} is contributed by the reduction in upward flux from the troposphere, 1.55 Wm^{-2} by the increased downward flux from the stratospheric CO_2 increase, and -0.15 Wm^{-2} by the decreased solar flux at the tropopause (Lal and Ramanathan, 1984).

The response of the climate system to the direct radiative forcing of the increased CO_2 when only the surface temperature is allowed to change is given by Eq. (1), with $f = 0$ and $\Delta Q = \Delta R_T$, and by Eq. (2) as

$$(\Delta T_s)_o = G_o \, \Delta R_T = \frac{T_s(1 \times CO_2)}{(1 - \alpha_p) \, S} \, \Delta R_T \, .$$

Taking $S = 1370$ Wm^{-2}, $\alpha_p = 0.3$ and T_s as the observed surface air temperature $T_a = 288$ K gives $G_o = 0.3°C/(Wm^{-2})$. Thus for $\Delta R_T = 4$ Wm^{-2},

$(\Delta T_s)_o = 1.2°C$. This value of $(\Delta T_s)_o$ is in agreement with what has been obtained by RCMs without feedbacks (see Schlesinger 1985, 1988a).

The feedback f of the CO_2-induced surface air temperature warming given by RCMs can be determined from Eq. (1) written as

$$f = 1 - \frac{(\Delta T_s)_o}{\Delta T_s} , \tag{3}$$

together with the above estimate of $(\Delta T_s)_o$. Thus, for the $0.48 \leq \Delta T_s \leq 4.2°C$ range simulated by RCMs, $-1.5 \leq f \leq 0.7$. Several physical mechanisms are thought to be the cause of this wide range in the feedback of these models. For increasing T_s these mechanisms include: 1) the increase in the amount of water vapor in the atmosphere as a consequence of the near-constancy of the relative humidity, 2) the change in the temperature lapse rate, 3) the increase in the cloud altitude as the clouds maintain their temperature, 4) the change in cloud amount, 5) the change in the cloud optical depth, and 6) the decrease in surface albedo. The feedbacks of these physical processes, as determined by applying Eq. (3) to and ensemble of RCM simulations in which the feedbacks were added sequentially (see Schlesinger 1985, 1988a), are summarized in Table 1. This table shows that: 1) the water vapor, cloud altitude and surface albedo feedbacks are positive, with values that decrease in that order; 2) the cloud optical depth feedback is negative; 3) the temperature lapse rate feedback is either positive or negative, depending on whether the lapse rate is controlled by baroclinic adjustment (BADJ) or convective (MALR or PC) processes; and 4) the cloud cover feedback is unknown. However, as shown by Eq. (1) and Fig. 2, the influence of any of these feedbacks on the response of the climate system depends nonlinearly on the sum of the other feedbacks. For example, the addition of cloud altitude feedback with $f = 0.2$ would increase ΔT_s by

Table 1. Summary of the feedbacks f in RCM and GCM simulations of CO_2-induced surface air temperature change.

Feedback Mechanism	RCM[a]	GCM GISS[b]	GCM GFDL[c]
Water Vapor	0.3 to 0.4	0.66	0.41
Lapse Rate[d]			
BADJ	0.1		
MALR	-0.25 to -0.4		
PC	-0.65		
Total		-0.26	0.05
Cloud			
Altitude	0.15 to 0.30		
Cover	Unknown		
Altitude & Cover		0.22	0.09
Optical Depth	0 to -1.32		
Surface Albedo	0.14 to 0.19	0.09	0.13
Total	-1.5 to 0.71	0.71	0.68

a. Based on the analysis of Schlesinger (1985, 1988a).
b. Based on the results of Hansen et al. (1984).
c. In this analysis a value of $\Delta R_T = 4.3$ Wm^{-2} is assumed. This value is based on the change in the net radiation at the top of the atmosphere given by Wetherald and Manabe (1988), $\Delta R_o = 2.28$ Wm^{-2}, and the difference between the ΔR_T and ΔR_o results for this radiation model averaged over the five atmospheric profiles of the Intercomparison of Radiation Codes used in Climate Models (ICRCCM) study (Ellis, 1987, personal communication).
d. BADJ, MALR and PC denote baroclinic adjustment, moist adiabatic adjustment and penetrative convection, respectively.

1.6°C if added to a system with an existing feedback of 0.5, but would increase ΔT_s by only 0.5°C if added to a system with no existing feedback.

2.3. General circulation models

While EBMs and RCMs calculate only the surface temperature and the vertical temperature profile, respectively, GCMs calculate the geographical distribution of an ensemble of climatic quantities which includes the vertical profiles of atmospheric temperature, water vapor and velocity, and the surface pressure, precipitation, soil water and snow. In addition, GCMs used for climatic-change simulations must calculate the geographical distributions of the sea surface temperature (SST) and sea ice extent. (See Schlesinger 1984 and 1988b for further information on GCMs.) To study CO_2-induced equilibrium climatic changes with a GCM requires two simulations, a $1xCO_2$ simulation with a CO_2 concentration generally taken to be 300-330 ppmv, and an $NxCO_2$ simulation with N generally taken to be 2 or 4. Each of the simulations is begun from some prescribed initial conditions and is run until these conditions are forgotten and the simulated climate reaches its statistically-stationary equilibrium state. The difference between the $NxCO_2$ and $1xCO_2$ equilibrium climates are then taken to be the CO_2-induced equilibrium climate changes.

The earliest GCM simulations of CO_2-induced climatic change were performed with so-called "swamp models" of the ocean. In such a swamp ocean model the ocean has zero heat capacity and no horizontal or vertical heat transport. Therefore, the swamp ocean is like perpetually wet land and is always in thermodynamic equilibrium. Consequently, the time for the Earth-atmosphere system to reach its equilibrium climate with an atmospheric GCM/swamp ocean model depends only on the atmosphere and land surface, and generally requires about 300 days. While such models are economical of

computer time, they must be run without the seasonal insolation cycle to prevent the freezing of the ocean in the latitudes of the polar night. Consequently, these models simulate the CO_2-induced change only for a surrogate of the annual-mean climate, namely, that which is obtained for the annual-mean solar insolation. More recently, atmospheric GCMs have been coupled to prescribed-depth mixed-layer ocean models which have heat capacity and sometimes a prescribed additional oceanic heating which includes the effects of oceanic heat transport. These atmospheric GCM/prescribed-depth mixed-layer ocean models are run with the seasonal insolation cycle and generally require about 20 simulated years to reach their equilibrium climate. An additional 10 years is generally simulated to obtain estimates of the means and other statistics of the equilibrium climate.

The annual cycles of the equilibrium climatic changes induced by a doubling of the CO_2 concentration have been simulated by the GCM/mixed-layer ocean models of: 1) the Geophysical Fluid Dynamics Laboratory (GFDL, Wetherald and Manabe, 1986), 2) the Goddard Institute for Space Studies (GISS, Hansen et al., 1984), 3) the National Center for Atmospheric Research (NCAR, Washington and Meehl, 1984), 4) Oregon State University (OSU, Schlesinger and Zhao, 1988), and 5) the United Kingdom Meteorological Office (UKMO, Wilson and Mitchell, 1987). In the following two subsections the CO_2-induced changes in the surface air temperature and soil water simulated by these models are presented.

2.3.1. Surface air temperature change. The equilibrium changes in the global-mean surface air temperature ΔT_s simulated by the five models for a doubled CO_2 concentration are presented in Table 2, together with the global-mean precipitation changes ΔP. This table shows that the simulated

Table 2. Changes in the global-mean surface air temperature (T_s) and precipitation rate (P) simulated by atmospheric GCM/mixed-layer ocean models for a CO_2 doubling.

Model/Study	ΔT_s (°C)	ΔP (% of $1xCO_2$ value)
GFDL/Wetherald & Manabe (1986)	4.0	8.7
GISS/Hansen et al. (1984)	4.2	11.0
NCAR/Washington & Meehl (1984)	3.5	7.1
OSU/Schlesinger & Zhao (1988)	2.8	7.8
UKMO/Wilson & Mitchell (1987)	5.2	15.0

CO_2-induced changes in the annual mean, global-mean surface air temperature range from 2.8 to 5.2°C, and the corresponding changes in precipitation from 7.1 to 15% of their $1xCO_2$ values. Furthermore, this table shows that the size of ΔP is positively correlated with the size of ΔT_s, this occurring as a result of the Clausius-Clapeyron relation between the saturation vapor pressure of water vapor and temperature.

A partial explanation for the range of ΔT_s, and thus of ΔP, is provided by Fig. 3 which displays the CO_2-induced warming plotted versus the annual-mean, global-mean surface air temperature of the simulated $1xCO_2$ climate. This figure shows that the warmer the $1xCO_2$ control climate, the smaller the CO_2-induced warming. This is due in part to the decrease in the positive ice-albedo feedback with increasing $1xCO_2$ temperature as a result of there being less sea ice and snow. From this is appears that the CO_2-induced changes in temperature and precipitation simulated by these models would be in better agreement if their $1xCO_2$ global-mean surface air temperature were in better agreement. Furthermore, it is tempting to conclude that the resulting common model temperature and precipitation sensitivities would be correct if the common $1xCO_2$ surface air temperature were in agreement with the observed temperature, perhaps through the use of the "Flux Correction Method."[1] However, while this is a necessary condition for the common

[1]In this method, which was employed by the GISS and UKMO models, an oceanic heating is determined for each calendar month at each ocean grid point from a $1xCO_2$ simulation with the atmospheric GCM using the observed annual cycle of SST as its lower boundary condition over the ocean. This heating field is then prescribed in both the $1xCO_2$ and $2xCO_2$ simulations with the GCM/mixed-layer ocean model, thereby helping the model to reproduce the observed SST distribution in the $1xCO_2$ simulation. However, although the prescribed oceanic heating includes the effects of the oceanic heat transports, it also includes a compensation for the air/sea heat flux errors of the atmospheric GCM in its simulation with the observed SSTs. Therefore, this "Flux Correction Method" is not a physically-based method. Furthermore, its use in both the $1xCO_2$ and $2xCO_2$ simulations does not allow the oceanic heat transport effects to change and contribute to the CO_2-induced climatic change.

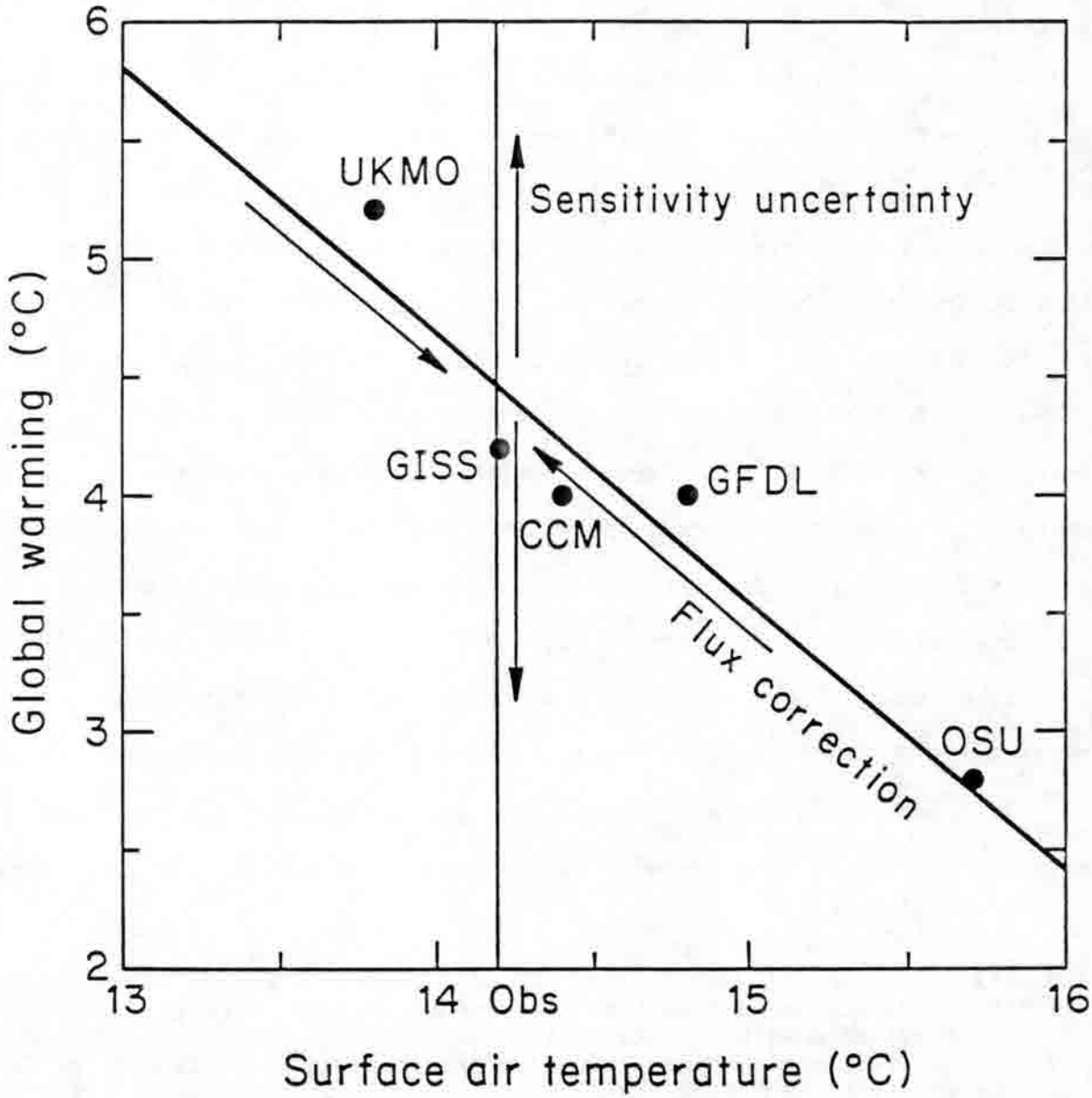

Fig. 3. The global-mean surface air temperature warming simulated for a CO_2 doubling by five GCMs [the GFDL model (Wetherald and Manabe, 1986), the GISS model (Hansen et al., 1984), the NCAR model (Washington and Meehl, 1984), the OSU model (Schlesinger and Zhao, 1988), and the UKMO model (Wilson and Mitchell, 1987)] versus their simulated $1xCO_2$ global-mean surface air temperature. "Obs" indicates the observed global-mean surface air temperature based on the Data of Jenne (1975). (Adapted from Cess and Potter, 1988).

sensitivities of the models to be in agreement with the sensitivities of nature, it is not a sufficient condition as is indicated by the vertical arrows labelled sensitivity uncertainty in Fig. 3. In fact, the potential for such a disparity is evidenced by Table 1 which shows that although the GISS and GFDL models simulate similar values of ΔT_s (Fig. 3), they do so with feedbacks that differ in both magnitude and sign, this despite the approximate agreement of their simulated values of T_s for the $1xCO_2$ climate. Consequently, to establish the correctness of the models' temperature and precipitation sensitivities when they simulate the present climate correctly requires the simulation of at least one climate different from that of the present, for example, that of Wisconsin Ice Age 18,000 years before the present, and the comparison of such a simulated paleoclimate with observations. This requirement for model validation is a fundamental and inherently-difficult problem in climate modeling and simulation (Schlesinger and Mitchell, 1985, 1987). This notwithstanding, it is of interest here to present and compare further results of the CO_2-induced climatic changes simulated by these models.

The time-latitude distributions of the zonal-mean surface air temperature changes simulated by the five models for doubled CO_2 are presented in Fig. 4. This figure shows that the CO_2-induced temperature changes increase from the tropics, where the values range from about 2°C for the NCAR and OSU models to about 4°C for the GISS and UKMO models, toward the poles, and that the seasonal variations of the CO_2-induced surface temperature changes are small between 50°S and 30°N and are large in the regions poleward of 50° latitude in both hemispheres. In the Northern Hemisphere a warming minimum of about 2°C is simulated near the pole by all five models in summer. The models also simulate a warming maximum in fall with values that range from 8°C for the NCAR model to 16°C for the GFDL and

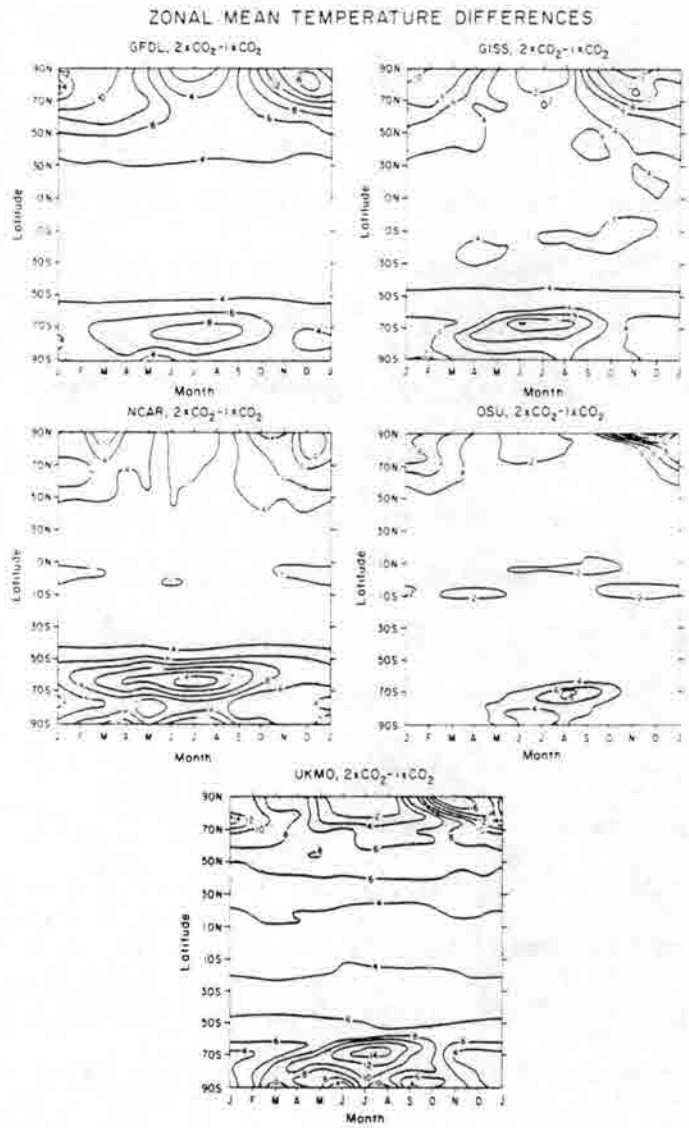

Fig. 4. Time-latitude distribution of the zonal-mean surface air temperature change (°C), $2xCO_2$-$1xCO_2$, simulated by: (a) the GFDL model by Wetherald and Manabe (1986); (b) the GISS model by Hansen et al. (1984); (c) the NCAR model by Washington and Meehl (1984); (d) the OSU model by Schlesinger and Zhao (1988); and (e) the UKMO model by Wilson and Mitchell (1987). Stipple indicates temperature increases larger than 4°C.

UKMO models. This maximum extends into winter in all the simulations except that of NCAR which instead exhibits a warming minimum near the pole. The NCAR model also simulates another polar warming minimum in spring that is not found in the other simulations. In the Southern Hemisphere all five models simulate a maximum warming in winter and a minimum warming in summer. The summer warming maximum occurs near the Antarctic coast in all five simulations and ranges from 8°C in the GFDL and OSU simulations to 14°C in the NCAR and UKMO simulations.

The geographical distributions of the $2xCO_2$-$1xCO_2$ surface air temperature changes simulated for December-January-February (DJF) ad June-July-August (JJA) by the five models are presented in Figs. 5 and 6 respectively. These figures show that all five models simulate a CO_2-induced surface air temperature warming virtually everywhere. In general, the warming is a minimum in the tropics during both seasons, at least over the ocean, and increases toward the winter pole. The tropical maritime warming minimum ranges from about 2°C in the NCAR and OSU simulations to about 4°C in the GFDL, GISS and UKMO simulations. Maximum warming in DJF occurs in the Arctic in all the simulations except that of NCAR which instead exhibits a warming maximum near 65°N. The maximum warming in JJA occurs around the Antarctic coast in all five simulations. The locations of the wintertime warming maxima in both hemispheres coincide with the locations where the $1xCO_2$ sea ice extent retreats in the $2xCO_2$ simulation. The magnitude of the wintertime warming maxima in the Northern Hemisphere ranges from 10°C in the GISS and OSU simulations to 20°C in the UKMO simulation, and in the Southern Hemisphere it ranges from 10°C in the OSU simulation to 20°C in the UKMO simulation. In JJA there is a warming minimum in the Arctic of about 2°C in all five simulations.

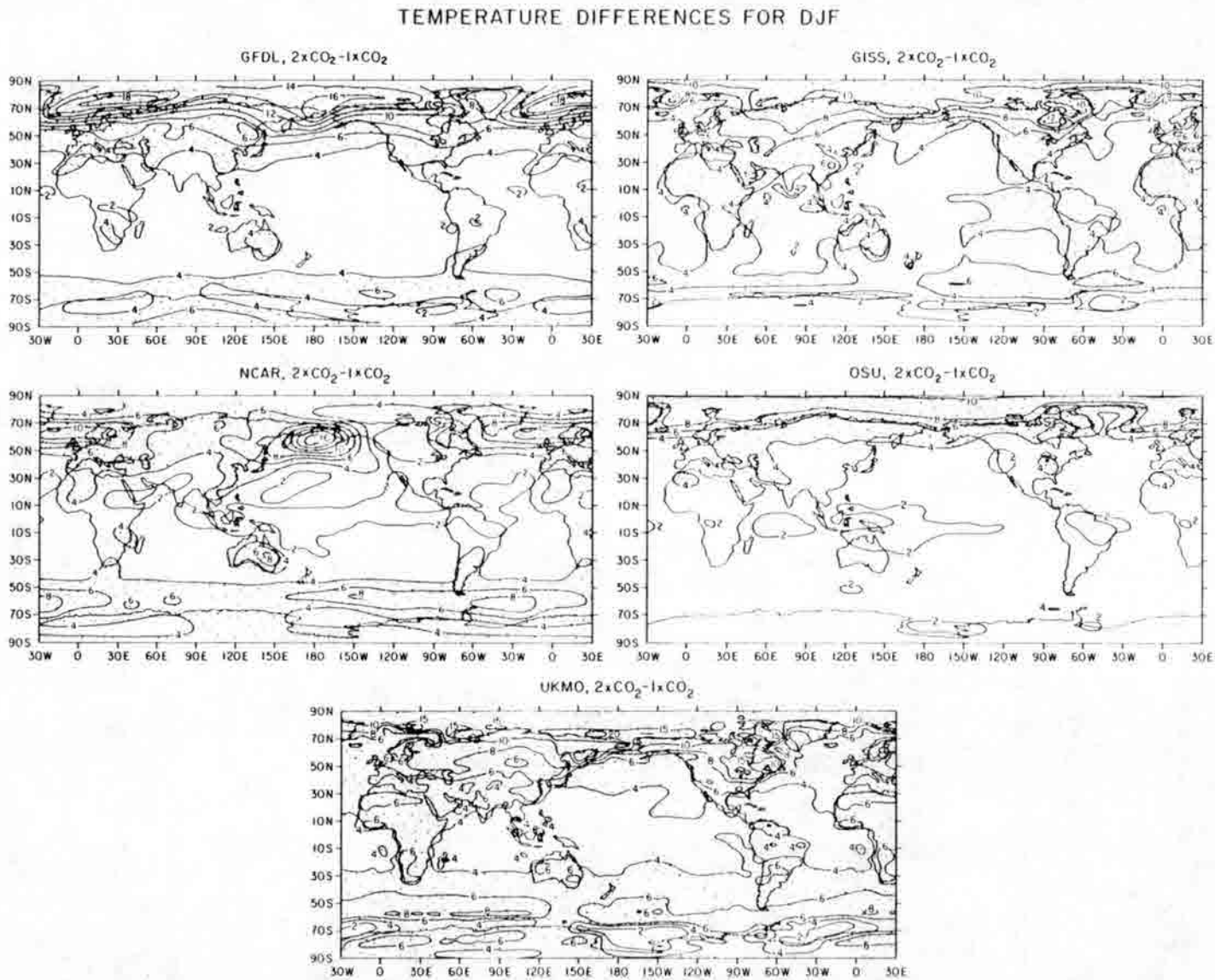

Fig. 5. Geographical distribution of the surface air temperature change (°C), $2xCO_2$-$1xCO_2$, for DJF simulated by: (a) the GFDL model by Wetherald and Manabe (1986); (b) the GISS model by Hansen et al. (1984); (c) the NCAR model by Washington and Meehl (1984); (d) the OSU model by Schlesinger and Zhao (1988); and (e) the UKMO model by Wilson and Mitchell (1987). Stipple indicates temperature increases larger than 4°C.

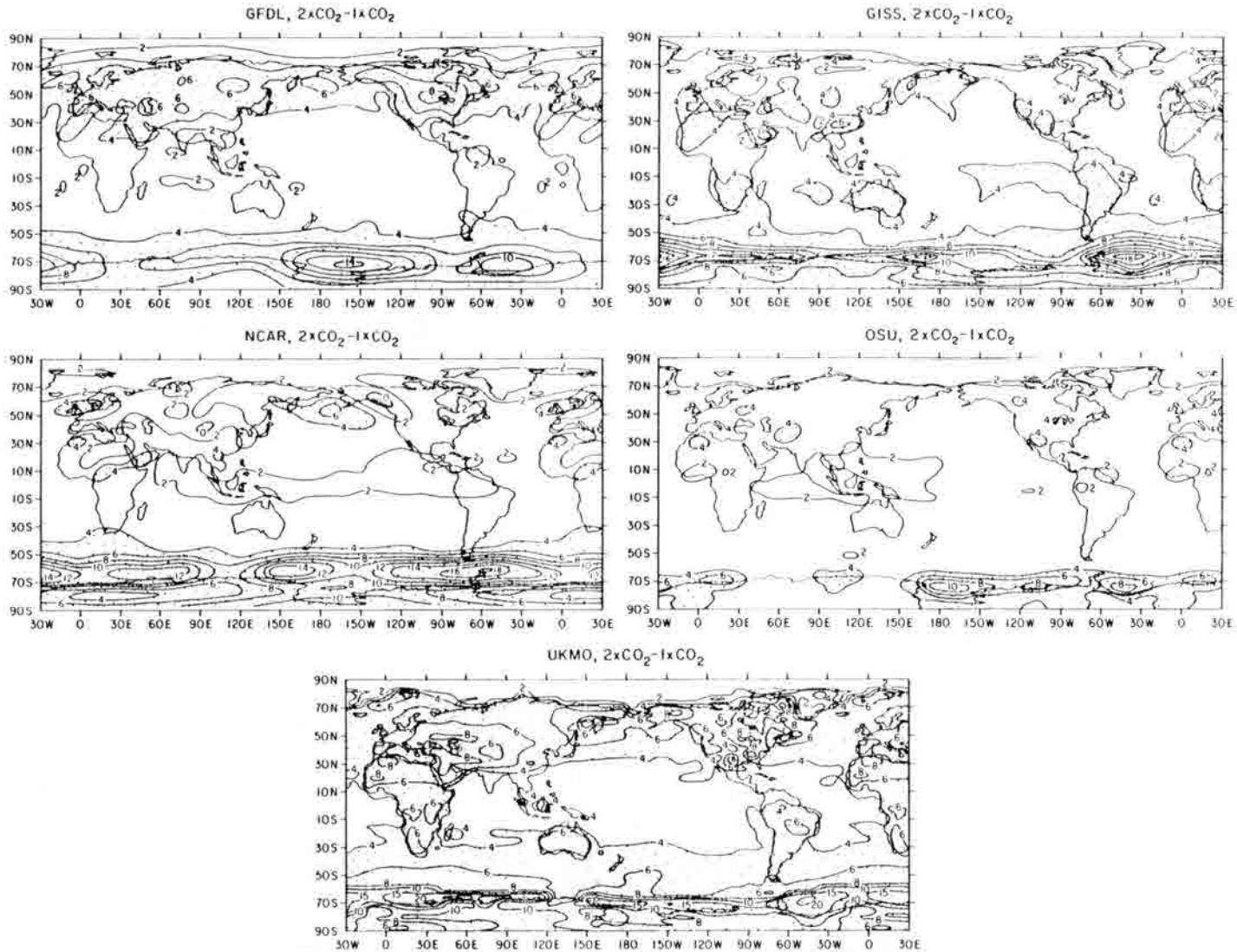

Fig. 6. As in Fig. 5, except for JJA.

Figures 5 and 6 also show that although there are similarities in the CO_2-induced regional temperature changes simulated by the models, there are significant differences in both their magnitude and seasonality. For example, in North America the wintertime warming generally increases with latitude in the GFDL, GISS and UKMO simulations with values of 4°C in the south and 10°C in the north, while both the NCAR and OSU simulations exhibit a warming minimum of 2°C centered over Canada and over the Pacific Northwest, respectively. Also, the CO_2-induced warming in summer compared to that in winter is simulated to be smaller by the GISS and NCAR models, to be comparable by the GFDL, OSU and UKMO models, and to be larger by the NCAR model. Further similarities and differences can be seen for the CO_2-induced temperature changes simulated for the other continents.

2.3.2. Soil water change. The time-latitude distributions of the zonal-mean soil water change over ice-free land simulated by the five models for doubled CO_2 are presented in Fig. 7. This figure shows that all five models simulate an increased soil water during winter in the Northern Hemisphere from about 45°N to 70°N. In northern hemisphere summer the GISS and NCAR models simulate a minimum increase in soil water, while the GFDL, OSU and UKMO models simulate a decreased soil water from about 30°N to 70°N.

The geographical distributions of the CO_2-changes in soil water over ice-free land simulated by the models for DJF and JJA are presented in Figs. 8 and 9, respectively. As was evidenced by the zonal-mean soil water changes shown in Fig. 7, all five models simulate a moistening of the soil over much of Eurasia and North America in DJF. On the other hand, the GISS and NCAR models simulate both regions of increased and decreased soil water over Eurasia and North America in JJA, while the GFDL, OSU and UKMO models simulate a desiccation virtually everywhere in the Northern Hemisphere

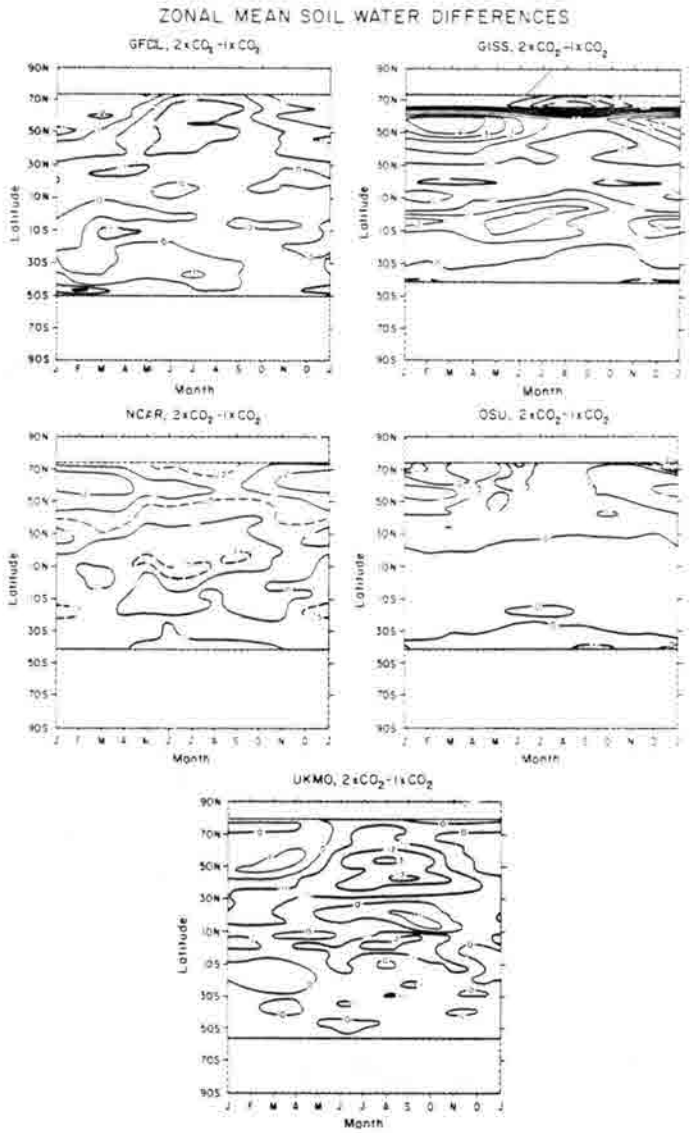

Fig. 7. Time-latitude distribution of the zonal-mean soil water change (cm), $2xCO_2$-$1xCO_2$, only over ice-free land simulated by: (a) the GFDL model by Wetherald and Manabe (1986); (b) the GISS model by Hansen et al. (1984); (c) the NCAR model by Washington and Meehl (1984); (d) the OSU model by Schlesinger and Zhao (1988); and (e) the UKMO model by Wilson and Mitchell (1987). Stipple indicates a decrease in soil water, hatching indicates latitudes where there is no ice-free land.

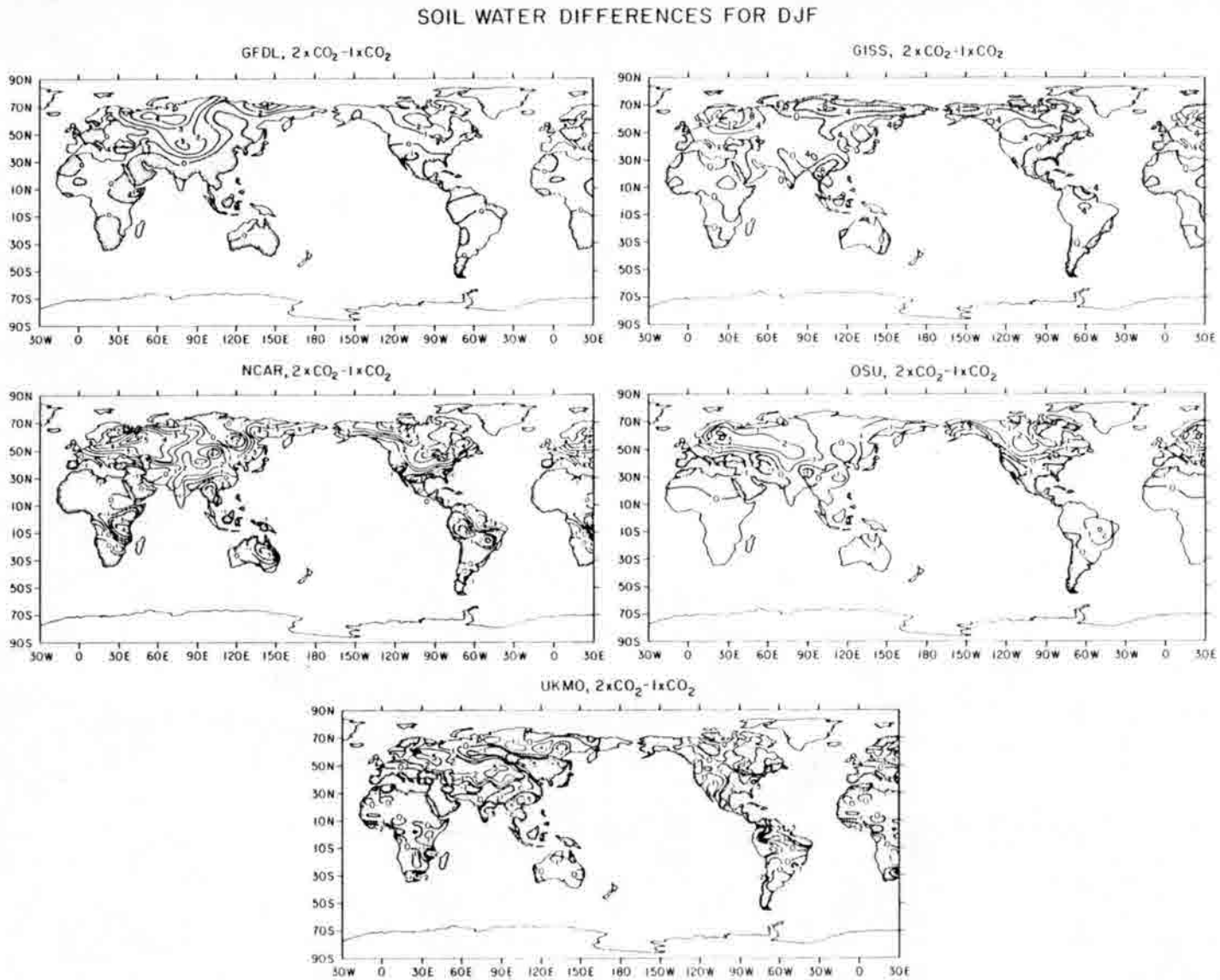

Fig. 8. Geographical distribution of the soil water change (cm), $2xCO_2$-$1xCO_2$, for DJF simulated by: (a) the GFDL model by Wetherald and Manabe (1986); (b) the GISS model by Hansen et al. (1984); (c) the NCAR model by Washington and Meehl (1984); (d) the OSU model by Schlesinger and Zhao (1988); and (e) the UKMO model by Wilson and Mitchell (1987). Stipple indicates a decrease in soil water.

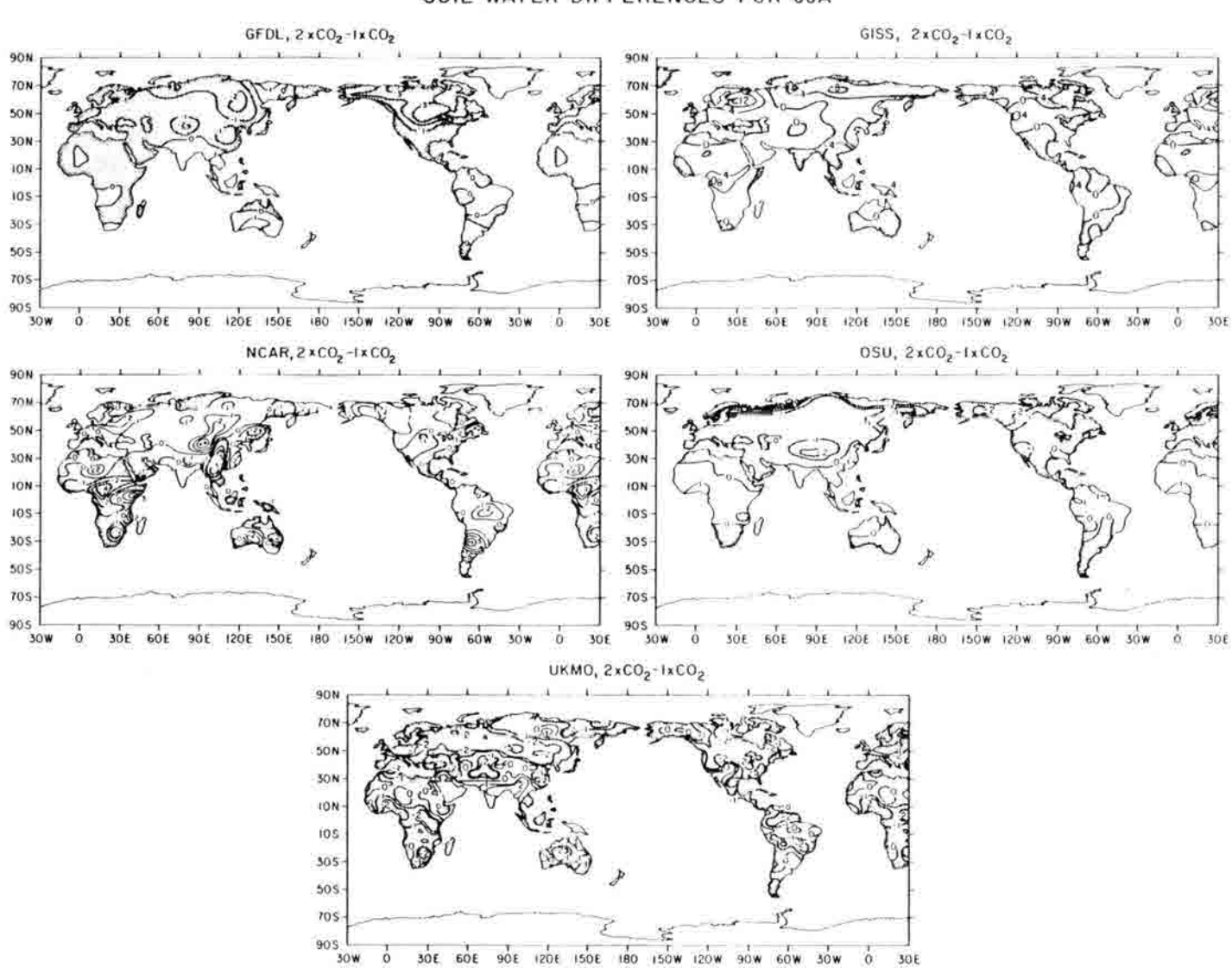

Fig. 9. As in Fig. 8, except for JJA.

during summer. A similar desiccation of the northern hemisphere soil was first obtained in the "annual-mean" simulations with atmospheric GCM/swamp ocean models and with the first annual-cycle simulation with an atmospheric GCM/prescribed-depth mixed-layer ocean model (see Schlesinger and Mitchell 1985, 1987).

3. CO_2-Induced Transient Climate Change

As discussed in the Introduction the CO_2 concentration has increased from about 288 ppmv in 1861 to 344 ppmv in 1984 (Siegenthaler and Oeschger, 1987; Keeling and Boden, 1986). The equilibrium surface temperature increase corresponding to this CO_2 increase can be written by Eq. (1) as

$$\Delta T_s = G_f \Delta Q \ ,$$

where the direct radiative forcing ΔQ can be scaled to that for a CO_2 doubling, ΔQ_{2x}, by (Augustsson and Ramanathan, 1977)

$$\Delta Q = \Delta Q_{2x} \left[\frac{\ln[C(1984)/C(1861)]}{\ln 2} \right] \ ,$$

where C is the CO_2 concentration. Combining these equations and noting that $(\Delta T_s)_{2x} = G_f \Delta Q_{2x}$ gives

$$\Delta T_s = (\Delta T_s)_{2x} \left[\frac{\ln[C(1984)/C(1861)]}{\ln 2} \right] \ . \qquad (4)$$

If we assume that $(\Delta T_s)_{2x} = 4°C$ based on the results from the GFDL, GISS, NCAR, OSU and UKMO atmospheric GCM/mixed-layer ocean model equilibrium simulations, then for the CO_2 concentrations above, $\Delta T_s = 1.0°C$. However, the reconstructed global-mean surface air temperature record (Jones et al.,

1986) indicates a warming from 1861 to 1984 of about 0.6°C. Does this difference mean that the gain G_f of our climate models is about twice as large as that of nature? The likely answer is no because the actual response of the climate system lags the equilibrium response because of the thermal inertia of the ocean. This can be illustrated by the energy-balance model

$$C_s \frac{d\Delta T_s}{dt} = \Delta Q - \frac{\Delta T_s}{G_f} ,$$

where C_s is the heat capacity of the upper ocean. When equilibrium is achieved, $d\Delta T_s/dt = 0$ and $(\Delta T_s)_{eq} = G_f \Delta Q$ as in Eq. (1). However, the transient solution

$$\Delta T_s(t) = (\Delta T_s)_{eq} \left(1 - e^{-t/\tau_e}\right)$$

shows that equilibrium is approached exponentially with a characteristic "e-folding" time $\tau_e = C_s G_f$, which is the time required to reach $1 - e^{-1}$ or 63% of the equilibrium response. In the following, the studies of this lag of the climate system are reviewed.

3.1. Results for an abrupt CO_2 increase

The transient response of the climate system to an abrupt CO_2 increase has been investigated with planetary energy-balance, radiative-convective and simplified atmospheric general circulation models in conjunction with box-diffusion, box-upwelling-diffusion and two-box ocean models. The box-diffusion ocean model consists of a fixed-depth mixed layer (the box) surmounting the thermocline and deep ocean in which vertical heat transport

is treated as a diffusive process with a prescribed thermal diffusivity κ. The box-upwelling-diffusion ocean model is a box-diffusion model with a prescribed oceanic upwelling velocity W. The two-box ocean model is comprised of a fixed-depth mixed-layer box and an intermediate-water box which exchange heat vertically with a prescribed ventilation time. A transient simulation with a global, coupled atmosphere/ocean general circulation model has also been performed. In the following we summarize the results from these simple and more-comprehensive models.

3.1.1. Results from simplified models. The results from six studies of the transient response to abrupt heating are presented in Table 3. Hoffert et al. (1980) using a box-upwelling-diffusion ocean model, and Schneider and Thompson (1981) using a two-box ocean model, obtained e-folding times of about 10 to 20 years. A slightly larger e-folding time of 25 years was obtained by Bryan et al. (1982) and Spelman and Manabe (1984) with a simplified coupled atmosphere-ocean general circulation model in which the geographical domain was restricted to a 120°-longitude sector extending from equator to pole, with the western half of the sector occupied by land at zero elevation and the eastern half by ocean with a uniform depth of 5000 m. On the other hand, Hansen et al. (1984) used a box-diffusion ocean model and obtained 27-, 55- and 102-year e-folding times corresponding to assumed climate system gains G_f of 0.465, 0.698 and 0.977°C/(Wm^{-2}), respectively. Bryan et al. (1984) used an uncoupled global oceanic general circulation model and found an e-folding time of about 100 years in response to an imposed 0.5°C upper-ocean surface warming. Lastly, Siegenthaler and Oeschger (1984) obtained a 60-year e-folding time in their study using a box-diffusion model.

Table 3. The e-folding time τ_e for abrupt heating from selected climate model studies.

Study	Model	τ_e (years)
Hoffert et al. (1980)	Planetary energy-balance climate model and a box-upwelling-diffusion ocean model	8-20
Schneider and Thompson (1981)	Planetary energy-balance model and a two-box ocean model	13
Bryan et al. (1982) Spelman and Manabe (1984)	Coupled atmosphere-ocean general circulation model with simplified geography and topography	25
Hansen et al. (1984)	Radiative-convective climate model and a box-diffusion ocean model	27 55 102
Bryan et al. (1984)	Global oceanic general circulation model	100
Siegenthaler and Oeschger (1984)	Planetary energy-balance climate model and a box-diffusion ocean model	60

The studies presented in Table 3 indicate that the e-folding time τ_e lies between 10 and 100 years. If $\tau_e \approx$ 10 years, then the actual response of the climate system would be quite close to the equilibrium response and the disparity between the latter for the 1861-to-1984 warming and the corresponding observed warming would mean that the gain of our climate models is larger than that of nature. On the other hand, if $\tau_e \approx$ 100 years, then the actual response of the climate system would be quite far from the equilibrium response, thus indicating that the gain of our climate models may be correct.

The factors that contribute to the wide range in τ_e have been discussed by Wigley and Schlesinger (1985) from their analytical solution for the energy-balance climate/box-diffusion ocean model. These authors found that τ_e depends quadratically on the climate system gain G_f and linearly on the thermal diffusivity κ. When a box-upwelling-diffusion model is used instead, the resultant e-folding time of the numerical solution can be expressed as shown in Fig. 10 by $\tau_e = 92.57\ G^{1.93}\ \kappa^{0.94}\ \exp(-0.15\ G^{0.97}\ \kappa^{0.09}\ W^{0.78})$. However, in view of this dependence of τ_e on G_f, κ and W, quantities which are prescribed in an energy-balance climate upwelling-diffusion ocean model, the determination of whether $\tau_e \approx$ 10 or 100 years requires a global, coupled atmosphere-ocean general circulation model in which these quantities are self-determined. The results from a simulation with such a model are described below.

3.1.2. Results from a global, coupled atmosphere-ocean GCM. To investigate the transient response of the climate system, $1xCO_2$ and $2xCO_2$ simulations have been performed with the OSU coupled atmosphere-ocean general circulation model (Schlesinger et al., 1985; Schlesinger and Jiang, 1987). The atmospheric component of the coupled model is basically the two-layer

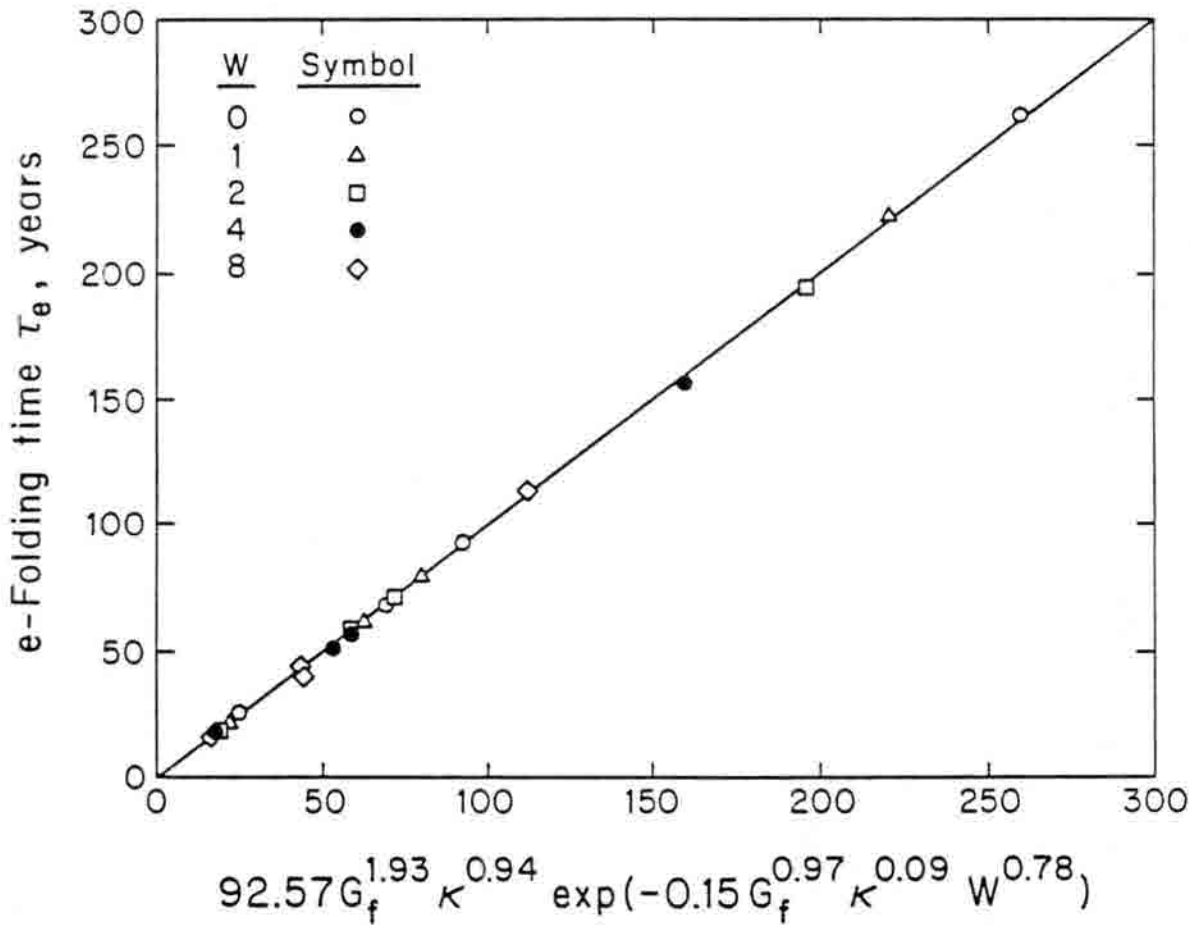

Fig. 10. The e-folding time τ_e for an abrupt heating perturbation versus $92.57\ G_f^{1.93}\ \kappa^{0.94}\ \exp(-0.15\ G_f^{0.97}\ \kappa^{0.09}\ W^{0.78})$. The data points were obtained from a numerical solution of a box-upwelling-diffusion model for upwelling velocities W = 0, 1, 2, 4 and 8 m yr^{-1}. The fit (straight line) was obtained by regression.

AGCM described by Schlesinger and Gates (1980) and documented by Ghan et al. (1982). The oceanic component of the coupled model is basically the six-layer oceanic general circulation model (OGCM) developed by Han (1984 a, b) and extended by him to include the Arctic Ocean. The coupled model predicts the temperatures and velocities of the atmosphere and ocean, the atmospheric surface pressure and water vapor, the oceanic salinity, the land surface temperature and water content, the sea ice thickness, the snow mass and clouds, and includes both the diurnal and seasonal variations of solar radiation. The coupled model is global, has realistic continent/ocean geography and land and ocean-bottom topographies, and is integrated synchronously, that is, both component models simulate the same period of time. The $1xCO_2$ and $2xCO_2$ simulations differed only in their CO_2 concentrations (326 and 652 ppmv, respectively), both were started from the same initial conditions, and each was integrated for 20 years. The evolution of the difference between the $2xCO_2$ and $1xCO_2$ simulations thus represents the transient climate change induced by an abrupt CO_2 doubling.

The evolution of the change in global-mean temperature induced by the doubled CO_2 concentration is shown in Fig. 11 in terms of the vertical distribution of monthly-mean $2xCO_2$-$1xCO_2$ temperature differences for the atmosphere and ocean. The top panel of Fig. 11 shows an initially-rapid and vertically-uniform warming of the atmosphere followed by a progressively-slowing atmospheric warming. The bottom panel of Fig. 11 also shows an initially-rapid warming of the sea surface followed by a progressively-slowing warming. Figure 11 indicates that this decrease with time in the warming rate of the atmosphere and sea surface is the result of a downward transport and sequestering of heat into the interior of the ocean.

The temperature changes shown in Fig. 11, when normalized by the equilibrium temperature change, define the climate response function for the

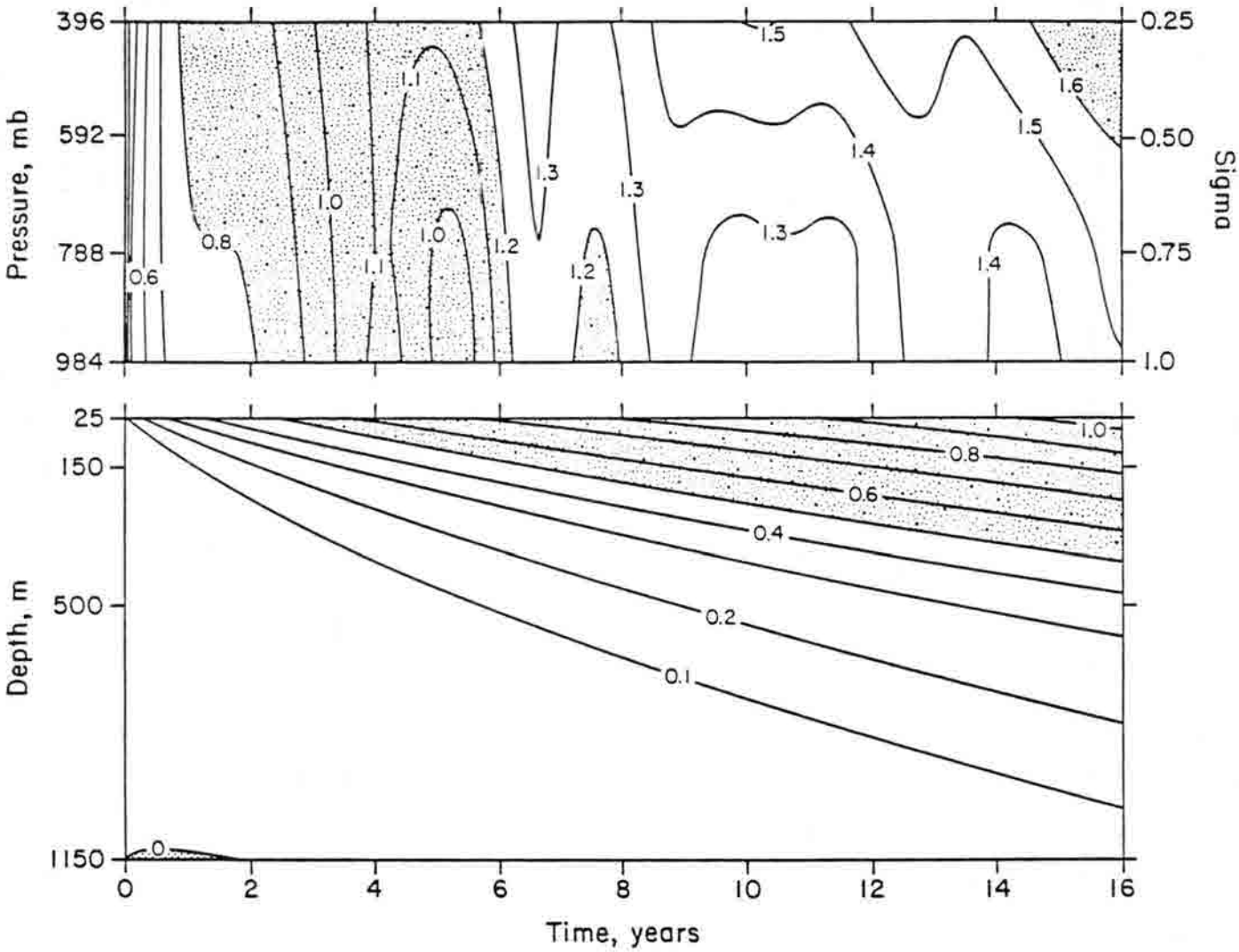

Fig. 11. Latitude-vertical distribution of the $2xCO_2$-$1xCO_2$ difference in the annual-mean, zonal-mean temperatures (°C) of the atmosphere (above) and ocean (below) for year 16. Atmospheric warming from 0.8 to 1.2°C and larger than 1.6°C is shown by light stipple, as is oceanic warming larger than 0.5°C, while oceanic cooling is indicated by heavy stipple. (From Schlesinger et al., 1985).

global-mean temperature. Clearly, these coupled atmosphere/ocean GCM simulations were not of sufficient duration for the equilibrium change to have been attained. However, an estimate of the equilibrium temperature change and the vertical transport characteristics of the ocean have been obtained from a representation of the time evolution of Fig. 11 by a simple one-dimensional climate/ocean model (Schlesinger et al. 1985). An energy-balance climate/multi-box ocean model gives an excellent representation of the evolution shown in Fig. 11 with self-determined parameters for which the estimated equilibrium temperature change is 2.8°C. The effective ocean thermal diffusivity κ, by which all vertical heat transport is parameterized in the simple multi-box ocean model representation, is 3.2 cm^2s^{-1} at the 50 m level, 3.8 cm^2s^{-1} at the 250 m level, and 1.5 cm^2s^{-1} at the 750 m level. The mass-averaged effective ocean thermal diffusivity of κ = 2.25 cm^2s^{-1} is in agreement with the best estimate based on the value required by a box-diffusion ocean model to reproduce the observed penetration of bomb-produced radionuclides into the ocean (Broecker et al., 1980; Siegenthaler, 1983). Moreover, an energy-balance climate/box-diffusion ocean model with κ = 2.25-2.50 cm^2s^{-1} is successful in reproducing the evolution of the $2xCO_2$-$1xCO_2$ differences in the surface air and ocean surface layer temperatures simulated by the coupled atmosphere/ocean GCM. Consequently, it appears that the coupled model transports heat from the surface downward into the ocean at a rate which is commensurate with the rate observed for the downward transport of radionuclides.

The climate response function obtained from the energy-balance climate/multi-box ocean model representation of the coupled model $2xCO_2$-$1xCO_2$ temperature evolution is shown in Fig. 12 where a projection with the simple model has been made to year 200 after the abrupt CO_2 doubling. It is seen that the response function is not simply $1-\exp(-t/\tau_e)$, as it would be

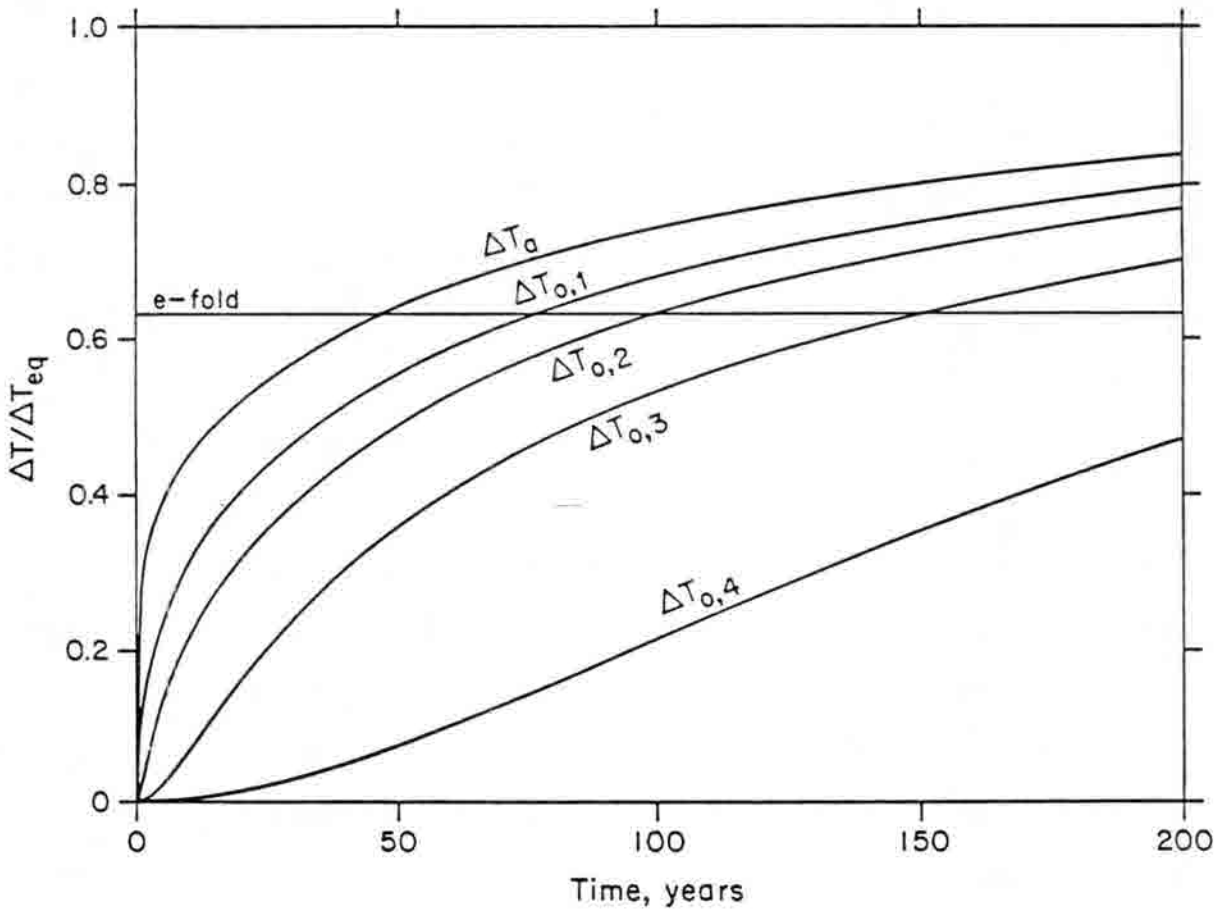

Fig. 12. Energy-balance climate/multi-box ocean model projection to year 200 of the evolution of the $2xCO_2$-$1xCO_2$ difference in global-mean surface air temperature (ΔT_a) and oceanic temperature ($\Delta T_{o,k}$, k = 1, 2, 3, 4) as a fraction of the equilibrium temperature difference (ΔT_{eq}). The horizontal line labelled e-fold indicates the level at which $\Delta T/\Delta T_{eq} = 1-1/e \approx 0.63$. (From Schlesinger et al., 1985).

if only the oceanic mixed layer warmed without transporting heat to the thermocline and deeper ocean. Thus, the response function cannot be characterized by a single parameter such as τ_e. Nevertheless, the time to reach 63% of the equilibrium is useful for comparison with earlier studies (Table 3). Figure 12 shows that such an "e-folding time" is about 50-100 years.

3.2. Results for a time-dependent CO_2 increase

The results presented in the preceding section have been for the transient response of the climate system to an instantaneous doubling of the CO_2 concentration. However, the CO_2 concentration has not abruptly changed in the past, nor is it likely to in the future. Instead the CO_2 concentration has increased more or less continuously since the dawn of the industrial revolution.

Both Hansen et al. (1984) and Wigley and Schlesinger (1985) estimated the temperature change from 1850 to 1980 induced by the increasing CO_2 concentration during this 130-year period. Figure 13, based on the study of Wigley and Schlesinger (1985) in which the 1850 CO_2 concentration was taken as 270 ppmv, shows the 1850-1980 surface temperature change versus the equilibrium surface temperature change for a doubled CO_2 concentration. Again let us assume that the latter is 4°C. If the climate system had no thermal inertia, the 1850-1980 surface temperature change would be in equilibrium with the instantaneous 1980 CO_2 concentration, and the warming would be given by an equation similar to Eq. (4). As shown in Fig. 13, this instantaneous equilibrium warming would be 1.3°C. However, when the heat capacity and vertical heat transport of the ocean are considered, as shown by the curves for the oceanic thermal diffusivities κ = 1 and κ = 3 $cm^2 s^{-1}$, the 1850-1980 warming is reduced to about 0.5 to 0.7°C, a range which does

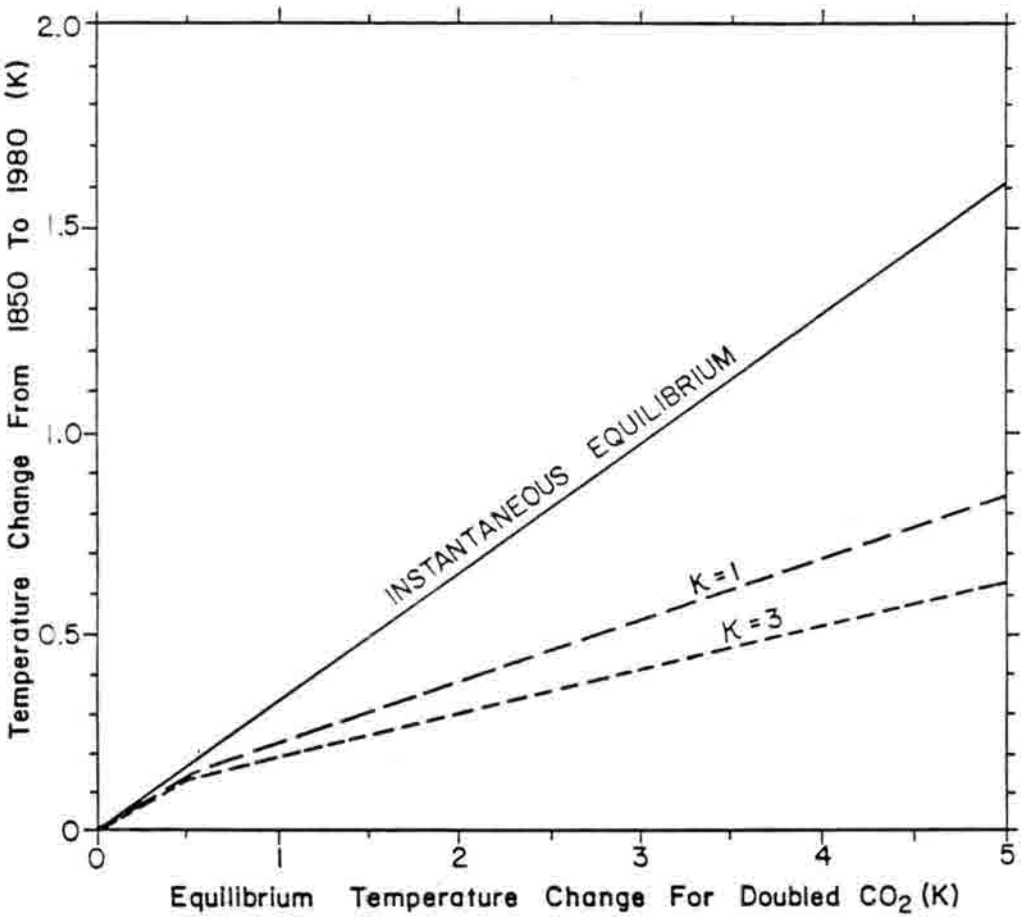

Fig. 13. The temperature change from 1850 to 1980 versus the equilibrium temperature change for doubled CO_2. The instantaneous equilibrium curve is given by Eq. (5). The curves $\kappa = 1$ an $\kappa = 3$ $cm^2 s^{-1}$ are from the results of Wigley and Schlesinger (1985).

not conflict with the observational record. Consequently, it appears that the climate system gain of about 1°C/(Wm^{-2}) obtained by the most recent GCM equilibrium simulations may be reasonably correct.

Figure 13 also shows that even if the CO_2 concentration were to increase no further in the future, the Earth's surface temperature would continue to increase by about 0.7°C in its approach to its new equilibrium value. This demonstrates the "Catch-22" nature of the CO_2-induced climatic-change issue: The present warming is "small" and perhaps within the natural variation of climate because the ocean sequesters heat within its interior, but, because of this, when the warming becomes demonstrably evident, continued future warming is inevitable, even if the CO_2 concentration were prevented from increasing further.

4. Summary

In this paper we have reviewed the simulations of CO_2-induced equilibrium and transient climatic change made by energy-balance, radiative-convective and general circulation models. The equilibrium climatic-change simulations have been characterized in terms of the direct radiative forcing of the increased CO_2, the response of the climate system in the absence of feedback processes, and the feedbacks of the climate system. The transient climatic-change simulations have been characterized in terms of the e-folding time of the response of the climate system.

For a doubling of the CO_2 concentration the direct radiative forcing is about 4 Wm^{-2} for the surface-troposphere system. In the absence of feedbacks the gain (output/input) of the climate system is about 0.3°C/(Wm^{-2}) and the change in the surface air temperature is therefore about 1.2°C. Surface energy-balance models (SEBMs) have given a warming induced by a CO_2 doubling of about 0.2 to 10°C. This wide range is the

result of the inherent difficulty in specifying the behavior of the atmosphere in SEBMs. Radiative-convective models (RCMs) have given a warming of about 0.5 to 4.2°C for a CO_2 doubling. This range is the result of water vapor feedback, lapse rate feedback, surface albedo feedback, cloud altitude feedback, cloud cover feedback and cloud optical depth feedback. General circulation models (GCMs) have given warming of about 1.3 to 5.2°C for a CO_2 doubling. This also is the result of the feedbacks listed above, except that due to cloud optical depth feedback which has not yet been included in the GCM simulations of CO_2-induced climatic change.

The most recent simulations of CO_2-induced climatic change by the GFDL, GISS, NCAR, OSU and UKMO atmospheric GCM/mixed-layer ocean models have been presented. The changes in the annual-mean, global-mean surface air temperature simulated by these models for a CO_2 doubling range from 2.8 to 5.2°C, and the corresponding changes in precipitation from 7.1 to 15% of their $1xCO_2$ values. The CO_2-induced zonal-mean surface air temperature changes exhibit a seasonal variation which increases from the tropics toward the poles. The geographical distributions of the CO_2-induced temperature change display a warming virtually everywhere in both winter and summer. The warming is a maximum in the winter polar region where the $1xCO_2$ sea ice retreats poleward in the $2xCO_2$ simulation, and is a minimum in the summer polar region and in the tropics during both seasons. Over the continents the CO_2-induced warming simulated by the models exhibits qualitative differences in seasonality and quantitative differences in magnitude. The geographical distributions of the CO_2-induced soil water change simulated by all the models reveal a moistening of the northern hemisphere continents in winter. A drying of much of the northern hemisphere continents in summer is simulated by the GFDL, OSU and UKMO models, but not by the GISS and NCAR models.

The simulations of CO_2-induced transient climatic change by simplified models have given an e-folding time τ_e of about 10-100 years for the response of the climate system to an abrupt increase in the CO_2 concentration. Simplified analytical and numerical analyses show that this wide range in the estimates of τ_e is the result of the dependence of τ_e on three parameters of the climate system, namely, its gain and the oceanic upwelling velocity and effective thermal diffusivity. A simulation with a global coupled atmosphere/ocean general circulation model indicates that τ_e is 50-100 years as a result of the transport of the CO_2-induced surface heating into the interior of the ocean. Theoretical studies for a time-dependent CO_2 increase between 1850 and 1980 demonstrate that this sequestering of heat into the ocean's interior is responsible for the concomitant warming being only about half that which would have occurred in the absence of the ocean. These studies also reveal that the climate system will continue to warm towards its as-yet unrealized equilibrium temperature change, even if there is no further increase in the CO_2 concentration.

5. Conclusion

The five most recent simulations of the equilibrium climatic changes induced by a doubling of the CO_2 concentration have been made with atmospheric general circulation models coupled to prescribed-depth mixed layer models of the ocean. These ocean models do not include in a physical way the horizontal transports of heat, momentum and salinity (see footnote 1) which are fundamental to the maintenance and change of the general circulation of the ocean. Such models cannot therefore correctly simulate the sea surface temperature (SST) distribution which is of paramount importance for the general circulation of the atmosphere. Therefore, such atmospheric GCM/mixed-layer ocean models cannot correctly simulate the

regional distribution of climate for either $1xCO_2$ or $2xCO_2$. Since only oceanic GCMs can simulate the horizontal and vertical transport upon which the SST and regional climates intimately depend, it is imperative that future simulations of CO_2-induced equilibrium climatic change be performed with coupled atmosphere/ocean GCMs.

A necessary condition for the acceptance of a coupled atmosphere/ocean model's simulation of a CO_2-induced equilibrium and/or transient climatic change is the validation of the model's simulation of the present ($1xCO_2$) climate by comparing it with the observed present climate. A rudimentary model validation has been performed by Schlesinger and Mitchell (1985) for the $1xCO_2$ simulations by the GFDL, GISS and NCAR models, and similar validations have been performed for the OSU and UKMO models by Schlesinger and Zhao (1988) and by Wilson and Mitchell (1987), respectively. These model validation studies show that, although the GCMs are the only type of model in the climate model hierarchy that can simulate the climate on the regional scale, they do so not without error, particularly for the components of the hydrological cycle such as precipitation. Therefore, further improvement in the simulation of CO_2-induced climate change requires the systematic analysis of the factors that contribute to the errors in the models' simulations of the present climate, and the subsequent correction of those errors. This will likely require the improvement of the methods used by the models for both the explicitly-resolved and parameterized physical processes, the former by a comparison of the solutions of the models' numerical methods with both exact solutions and the results of laboratory studies for simplified cases, and the latter by intercomparison studies among the models and observations following the approach of the Intercomparison of Radiation Codes in Climate Models (ICRCCM) program (Luther and Fouquart, 1984).

The successful validation of a model's simulation of the present climate, while a necessary condition for the acceptance of its simulated CO_2-induced climatic change, is not a sufficient condition for this purpose. While in all likelihood such a sufficient condition does not exist, there is a second necessary condition, namely, that the model correctly simulate a climate different from that of the present. Thus, to increase confidence that the CO_2-induced climatic changes simulated by the models are correct at the regional scale, the model validation methodology described above for the present climate must also be applied to at least one other climate such that of the Wisconsin Ice Age 18,000 years before the present.

Acknowledgements. I would like to thank Syukuro Manabe and Richard Wetherald of the Geophysical Fluid Dynamics Laboratory; James Hansen, Gary Russell, Andrew Lacis and David Rind of the Goddard Institute for Space Studies; Warren Washington and Gerald Meehl of the National Center for Atmospheric Research; and John Mitchell of the United Kingdom Meteorological Office for making their results available to me. I express my gratitude to Dean Vickers for performing some of the calculations herein, and to John Stark, Larry Holcomb and Linda Haygarth for drafting. This study was supported by the National Science Foundation and the U.S. Department of Energy under grant ATM 87-12033.

REFERENCES

Augustsson, T., and V. Ramanathan, 1977: A radiative-convective model study of the CO_2 climate problem. J. Atmos. Sci., **34**, 448-451.

Broecker, W. S., T.-H. Peng and R. Engh, 1980: Modeling the carbon system. Radiocarbon, **22**, 565-598.

Bryan, K., F. G. Komro, S. Manabe and M. J. Spelman, 1982: Transient climate response to increasing atmospheric carbon dioxide. Science, **215**, 56-58.

Bryan, K., F. G. Komro and C. Rooth, 1984: The ocean's transient response to global surface temperature anomalies. In Climate Processes and Climate Sensitivity, Maurice Ewing Series, 5, J. E. Hansen and T. Takahashi, Eds., American Geophysical Union, Washington, D.C., 29-38.

Budyko, M. I., 1969: The effect of solar radiation variations on the climate of the earth. Tellus, **21**, 611-619.

Cess, R. D., and G. L. Potter, 1988: A methodology for understanding and intercomparing atmospheric climate feedback processes within general circulation models. J. Geophys. Res. (in press).

Gates, W. L., 1976a: Modeling the ice-age climate. Science, **191**, 1138-1144.

Gates, W. L., 1976b: The numerical simulation of ice-age climate with a global general circulation model. J. Atmos. Sci., **33**, 1844-1873.

Ghan, S. J., J. W. Lingaas, M. E. Schlesinger, R. L. Mobley and W. L. Gates, 1982: A documentation of the OSU two-level atmospheric general circulation model. Report No. 35, Climatic Research Institute, Oregon State University, Corvallis, OR, 395 pp.

Han, Y.-J., 1984a: A numerical world ocean general circulation model, Part I. Basic design and barotropic experiment. Dyn. Atmos. Oceans, **8**, 107-140.

Han, Y.-J., 1984b: A numerical world ocean general circulation model, Part II. A baroclinic experiment. Dyn. Atmos. Oceans, **8**, 141-172.

Hansen, J., A. Lacis, D. Rind, G. Russell, P. Stone, I. Fung, R. Ruedy and J. Lerner, 1984: Climate sensitivity: Analysis of feedback mechanisms. In Climate Processes and Climate Sensitivity, Maurice Ewing Series, 5, J. E. Hansen and T. Takahashi, Eds., American Geophysical Union, Washington, D.C., 130-163.

Hoffert, M. I., A. J. Callegari and C.-T. Hsieh, 1980: The role of deep sea heat storage in the secular response to climate forcing. J. Geophys. Res., **85**, 6667-6679.

Imbrie, J., and K. P. Imbrie, 1979: Ice Ages, Solving the Mystery. Enslow Publishers, Short Hills, NJ, 224 pp.

Jenne, R., 1975: Data sets for meteorological research. NCAR Tech. Note TN/1A-III, National Center for Atmospheric Research, Boulder, CO, 194 pp.

Jones, P. D., T. M. L. Wigley and P. B. Wright, 1986: Global temperature-variations between 1861 and 1984. Nature, **322**, 430-434.

Keeling, C. D., and T. A. Boden, 1986: Atmospheric CO_2 Concentrations - Mauna Loa Observatory, Hawaii 1958-1986. Carbon Dioxide Information Center (CDIC) Numeric Data Collection, NDP-001/R1, Oak Ridge National Laboratory, 17 pp. with addenda.

Lal, M., and V. Ramanathan, 1984: The effects of moist convection and water vapor radiative processes on climate sensitivity. J. Atmos. Sci., **41**, 2238-2249.

Luther, F. M., and Y. Fouquart, 1984: The Intercomparison of Radiation Codes in Climate Models (ICRCCM): Longwave Clear-Sky Calculations. World Meteorological Organization Report WCP-93, Geneva, Switzerland, 37 pp.

Nature, 1987: Summary of letter to Nature by Roeckner et al., v.

Nordhaus, W. D., and G. W. Yohe, 1983: Future paths of energy and carbon dioxide emissions. In Changing Climate, National Academy of Sciences, Washington, D.C., 87-153.

Ramanathan, V., M. S. Lian and R. D. Cess, 1979: Increased atmospheric CO_2: Zonal and seasonal estimates of the effects on the radiation energy balance and surface temperature. J. Geophys. Res., **84**, 4949-4958.

Rasool, S. I., and S. H. Schneider, 1971: Atmospheric carbon dioxide and aerosols: Effects of large increases on global climate. Science, **173**, 138-141.

Rotty, R. M., and C. D. Masters, 1985: Carbon dioxide from fossil fuel combustion: trends, resources, and technological implications. In Atmospheric Carbon Dioxide and the Global Carbon Cycle, J. R. Trabalka, Ed., U.S. Department of Energy, DOE/ER-0239, 63-80.

Schlesinger, M. E., 1984: Climate model simulations of CO_2-induced climate change. In Advances in Geophysics, **26**, B. Saltzman, Ed., Academic Press, New York, 141-235.

Schlesinger, M. E., 1985: Feedback analysis of results from energy balance and radiative-convective models. In The Potential Climate Effects of Increasing Carbon Dioxide, M. C. MacCracken and F. M. Luther, Eds., U.S. Department of Energy, DOE/ER-0237, 280-319. (Available from NTIS, Springfield, Virginia.)

Schlesinger, M. E., 1988a: Quantitative analysis of feedbacks in climate model simulations of CO_2-induced warming. In Physically-Based Modelling and Simulation of Climate and Climate Change, Vol. II, M. E. Schlesinger, Ed., NATO Advanced Study Institute Series, Reidel, Dordrecht 653-736, (in press).

Schlesinger, M. E., 1988b: Physically-Based Modelling and Simulation of Climate and Climatic Change, Vol. I & II, M. E. Schlesinger, Ed., NATO Advanced Study Institute Series, Reidel, Dordrecht (in press).

Schlesinger, M. E., and W. L. Gates, 1980: The January and July performance of the OSU two-level atmospheric general circulation model. J. Atmos. Sci., **37**, 1914-1943.

Schlesinger, M. E., and J. F. B. Mitchell, 1985: Model projections of the equilibrium climatic response to increased CO_2. In The Potential Climatic Effects of Increasing Carbon Dioxide, M. C. MacCracken and F. M. Luther, Eds., DOE/ER-0237, U.S. Department of Energy, Washington, D.C., 81-147. (Available from NTIS, Springfield, Virginia.)

Schlesinger, M. E., and J. F. B. Mitchell, 1987: Climate model simulations of the equilibrium climatic response of increased carbon dioxide. Rev. of Geophys., **25**, 760-798.

Schlesinger, M. E., and X. Jiang, 1987: The transport of CO_2-induced warming into the ocean: An analysis of simulations by the OSU coupled atmosphere-ocean general circulation model. Climate Dynamics (in press).

Schlesinger, M. E., and Z.-C. Zhao, 1988: Seasonal climatic changes induced by doubled CO_2 as simulated by the OSU atmospheric GCM/mixed-layer ocean model. J. Climate (submitted).

Schlesinger, M. E., W. L. Gates and Y.-J. Han, 1985: The role of the ocean in CO_2-induced climate warming: Preliminary results from the OSU coupled atmosphere-ocean GCM. In Coupled Ocean-Atmosphere Models, J. C. J. Nihoul, Ed., Elsevier, Amsterdam, 447-478.

Schneider, S. H., and S. L. Thompson, 1981: Atmospheric CO_2 and climate: Importance of the transient response. J. Geophys. Res., **86**, 3135-3147.

Sellers, W. D., 1969: A global climate model based on the energy balance of the earth-atmosphere system. J. Appl. Meteor., **8**, 392-400.

Siegenthaler, U., 1983: Uptake of excess CO_2 by an outcrop-diffusion model of the ocean. J. Geophys. Res., **88**, 3599-3608.

Siegenthaler, U., and H. Oeschger, 1984: Transient temperature changes due to increasing CO_2 using simple models. Ann. of Glaciology, **5**, 153-159.

Siegenthaler U., and H. Oeschger, 1987: Biosphere CO_2 emissions during the past 200 years reconstructed by deconvolution of ice core data. Tellus, **39B**, 140-154.

Spelman, M. J., and S. Manabe, 1984: Influence of oceanic heat transport upon the sensitivity of a model climate. J. Geophys. Res., **89**, 571-586.

Washington, W. M., and G. A. Meehl, 1984: Seasonal cycle experiment on the climate sensitivity due to a doubling of CO_2 with an atmospheric general circulation model coupled to a simple mixed-layer ocean model. J. Geophys. Res., **89**, 9475-9503.

Wetherald, R. T., and S. Manabe, 1986: An investigation of cloud cover change in response to thermal forcing. Climate Change, **8**, 5-23.

Wetherald, R. T., and S. Manabe, 1988: Cloud feedback processes in a general circulation model. J. Atmos. Sci., **45** (in press).

Wigley, T. M. L., and M. E. Schlesinger, 1985: Analytical solution for the effect of increasing CO_2 on global-mean temperature. Nature, **315**, 649-652.

Wilson, C. A. and J. F. B. Mitchell, 1987: A doubled CO_2 climate sensitivity experiment with a global climate model including a simple ocean. J. Geophys. Res., **92**, 13,315-13,343.

II. The Climate Record

H. Ellsaesser

H. Dias and T. Karl

T. Karl

P. Michaels et al.

N. Doesken and J. Kleist

R. Jarrett

Interpretation of our Present Terrestrial Climatic Record

Hugh W. Ellsaesser
Participating Guest Scientist
Atmospheric and Geophysical Sciences Division
Lawrence Livermore National Laboratory
P.O. Box 808
Livermore, California 94550

Abstract

Detailed studies of profiles of $\delta^{18}O$ in oceanic and glacial cores and of pollen deposits in bogs indicate that the terrestrial climatic system, consisting of the atmosphere, hydrosphere, lithosphere and biosphere, is capable of oscillations with amplitudes, such as that of the Melisey II stadial of northern France, approaching or equaling that of the glacial-interglacial cycle but on time scales too short for the usually envisioned transfer of mass between the oceans and continental glaciers. Abrupt oscillations or shifts to new equilibrium are well documented in the Bolling-Allerod warming and Younger Dryas readvance, the 0.4°C rise in NH continental air temperature circa 1920 and the year-to-year oscillations in NH continental air temperatures from 1976 to 1984.

Such abrupt oscillations defy explanation in terms of external forcing functions and suggest rather internal rearrangements within the climate system as the driving mechanism. Suggestions are made as to mechanisms for possible internal rearrangements which might lead to different hemispheric or global mean surface temperatures.

INTRODUCTION

The oxygen isotope ^{18}O in the form $H_2^{18}O$ has become the principal tracer in the reconstruction of past climates. This is due basically to the lower

vapor pressure and molecular diffusivity of the $H_2^{18}O$ molecule compared to the more abundant $H_2^{16}O$. These lead to a successively progressive depletion of the heavier molecule in a water vapor sample, evaporated from the ocean and progressively condensed and precipitated as it moves to higher latitudes and altitudes at a rate between 0.6 and 1.3°/$_{oo}$ $\delta^{18}O$ for each degree of cooling of the condensation temperature. Accordingly, snow accumulating on the Greenland ice cap has a $\delta^{18}O$ isotopic ratio of roughly -30 to -40°/$_{oo}$ and that accumulating in central Antarctica up to -60°/$_{oo}$. With a build-up of ice depleted in ^{18}O, the mean oceanic waters become heavier at a rate of about 1°/$_{oo}$ per 100 m drop in sea level. At the Pleistocene glacial maximum the oceans were about 1.2°/$_{oo}$ heavier than now and for an ice free planet they would be about 0.9°/$_{oo}$ lighter than now (Shackleton, 1982). In addition to this effect, there is a small oxygen isotopic fractionation between water and calcite which at equilibrium depends only on temperature, amounting to about 0.25°/$_{oo}$ enrichment in ^{18}O for each 1°C decrease in the temperature at which the calcite is biologically precipitated (Shackleton, 1982). Thus, for an average 2.3°C warming of the ocean surface since the last glacial maximum, the major portion of the variations in $\delta^{18}O$ in oceanic cores, even for planktonic or surface dwelling nanofossils, is due to the fluctuations in ice volume rather than to changes in temperature. However, for ice cores from Greenland or Antarctica, the 5- to 10-fold larger variations in $\delta^{18}O$ are believed to be almost entirely due to changes in the temperature at which the water vapor was condensed from the atmosphere.

From the roughly 1.6°/$_{oo}$ oscillation of $\delta^{18}O$ in oceanic cores and the 5 to 11°/$_{oo}$ oscillations in polar ice cores, we have come to think of the Pleistocene climate as flipping between two equilibrium states, a glacial and an interglacial. However, as these cores have been sampled in greater detail, they seem to reveal two somewhat contradictory qualities; abrupt

short period fluctuations but great stability in the sense of returning to and oscillating about the preexisting mean state. These two properties appear typical of the terrestrial climate on all time scales. That is, despite the amplitude, abruptness or time scale of climatic perturbations, the system appears to have a built-in memory which allows it, most of the time, to return to the original mean state, although occasionally, it shifts to a new equilibrium. In the extremes of the glacial-interglacial cycle, we even see evidence of a long-term memory of a prior equilibrium not experienced for up to nearly 10^5 years.

Dansgaard et al. (1972, 1982) have described a $\delta^{18}O$ spike in the Camp Century ice core comparable to those of the glacial-interglacial transition (~10°/$_{oo}$, see Figure 1) occurring almost instantaneously (within 100 years) and recovering to the preexisting mean level within 1000 years. Moreover, the implied sudden cooling was confirmed by the Melisey II Glacial between the St. Germain I and II Interglacials in the Grande Pile pollen record of northeastern France (see Figure 2). The Melisey II was so cold that the local forests completely died out and were replaced by a very open landscape with new plant species adapted to a dry, cold climate (Woillard, 1978).

Dansgaard et al. (1982) also noted $\delta^{18}O$ fluctuations with double amplitudes of 4-5°/$_{oo}$ present throughout the Wisconsin Glacial portions of both the Dye 3 and Camp Century ice cores (see Figure 3). Besides their congruence in cores taken 1400 km apart, at least some of these spikes correspond with previously identified climatic events such as the Bolling-Allerod warm period and the Younger Dryas readvance recorded over wide geographical areas.

Ruddiman and McIntyre (1981) conducted a detailed study of North Atlantic cores during the last deglaciation. They related the Bolling-Allerod (13000-11000 BP) warming and the Younger Dryas (11000-10000 BP)

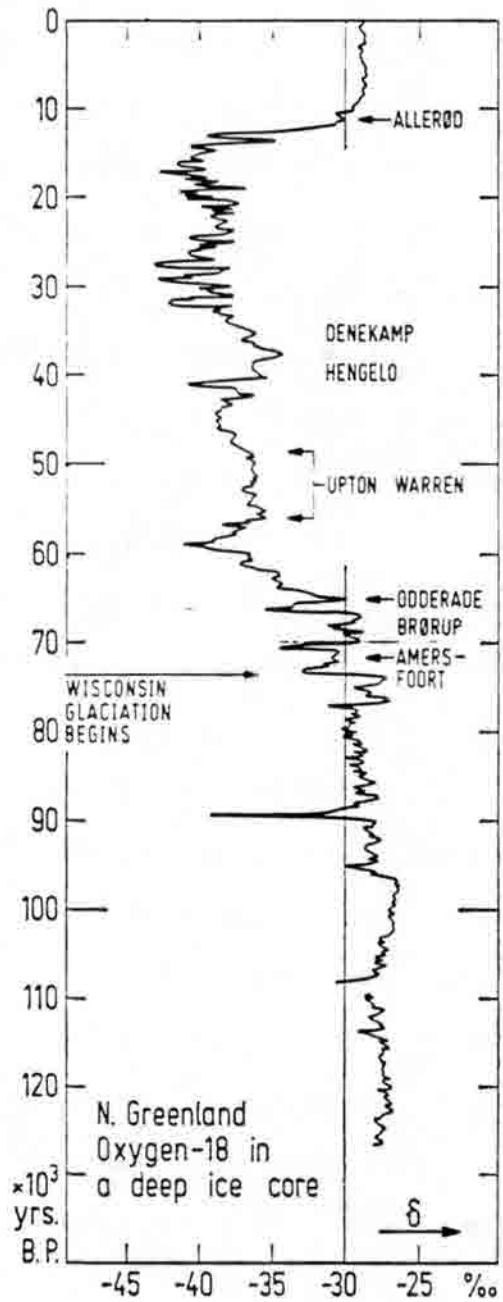

Figure 1. Camp Century Greenland ice core $\delta^{18}O$ profile, showing a deep drop just before 90,000 BP which appears instantaneous (~100 years) within the resolution of the data (adapted from Dansgaard et al, 1972).

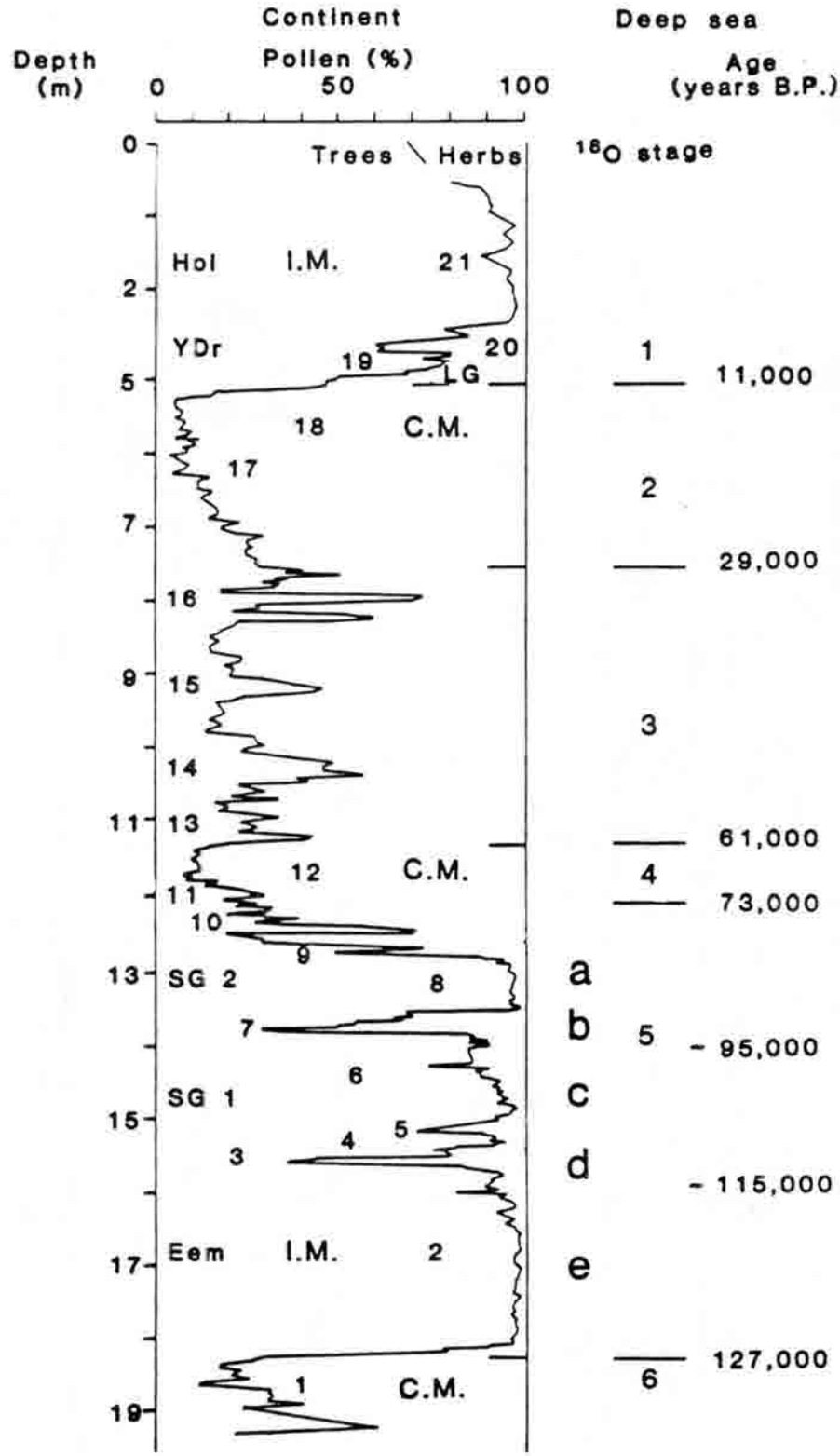

Figure 2. Continental time series of total tree and shrub pollen versus herb pollen from Grande Pile Peat Bog in northeastern France. SG 1 and 2 identify St. Germain I and II Interglacials, labeled as stages 6 and 8 with stage 7, the Melisey II glacial, between them (adapted from Woillard and Mook, 1982).

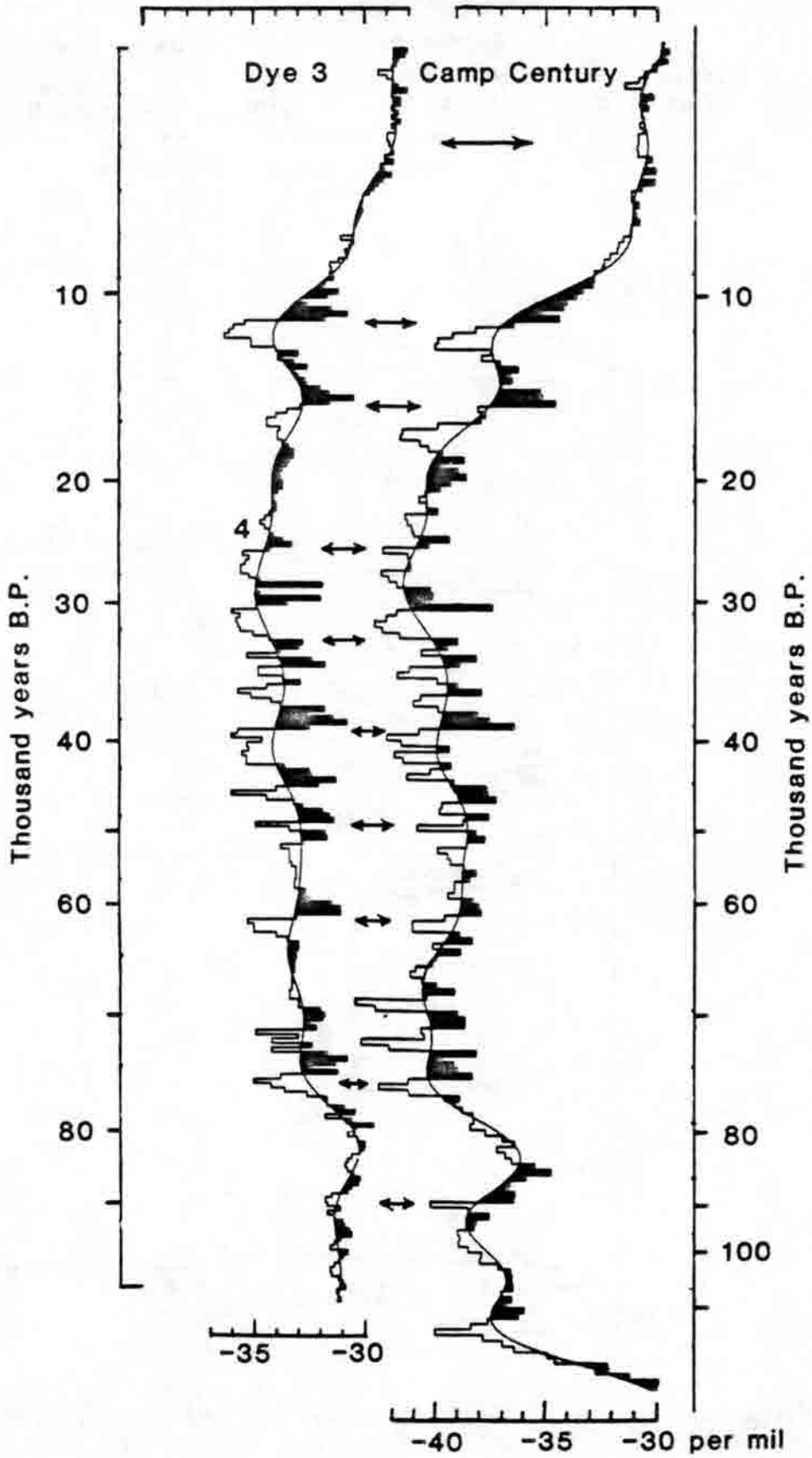

Figure 3. The deepest 300 m of the Dye 3 and Camp Century Greenland ice core $\delta^{18}O$ profiles with arrows indicating similar details.

cooling to large migrations in the North Atlantic polar front and corresponding large changes in the area of near freezing surface water north of the front. From the continental evidence they demonstrated that this temperature cycle was centered on the North Atlantic and adjacent areas of Europe and was not convincingly revealed in North American pollen records west of the Canadian maritimes.

The point of this review is to bring out the strong indications that the terrestrial climatic system is capable of abrupt transitions between the glacial and interglacial temperature climates without the large shifts in continental glaciation and sea level we normally associate with this transition. In the case of the Bolling-Allerod to Younger Dryas cycle, the temperature changes appear to have been controlled by wide swings in the position of the North Atlantic polar front although the reasons for these swings remain unknown. Equally unknown is whether the position of the oceanic polar front responded to the changes in the mean hemispheric temperature or whether it was responsible for the changes in temperature. First we must learn what determines the positions of these lines of convergence in the oceans.

Kelly et al. (1985) and Ellsaesser et al. (1986), among others, have pointed out that the major part of the NH warming of the past century occurred in a 2-year period centered about 1920 and that since that time the temperature has oscillated about a mean ~0.4°C warmer than during the preceding 40 years (see Figure 4). Ellsaesser et al (1986) pointed out that this warming also was centered on the North Atlantic and suggested that it might have been due to a small shift in the position of the North Atlantic polar front similar to that described by Ruddiman and McIntyre (1981).

These observations suggest that the concept of the terrestrial climate system as a passive thermal reservoir of prescribed heat capacity and

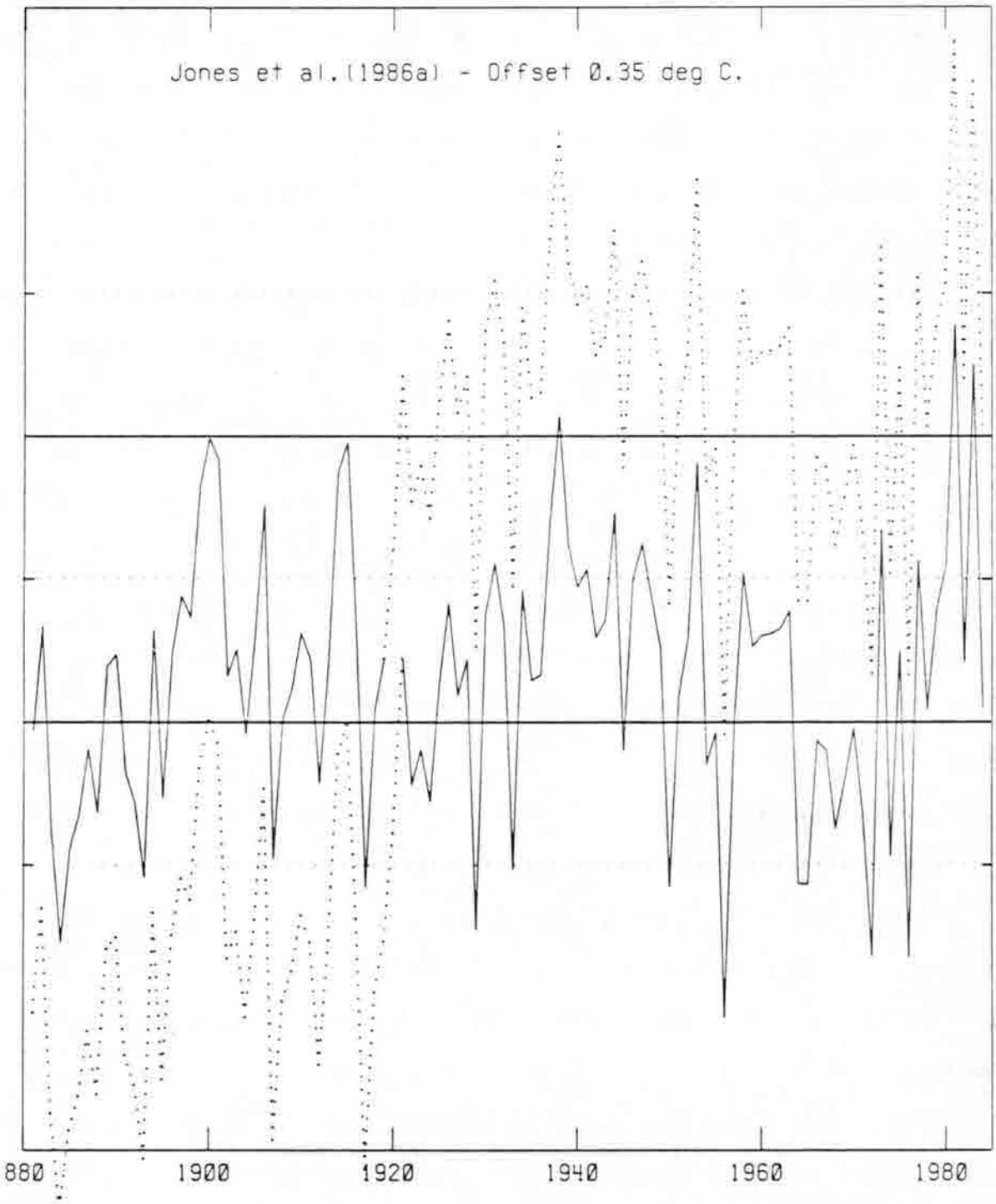

Figure 4. The NH mean temperature departures from the 1951-1970 normal of Jones et al. (1986a) plotted twice with an offset of 0.35°C. The post-1919 portion of the upper curve and pre-1921 portion of the lower curve are dotted to illustrate the degree to which the remaining solid curves reflect a normal trendless curve and thus the abruptness of the transition of the NH temperature from one mean to another 0.35°C warmer (from Ellsaesser et al., 1986).

thermal conductivity or relaxation time is unlikely to be very useful. This was also the conclusion of Oliver (1976) when he attempted empirically to model the response to volcanic clouds by this approach. Also, as Oliver (1976) pointed out, there are as many spikes in the mean annual temperature record as there are dips; while volcanoes might cause the dips, what is the cause of the spikes? In fact, aside from 1979-80, there was from 1972 through 1984 a see-saw in the NH land temperature record to such an extent that the sign of the trend reversed each year. I cannot conceive of any scenario of driving mechanisms capable of explaining this or the equally random but much more extreme and longer period fluctuations suggested by the $\delta^{18}O$ records of the Greenland ice cores throughout the Wisconsin glaciation shown in Figure 3. Accordingly, I believe we have to conclude that the terrestrial climate system is a dynamic entity capable of internal rearrangements leading to changes in mean surface temperature of the amplitudes and on the time scales suggested by the data I have reviewed. Since this report was first written, Broecker (1987) has provided strong support for their point of view.

THE TERRESTRIAL CLIMATE SYSTEM

The atmosphere, hydrosphere and biosphere essentially represent a planetary surface temperature control system in which radiative transport is the primary mechanism for transporting energy only above the moist layer. Within the moist layer, energy redistribution is accomplished primarily by the far more efficient means of advection and convection in both the atmosphere and hydrosphere with judicious use of latent energy for cooling hot spots, warming cold spots and transporting of energy from the planetary surface to the top of the moist layer.

Viewed in planetary steady state perspective, the colder the polar regions of the planet, the smaller the energy loss to space and the smaller the energy transport from lower latitudes required to maintain the existing temperature. Thus, the polar regions appear to be part of a negative feedback regulatory system for the surface temperature of the planet. If the planet becomes too cold, the poles cool, reducing the ejection of energy to space and allowing the planet to warm. If the planet becomes too warm, the poles warm up, increasing the rate of ejection of energy to space. The addition of sea ice greatly increases the amount of negative feedback. The ice cover drastically reduces the loss of latent and sensible heat from the ocean to the atmosphere and also allows the interface with the atmosphere to cool substantially below the freezing point of sea water, thus also reducing the radiative loss of IR to both the atmosphere and to space. Accompanying this negative feedback on the planetary mean surface temperature there is a simultaneous thermostatic control applied to extremes of surface temperature in both high and low latitudes. This occurs in the form of local release of latent heat as sea ice freezes and in the formation of dense brine which sinks to form bottom water and provides part of the driving mechanism for the thermohaline circulation of the oceans. This does not merely slow winter cooling of the oceanic surface in high altitudes, but in combination with the trade wind driven divergence provides surface cold water at low latitudes for storage of solar energy rather than its immediate local release to the atmosphere by evaporation of sea water (Csanady, 1984). The eventual effect of an acceleration or increase in the volume of the thermohaline circulation would appear to be a slight cooling and slowing of the hydrological cycle in low latitudes followed by a longer term increase in the flux of heat by the oceans from low to high latitudes, that is, a shift in the partitioning of solar energy absorbed by the oceans in low

latitudes from immediate evaporation to storage in the photic layer of the oceans as well as an increase in the rate of transport of the surface layer and its contained heat toward the poles.

Over land we find similar, if weaker, limiting processes brought into play by extremes of surface temperature in the form of surface inversions limiting the loss of radiation to space and large-scale deserts in subtropical latitudes capable of radiating more energy to space than they receive from the Sun. Once these latter areas become established, a positive feedback field of subsidence is developed which permits them to become self-sustaining, if not self-expanding (Charney et al., 1975). Bryson (Bryson et al., 1964; Bryson and Baerreis, 1967) had earlier hypothesized that the dust from the desert floor increased the radiative divergence of the IR emission of the atmosphere, leading to subsidence which then maintained or amplified the desertification. I expanded the concept into an ice-age theory, in which the self-expanding subtropical deserts cool the planet enough to induce a glacial and the expanding ice caps eventually force the wave cyclone track of the westerlies sufficiently equatorward to quench the deserts. Their return to a positive radiation balance then heats the planet enough to melt the ice caps and start the cycle over again (Ellsaesser, 1975).

Within the free atmosphere we find another thermostatic mechanism brought into play in the form of the polar vortices of winter. To a considerable extent these insulate the energy losing winter polar caps from the rest of the atmosphere and allow them to cool to a much lower temperature, thus slowing the radiative loss of energy to space. The system is significantly more efficient in the Antarctic than in the Arctic, in that the winter cooling in the Antarctic is greater both at the surface and in

the stratosphere. Another thermostatic mechanism of tremendous thermo-capacity is the so-called outcrop regions of the polar oceans where the seasonal cycle of ocean surface temperature, in the SH at least, is comparable to that in the tropics, due to the convective overturning of water to great depths (van Loon, 1966). Here again, we find greater efficiency in the SH than in the NH in that a substantial area of the southern oceans between 45°S and 55°S has an annual temperature range of less than 3°C (Taljaard and van Loon, 1984, p. 517) while we find only a small area in the North Atlantic, between Iceland and Spitzbergen, with a range this low. So far as I am aware, essentially no attention has been directed to where and how the oceans replace the huge winter losses from these thermal reservoirs. Considering the normal negative net radiative balance of higher latitudes, in situ absorption of solar radiation alone does not appear sufficient.

With so many circulation dependent negative feedbacks and thermostatic mechanisms controlled by local and regional conditions, it is not surprising that the mean hemispheric and global average temperatures jump around quite erratically from year to year. Other than the positive feedback of desertification, however, none of these mechanisms appear to offer an explanation for relatively consistent trends in one particular direction or for abrupt jumps to new equilibrium states.

CLIMATIC EFFECTS OF VOLCANOES

I have spent considerable time reviewing the studies of the climatic effects of volcanoes (Ellsaesser, 1977, 1983, 1986). In this subject, as in others, I was again amazed at the domination of the current paradigm (Sagan, 1987) over logical analysis. Most research studies seem to consist of a summarization of the data which appear to support the prevailing paradigm

and a disregard of those data which contradict or fail to support it, completely overlooking the fact that it is such nonconformities which most frequently lead to new knowledge. The inconsistent or nonsupportive data are quite evident in the case of the climatic effects of volcanoes. As Rampino et al. (1979) have clearly shown, the available data are more consistent with the proposition that abrupt cooling is followed by volcanic eruptions than with the converse, that volcanic eruptions are followed by cooling. Yet the paradigm that volcanic aerosol layers increase the planetary albedo and thus lead to surface cooling remains firmly fixed in the minds of most meteorologists and particularly in the minds of those engaged in climate modeling.

Stan Grotch of our Laboratory has computer analyzed the NH data set of Jones et al. (1986a) for volcanic effects. For a small subset of what are believed to be the major eruptions, he finds support for the finding of Kelly and Sear (1984) that maximum cooling sets in within about 2 months and becomes essentially undetectable within 6 to 12 months after the eruption. However, the exceptions to this for some of the presumed largest eruptions are such as to still leave doubt that volcanoes produce any detectable systematic effect in hemispheric mean surface temperature. And of course, if Kelly and Sear (1984) are correct that the maximum effect in the hemisphere of the eruption appears within 2 months of the eruption, then many other studies are in error. (It should be noted that even in their selection of NH eruptions for superposed epoch analysis, the cooling begins before the eruptions.)

CLIMATIC EFFECT OF CARBON DIOXIDE

Looking at the compilation of global surface temperature data in Figure 5, it is very difficult to claim that increasing CO_2 has had any effect on temperature since 1938. The warming since 1976 has been too rapid, and some explanation is required as to what was happening between 1938 and 1976. Similarly, it is difficult to attribute the warming up to 1938 to the approximately 5 ppm increase in atmospheric CO_2 (Esser, 1987) which could have been due to the burning of fossil fuels by that date, particularly since the approximately 40 ppm added since that date (Esser, 1987) hasn't done much. Thus, if any of the warming of the past century is to be attributed to anthropogenic CO_2 it has to be the roughly 100 to 200 GtonC [gigatons carbon] earlier released from the biosphere due to the forest removal and the spread of agriculture.

A possible, and even tempting, interpretation of the available data, is that in the Holocene, the mean NH temperature reached its peak in the Climatic Optimum 4500-8000 BP and has since been drifting toward the next glacial. The reason for the termination of the Little Ice Age (1430-1850 AD) and its recognition as a cold period is the additional greenhouse effect that was provided by the anthropogenically released biospheric CO_2 variously estimated to range from 62 to 260 GtonC and believed to be most probably in the range 90-180 GtonC (Houghton et al., 1985). Using the atmospheric fraction of 58%, determined from the fossil fuel consumed during the period of the Mauna Loa record, this could have increased the atmospheric CO_2 content by about 25-50 ppm. But from our best estimates of past atmospheric levels, it could have increased the atmospheric content by no more than from 240 to 280 ppm up to about 290 ppm, or 10-50 ppm. This

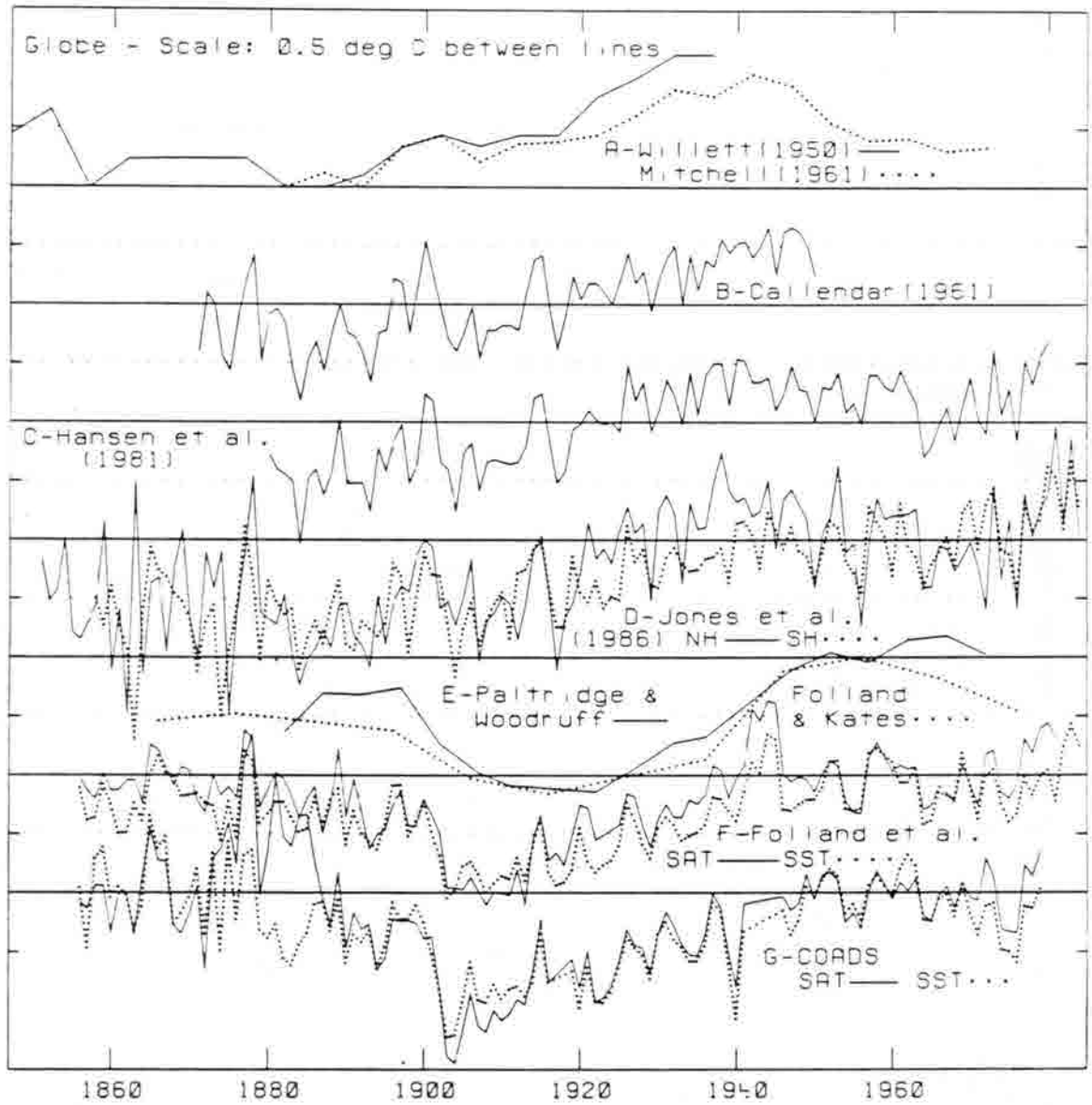

Figure 5. Estimates of observed changes in global mean temperature. Curve A: (solid curve) Willett (1950) as corrected by Mitchell (1961) and (dotted curve) Mitchell (1961) as updated by Lamb (1981) 5-year mean departures from 1880-1884 normal. Curve B: Callendar (1961) annual mean 60°S-60°N departures from 1901-1930 normal. Curve C: Hansen et al. (1981) annual mean departures from 1881-1980 normal. Curves D: Jones et al (1986a,b) annual mean departures from 1951-1970 normals (solid curve, NH; dotted curve, SH). Curves E: (solid curve) Paltridge and Woodruff (1981) 5-year mean SST and land surface air temperature departures using primarily ship data, renormalized to 1951-1960 and (dotted curve) Folland and Kates (1984) 5-year mean ship SST departures from 1951-1960 normal with linear in time correction for switch from bucket to injection water temperatures. Curves F: Folland et al. (1984) annual mean ship (solid curve) SST departures from 1951-1970 normals. NSATs corrected for ship size and SSTs for switch from bucket to intake water temperatures. Curves G: COADS annual mean ship (solid curve) SAT and (dotted curve) SST departures from 1951-1970 normals with corrections of Folland et al. (1984) and war years 1918-1919 and 1942-1945 omitted (adapted from Ellsaesser et al., 1986).

would also be consistent with a lower atmospheric fraction, as would be expected with a lower rate of release to the atmosphere. These latter changes represent fractional increases of 3.5 to 21%, and assuming a 3°C temperature increase for a CO_2 doubling, would give an equilibrium warming of 0.15 to 0.9°C.

The numbers would fit if the preindustrial level of CO_2 was 260 ppm or below, and if valid, indicate that we are already committed for at least as much additional warming as has occurred since the Little Ice Age because of the fossil fuel CO_2 already in the atmosphere. However, before we begin to evacuate low-lying coastal cities, it behooves us to remember that between the Altithermal and the Little Ice Age, other warming and cooling periods have been identified, the causes for which remain unknown. And as long as the causes for such oscillations remain unknown, they cannot be ruled out as the cause of the termination of the Little Ice Age. Studies continue to appear (e.g., see Pachur and Kropelin, 1987) indicating substantially less aridity in the present subtropical desert areas during the Altithermal. The apparent coincidence in time of cooling following the Altithermal and expansion and intensification of the subtropical deserts suggests a cause and effect relationship which may indeed play a role in the initiation of the next glacial. The ability of the glacial cap to expand sufficiently to force mid-latitude precipitation systems to quench the subtropical deserts is less well documented.

If the warming of the past 100-200 years is not due to the biospheric pulse to atmospheric CO_2, then there is very little reason for believing what our climate models are now saying about the effect of the fossil fuel pulse to atmospheric CO_2. Moreover, if we cannot look forward to a CO_2-induced warming, we might wish to give some thought to reversing the process of desertification before the ice caps start growing again.

ACKNOWLEDGEMENT

This work was performed under the auspices of the Carbon Dioxide Research Division of the Office of Energy Research, U.S. Department of Energy by the Lawrence Livermore National Laboratory, Livermore, California under contract W-7405-Eng-48.

REFERENCES

Broecker, W. S., Unpleasant surprises in the greenhouse? Nature, 328, 123-126, 1987.

Bryson, R. A. and D. A. Baerreis, Possibilities of major climatic modification and their implications: Northwest India, a case for study, Bull. Amer. Meteor. Soc., 48, 136-142, 1976.

Bryson, R. A., C. W. Wilson and P. M. Kuhn, Some preliminary results from radiation sonde ascents over India, in Symposium on Tropical Meteorology, Rotorua, New Zealand, November 1963, pp. 501-516, New Zealand Meteorological Service, Wellington, 1964.

Callendar, G. S., Temperature fluctuations and trends over the Earth, Quart. J. Roy. Met. Soc., 87, 1-12, 1961.

Csanady, G. T., Warm water mass formation, J. Phys. Oceano., 14, 264-275, 1984.

Dansgaard, W., A. J. Johnson, H. B. Clausen and C. C. Langway, Speculations about the next glaciation, Quat. Res., 2, 396-398, 1972.

Dansgaard, W., H. B. Clausen, N. Gundestrup, C. U. Hammer, S. F. Johnsen, P. M. Kristinsdottir and N. Reeh, A new Greenland deep ice core, Science, 218, 1273-1277, 1982.

Ellsaesser, Hugh W., The role of deserts on global climate, EOS, 56(12), 998, 1975.

Ellsaesser, Hugh W., Comments on 'Estimate of the global change in temperature, surface to 100 mb, between 1958 and 1975,' Mon. Wea. Rev., 105, 1201-1202, 1977.

Ellsaesser, Hugh W., Isolating the climatogenic effects of volcanoes, Rpt. UCRL-89161, Lawrence Livermore National Laboratory, Livermore, CA 94550, 1983 (presented at Meeting of Experts on Anthropogenic Climatic Change, 4-10 July 1983, Leningrad, USSR).

Ellsaesser, Hugh W., Comments on 'Surface temperature changes following the six major volcanic episodes between 1780 and 1980,' J. Clim. Appl. Meteorol., 25(8), 1184-1185, 1986.

Ellsaesser, H. W., M. C. MacCracken, J. J. Walton and S. L. Grotch, Global climatic trends as revealed by the recorded data, Rev. Geophys., 24(4), 745-792, 1986.

Esser, Gerd, Sensitivity of global carbon pools and fluxes to human and potential climatic impacts, Tellus, 398, 245-260, 1987.

Folland, C. K. and F. Kates, Changes in decadally averaged sea surface temperature over the world, 1861-1980. In Milankovitch And Climate, A. Berger, J. Imbrie, J. Hays, G. Kukla and B. Saltzman (eds.), Part II, pp. 721-727, D. Reidel, Hingham, MA, 1984.

Folland, C. K., D. E. Parker and F. E. Kates, Worldwide marine temperature fluctuations 1856-1981, Nature, 310, 670-673, 1984.

Hansen, J., D. Johnson, A. Lacis, S. Lebedeff, P. Lee, D. Rind and G. Russell, Climate impact of increasing atmospheric carbon dioxide, Science, 213, 957-966, 1981.

Houghton, R. A., W. H.Schlesinger, S. Brown and J. F. Richards, Carbon dioxide exchange between the atmosphere and terrestrial ecosystems, in Atmospheric Carbon Dioxide and the Global Carbon Cycle, Rep. DOE/ER-0239, pp. 113-140, U.S. Dept. of Energy, Carbon Dioxide Res. Div., Natl. Tech. Inf. Serv., Springfield, VA, 1985.

Jones, P. D., S. C. B. Raper, R. S. Bradley, H. F. Diaz, P. M. Kelly and T. M. L. Wigley, Northern hemisphere surface air temperature variations 1851-1984, J. Clim. Appl. Meteorol., 25, 161-179, 1986a.

Jones, P. D., S. C. B. Raper and T. M. L. Wigley, Southern hemisphere air temperature variations, 1851-1984, J. Clim. Appl. Meteorol., 25, 1213-1230, 1986b.

Kelly, P. M. and C. B. Sear, Climatic impact of explosive volcanic eruptions, Nature, 311, 740-743, 1984.

Kelly, P. M., P. D. Jones, T. M. L. Wigley, R. S. Bradley, H. F. Diaz and C. M. Goodess, The extended northern hemisphere surface air temperature record: 1851-1984, in 3rd Conference On Climatic Variations And Symposium On Contemporary Climate: 1850-2100, pp. 35-36, American Meteorological Society, Boston, MA, 1985.

Mitchell, J. M., Jr., Recend secular changes of global temperature, Ann. N. Y. Acad. Sci., 95, 235-250, 1961.

Oliver, R. C., On the response of hemispheric mean temperature to stratospheric dust: An empirical approach, J. Appl. Meteorol., 15, 933-950, 1976.

Paltridge, G. and S. Woodruff, Changes in global surface temperature from 1880 to 1977 derived from historical records of sea surface temperature, Mon. Wea. Rev., 109, 2427-2434, 1981.

Pachur, H.-J., S. Kropelin and Wadi Howar: Paleoclimatic evidence from an extinct river system in the Southeastern Sahara, Science, 237, 298-300, 1987.

Rampino, M. R., S. Self and R. W. Fairbridge, Can rapid climate change cause volcanic eruptions?, Science, 206, 826-829, 1979.

Ruddiman, W. F. and A. McIntyre, The North Atlantic Ocean during the last deglaciation, Palaeogeogr. Palaeocli. Palaeoecol., 35, 145-214, 1981.

Sagan, Leonard A., What is hormesis and why haven't we heard about it before?, Health Physics, 52(5), 521-523, 1987.

Shackleton, N. J., The deep-sea sediment record of climate variability, Prog. in Oceano., 11, 199-218, 1982.

Taljaard, J. J. and H. van Loon, Climate of the Indian Ocean South of 35 S, World Survey of Climatology, 15, 505-601, 1984.

van Loon, Harry, On the annual temperature range over the Southern Oceans, The Geographical Review, 56(4), 497-515, 1966.

Willett, H. C., Temperature trends of the past century, Centen. Proc. R. Meteorol. Soc., Spec. Vol., 195-206, 1950.

Woillard, Genevieve M., Grande Pile Peat Bog: A continuous pollen record for the last 140,000 years, Quat. Res., 9, 1-21, 1978.

Woillard, G. M. and W. G. Mook, Carbon-14 dates at Grande Pile: Correlation of land and sea chronologies, Science, 215, 159-161, 1982.

Temperature Trends and Urban Effects in the Contiguous United States

Henry F. Diaz
NOAA/ERL
325 Broadway
Boulder, Colorado 80303

Thomas R. Karl
National Climatic Data Center
National Oceanic and Atmospheric Administration
Federal Building
Asheville, North Carolina 28801

1. Introduction

Physical modelling of the global climate system suggests that increasing atmospheric concentrations of greenhouse gases should have had and will increasingly have a warming effect on surface temperature over the earth. The models are currently ambiguous as to the regional impact of these changes, but they generally agree that temperature increases will be greater toward higher latitudes of both hemispheres.

The computation of surface air temperature trends in North America as in other parts of the world is complicated by the urban warming bias, which to an unknown degree affects all available observation networks. Here, we examine mean temperature trends within the contiguous 48 states, and compare maximum and minimum temperature regionally as a function of station population.

2. Data

The data used comes from the Historical Climatology Network (HCN) developed by Karl and co-workers at the National Climatic Data Center in Asheville, NC. Adjustments have been applied to the data to correct such non-climatic biases as time of observation changes and minor station moves. No correction based on population differences has been applied to the data.

3. Analysis

The degree of influence of urbanization in modifying the mean daily temperature depends on a number of factors among which are the increase in thermal mass of the city, reduction of evaporation, waste heat, and geographical factors such as the immediate local terrain (i.e., whether it is located on a valley floor, a plateau, in the continental interior or on the coast). Furthermore, urban warming should affect the minimum and maximum temperature differently (Landsberg, 1981). Likewise, a true climate drift toward higher mean temperature may differentially change the maximum and minimum temperatures (Karl et al., 1984; Karl et al., 1986). It has also been shown that the intensity of the urban heat islands increases with growth in population (Mitchell, 1953; Landsberg, 1981; Ackerman, 1985; Oke, 1973; Oke, 1978).

Figure 1 gives the distribution of stations across the contiguous United States used in this study. State climatic division boundaries and state boundaries are also outlined. Using a combination of topographic relief and vegetation characteristics, a set of 23 subregions were identified which allowed for further climate differentiation. These 23 regions are homogeneous in terms of their annual cycle and interannual variance characteristics. The region boundaries are illustrated in Fig. 2. We note that the difference in temperature between the current network of principal observing stations in the U.S. (the so-called first and second order stations) and the remaining set of cooperative observing stations is large and has been rising steadily for several decades (Fig. 3).

The first analysis involved averaging the station annual mean temperatures by region according to their population. Four population categories were used: <2,000; 2,000-10,000; 10,000-100,000 and >100,000. Figures 4-5 give the difference in long-term mean temperature between the different population groups for the mean and the average minimum temperature. The graphs show the lowest, median and highest difference in mean temperature stratified by station population within each region. For the minimum temperature, for example, where the population related differences appear to be greatest, out of 21 regions with available data the median difference between means of stations with populations less than 2,000 and those with populations between 2,000 and 10,000 is about 0.25°C. For the next population category (10,000-100,000), based on 20 out of 23 regions, it is about 0.8°C; and differences between means of stations >100K and <2,000 is 1.8°C (though derived from only 8 of the 23 regions). For mean temperature the median differences are 0.6, 1.2 and 0.9 for the same corresponding population categories (see Fig. 4).

About 60% of the stations shown in Fig. 1 have populations less than 10,000. Differences in temperature were calculated between successive 40-year means according to the population categories given above; they are shown in Fig. 6 for the average temperature. For example, the median difference in temperature between 1900-41 and 1942-84 for stations with population greater than 100K was greater than the corresponding temperature change for stations with population less than 2,000 by 0.05°C. This is using regional averages of these stations according to Fig. 2. However, the results for the other categories show less warming between these two periods for the other two population categories (-0.1°C for 2-10K and -0.05 for 10-100K). A look at the spatial distribution of these anomaly differences (not shown) reveals the presence of spatial coherence. These complex relationships between population, and spatial and temporal temperature changes are explored in Karl et al. (1987).

Figures 7-11 show annual and seasonal temperature anomalies for the contiguous United States for the period 1901-84 for both the HCN dataset and the corresponding averages using the 5° x 10° latitude/longitude gridpoints described in Jones et al. (1986). Anomalies were calculated from a reference mean of 1951-70. While the agreement is excellent at all frequencies, the Jones et al. record appears to be colder in the earlier decades, which lead to generally greater linear warming trends (see Table 1). The data from the HCN indicates that since 1900, temperatures in the contiguous United States exhibit no significant trend, although they have displayed considerable variability from year to year, and in some instances, such as the remarkable warm period during the 1930s, extended periods of departures of one sign. Both sets also display the well-known

Fig. 1. Spatial distribution of stations in the historical climatology network (HCN).

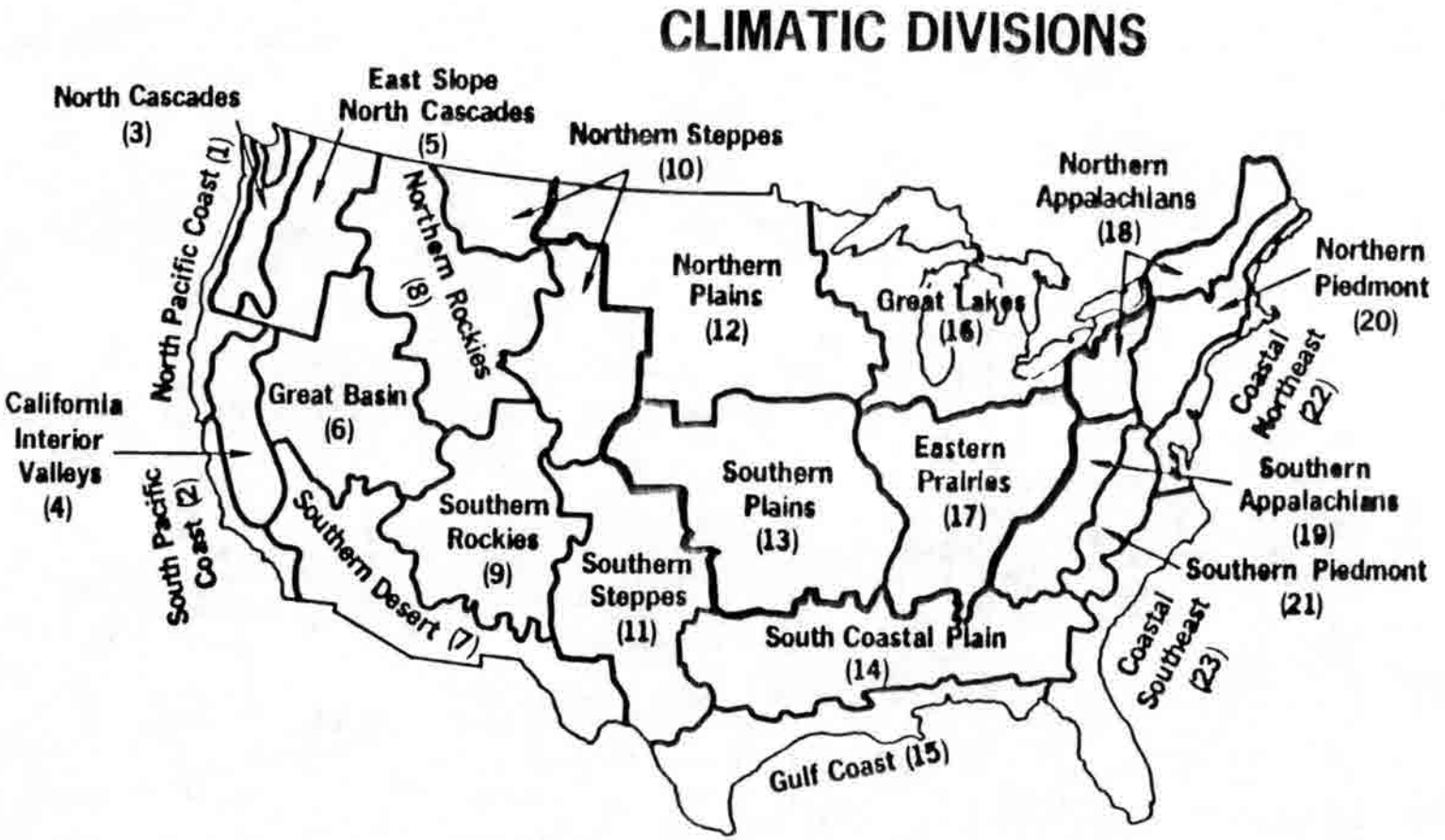

Fig. 2. Regional boundaries of climatic subdivisions (regions) designed to maximize climatic homogeneity.

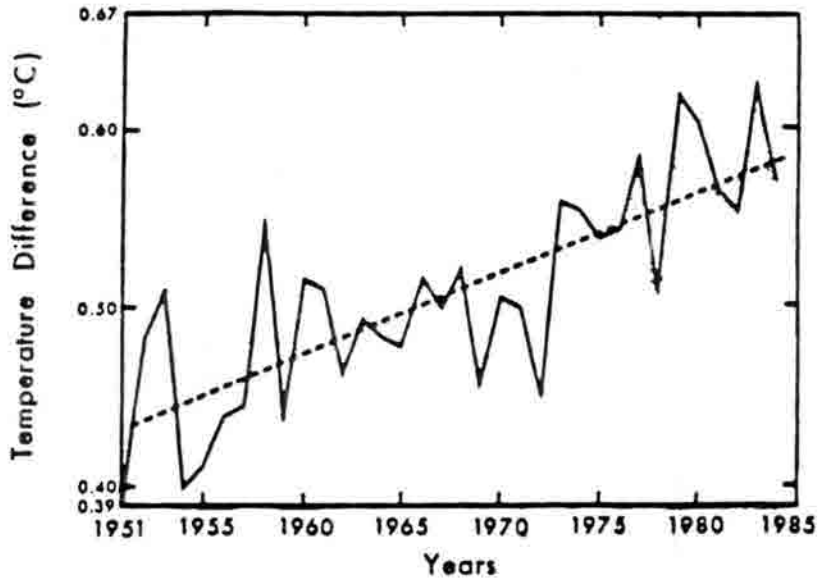

Fig. 3. Difference between first and second order stations mean temperature and all stations within the contiguous United States.

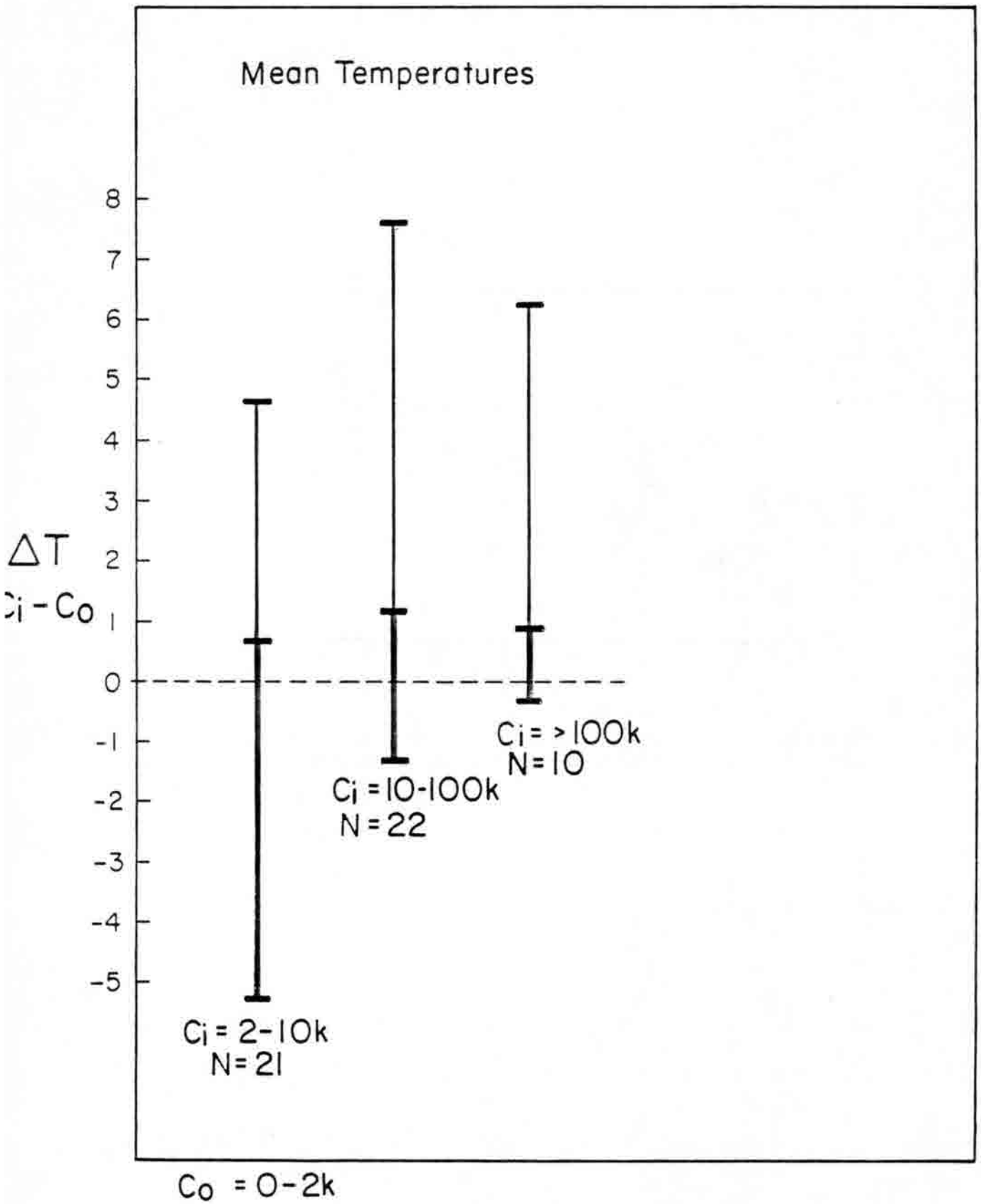

Fig. 4. Range of differences in average regional temperature between sets of stations with populations less than 2,000 and those with the indicated populations (2-10K; 10-100K and >100K). The value for N indicates the number of regions (shown in Fig. 2) for which comparisons were available.

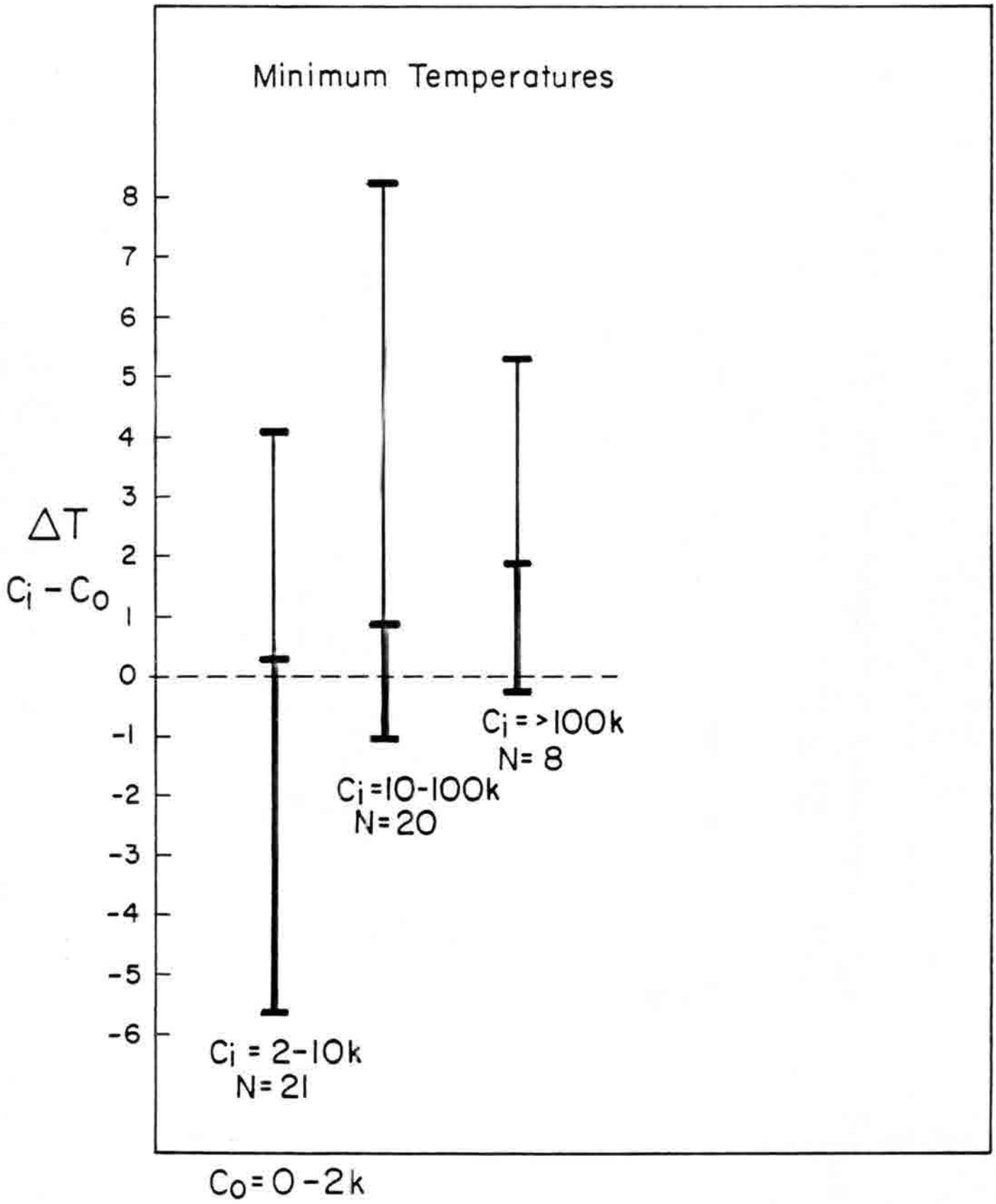

Fig. 5. Same as for Fig. 4, except for average minimum temperature.

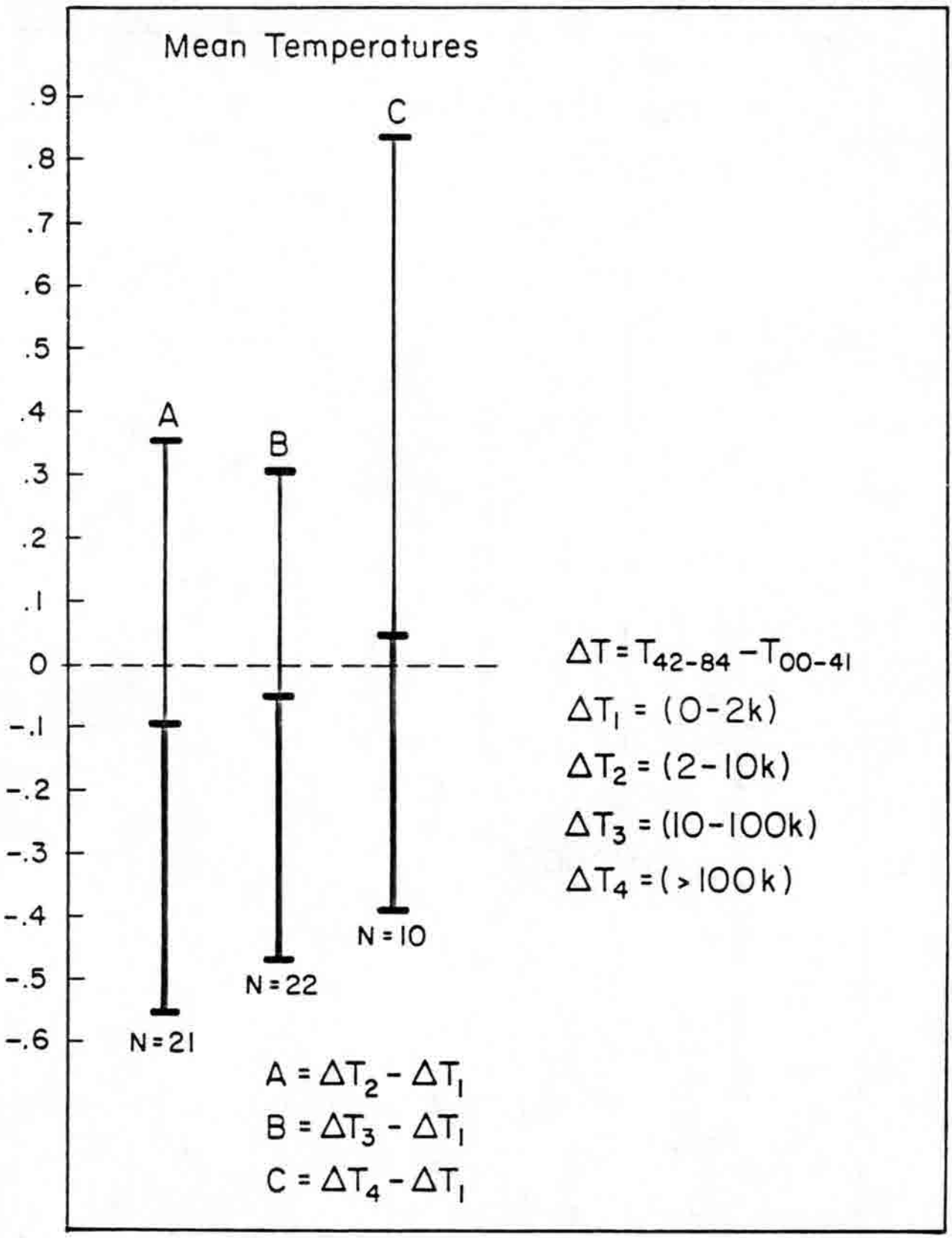

Fig. 6. Differences in temperature changes (1942-84 minus 1900-41) according to station population.

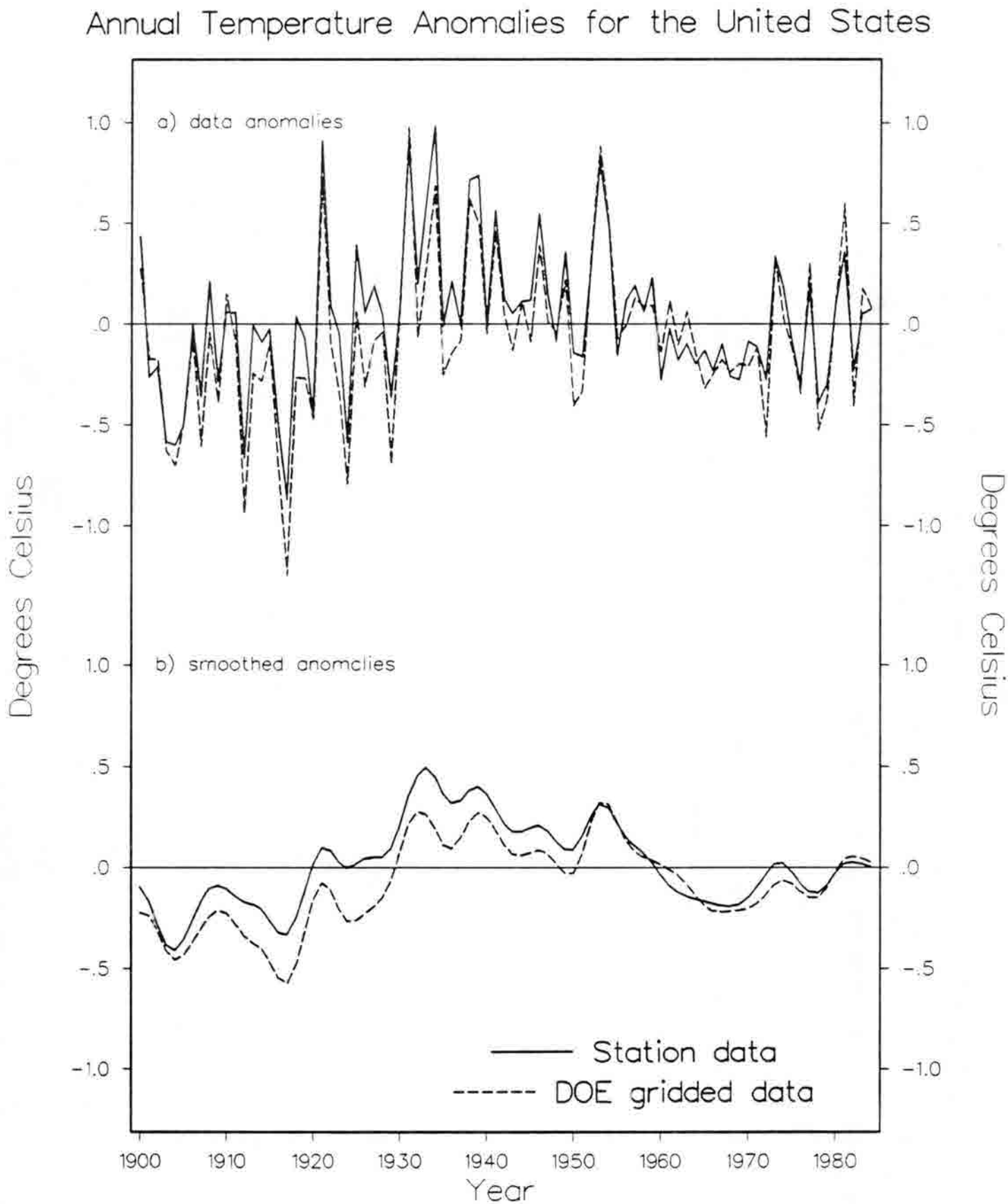

Fig. 7. Annual mean temperature anomalies (in °C) for the contiguous United States based on the HCN station group (solid line) and a gridded average extracted from data described in Jones et al., 1986 (dashed line). The station coverage is shown in Fig. 1; the reference period is taken as 1951-70.

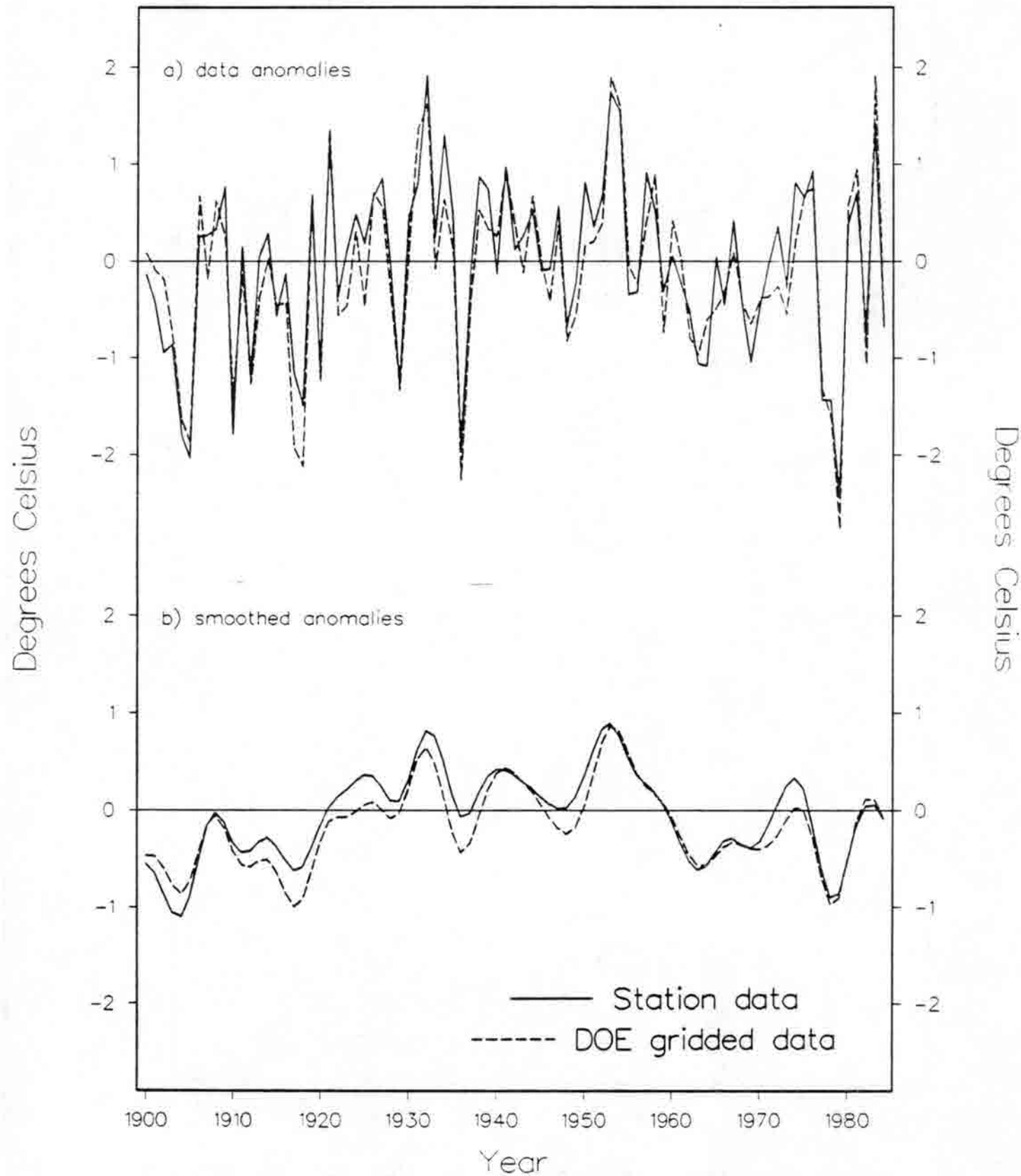

Fig. 8. As for Fig. 7, except for winter (December-February) mean temperature.

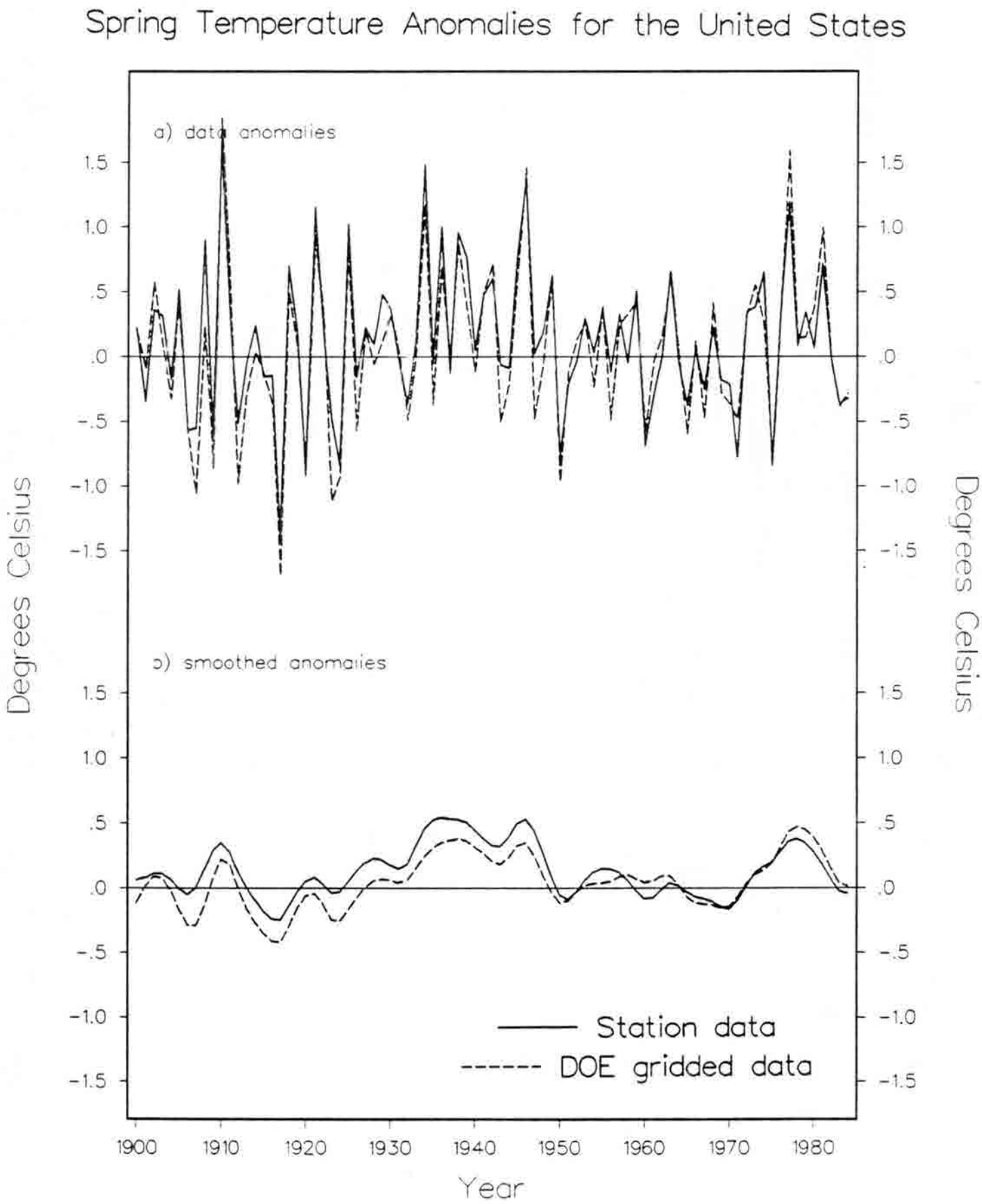

Fig. 9. As for Fig. 7, except for spring (March-May) mean temperature.

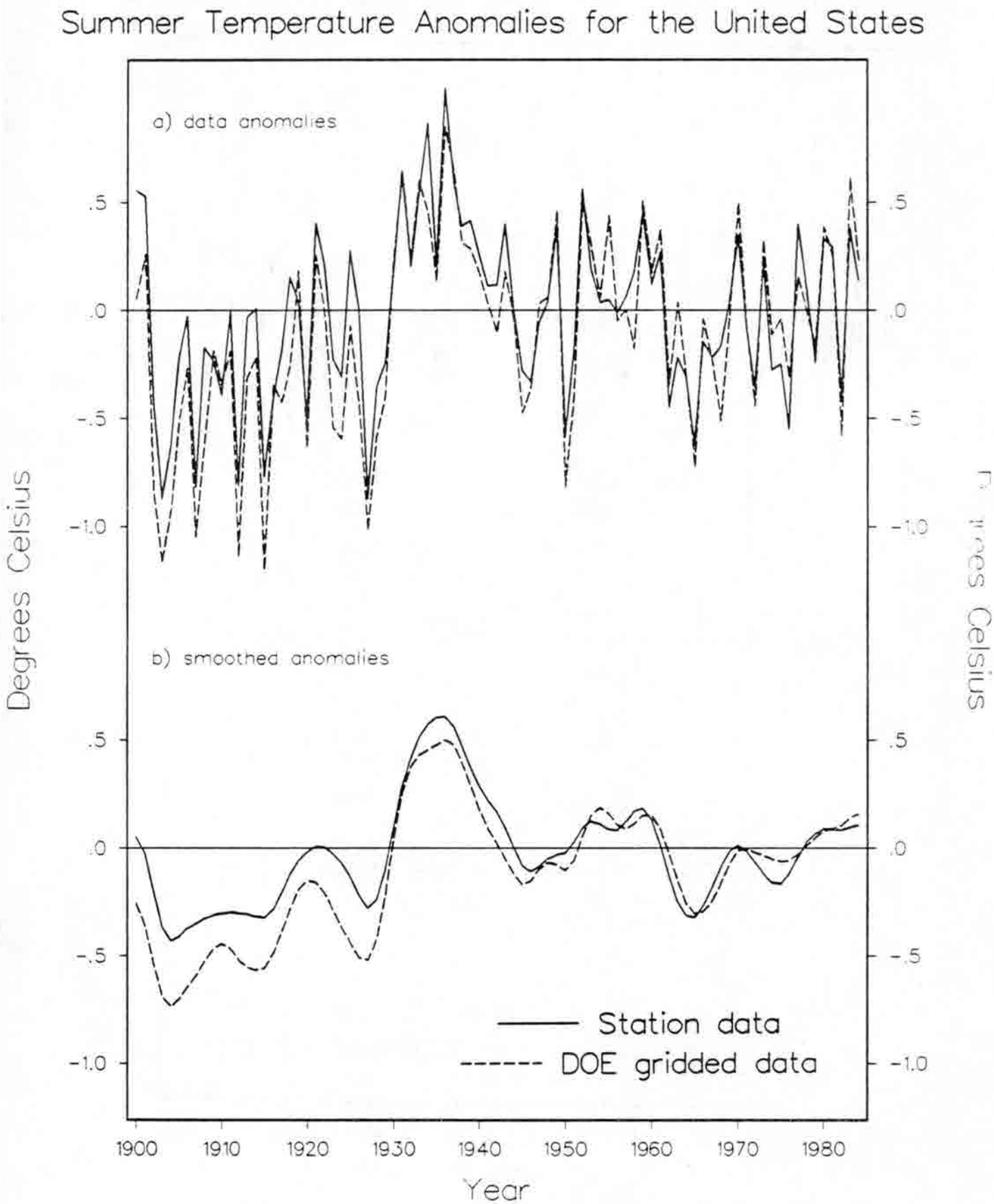

Fig. 10. As for Fig. 7, except for summer (June-August) mean temperature.

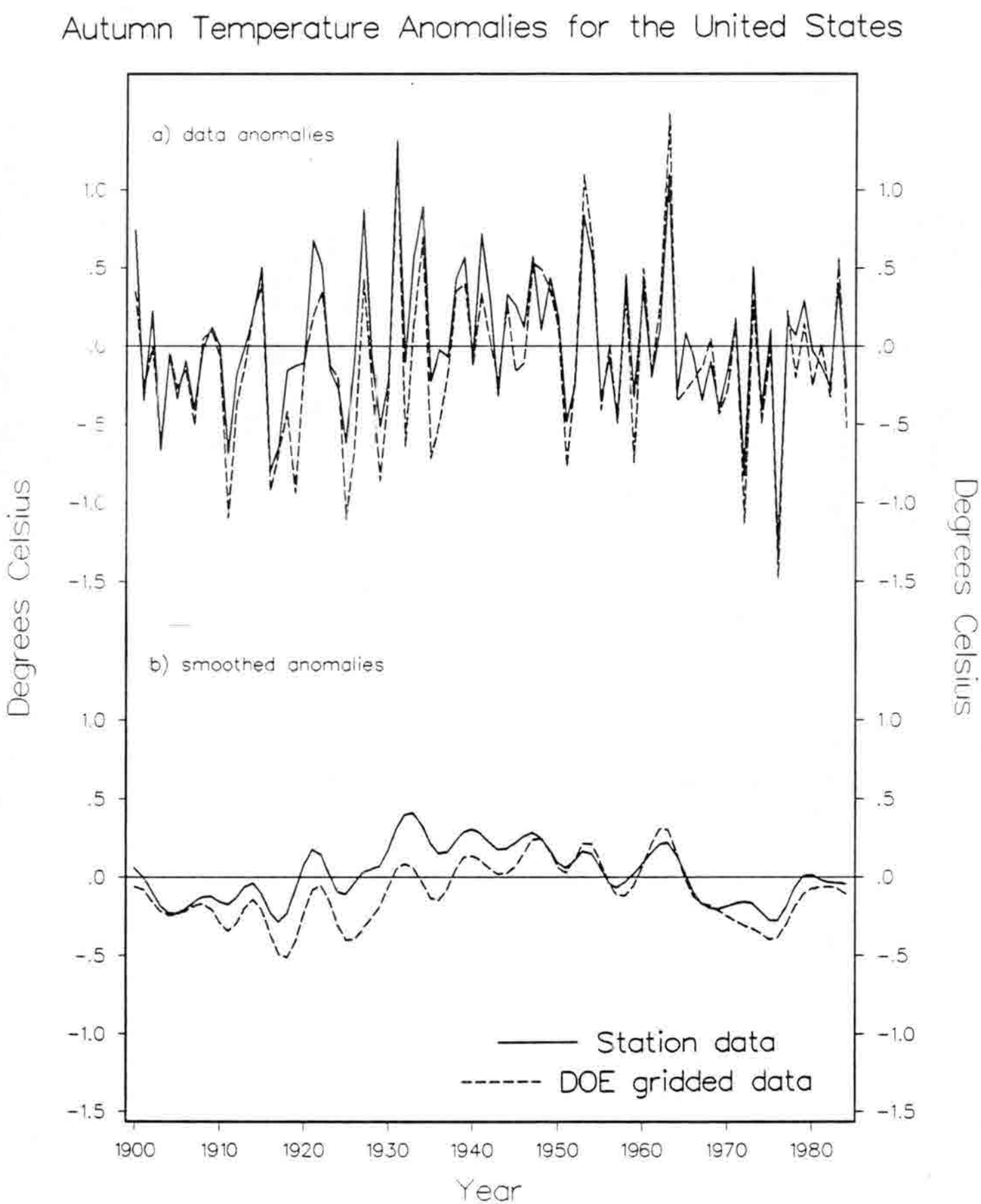

Fig. 11. As for Fig. 7, except for autumn (September-November) mean temperature.

Table 1

Linear Trend for the period 1900-84 (in °C per decade) and statistical significance against the null hypothesis of zero trend for the HCN Network and the equivalent time series based on a U.S. grid using data taken from Jones et al. (1986), referred to as the DOE data. One asterisk (*) denotes significance at 5% level; two asterisks (**) at the 1% level.

Season	Slope (°C/decade)
Historical Climatology Network	
Winter (DJF)	.030
Spring (MAM)	-.001
Summer (JJA)	.023
Fall (SON)	-.000
Annual	.013
DOE Gridded U.S. Temperatures	
Winter (DJF)	.027
Spring (MAM)	.027
Summer (JJA)	.068 (**)
Fall (SON)	.017
Annual	.036 (*)

early "cool" period, middle "warm" period and the recent 2-3 decades of intermediate temperatures (Diaz and Quayle, 1980).

The northern midsection of the contiguous U.S. is likely to exhibit relatively greater amplitude of temperature variation due to its interior continental climate. Accordingly, the temperatures for subregions 12, 13, 16, and 17 were averaged together by season and the results are shown in Fig. 12. While, as expected, the temperature range is much larger than for the HCN network as a whole, with differences as large as 6°C between warm and cold years, the overall trends are still near zero.

4. Conclusions

The following may be concluded regarding surface mean temperatures in the United States. Based on averages derived from a set of 723 stations across the contiguous 48 states which have been adjusted to the extent possible to account for non-climatic biases, the seasonal and annual mean temperatures exhibit no statistically significant trend since 1900. The temperature series display mainly interannual and decadal-scale (10-40 years)) variability. Based on this and other analyses, we advance the following recommendations for further diagnostic and modelling studies.

- General circulation models should be run with evolving boundary conditions such as the observed surface temperature conditions of the past 50 or so years as both a test of the model's ability to reproduce observed spatial and temporal variability as well as an aid in trying to understand climate processes at decadal and longer time scales.

- GCM experiments could be run to try to replicate such observed past behavior as the development and termination of quasi-stable climate regimes such as the North Atlantic warming in the 1920s, ENSO variability, the on-going African drought and the 1930s warm and dry U.S. regime.

We thank Mr. Jon Eischeid of CIRES for assistance in processing the voluminous data and producing the time series plots.

References

Ackerman, B., 1985: Temporal march of the Chicago heat island. J. Clim. Appl. Meteor., 24, 547-554.

Diaz, H. F. and R. G. Quayle, 1980: The climate of the United States since 1895: spatial and temporal changes. Mon. Wea. Rev., 108, 249-266.

Jones, P. D., S. C. B. Raper, R. S. Bradley, H. F. Diaz, P. M. Kelly, and T. M. L. Wigley, 1986: Northern hemisphere surface air temperature variations, 1851-1984. J. Clim. Appl. Meteor., 25, 161-179.

Karl, T. R., G. Kukla, and J. Gavin, 1984: Decreasing diurnal temperature range in the United States and Canada from 1941 through 1980. J. Clim. Appl. Meteor., 23, 1489-1504.

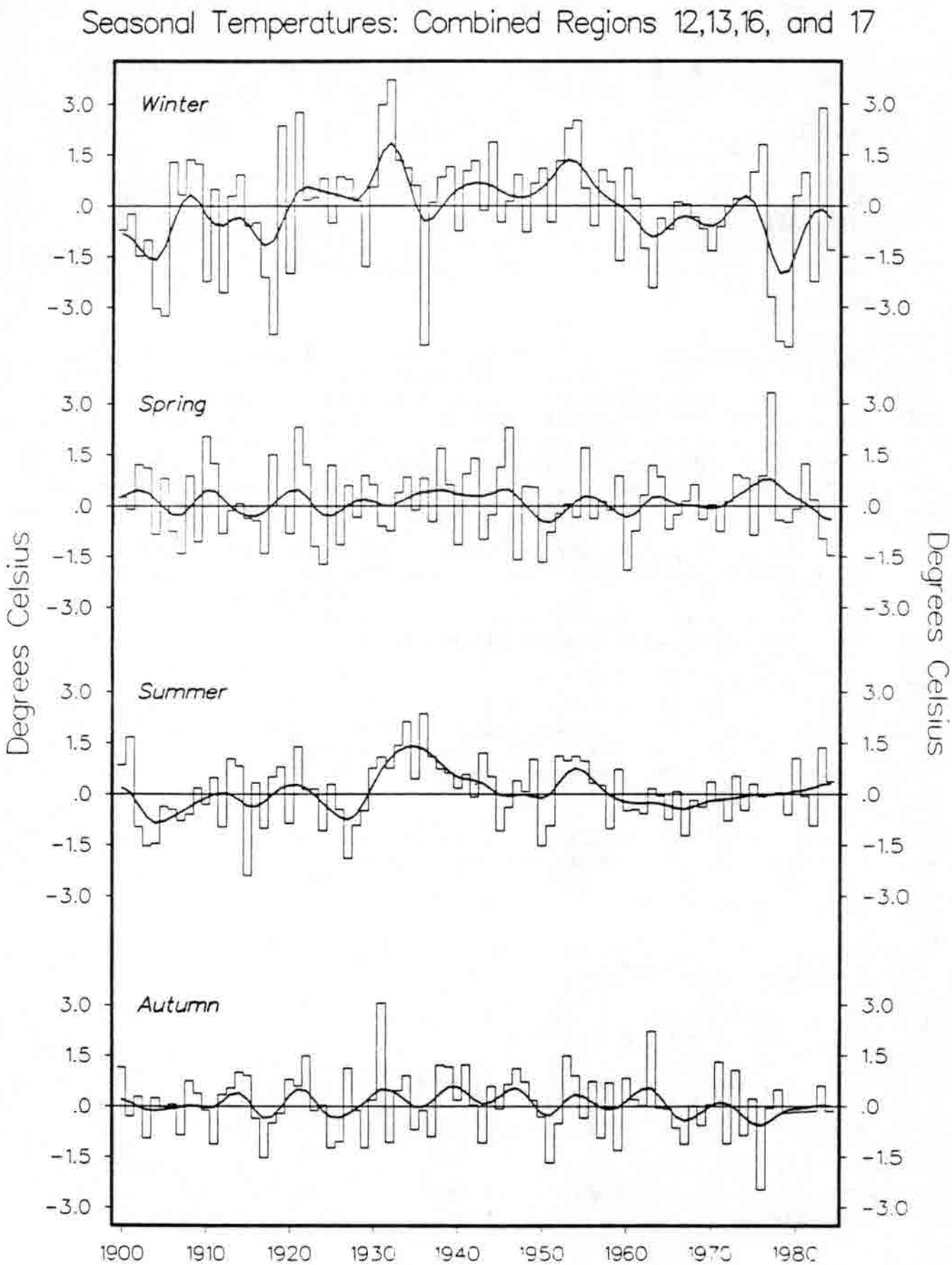

Fig. 12. Combined seasonal and annual mean temperature anomalies (°C, from 1951-70 means) for the four regions outlined by the bolder black line in Fig. 2).

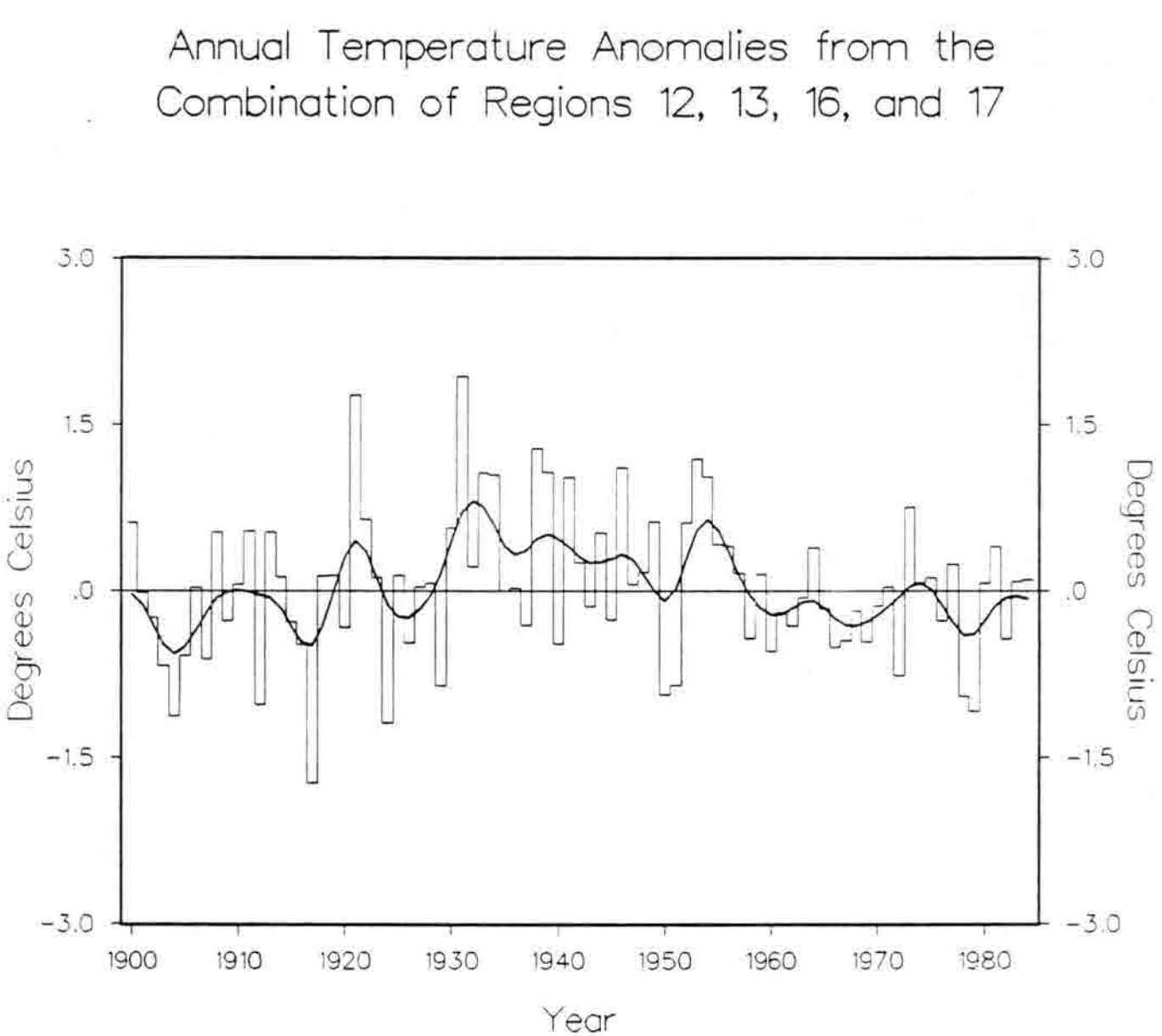

Figure 12 (cont.)

Karl, T. R., G. Kukla, and J. Gavin, 1986: Relationship between decreased temperature range and precipitation trends in the United States and Canada, 1941-80. J. Clim. Appl. Meteor., 25, 1878-1886.

Karl, T. R., H. F. Diaz, and G. Kukla, 1987: Urbanization: Its detection and effects on the U.S. climate record (submitted).

Landsberg, H. E., 1981: The Urban Climate. Academic Press, 185 pp.

Mitchell, J. M., Jr., 1953: On the causes of instrumentally observed secular temperature trends. J. Meteor., 10, 224-261.

Oke, T. R., 1973: City size and the urban heat sialnd. Atmos. Environ., 7, 769-779.

Oke, T. R., 1978: Boundary Layer Climates. Methuen and Co. Ltd., London, 372 pp.

Multi-Year Fluctuations of Temperature and Precipitation: The Gray Area of Climate Change

Thomas R. Karl
National Climatic Data Center
National Environmental Satellite Data and Information Center
National Oceanic and Atmospheric Administration
Federal Building
Asheville, North Carolina 28801

Abstract

The issue of whether the secular climate (twentieth century) is stationary or changing to some new semi-permanent state is clouded by the presence of so-called "climate fluctuations." The twentieth century climate record of the United States reveals a substantial number of decadal fluctuations which occur in all seasons for both temperature and precipitation. Recent examples of such behavior include changes in winter and summer temperature variability and increases in transition season precipitation. Statistical evidence suggests that a substantial portion of these fluctuations, even those which are remarkably unusual, are merely manifestations of a stochastic process which possesses weak year-to-year persistence as viewed from an a posteriori perspective. The implications of this result are particularly important with respect to the formulation of physical causes of the fluctuations. The results emphasize the desirability of well-founded clearly-stated a priori theories of climate change as well as the limited usefulness of widely used climate normals.

1. Background

It has been well established that the secular near-surface climate record contains variations on many time scales ranging from week-to-week to decade-to-decade (Lamb and Johnson, 1961; Mitchell, 1976; Douglas et al.,

1982; Walsh et al., 1983; Karl and Riebsame, 1984). Some researchers have linked these variations to changes in circulation and/or sea surface temperatures (Namias, 1978; van Loon and Williams, 1982; Rasmusson, 1983; Diaz, 1986) while others have attempted to relate them to the volcanic record, solar variations, and greenhouse gases (Hansen et al., 1981; Gilliland and Schneider, 1984). Despite some progress, particularly with respect to month-to-month and season-to-season variations of climate (Namias, 1978; Klein, 1983), the explanation of multi-year fluctuations in the climate record remains a major problem in our fundamental comprehension of the Earth's climate system (Gates and MacCracken, 1985). In particular, it compounds the problem of detecting the climatic effects of increasing atmospheric concentrations of carbon dioxide and other greenhouse trace gases (Madden and Ramanathan, 1980).

The biophysical and socio-economic impacts of recent fluctuations are quite noteworthy (Karl and Young, 1986; Changnon, 1987; Quinn, 1986; Karl et al., 1984). The extreme wetness of recent decades has raised lake levels of the Great Salt Lake and the Great Lakes, and forced state, local, and federal governments into a reaction mode to help ameliorate the social and economic impacts of these high lake levels (Kay and Kiaz, 1985; Changnon, 1987). Moreover, the impacts of long past fluctuations have also been documented. The prolonged heat and dryness of the 1930s not only severely reduced agricultural production, but it affected the social and economic fabric of those living in the Great Plains (Warrick, 1980). The decreased variability of the 1960s has been linked to remarkable increases in agricultural production during this time (Thompson, 1975). Obviously, the importance of an adequate understanding of the nature of these and other multi-year climate fluctuations is not limited to the climatological community, but span many disciplines (Kates, 1980).

Figure 1 depicts the climate record of the United States for the past century. The data used in these time series are described by Karl et al. (1984). Essentially they are areally averaged means of seasonal and annual temperature and total precipitation from 344 climate divisions in the contiguous United States. Adjustments to the data include a time of observation bias for the temperature (Karl et al., 1986). An inspection of these time series reveals a number of rather abrupt transitions in the series, which persist for up to several decades, where the mean or standard deviation appears inconsistent with the rest of the climate record. The largest of these shifts or climate fluctuations are identified in the first four columns of Tables 1 and 2. These tables contain a number of climate fluctuations which persist from 5 to 39 years. They were identified by an "ad hoc" search of the time series for what appeared to be an unusual sequence of departures from the expected values. (Only those events later found to be infrequent in recurrence, via statistical methods, are reported). No event overlaps another event for the same statistic of interest, i.e., changes in the average (or level) or variability. Fluctuations related to changes in level are denoted in Tables 1 and 2 by "Mean" or "Thresh." This implies a change in level over some specified period of time either in the form of a change in the mean (Mean) or as an unexpected number of years at or above/below some threshold value (Thresh). Changes in variability are indicated by changes in the standard deviation (Std) or a specified number of years (data points) in a sequence of years whose absolute value is above (increased variability) or below (decreased variability) some threshold value (Va). Recent fluctuations include the change in wintertime temperature variability, wintertime precipitation variability, and increases in transition season precipitation.

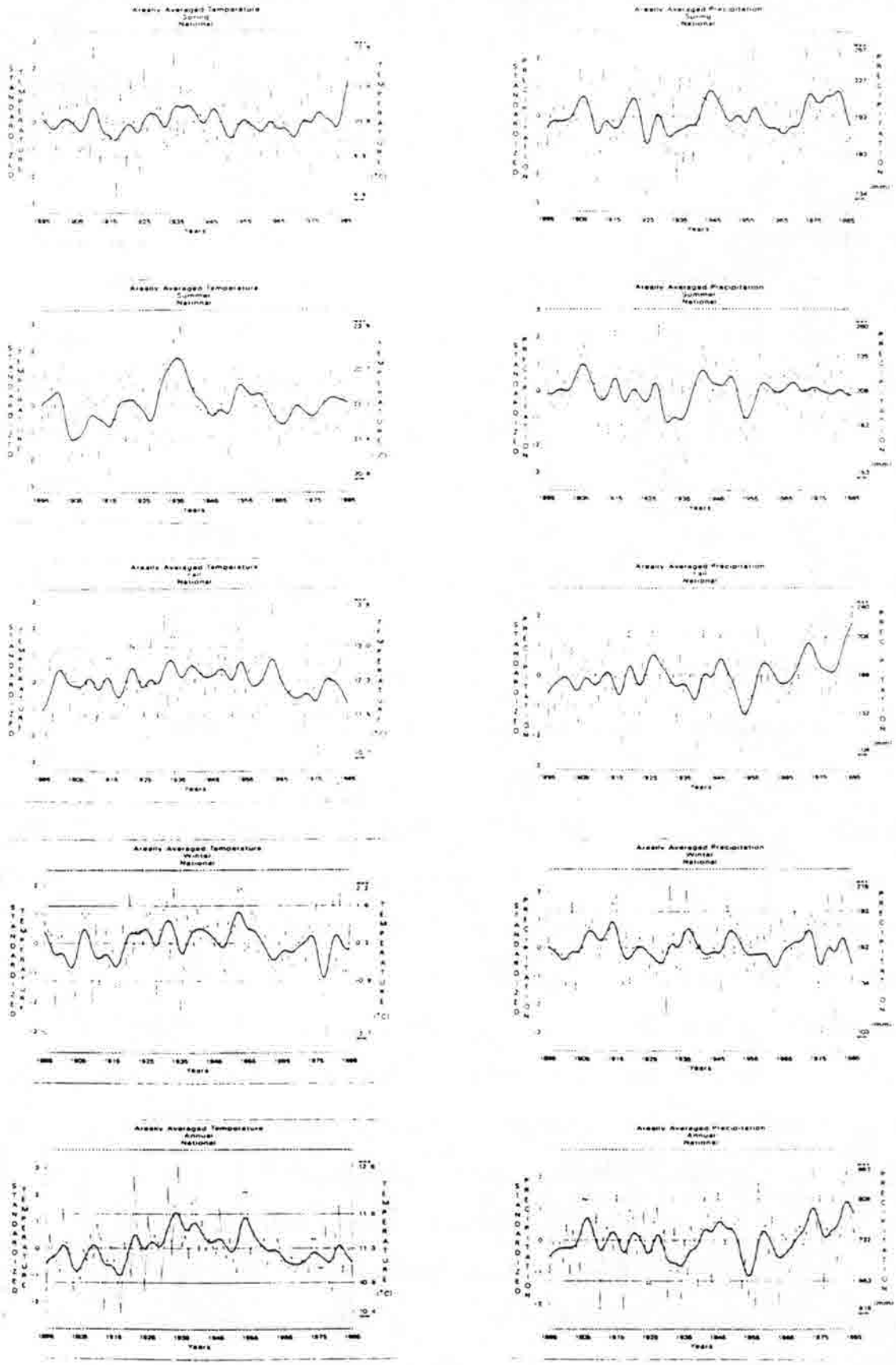

Figure 1. Time series of areally averaged seasonal and annual mean temperature and total precipitation for the U.S. The standardized values are derived from the normal distribution for temperature and the gamma distribution (maximum likelihood estimates for precipitation. The smoothed curve is a nine-point binomial filter with truncated endpoints. The horizontal lines reflect the mean and ± 1.282 standardized departures from the mean (upper and lower 10% of the data).

Table 1. Observed climate fluctuations from the normalized temperature climate record and the results of simulating these fluctuations in various autoregressive moving average (ARMA) models of order indicated by the parenthetical expressions. BIC implies Bayesian Information Criteria and AIC Akaike Information Criteria. The first term in parenthesis after the AIC or BIC represents the AR order and the second the MA order. The coefficients of the ARMA model are also given (models of order zero have coefficients of zero). "Thresh" implies a series of values above or below some threshold value, "Std" implies the standard deviation, and "Va" implies a series of values whose absolute value is above or below some predetermined value. Also given is the 5 and 95% confidence interval of the return period of the climate fluctuation and the percent of simulated time series of length 92 years which had fluctuations as large or larger as those observed.

TEMPERATURE

TYPE	LIMITS	YEARS	YEARS SELECTED	RETURN PERIODS BIC	RETURN PERIODS AIC	% OF SIMULATIONS>LIMITS BIC	% OF SIMULATIONS>LIMITS AIC
SPRING — BIC (0,0); AIC (0,0)							
Std	≥1.376	1906-25	20	531-576	531-576	6.54	6.54
Va	≤/1.218/	1951-74	24 of 24	1712-2025	1712-2025	2.06	2.06
SUMMER — BIC (0,1), θ_1=0.343; AIC (0,3), θ_1=0.300, θ_2=-0.085, θ_3=0.405							
Mean	≤-0.887	1902-17	16	1339-1521	767-843	1.74	4.18
Thresh	≥0.602	1930-40	11 of 11	65410-368757	22826-45064	0.04	0.14
Va	≤/1.169/	1954-85	31 of 32	2295-2776	1862-2218	1.52	1.88
FALL — BIC (0,0); AIC (0,0)							
Thresh	≤0.784	1964-85	22 of 22	4009-5193	2646-3289	4.92	4.92
WINTER — BIC (0,0); AIC (1,1), ϕ_1=-0.827, θ_1=0.981							
Va	≤/1.038/	1954-74	21 of 21	5470-7397	4540-6106	0.62	1.14
Va	≥/0.593/	1975-85	11 of 11	1432-1646	1385-1619	5.30	4.64
ANNUAL — BIC (0,0); AIC (1,0), ϕ_1=0.171							
Thresh	≤0.479	1895-1920	24 of 26	1105-1252	630-694	3.54	7.18
Std	≥1.304	1912-41	30	729-807	700-765	1.88	2.22
Mean	≥0.524	1921-59	39	7776-11442	2166-2588	0.00	0.06
Thresh	≤-0.061	1960-85	20 of 26	1787-2099	889-991	1.62	3.80
Std	≤0.502	1955-77	23	14198-22954	10735-15911	0.14	0.26
TYPE	LIMITS	YEARS	YEARS SELECTED	RETURN PERIODS BIC	RETURN PERIODS AIC	% OF SIMULATIONS>LIMITS BIC	% OF SIMULATIONS>LIMITS AIC

Table 2. Same as Table 1 except for precipitation.

PRECIPITATION

SPRING — BIC (0,0); AIC (0,1), θ_1=0.092

TYPE	LIMITS	YEARS	YEARS SELECTED	RETURN PERIODS BIC	RETURN PERIODS AIC	% OF SIMULATIONS>LIMITS BIC	% OF SIMULATIONS>LIMITS AIC
Va	≥/0.580/	1922-39	17 of 18	6048-8287	5735-7714	0.96	0.92
Thresh	≥0.294	1942-48	7 of 7	1266-1484	829-927	5.48	8.34
Thresh	≥-0.070	1973-84	12 of 12	4009-5193	2646-3289	1.34	2.18

SUMMER — BIC (0,0); AIC (0,1), θ_1=0.193

Va	</0.727/	1895-1904	10 of 10	1130-1291	990-1118	6.38	6.88
Mean	≤-1.367	1929-36	8	16895-30479	4069-5487	0.06	0.74
Va	≤/0.946/	1959-74	16 of 16	2429-2956	2010-2400	2.38	2.72

FALL — BIC (1,0), ϕ_1=0.141; AIC (1,0), ϕ_1=0.141

Thresh	≤-1.856	1952-56	3 of 5	2668-3365	2268-3365	2.06	2.06
Mean	≥0.751	1970-85	16	764-857	764-857	4.46	4.46

WINTER — BIC (0,0); AIC (2,0), ϕ_1=0.045, ϕ_2=0.326

Thresh	≥0.005	1905-15	10 of 11	466-504	1158-1318	13.78	5.26
Std	≥1.953	1976-82	7	2591-3184	910-1017	1.44	4.44
Va	≥/2.006/	1930-36	3 of 7	936-1037	581-637	6.74	10.00

ANNUAL — BIC (0,0); AIC (0,1), θ_1=0.131

Mean	≤-1.370	1952-56	5	1130-1157	555-609	4.80	10.42
Thresh	≥-0.140	1968-85	16 of 18	1226-1388	741-820	4.36	6.98

TYPE	LIMITS	YEARS	YEARS SELECTED	RETURN PERIODS BIC	RETURN PERIODS AIC	% OF SIMULATIONS>LIMITS BIC	% OF SIMULATIONS>LIMITS AIC

There are at least three possibilities why the search for the explanation of multi-year climate fluctuations has not proven very satisfying. First, the fluctuations themselves may merely be a consequence of searching the climate record a posteriori for an unusual sequence of events. In such a search, particularly if the climate system possesses some weak year-to-year persistence or memory, the clustering of anomalous years to form multi-year climate fluctuations may merely be a chance event, and it is not necessary to invoke some additional physical mechanism(s) linking these years together. On the other hand, it has been suggested by Mandelbrot and Van Ness (1968) and Mandelbrot and Wallis (1969a,b) that geophysical time series possess an infinite memory, a characteristic that can be described and modeled by random processes such as "fractional Brownian noises" as well as other statistical models, i.e., autoregressive integrated moving average (ARIMA) models (O'Connell, 1971) or as sums of broken line processes (Rodriquez-Iturbe et al., 1972). These statistical models have been used to describe the so-called Hurst phenomenon (Hurst, 1957)[1]. Thirdly, the time series may contain some subtle mechanism(s) or feedbacks, intrinsic or extrinsic to the climate system itself, which only became important at irregular intervals. As yet these mechanisms have not been adequately characterized or discovered. It is the purpose of this work to weigh some of the empirical evidence in support of each of these possibilities.

[1]The Hurst phenomenon defies the hypothesis that a hydrological time series can be characterized by a random series in which observations separated by large segments of time can be considered independent.

2. Method

The question to be addressed with respect to all of the observed climate fluctuations can be formulated in the null hypothesis: "The observed climate fluctuations are well described by a stationary time series which can be described by a low-order ARMA process". If this were the case, then the apparent unusual events in Tables 1 and 2 would represent nothing more than the result of an a posteriori search of the climate record for unusual events. The term stationary that is used here implies that the mean, variance, and autocorrelation are invariant over time. The alternate hypothesis, in lieu of the rejected null hypothesis is: "The climate record is either non-stationary, cannot be described by a low order ARMA or both". This would probably imply that the climate record contains fluctuations that must in part be explained by some intrinsic and/or extrinsic process which acts to produce low-frequency variations in the mean and variance. Such variations may, of course, be expressable in terms of other statistical models such as higher-order ARMAs, low-order ARMAs with irregular intervention or other long-range dependence models such as those described earlier.

With respect to the alternate hypothesis, Lorenz has recently run a 400-year integration (after equilibrium) of a low-order global model (Lorenz, 1984; Lorenz, 1986). The model includes viscous and thermal damping, evaporation and precipitation, and radiative heating and cooling. The cloud cover is a preassigned function of the relative humidity, and the albedo depends in turn upon the cloud cover. He has unintentionally produced what appears to be a sequence of climate fluctuations not unlike those observed in the U.S. climate record (Figure 2). Lorenz attributes these fluctuations to the internal dynamics in his model, namely a feedback between clouds and albedo. Such a mechanism may not manifest itself in the

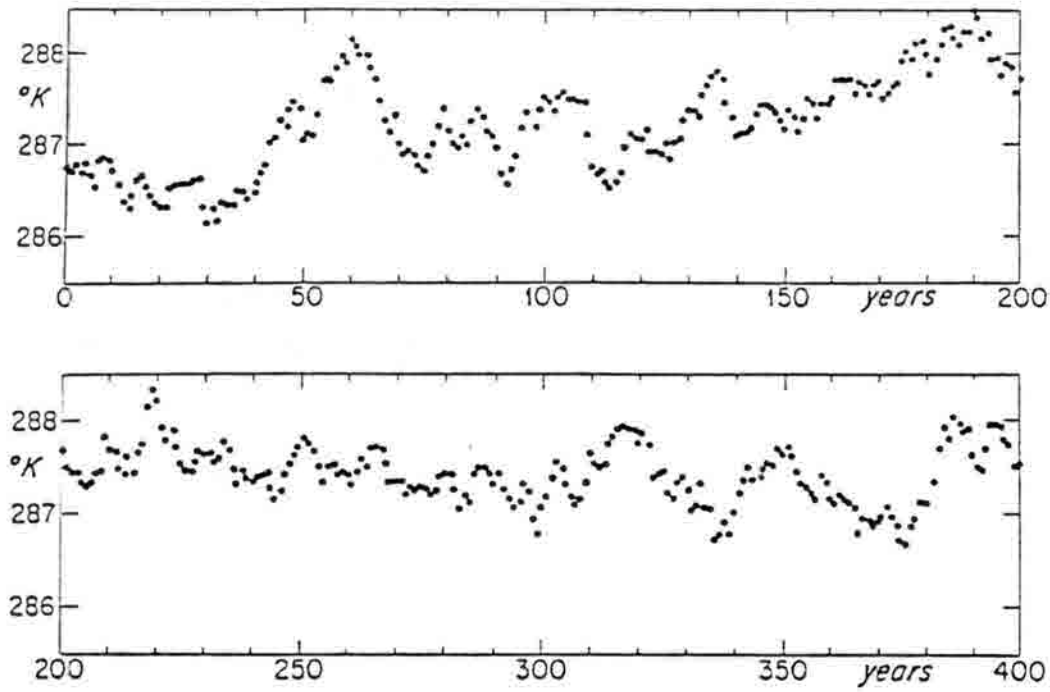

Figure 2. Annual mean values of the globally-averaged temperatures during 400 consecutive years in Lorenz's low-order model. The initial state, year zero, follows a 50-year integration of the model.

form of simple persistence of anomalies of like sign, i.e., time invariant autocorrelations. That is to say, the climate system may become unstable at some point such that the cold (warm) anomalies associated with high (low) albedo and cloud cover lead to reduced (increased) evaporation and subsequent decreases (increases) in cloud cover and hence warm (cold) anomalies. This may occur over a period of years, or perhaps rather suddenly. Of course, this does not imply that such a mechanism is operating in the Earth's climate system, but it does suggest, as Lorenz states, "climate fluctuations may depend on mechanisms which seem so secondary they are often omitted in theoretical investigations or as yet remain to be discovered". In contrast to such an internal mechanism, numerous extrinsic forcings may also be postulated. This includes changes in solar output, volcanic eruptions, anthropogenic effects, etc.

In the context of the formulated null and alternate hypotheses, each time series of standardized temperature and precipitation (standardized via the normal and gamma distributions, respectively) was modeled using an autoregressive moving average (ARMA) model (Box and Jenkins, 1976). The model can be written as:

$$Y_t = \sum_{i=1}^{p} \phi_i Y_{t-1} + \sum_{j=1}^{q} \theta_j a_{t-j} + a_t \qquad (1)$$

where Y_t is the value of the time series at time t; ϕ_i is the ith autoregressive (AR) coefficient; θ_j is the jth moving average (MA) coefficient; and a_t is random noise (or a shock) at time t. The order of the model is expressed as p,q and represented as ARMA (p,q). The distribution of a_t is assumed normal with mean zero and standard deviation

σ_a. As Priestly (1981) points out, most stationary processes which arise in practice can be fitted by an ARMA model.

From Eq. 1 it can be seen that when p and q are zero the model represents a white noise or uncorrelated time series. Furthermore, ARMA (0,q) models can be characterized as having finite persistence, i.e., the random noise in the model persists for exactly q observations. By comparison, ARMA (p,0) models can be characterized as having infinite, but geometrically decaying persistence of the random noise component. Specifically, for an ARMA (1,0) process this is simply:

$$Y_t = \sum_{i=0}^{\infty} \phi_1^i \, a_{t-1} \quad . \tag{2}$$

This implies that an AR(1) is equivalent to an MA(∞) with the magnitude of the coefficients θ_j (Eq. 1) decaying geometrically. If ϕ_1 is large (approaches 1) the model verges on non-stationarity and long-range dependence is contained within the model. Large coefficients of ϕ_1 (≥ 0.7) in the AR(1) can easily produce time series which appear non-stationary, but in fact are stochastic and non deterministic. When ϕ_1 is small (< 0.4), the memory of past observations is short. The average impact of shock a_{t-4} at t is about 2.5% of the shock at a_t. For higher-order autoregressive processes, AR(p), the decay of the random shock is not a simple function of the (ϕ_p)s. Nonetheless, even for an ARMA (2,0) when $\phi_1+\phi_2$ are small (i.e., less than 0.4) the impact of the random shock by a_{t-4} can be shown to be rather small (2.5% of the sum of the shocks a_t, a_{t-1}, a_{t-2}, and a_{t-3}; McCleary and Hay, 1980). On the other hand, when ϕ_1 and ϕ_2 are both present this can lead to cyclic behavior in the time series. When both ϕ_1 and θ_1 are present in the model and of opposite sign, but similar magnitude, the

ARMA (1,1) has parameter redundancy. It can be shown, if $-\phi_1 = \theta_1$, that the ARMA (1,1) reduces to an ARMA (0,0).

Given the form of the model (Eq. 1) the problem remains as to the determination of the appropriate order of the model. Information theoretic concepts are used in two general information criteria in order to identify the appropriate order of the ARMA for each of the series depicted in Figure 1. The Akaike and Schwarz's Bayesian information criteria were used (Schwarz, 1978; Priestly, 1981). They can be represented by:

$$\text{AIC } (p,q) = n \ln(\sigma^2) + 2(p+q+1) \tag{3}$$

and

$$\text{BIC } (p,q) = n \ln(\sigma^2) + \ln(n)(p+q+1) \ , \tag{4}$$

where n is the number of observations in the time series and σ^2 is the residual mean sum of squares of the one-step ahead forecast for Y_t (Priestly, 1981; Harvey, 1981), i.e., σ^2 is the variance of a_t. The most appropriate order of the model is found when the AIC (p,q) or BIC (p,q) are at a minimum. It should be noted that the AIC tends to overestimate the true order of an AR model (Priestly, 1981), but the BIC procedure is more parsimonious for $n \geq 8$, i.e., BIC (p+q) $\leq$ AIC (p+q).

The maximum order allowed is constrained by: $p \leq 2$, $q \leq 4$, and $p+q \leq 4$. This assumption is consistent with the hypothesis of a low-order ARMA process. Higher-order models could (and will later) be fitted, but their physical interpretation is often difficult. As Katz (1982) points out, the choice of the appropriate order for Eqs. 3 and 4 can be interpreted as weighing two pieces of information. The first term to the right of the equality measures how well the ARMA model fits the observed data, and the second term is a penalty function for the number of terms in the model plus

the removal of the mean. The coefficients of the ARMA model (ϕ and θ) are determined iteratively by minimizing the residuals of the model. This requires estimation of each a_t using observed data. Forward recursions and a backcasting method are used to calculate a_t (Box and Jenkins, 1976) thereby finding the coefficients which minimize the errors of predicting Y_t.

Once the model is selected in accordance with an information criterion, it is then possible to evaluate whether the identified climate fluctuations are consistent with the null hypothesis, i.e., the apparent clustering of anomalous years to form multi-year climate fluctuations is an artifact of an a posteriori search of the climate record which can be modeled by a low-order ARMA. This is accomplished in two separate Monte Carlo experiments.

The first experiment has two parts. First, the average return period of each of the identified climate fluctuations is estimated using the appropriate ARMA model. This is found by generating 100 realizations of a time series of length n = 10,000. Next, the frequencies of occurrence of the various types of climate fluctuations are calculated over the specified period of years (time steps) as listed in Tables 1 and 2, i.e., changes in level or variability. Ninety-five percent confidence intervals of the average return period are estimated by use of the expression:

$$s_N = s/\sqrt{N} \quad , \tag{5}$$

where s is the standard deviation of the total number of events across the 100 simulations (N) and s_N is an estimate of the uncertainty of the mean frequency of occurrence of the events as determined from the 100 simulations (Panofsky and Brier, 1968). This method is also described in earlier work (Karl et al., 1984). The rationale of this approach is simply that if many

of the climate fluctuations have long return periods this may be inconsistent with the null hypothesis, and it also serves to indicate the unlikelihood of many of these fluctuations. Next, the percent frequency of simulated time series which contained climate fluctuations which met or exceeded the observed climate fluctuations listed in Tables 1 and 2 were calculated in the second portion of the first Monte Carlo experiment. In this experiment N = 5,000 (simulations) and each simulated series had length n = 92 (at least as many years of data as contained in each season in Figure 1). Again, the appropriate ARMA model was used based on the AIC and BIC.

If the Monte Carlo simulations were based on a priori information then two times the calculated percent of time series which contain the observed climate fluctuations could be viewed as a two-tailed critical significance level for use in the acceptance[2] or rejection of the null hypothesis. As the simulations are a posteriori the fact that few simulations contain the observed climate fluctuation merely indicates that the null hypothesis may be inconsistent with the observations. That is, it is a necessary but not a sufficient condition to reject the null hypothesis. This is because when searching for unusual events from an a posteriori perspective, if given enough degrees of freedom, it may often be possible to find some unlikely event, even from a purely stochastic process.

For example, in 92 throws of a six-sided die, if many degrees of freedom are allowed with respect to identifying some unusual sequence it may be quite easy to find some strange sequence such as a highly unlikely sequence of one's and six's embedded in the 92 tosses or various

[2]The term acceptance is used loosely to imply that the null hypothesis is not inconsistent with the observed data.

combinations of other numbers. So, before the null hypothesis can be regarded as inconsistent with the observed data, it is necessary to determine how often such unlikely events can be found from purely stochastic processes. The second Monte Carlo experiment addresses this problem.

Twenty stochastic time series, each of length $n = 92$, were generated (Figures 3 and 4) using the 20 ARMA models (10 using the BIC and 10 using the AIC) developed from the observed time series of temperature and precipitation. The outputs of these time series models were treated exactly as if they were the observed data, and the second portion of the first Monte Carlo experiment was repeated using these stochastic time series. The only difference was that the number of Monte Carlo simulations, N, varied from 1,000 to 10,000, the exact number proportional to the unusualness of the observed event. If many of the stochastically generated time series contain unusual events, i.e., climate fluctuations, then this would be consistent with the null hypothesis, despite what may have been implied based on the first Monte Carlo experiment.

3. Results

The results of the first Monte Carlo experiment are given in Tables 1 and 2. They suggest that the climate record does, indeed, contain a large number of "unusual events." Of the 10 time series modeled, unusual climate fluctuations occurred in every season. A total of 26 fluctuations were found. In each of these fluctuations at least one of the two information criteria indicated that the fluctuation was expected to recur in less than 10 percent of the simulations. These fluctuations were about equally divided between changes in level and changes in variability. The fluctuations are just as frequent with respect to precipitation as they are with respect to temperature. Given the number of unusual climate fluctuations it

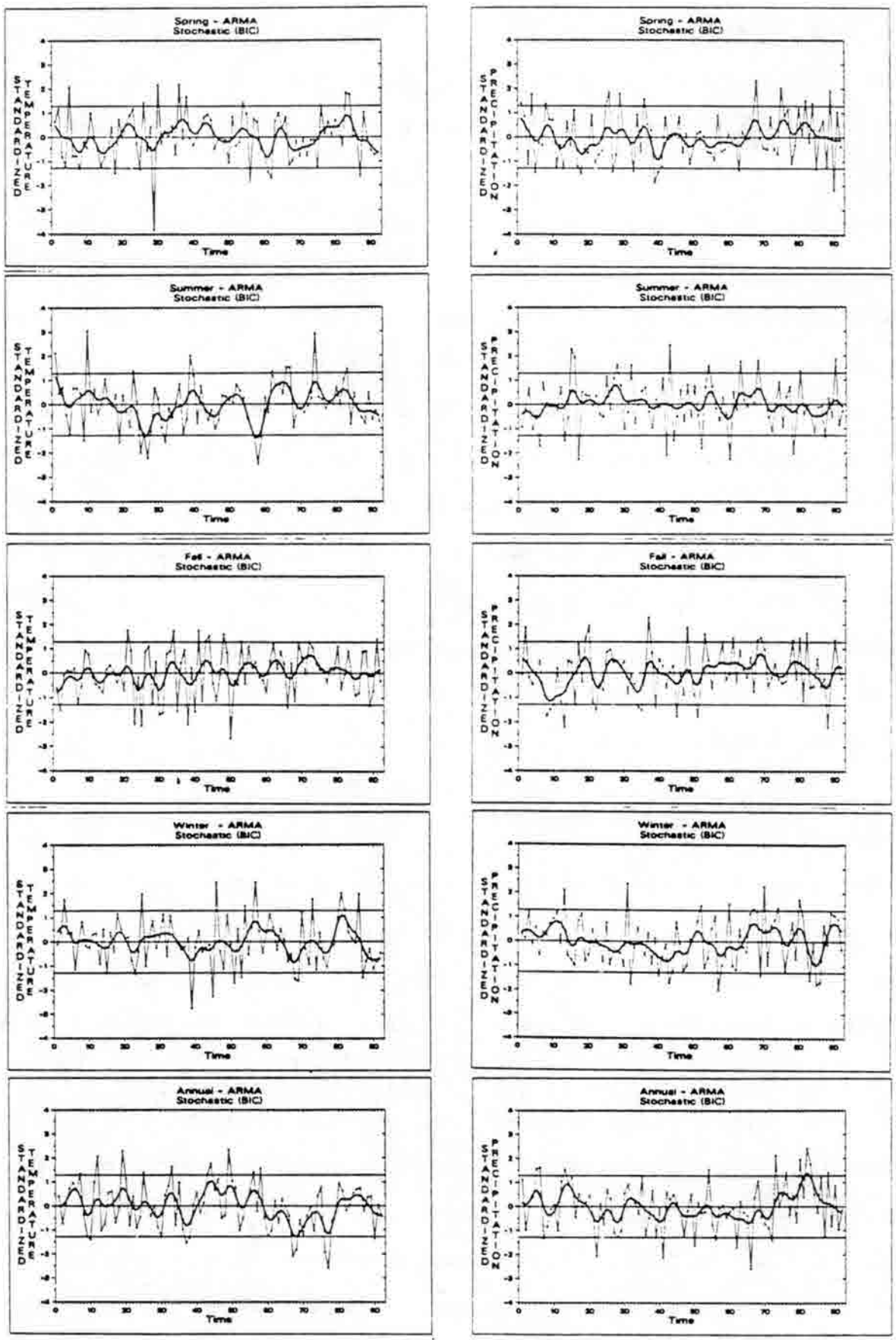

Figure 3. Same as Fig. 1 except the time series are stochastically generated by the ARMA models using the BIC.

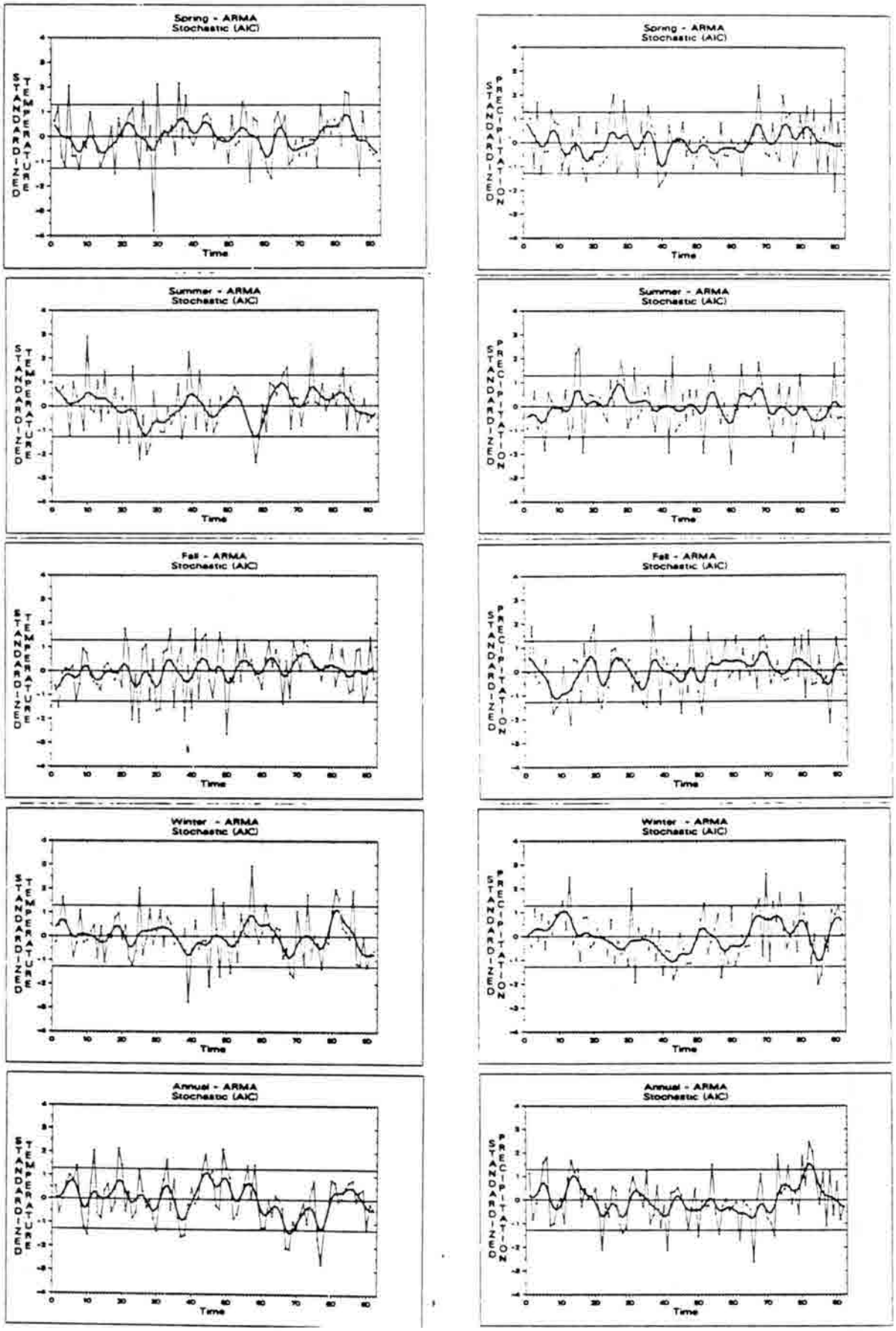

Figure 4. Same as Fig. 3 except the AIC is used.

is quite obvious why the terminology "climate fluctuation" was officially introduced into the climate community by the World Meteorological Organizaton (Mitchell et al., 1966).

At this point it is very tempting to infer that the null hypothesis is invalid, and in order to adequately describe the observed phenomena in the time series in a concise manner some high-order model or some type of intervention analysis would be desirable. For example, the character of the time series could change at some time, t, and then change again at some time, t+i; where i is the length of the fluctuation. There is no reason why these fluctuations must be periodic.

This would invite many theories of climate forcings particularly those proposed years ago by Lorenz (1963) (cf. Figure 2). The evidence from the second Monte Carlo experiment, however, indicates that this viewpoint must be tempered with caution.

The results of the second Monte Carlo experiment are provided in Tables 3 and 4. In these tables the percent of simulations exceeding specific threshold values were based on 1,000 simulations when reported to tenths and 10,000 simulations were reported to hundredths. There are numerous fluctuations depicted in Tables 3 and 4 which are rather unusual, and one such fluctuation was found to be very rare. Specifically, the high variability of the temperature, related to the white noise process corresponding to the fall season, was found in only 2 of 10,000 simulations. Table 5 provides a comparison of the frequency of climate fluctuations for the stochastically generated data compared to the observed data. It is immediately apparent that despite the large number of climate fluctuations identified for the observed series many such fluctuations can be generated from a purely stochastic low-order model with weak or no persistence whatsoever.

Table 3. Same as Table 1 except the climate fluctuations are stochastically generated.

TEMPERATURE

	B	I	C		A	I	C
		TIME	% OF		TIME	% OF	
		TIME	STEPS	SIMULATIONS	TIME	STEPS	SIMULATIONS
TYPE	LIMITS	STEPS	SELECTED	>LIMITS	LIMITS	STEPS	SELECTED	>LIMITS
SPRING — BIC (0,0); AIC (0,0)								
Std	≥1.879	23-30	8	1.2	≥1.879	23-30	8	1.2
Thresh	≤-0.058	67-75	8 of 9	4.6	≤-0.058	67-85	8 of 9	4.6
SUMMER — BIC (0,1), θ_1=0.343; AIC (0,3), θ_1=0.300, θ_2=-0.085, θ_3=0.405								
Thresh	≥-0.182	62-83	20 of 22	3.4	≥-0.180	62-83	20 of 22	5.6
FALL — BIC (0,0); AIC (0,0)								
Std	≤0.548	3-20	18	5.8	≤0.548	3-20	18	5.8
Va	≥/1.104/	21-51	20 of 30	0.02	≥/1.104/	21-51	20 of 30	0.02
WINTER — BIC (0,0); AIC (1,1), ϕ_1=-0.827, θ_1=0.981								
Va	≥/0.949/	68-90	13 of 23	12.6	≥/1.061/	68-90	13 of 23	4.6
ANNUAL — BIC (0,0); AIC (1,0), ϕ_1=-0.171								
Mean	≥0.824	42-51	10	10.0	≥0.912	42-51	10	15.2
Mean	≤-0.701	59-79	21	0.2	≤-0.783	59-79	21	0.4
TYPE	LIMITS	TIME STEPS	TIME STEPS SELECTED	% OF SIMULATIONS >LIMITS	LIMITS	TIME STEPS	TIME STEPS SELECTED	% OF SIMULATIONS >LIMITS
	B	I	C		A	I	C	

Table 4. Same as Table 2 except the climate fluctuations are stochastically generated.

PRECIPITATION

	B	I	C		A	I	C
			TIME	% OF		TIME	% OF
		TIME	STEPS	SIMULATIONS		STEPS	SIMULATIONS
TYPE	LIMITS	STEPS	SELECTED	>LIMITS	LIMITS	STEPS	SELECTED	>LIMITS
SPRING — BIC (0,0); AIC (0,1), θ_1=0.092								
Va	≥/1.044/	1-41	20 of 30	1.8	≥/0.971/	1-41	20 of 41	8.6
Std	≤0.557	42-62	21	2.4	≤0.550	42-62	21	3.8
SUMMER — BIC (0,0); AIC (0,1), θ_1=0.193								
NULL								
FALL — BIC (1,0), ϕ_1=0.141; AIC (1,0), ϕ_1=0.141								
Thresh	≥-0.748	52-80	29 of 29	0.8	≥-0.748	52-80	29 of 29	0.8
WINTER — BIC (0,0); AIC (2,0), ϕ_1=0.045, ϕ_2=0.326								
Thresh	≥-0.118	1-13	12 of 13	9.8	≥-0.181	1-13	11 of 13	50.6
Va	≥/0.909/	66-74	8 of 9	5.8	≥/0.851/	66-74	8 of 9	15.4
ANNUAL — BIC (0,0); AIC (0,1), θ_1=0.131								
Thresh	≤0.212	55-66	12 of 12	4.8	≤0.042	55-67	13 of 13	1.2
Va	≥/0.848/	5-15	9 of 11	13.8	≥/0.899/	5-15	9 of 11	9.0
TYPE	LIMITS	TIME STEPS	TIME STEPS SELECTED	% OF SIMULATIONS >LIMITS	LIMITS	TIME STEPS	TIME STEPS SELECTED	% OF SIMULATIONS >LIMITS
		B	I	C		A	I	C

Table 5. Number of fluctuations which were identified in the observed and stochastically generated data which are expected to occur in less than 10%, 5%, 1%, or 0.1% of the time series of length, n = 92, based on both the AIC and BIC.

	OBSERVED DATA	STOCHASTICALLY GENERATED DATA
<10%	24	10
<5%	18	7
<1%	6	3
<0.1%	1	1

The question was pursued regarding whether high-order ARMA models would more readily reproduce the observed climate fluctuations. For this purpose, the maximum order of the models which either the BIC or AIC would evaluate was increased to $p \leq 20$ if $q = 0$, $q \leq 20$ if $p = 0$, and $p + q \leq 10$. Tables 6 and 7 indicate that in five of the 10 seasons a higher-order ARMA was selected based on the AIC, but using the BIC a high-order model was selected in only two of the 10 seasons. As indicated in the tables, the use of high-order ARMA models cannot readily explain the observed climate fluctuations. Some fluctuations do appear to recur with increased frequency, but some fluctuations are found less often.

4. Discussion and Conclusions

Several points need to be addressed regarding the results and the implications of the results. These include:

1) Should any significance be attached to the fact that more than twice as many fluctuations were identified in the observed data compared to the stochastic data?
2) If no significance is attached to the differences, does this imply that all the climate fluctuations identified in the observed data are likely to be the result of a purely stochastic process?
3) What are the implications of these results in detecting semi-permanent climate change?
4) Do these results have any bearing on the use of climate normals?

The first two points are related and they will be treated together. It is difficult to ascribe much significance to the fact that the observed data contain more fluctuations than the stochastic data for several reasons. First, the models themselves may not be perfectly identified. For example, the order of the model may be too low or too high for the observed data, but

Table 6 Comparison of the frequency of observed climate fluctuations as simulated by time series generated using high-order ARMAs versus low-order ARMAs. Model coefficients are the high-order model identified by AIC or BIC. Abbreviations are the same as in Table 1, NA implies not applicable.

TEMPERATURE

SPRING --- AIC (2,7); $\phi_{1...2}$ = -0.834, -0.582
$\theta_{1...7}$ = 0.658, 0.553, -0.448, -0.124, 0.237, -0.087, -0.231

				% OF SIMULATIONS>LIMITS			
			YEARS	LOW ORDER		HIGH ORDER	
TYPE	LIMITS	YEARS	SELECTED	BIC	AIC	BIC	AIC
Std	≥1.376	1906-25	20	NA	6.54	NA	13.76
Va	≤/1.218/	1951-74	24 of 24	NA	2.06	NA	4.37

SUMMER --- BIC (1,5); AIC (1,5); ϕ_1 = -0.640
$\theta_{1...5}$ = 0.946, 0.132, 0.381, 0.457, 0.357

Mean	≤-0.887	1902-17	16	1.74	4.18	9.92	9.92
Thresh	≥0.602	1930-40	11 of 11	0.04	0.14	0.35	0.35
Va	≤/1.169/	1954-85	31 of 32	1.52	1.88	2.23	2.23

ANNUAL --- BIC (5,4); AIC (5,4); $\phi_{1...4}$ = 0.255, -0.162, -0.059, 0.756
$\theta_{1...5}$ = -0.811, 0.432, 0.356, -0.949, -0.167

Thresh	≤0.479	1895-1920	24 of 26	3.54	7.18	1.61	1.61
Std	≥1.304	1912-41	30	1.88	2.22	29.21	29.21
Mean	≥0.524	1921-59	39	0.00	0.06	0.00	0.00
Thresh	≤-0.061	1960-85	20 of 26	1.62	3.80	0.07	0.07
Std	≤0.502	1955-77	23	0.14	0.26	5.16	5.16
TYPE	LIMITS	YEARS	YEARS SELECTED	BIC	AIC	BIC	AIC
				LOW ORDER		HIGH ORDER	
				% OF SIMULATIONS>LIMITS			

Table 7 Same as Table 6 except for precipitation.

PRECIPITATION

FALL --- AIC (4,3); $\phi_{1...4}$ = 0.391, -0.216, -0.866, 0.177
$\theta_{1...3}$ = -0.416, 0.358, 0.900

				% OF SIMULATIONS>LIMITS			
			YEARS	LOW ORDER		HIGH ORDER	
TYPE	LIMITS	YEARS	SELECTED	BIC	AIC	BIC	AIC
Thresh	≤-1.856	1952-56	3 of 5	NA	2.06	NA	0.13
Mean	≥0.751	1970-85	16	NA	4.46	NA	0.00

WINTER --- AIC (2,3); $\phi_{1...2}$ = -0.647, -0.796
$\theta_{1...3}$ = 0.703, 0.679, -0.262

Thresh	≥0.005	1905-15	10 of 11	NA	5.26	NA	5.86
Std	≥1.953	1976-82	7	NA	4.44	NA	8.63
Va	≥/2.006/	1930-86	3 of 7	NA	10.00	NA	13.22
TYPE	LIMITS	YEARS	YEARS SELECTED	BIC	AIC	BIC	AIC
				LOW ORDER		HIGH ORDER	
				% OF SIMULATIONS>LIMITS			

it is perfectly specified for the stochastic data. Second, the coefficients of each model are not known exactly, but they are known exactly in the stochastic model. Third, the observed data are transformed and standardized by the normal (temperature) and gamma (precipitation) distributions. The observed data are not likely to be perfectly represented by these distributions despite the fact that tests of normality of the standardized data (Skewness and Kurtosis tests) cannot reject such an assumption; but the stochastic data are perfectly represented by the normal distribution as they are generated from such a distribution. All of these differences lead to some of the uncertainty associated with any one model, and therefore enhance the chance of finding more unusual multi-year fluctuations in the observed data than would otherwise occur. On the other hand, the fact that rather large differences occur leaves open the possibility that some type of intervention model may be more appropriate or that the climate system contains long-range dependency. This suggests that some of the observed fluctuations have arisen due to any number of external or internal climate forcings. In fact, it could be argued with respect to changes in level that most of the contribution to the weak autocorrelations arise because of the climate fluctuations themselves. That is, the actual change in level leads to an apparent persistence in the full period of record. This is similar to the problem Klemes (1974) discusses in connection with the use of the infinite memory of the fractional Brownian model to explain Hurst's phenomenon. He uses the example of a perfectly stationary 10,000-year record of lake levels which at year 10,001 water begins to be secretly siphoned off the lake. In such a time series an analyst with a 20,000-year record would suspect, based on the spectral density of the time series, that the processes affecting lake levels have an infinite memory. Of course, such an assertion would be totally false. A more appropriate representation

of the process would include an intervention component at time, t = 10,001. In this regard the infinite memory of the process would vanish. Unfortunately, in practice without knowledge of such interventions the blind search for such breaks, as has been conducted in this article, produces so many discontinuities that the separation of deterministic from stochastic discontinuities is impossible with a priori information. The recent work of Lorenz (1984) and the results presented here, however, suggest that the challenge of developing methods and a model to test for feedbacks such as suggested by Lorenz (1984) may prove quite important.

The most important and robust conclusion that can be drawn from this analysis is in the form of a warning aimed at those who may be tempted to project ongoing climate fluctuations or those who propose physical explanations of climate fluctuations from an a posteriori view. Specifically, many (but not necessarily all) of the observed climate fluctuations, even the highly unusual events, are the result of a unique sequence of seasonal climate anomalies which need only be explained on a season-by-season basis with perhaps some physically-based weak year-to-year persistence of anomalies.

The implications of these results with respect to the detection of climate change are clear. During an ongoing unusual climate event, even one persisting for decades, it is extremely difficult to convincingly demonstrate through statistics that a climate change, i.e., a new mean or variance, is or has taken place without strong and clearly defined a priori reasons for suggesting that such a change is expected. Ellsaesser et al. (1986) have recently described this problem in context with the current effort to detect the effects of CO_2 and other greenhouse gases on the surface temperature record. Epstein (1982) also discusses this problem from

a Bayesian and Classical Statistics viewpoint with respect to a prior specification of the functional form of any expected climate change.

Finally, the results emphasize the limited usefulness of 30-year climate normals. This has been pointed out by many in the context of predicting next year's climate (Sabin and Shulman, 1985; Lamb and Changnon, 1981; Craddock, 1981; Court, 1967-68). But in addition, practically significant decadal fluctuations are often embedded within 30-year time averages. If, for example, climate normals are redefined every decade (as recommended by the World Meteorological Organization) it would be very desirable to model the historical data, perhaps using ARMA techniques, and simulate the probability of 2, 3, 4...30-year means and/or variances above or below various threshold values. Even if the climate system is non-stationary over periods of decades, these ARMA derived "normals" would prove much more useful for long-range operations and planning than the traditional 30-year means.

Acknowledgements

This work has been largely supported by the Carbon Dioxide Research Division of the Department of Energy under contract number DE-FG02-85ER60372 and the National Climate Program Office's support of CLIMPAX (the Climate Impact Perception and Adjustment Experiment).

The comments by Drs. Richard Katz, Tim Barnett, Jerome Namias, James Koss, and Robert Quayle on the first draft of this manuscript are gratefully acknowledged. Discussions with Drs. Edward Epstein and Edward Lorenz are also acknowledged. The work reported may not necessarily reflect their views.

REFERENCES

Box, G. E. P. and G. M. Jenkins, 1976: Time Series Analysis: Forecasting and Control, Holden-Day, San Francisco, CA, 575 pp.

Changnon, S. A., Jr., 1987: An assessment of climate change, water resources, and policy research. Water International, 12, 69-76.

Court, A., 1967-68: Climatic normals as predictions: Parts I-V. Sci. Rep. Air Force Cambridge Research Lab., Bedford, MA, Contract AF19 (628)-5176 (NTIS AD-657 358, AD-686 163, AD-672 268, AD-687 137, AD-687 138).

Craddock, J. M., 1981: Monitoring a changing climate series. J. Climatology, 1, 333-343.

Diaz, H. F., 1986: An analysis of twentieth century climate fluctuations in Northern North America. J. Clim. Appl. Meteor., 25, 1625-1657.

Douglas, A. V., D. R. Cayan and J. Namias, 1982: Large-scale changes in North Pacific and North American weather patterns in recent decades. Mon. Wea. Rev., 110, 1851-1862.

Ellsaesser, H. W., M. C. MacCracken, J. J. Walton and S. L. Grotch, 1986: Global climatic trends as revealed by the recorded data. Rev. of Geophys., 24, 745-792.

Gates, W. L. and M. C. MacCracken, 1985: The challenge of detecting climate change by increasing carbon dioxide. (U.S. Dept. of Energy, DOE/ER-0235, Washington, D.C. 20545) 1-12. M. C. MacCracken, F. M. Luther (Eds.), Detecting the Climatic Effects of Increasing Carbon Dioxide.

Gilliland, R. L. and S. H. Schneider, 1984: Volcanic CO_2 and solar forcings of northern and southern hemisphere surface air temperature. Nature, 310, 38-41.

Hansen, J., D. Johnson, A. Lacis, S. Lebedeff, P. Lee, D. Rind and G. Russell, 1981: Climatic impact of increasing atmospheric carbon dioxide. Science, 213, 957-966.

Harvey, A. C., 1981: Time Series Models, Phillip Allen Publ., 222 pp.

Hurst, H. E., 1957: A suggested statistical model of some time series which occur in nature. Nature, 180, 494.

Karl, T. R., R. E. Livezey and E. S. Epstein, 1984: Recent unusual mean winter temperatures across the contiguous United States. Bull. Amer. Meteor. Soc., 65, 1302-1309.

Karl, T. R. and W. E. Riebsame, 1984: The identification of 10- to 20-year temperature and precipitation fluctuations in the contiguous United States. J. Clim. Appl. Meteor., 23, 950-966.

Karl, T. R., C. N. Williams, Jr., P. J. Young and W. Wendland, 1986: A model to estimate the time of observation bias associated with monthly mean maximum, minimum, and mean temperatures for the United States. J. Clim. Appl. Meteor., 25, 145-160.

Karl, T. R. and P. J. Young, 1986: Recent heavy precipitation in the vicinity of the Great Salt Lake: Just how unusual? J. Clim. Appl. Meteor., 25, 353-363.

Kates, R. W., 1980: Climate and society: Lessons learned from recent events. Weather, 35, 17-25.

Katz, R. W., 1982: Statistical evaluation of climate experiments with general circulation models: A parametric time series modeling approach. J. Atmos. Sci., 39, 1446-1455.

Kay, P. A. and H. F. Diaz, eds., 1985: Problems and prospects for predicting Great Salt Lake levels. Center for Public Affairs and Administration, University of Utah, May, 1985, 309 pp.

Klein, W. H., 1983: Objective specification of monthly mean surface temperature from 700 mb heights in winter. Mon. Wea. Rev., 111, 674-691.

Lamb, H. H. and A. I. Johnson, 1961: Climatic variation and observed changes in the general circulation. Geogr. Ann., 41, 363-400.

Lamb, P. J. and S. A. Changnon, Jr., 1981: On the "best" temperature and precipitation normals: The Illinois situation. J. Appl. Meteor., 20, 1383- .

Lorenz, E. N., 1963: The mechanics of vacillation, J. Atmos. Sci., 20, 448-464.

Lorenz, E. N., 1984: Formulation of a low order model of a moist general circulation. J. Atmos. Sci., 41, 1933-1945.

Lorenz, E. N., 1986: The index cycle is alive and well. Namias Symposium, Lib. Cong. #86-50752, 188-196.

Madden, R. A. and V. Ramanathan, 1980: Science, 209, 763-768.

Mandelbrot, B. B. and J. R. Wallis, 1969a: Computer experiments with fractional Gaussian noises, 1, Averages and variances; 2, Rescaled ranges and spectra; 3, Mathematical appendix. Water Resour. Res., 5, 222-267.

Mandelbrot, B. B. and J. W. Van Ness, 1968: Fractional Brownian nations, fractional noises and applications. SIAM Rev., 4, 422-437.

Mandelbrot, B. B. and J. R. Wallis: Some long-run properties of geophysical records. Water Resour. Res., 5, 321-340.

McCleary, R. and R. A. Hay, Jr., 1980: Applied Time Series Analysis for the Social Sciences, Sage Publications, 331 pp.

Mitchell, J. M., Jr., 1976: An overview of climate variability and its casual mechanisms. Quaternary Research, 6, 481-493.

Mitchell, J. M., Jr., B. Dzerdzeevskii, H. Flohn, W. L. Hofmyer, H. H. Lamb, K. N. Kao and C. C. Wallen, 1966: Climatic Change Technical Note 79, World Meteorological Organization. WMO-No. 195, T.P. 100, Geneva, Switzerland, 79 pp.

Namias, J., 1978: Multiple causes of the North American abnormal winter of 1976-77. Mon. Wea. Rev., 106, 279-259.

Namias, J., 1978: Persistence of U.S. seasonal temperatures up to one year. Mon. Wea. Rev., 106, 121-131.

O'Connell, P. E., 1971: A single stochastic modeling of Hurst's law. In Proceedings of the International Symposium on Mathematical Mode in Hydrology, International Association of Scientific Hydrology, Warsaw, 327-358.

Panofsky, H. A. and G. W. Brier, Some Applications of Statistics to Meteorology, Penn. State Univ. (1968) (see Appendix III).

Priestly, M. B., 1981: Spectral Analysis and Time Series, Academic Press, 890 pp.

Quinn, F. H., 1986: Causes and consequences of the record high 1985 Great Lakes Water levels. Ameri. Meteor. Soc. Conf. on Climate and Water Management, Asheville, NC, 281-290.

Rasmusson, E. M. and J. M. Wallace, 1983: Science, 222, 1195-1201.

Rodriguez-Iturbe, I., J. M. Mejia and D. R. Dawdy, 1972: Streamflow stimulation, 1, A new look at Markovian models, fractional Gaussian noise and crossing theory; 2, the broken line process as a potential model for hydrological simulation. Water Resour. Res., 8, 921-941.

Sabin, T. E. and M. D. Shulman, 1985: A statistical evaluation of the efficiency of the climate normal as a predictor. J. Climatology, 5, 63-77.

Schwarz, G., 1978: Estimating the dimension of a model. Am. Statist., 6, 461-464.

Thompson, L. M., 1975: Weather variability, climatic change, and grain production. Science, 188, 535-541.

van Loon, H. and J. Williams, 1976: The connection between trends of mean temperature and circulation at the surface. Post I: Winter. Mon. Wea. Rev., 104, 1003-1011.

Walsh, J. E., D. R. Tucek and M. R. Peterson, 1982: Seasonal snow cover and short-term climate fluctuations over the United States. Mon. Wea. Rev., 110, 272-286.

Warrick, R. A., 1980: Drought in the Great Plains: A case study of research on the climate and society in the USA. In Ausubel, J. and Biswas, A. K. (Eds.), Climatic Constraints and Human Activities, 93-124, Pergamon, NY.

Nonthermometric Measurement of Recent Temperature Variability over the Coterminous United States, Southern Canada and Alaska

Patrick J. Michaels
David E. Sappington
Bruce P. Hayden
David Stooksbury
Center for the Study of Global Environmental Change, and
Department of Environmental Sciences
University of Virginia
Charlottesville, Virginia 22903

Abstract

We present a temperature proxy for the United States, southern Canada, and the surrounding oceans for 1885-1985 that does not suffer from station biases inherent in thermometric records. Calculated annual mean temperatures rose over the region approximately 1.7°C from 1895 to 1955, and then fell by 0.7°C from 1955 to 1975. By 1985, calculated temperatures were 0.3°C above the mean for the last 100 years. In the absence of other compensating factors, the results indicate secular temperature variability is approximately twice the thermometrically measured value.

A companion analysis of north Alaskan temperatures, where proxy records suggest major warming some time in the last century, shows no secular trend in mean temperature from 1948 through 1985.

The temperature proxy is based upon the 1000-500 mb thickness. 500 mb heights prior to 1948 were statistically estimated with cyclone frequency eigenvectors. Because the Alaskan cyclone data has not been tabulated, analysis there was only from 1948 through 1985.

1. Introduction

Kukla et al. (1986) recently noted a substantial warming of some United States temperature records resulting from local changes at stations with populations previously thought to be too small to promote "urban" warming. Over the last forty years they calculated that the U.S. first order station temperatures are progressively overestimated by approximately 0.12°C per decade. Jones et al. (1986) attempted to remove urban and site-change biases in hemispheric records, but the number of stations showing urban warming was proportionally very small when compared to that in Kukla et al. (1986). Nonetheless, Ellsaesser et al. (1986) compared virtually all available long-term records of hemispheric temperature including those of Jones et al. (1986) and found correlations averaging approximately 0.85 between various thermometric summaries.

There are several ongoing attempts to remove station bias from the thermometric records using population data, but recent ones, by Karl et al. (1987, in press) and Hansen (1987, in press) give conflicting results. In this paper, we report a temperature proxy for the last 100 years, over the United States and southern Canada, that does not suffer from site effects

and has very low instrumental bias. A companion analysis over Alaska extends back to 1948.

2. Cyclone Tracks and 500 mb Heights: United States and Southern Canada

We first calculated mean annual 500 mb heights based on the 23 stations that regularly report from 55 to 125 West and 22.5 to 55 North--roughly the United States, southern Canada, and the surrounding oceans (Figure 1). The length of record was from 1948-1980, which is the period of digitized data availability for the combined U.S. and Canadian regions; the Canadian data is not summarized after 1980. We found no reports in the refereed literature concerning systematic temporal biases in height figures over the region we studied.

The mean annual heights were then statistically related to eigenvectors of cyclone frequency over the region. The methodology for calculation of the eigenvectors is given in Hayden (1981). Temperate cyclones form and move along thickness gradients, so 500 mb height fields would be expected to relate to changes in cyclone frequency eigenvectors. Note that these eigenvectors describe large and persistent patterns of cyclone distribution, which should be associated with changes in the thickness field of similar dimension. The first five were entered as possible predictors of the mean 500 mb height over the region, but only two (the second and third; see Hayden (1981) for a map of weightings) were retained in the final equation with the inclusion limits set at $\alpha = .05$. Multiple correlation between the two fields was .73, and the relationship was significant at the .0001 level ($F_{2,30} = 11.73$).

The Hayden data does not include cyclone frequency counts over mountainous regions of the western U.S. during the period 1958-76; we empirically estimated these values from the existing eastern data prior to the regression between cyclone eigenvectors and 500 mb heights. We then used the empirical cyclone eigenvector/500 mb height equation to calculate mean annual 500 mb heights over the region from 1885 to 1985. Results are shown in Figure 2.

3. Temperature Reconstructions

The height curve bears considerable superficial resemblance to hemispheric and regional temperature histories, such as those of Diaz and Quayle (1980) or Jones et al. (1986). Perhaps coincidentally, 1895, the year of furthest south deep snow cover in North America (see Ludlam, 1982), also has the lowest calculated mean 500 mb height.

Using the calculated 500 mb heights and the observed mean surface pressure from the 5 X 5 degree historical record from the National Center for Atmospheric Research (1899-1980) we calculated the mean thickness (Z) of the lower half of the atmosphere over the study region. The hypsometric equation, relating thickness and temperature (see, for example, Barry and Perry, 1973) can then be used to calculate regional mean annual temperatures. These are shown in Figure 3.

Figure 4 shows a scatterplot between mean daily surface temperature and thickness departure from normal for over 350 randomly selected days in the

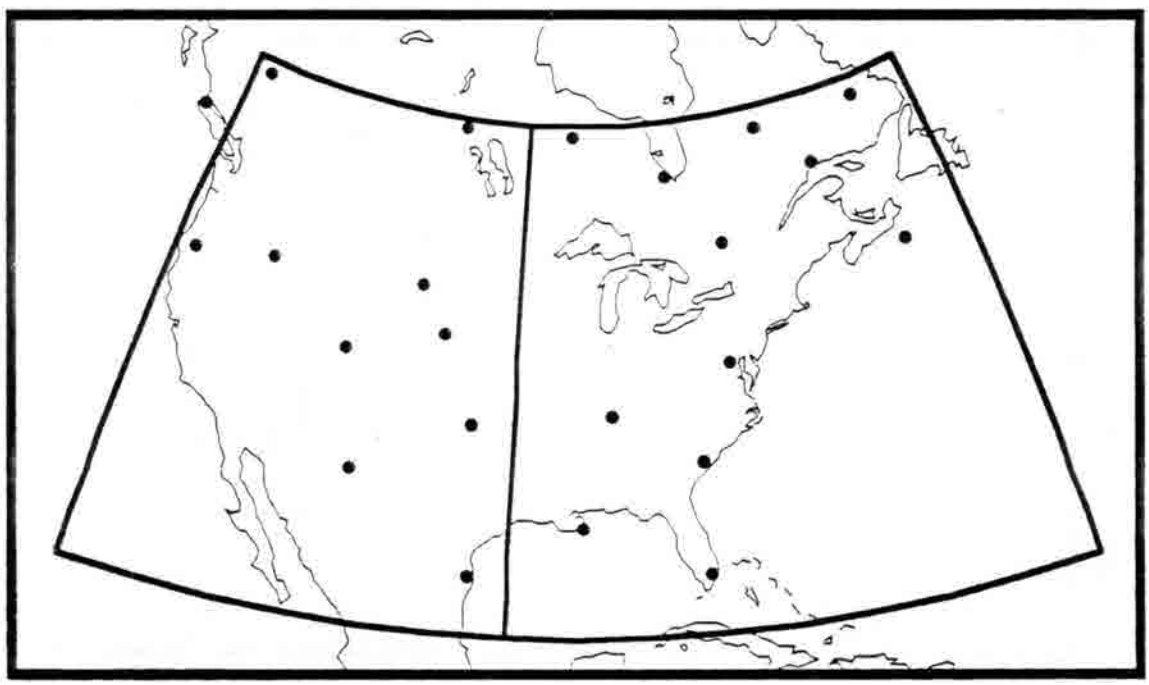

Fig. 1. Spatial domain over the U.S. and southern Canada. Dots indicate station locations for 500 mb data.

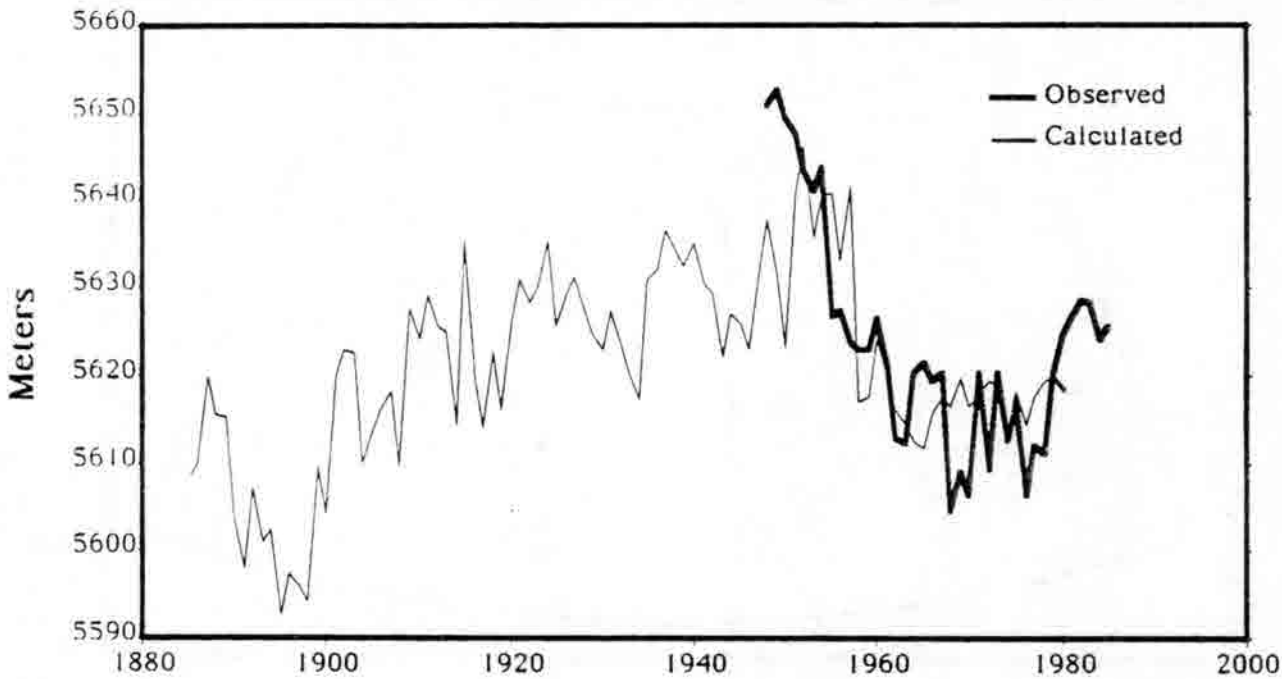

Fig. 2. Observed and calculated mean annual 500 mb height, 1885-1985.

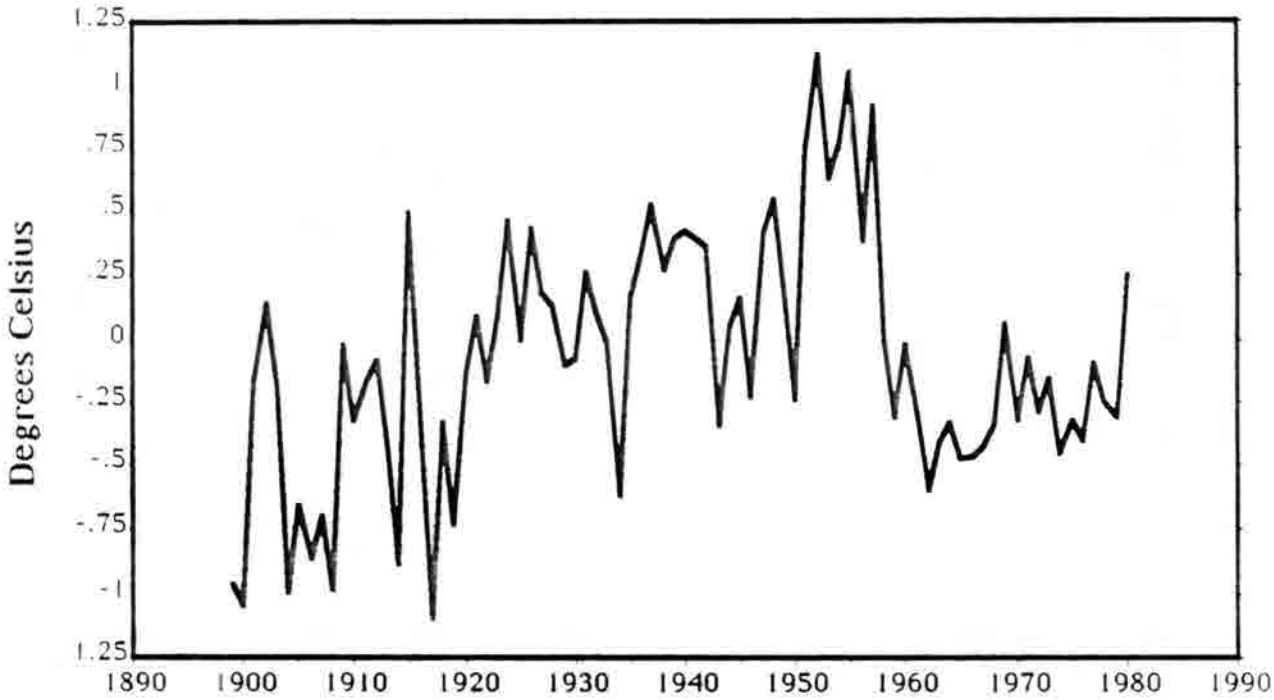

Fig. 3. Mean annual regional temperature 1899-1980, based upon 1000-500 mb thickness proxy calculations.

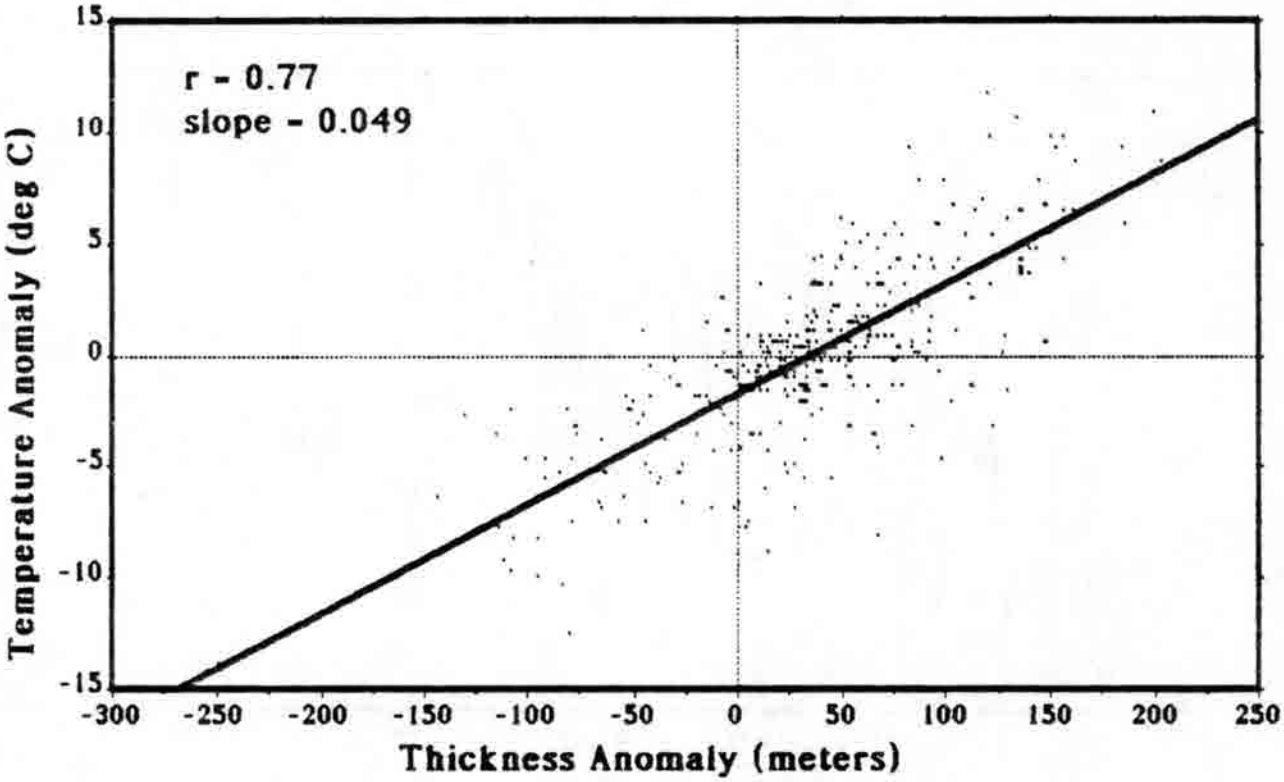

Fig. 4. Scatterplot of 1000-500 mb thickness departure from normal and mean daily temperature departure from normal for 365 randomly selected days.

U.S. As would be expected from the hypsometric equation, the relationship is linear with a slope of 0.049°C/meter change in thickness.

We found the mean warming over entire area between 1899 and 1955 was approximately 1.7°C and the subsequent cooling between 1955 and 1975 was 0.7°. By 1980, temperatures were approximately 0.3° above the mean for the last 85 years.

The gridded surface pressure record is currently unavailable for 1885-1898 and 1981-1985. However, mean annual temperature calculations can be made for the entire 101-year period by not adjusting for surface pressure changes; as shown in Figure 5, through the period of record, the amount of temperature change forced by surface pressure change alone is almost an order of magnitude less than that resulting from changes in 500 mb heights. Ten year running-mean values of the calculated temperature curve for 1885-1985 is shown in Figure 6, along with the gridded mean temperatures (ten year running means) from the same subregion that were used to construct the hemispheric means of Jones et al. (1986). Note that the secular changes from 1899 to 1980 that include the surface pressure adjustment (Figure 3) are not appreciably different from those that formed the running means in Figure 6.

4. Extension to Alaska

Lachenbruch and Marshall (1986) reported evidence that permafrost changes in Alaska might corroborate expected trace gas warming. Their methodology did not allow for discrimination between recent climatic changes and those that might have occurred over the last 100 years.

Our methodology allows for such a discrimination, without the problems normally associated with thermometric measurements. However, the lack of documented cyclone frequency data requires that our analysis be restricted to the observed period of combined surface pressure and 500 mb heights. This extends back only to 1948.

Figure 7 shows thickness-derived mean surface temperatures over the northern half of Alaska from 1948 through 1980; 500 mb station density there is not appreciably different than that in the lower 48 states, and consists of stations at Barrow, Kotzebue, Nome and Fairbanks. Figure 8 extends that analysis through 1985, but does not allow for the small adjustment in temperatures resulting from changes in surface pressure. An inspection of the two curves reveals that, as was the case for the coterminous U.S. and southern Canada, the temperature response to surface pressure adjustment is very small.

Both results show no systematic or significant warming since 1948. The apparent conclusion is that the warming shown in the Lachenbruch and Marshall report took place at a prior time, which is generally conceded to be before important trace-gas related changes would be expected to occur. This is particularly important in light of the high Northern latitude temperature changes predicted by all of the GCM simulations of trace-gas related warming.

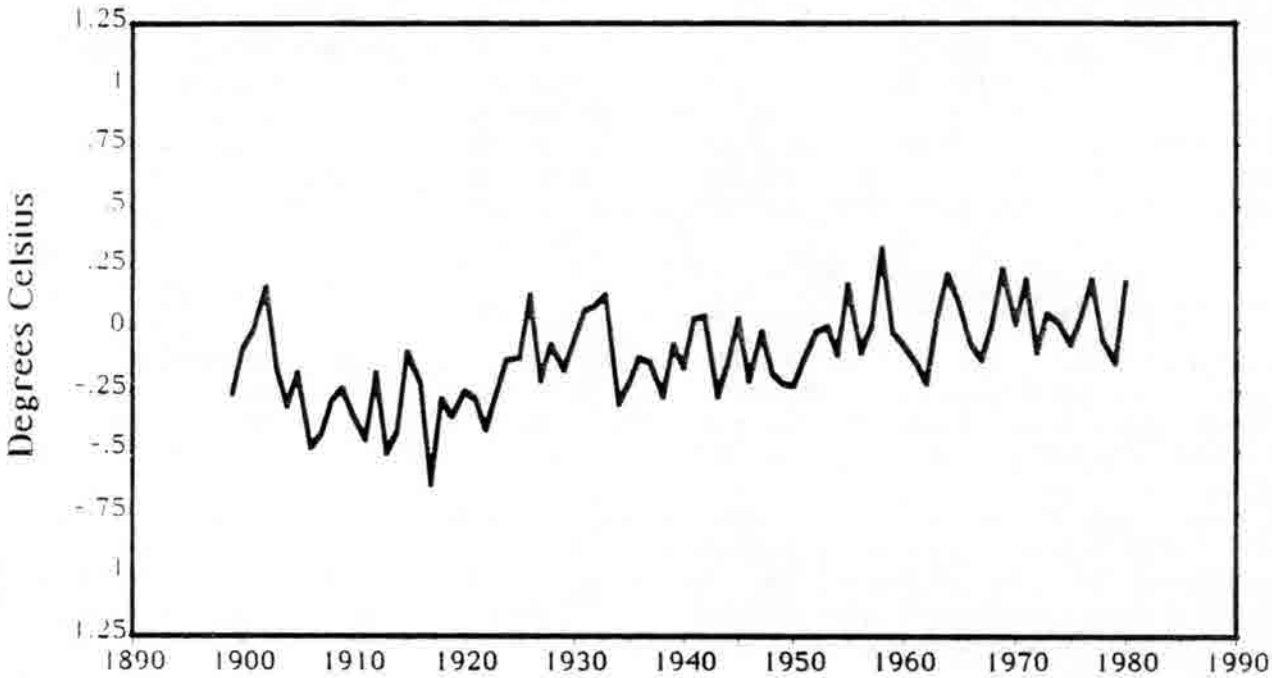

Fig. 5. Surface temperature adjustment implied by the change in mean annual surface pressure (assuming constant 500 mb height), 1899-1980.

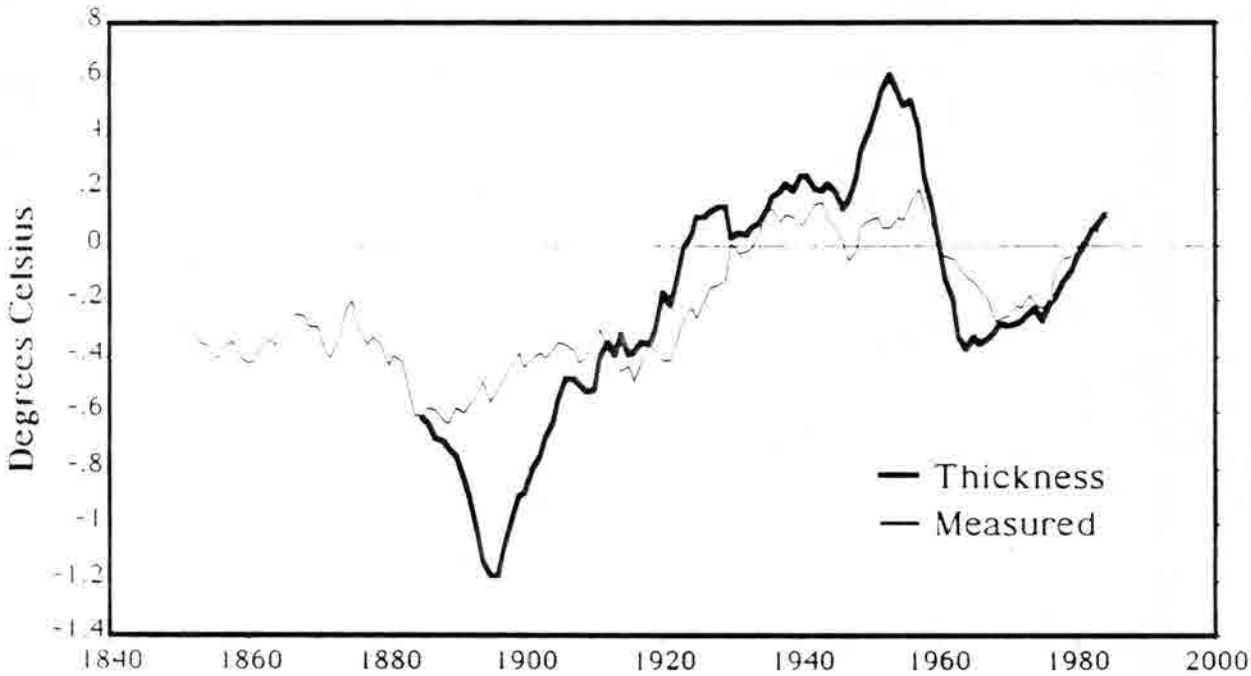

Fig. 6. Ten-year running mean curves of thickness proxy annual mean temperature (thick line) and measured temperatures for the same region from Jones et al. (1986).

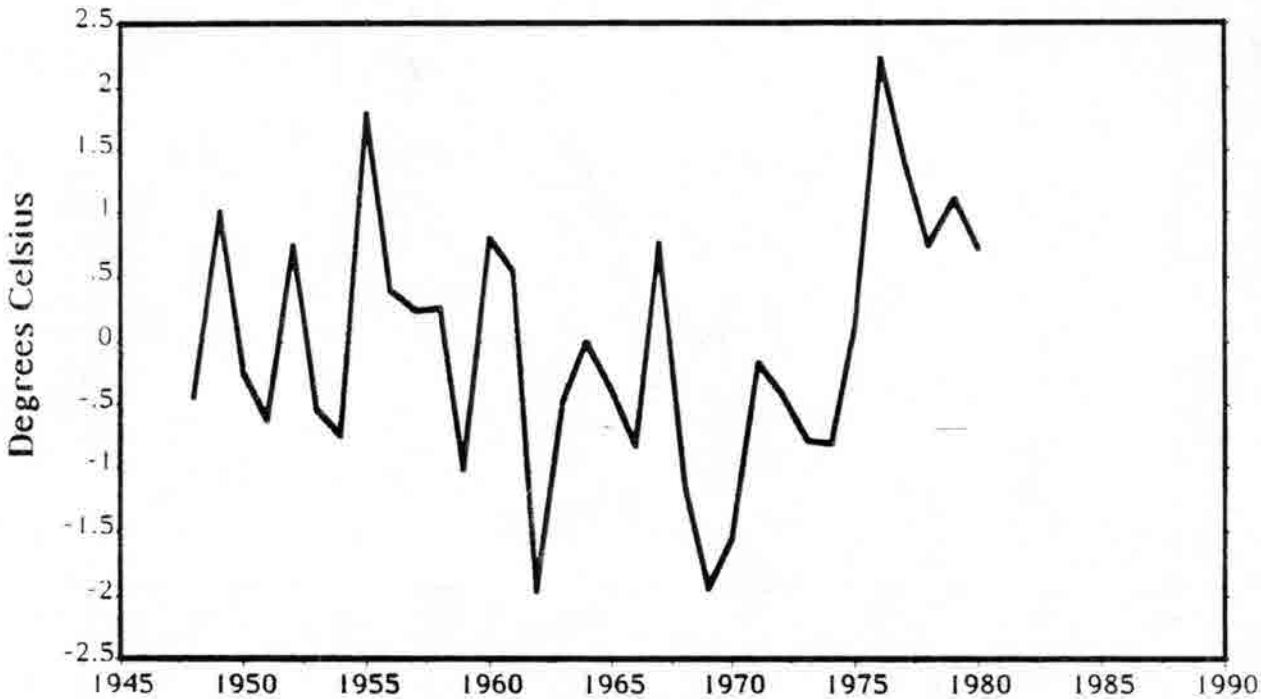

Fig. 7. North Alaskan mean temperature based upon observed 1000-500 mb thickness, 1948-1980.

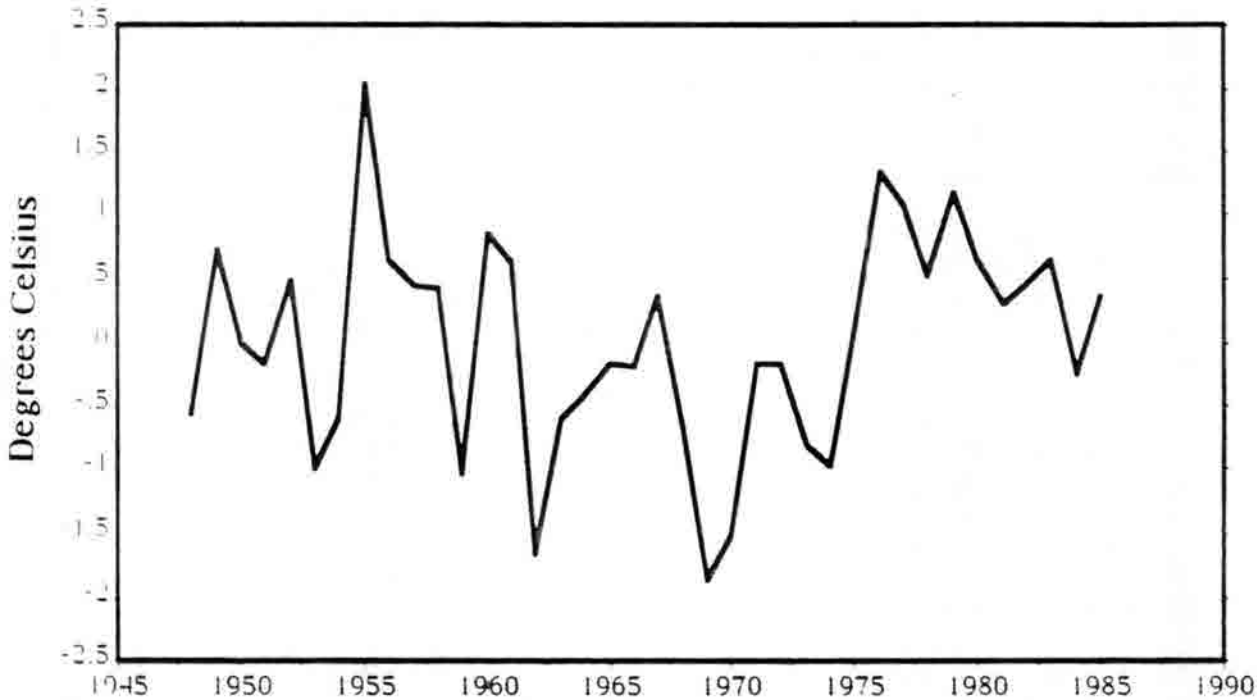

Fig. 8. North Alaskan mean temperature based upon observed 500 mb height changes, 1948-1985, without adjustment for surface pressure.

5. Discussion

The linear correlation coefficient between the 10-year smoothed thickness proxy temperature history, over the coterminous U. S. and southern Canada, and that of Jones et al. for the same period is .87; (Figure 9). This high value results mainly from coincident timing of the major warmup from 1900-1950, the rapid cooling that followed to the 1960's, and the recovery of temperatures through the 1980's. The most significant differences in the curves appear in the late-19th century, when Jones' data set begins to degrade and our regression approach is slightly beyond its calibration range. It is therefore impossible to presently state the reason for that difference.

However, the common perception that statistical models are valid only within their calibration range is not necessarily true; rather this only strictly holds if the boundary conditions determining such a model change as the independent variable exceeds the calibration region. There is no evidence that is true here.

The slope between Jones' smoothed data and our estimates was 0.48 for the period 1885-1985 in the model that neglects the effect of surface pressure change. When the surface pressure data can be used (1899-1980) neither the slope nor the correlation change significantly, with values of 0.49 and 0.85, respectively.

One might argue that these consistent differences result primarily because the two cyclone eigenvectors explain only slightly more than one-half of the variance in the 33-year record of mean 500 mb heights. However, in that case the model would be considered underfit and would tend to predict interannual temperature changes of less than those observed. Conversely, it is hard to accuse a model with a predictor/predictand ratio of 0.06 of being overfit.

The Alaskan results, which only extend from 1948 through 1985, argue that warming related to permafrost changes noted by Lachenbruch and Marshall (1986), occurred prior to 1948. This is earlier than what would be expected from anthropogenic trace gases.

Mitigating Factors

Changes in cloudiness can affect the thickness-temperature relation by raising nighttime temperatures and lowering daytime readings. Our use of daily means partially compensates for this behavior.

Two recent studies of U.S. cloudiness by Henderson-Sellers (1986) and Seaver and Lee (1987) do not support the proposition that either the history of Jones et al. (1986) or our derived curve is being affected by cloudiness. Henderson-Sellers found rather monotonic increases in U.S. cloud cover from 1900 through 1954, and Seaver and Lee found, on the aggregate, that this trend does not reverse through 1982, although they only compared the 1950-1982 period to a 1930-1936 base. This combination of findings is not consistent with the decline in smoothed mean temperature from 1950 to 1980 that appears in both curves.

Additional modifications to thickness-derived temperatures can occur because of increasing wind speed or surface moisture, but no recent findings

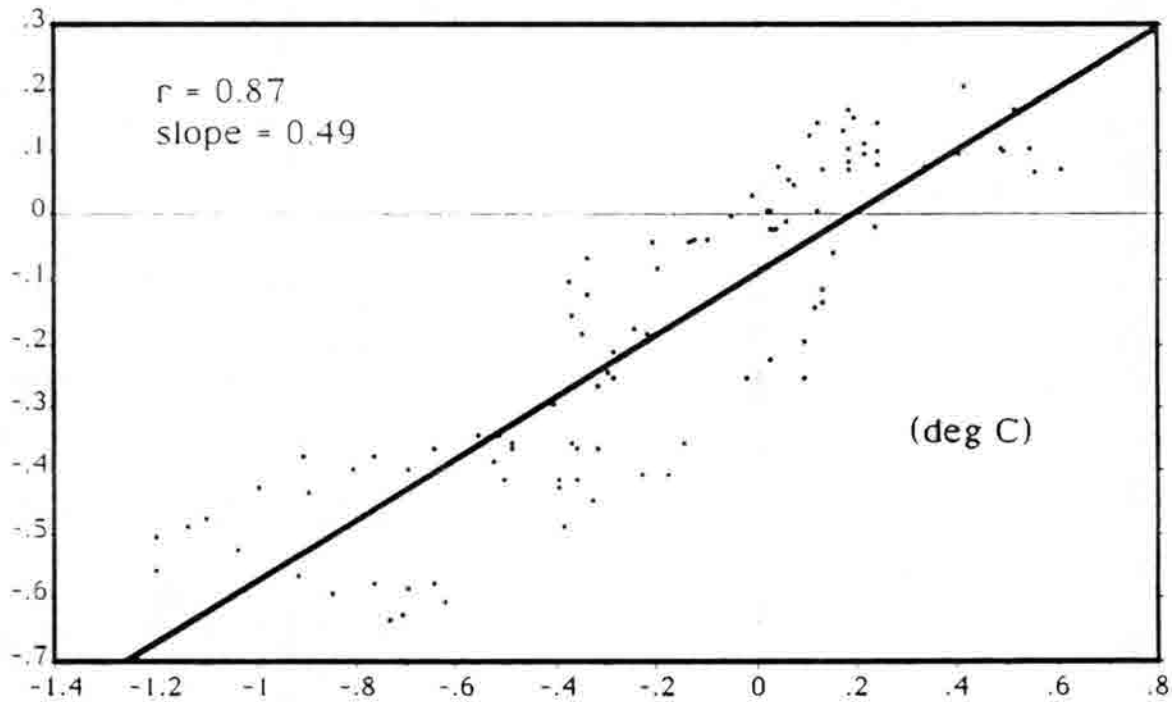

Fig. 9. Scatterplot of thickness proxy annual mean temperature (X) vs. measured temperatures (Y) for the same region from Jones et al. (1986) using data from Fig. 6.

correlate well with either curve. Bradley et al. (1987) note a secular rise in U.S. precipitation that is concurrent with a slight decrease in mean temperature, but note no other compensating secular trend through the major warmup of the first half of the twentieth century in this region.

Our results allow only a tentative conclusion that thermometric-based measurement underestimates secular climatic variability by a factor of two. Such a conclusion would be strengthened by inclusion of missing data cyclone data from the mountainous regions for 1958-76, rather than by their empirical estimation from eigenvectors over the remaining area. More convincing evidence would be reproducibility over other regions, such as Europe, much of Alaska, and a portion of the Far East, where suitable height and cyclone data exist. Our Alaskan analyses, which currently extend only back to 1948, also argue against any detectable anthropogenic trace-gas signal to date.

Our findings primarily corroborate the recent report by Wigley (1987) that indicates that GCM estimates of trace-gas related warming are either too high or suffer from oceanic thermal storage that cannot be accounted for by current theoretical estimates.

If it indeed turns out that observed variability remains twice the thermometrically measured value, there are several important ramifications:

Our estimates of the "natural variability" of temperature will have to be doubled, as the major warmup was prior to most of the rise in trace gases. Further, the predicted climatic change in these regions from trace gases may actually turn out to not be appreciably different in magnitude to one already experienced in the twentieth century. Determination of the causes of such climatic excursions remains a scientific challenge.

Secular variation of such magnitude may have considerable ecological effects. For example, assuming that a warmup of 1.7°C in the first half of the century over the U.S. and southern Canada was equally distributed throughout the seasons, the change in growing degree days in forest simulation models of Shugart (1984) would be sufficient to simulate a decline in eastern North American forests similar to ones currently ascribed to acid precipitation. Muller-Dombois (1987) recently argued that a substantial portion of the recent "dieback" of large forest regions is related to climatic variability of unknown magnitude and extent operating on mature even-aged stands.

Finally, a thickness-based temperature may prove to be more representative of the output of circulation model simulations of the present and future climate than the ground-based thermometric record, as local site effects and diurnal temperature redistributions are currently not specified because of computational limitations.

Acknowledgements

This research was supported by the Commonwealth of Virginia. I thank Thomas R. Karl of the National Climatic Data Center, David Policansky of the National Research Council, Alan Hecht of the National Climate Program Office, Michael MacCracken of Lawrence Livermore National Laboratory, and Alan Howard, H. G. Goodell, and Herman H. Shugart of the University of Virginia for valuable criticism. Ms. M. Mossler assisted in technical aspects of manuscript preparation.

REFERENCES

Barry, R. G., and Perry, A. H.: 1973, Synoptic Climatology: Methods and Application, Methuen, London, 555 pp.

Bradley, R. S., Diaz, H. F., Eischeid, J. K., Jones, P. D., Kelly, P. M., and Goodess, C. M.: 1987, 'Precipitation Fluctuations over Northern Hemisphere Land Areas Since the Mid-19th Century,' Science **237**, 171-175.

Diaz, H. F., and Quayle, R. G.: 1980, 'The Climate of the United States since 1895: Spatial and Temporal Changes,' Mon. Wea. Rev. **108**, 249-266.

Ellsaesser, H. W., MacCracken, M. C., Walton, J. J., and Grotch, S. L.: 1986, 'Global Climatic Trends as Revealed by the Recorded Data,' Rev. Geophys. **24**, 745-792.

Hansen, J.: 1987 (in press), 'Global Trends of Measured Surface Air Temperature,' accepted for publication in Science.

Hayden, B. P.: 1981, 'Secular Variation in Atlantic Coast Extratropical Cyclones,' Mon. Wea. Rev. **109**, 159-167.

Henderson-Sellers, A.: 1986, 'Increasing Cloud in a Warming World,' Cli. Chg. **9**, 267-309.

Jones, P. D., Raper, S. C. B., Bradley, R. S., Diaz, H. F., Kelly, P. M, and Wigley, T. M. L.: 1986, 'Northern Hemisphere Surface Air Temperature Variations, 1851-1984,' J. Climate Appl. Meteor. **25**, 161-183.

Karl, T. R.: 1987 (in press), CIRA symposium on Climatic Change, Colorado State University, Fort Collins, CO.

Kukla, G., Gavin, J., and Karl, T. R.: 1986, 'Urban Warming,' J. Climate Appl. Meteor. **25**, 1265-1272.

Lachenbruch, A. H., and Marshall, B. V.: 1986, 'Changing Climate: Geothermal Evidence from Permafrost in the Alaskan Arctic,' Science **234**, 689-696.

Ludlum, D. M.: 1982, The American Weather Book, Houghton Mifflin, Boston, 296 pp.

Muller-Dombois, D.: 1987, 'Natural Dieback in Forests,' Bioscience **37**, 575-582.

Seaver, W. L., and Lee, J. E.: 1987, 'A Statistical Examination of Sky Cover Changes in the Contiguous United States,' J. Clim. Appl. Meteor. **26**, 88-95.

Shugart, H. H.: 1984, A Theory of Forest Dynamics, Springer-Verlag, New York, 278 pp.

Wigley, T. M. L.: 1987, 'Relative Contributions of Different Trace Gases to the Greenhouse Effect,' Clim. Mon. **16**, 14-28.

Observed Variations in Cloudiness, Precipitation and Temperature in Colorado during the Past Century

Nolan J. Doesken
John Kleist
Colorado Climate Center
Department of Atmospheric Science
Colorado State University
Fort Collins, Colorado 80523

INTRODUCTION

Real or perceived changes (or potential changes) in the earth's climate resulting from Man's activities is a legitimate topic for research and scientific discussion on a global and international scale. Unlike many scientific concerns, the issue of potential climate change from increasing greenhouse gases is of great interest to a significant segment of the general public. The frequent and widespread attention given this topic by the news media in combination with the ever present public interest in weather and climate has made this topic one of special public concern. Within the past five years, it has become almost impossible to speak about climate to a lay audience without being subjected to many questions on the subject of the greenhouse effect and what it means for us here in Colorado.

When scientific issues become public issues, the role of public perception takes on special importance. In this case, if the public perceives the climate to be changing, and if greenhouse gases are perceived to be the most likely cause, then public support for research on these topics tends to be great. Similarly, when public interest is high, results from research efforts will likely be "front page" material and will lead to wider dissemination of results and greater public awareness and acceptance.

Why are we interested in public perception of this issue, and why are we using this to introduce this paper? From our experiences in Colorado we find that many people do have definitive perceptions about climate and climate change. Most believe that the climate is changing. These perceptions are based on information derived from a limited number of sources: local media and broadcast meteorologists, national media, and local personal observations and experience. Our office and others like us in other states enjoy a close relationship with the general public in our state. We often work closely with news media and broadcast meteorologists. As a result, we carry a substantial burden of responsibility since the information we provide can shape the perceptions of thousands of people within the state. What we observe here in Colorado, how we interpret what we observe, and how we relate that information to popular explanations such as the "greenhouse effect" can have a great impact on how the entire problem is viewed and perceived on the state and local level. Sure, maybe the northern hemisphere is warming 2 degrees Celsius, but what people here care about is what is happening right here in Colorado and how that may affect our future.

In this paper we will look at some of the long-term sources of climate data in Colorado. Observed trends and variations will be discussed in the context of the increasing greenhouse gases issue.

Long-term climate data in Colorado

Consistent sets of climatological observations in Colorado date back approximately 100 years into the late 1800's. Data on temperature and precipitation are available for a number of stations scattered across the state. Other types of data such as wind, pressure, humidity and cloudiness are available on a much more limited basis for a very small number of sites. The consistency of the temperature and precipitation data is quite good since the same type of instruments and observational procedures were used throughout the period of record. Station moves and observations times that could affect data consistency are usually traceable. Consistency of the observations of some of the other elements is harder to confirm. Over the long period of record there have been changes in instrumentation and there may have been changes in observational procedures that are not easy to identify.

Analysis

In this study the time series of three climatic elements are examined: mean temperature, precipitation and cloudiness. Only selected stations with good quality long-term records are analyzed. The locations of these stations are identified in Figure 1. Simple statistics are performed and visual comparisons among these separate time series are made in hopes of identifying any consistent indications of climatic change.

The number of cloudy days observed each year in Denver since 1873 are shown in Figure 2. A day is defined as "cloudy" when the average cloudcover, based on "frequent" observations is 8/10 or greater. The resulting time series has a dramatic and remarkable upward trend with a slope, based on linear regression, of +0.80 days/year. There are no obvious discontinuities in the graph which might suggest a change in cloudiness definition or observational practice during the period of record. Similar data were analyzed for Cheyenne, Wyoming and the results are shown in Figure 3. The slope of the trend at Cheyenne, +0.78, is only slightly less than Denver's although Cheyenne has been consistently cloudier than Denver throughout the 114-year period of record. Trends were also analyzed at Colorado Springs and Grand Junction, Colorado. Each of these stations has only approximately 40 years of cloudiness data. The results are not shown here graphically, but both stations have experienced significant increases over the past 40 years. Analyzed slopes were +0.81 days/year at Colorado Springs and +0.49 days/year at Grand Junction.

If this incredible increase in cloudiness over the past century is true, some sort of climate change seems to be taking place. With such a dramatic trend in cloudiness, it is logical to expect some related trends in other basic climate elements. Time series of precipitation data were examined at several locations in Colorado. Unfortunately, due to significant station moves, records at Denver and Colorado Springs could not be used for comparison. Time series for six locations in Colorado; Montrose and Grand Junction in west central Colorado, Fort Collins and Cheesman on the eastern slope of the Rockies, and Burlington and Cheyenne Wells on the eastern plains; are shown together in Figure 4. Smoothing was applied to

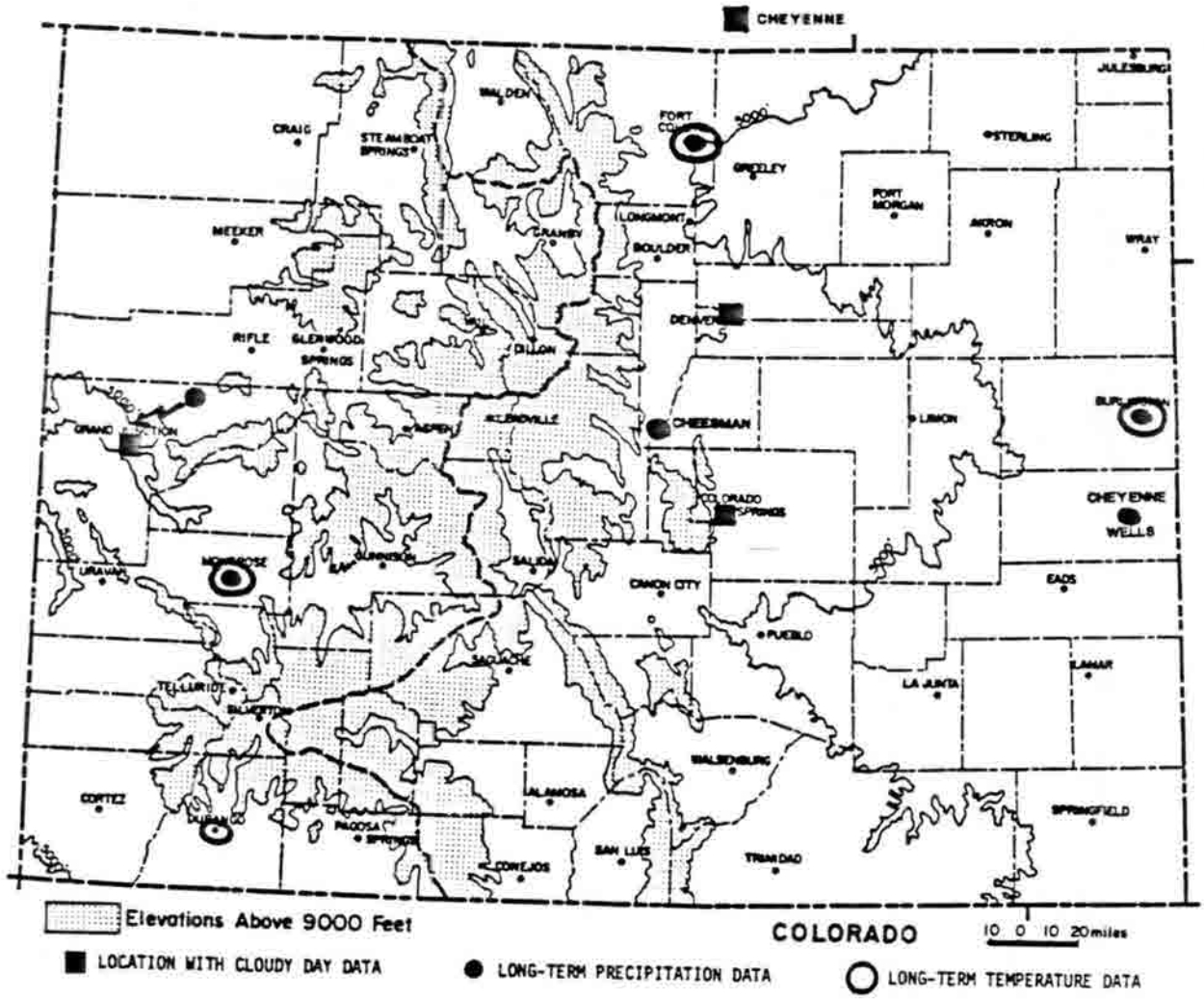

Figure 1. Locations with long-term climatological records used in this analysis.

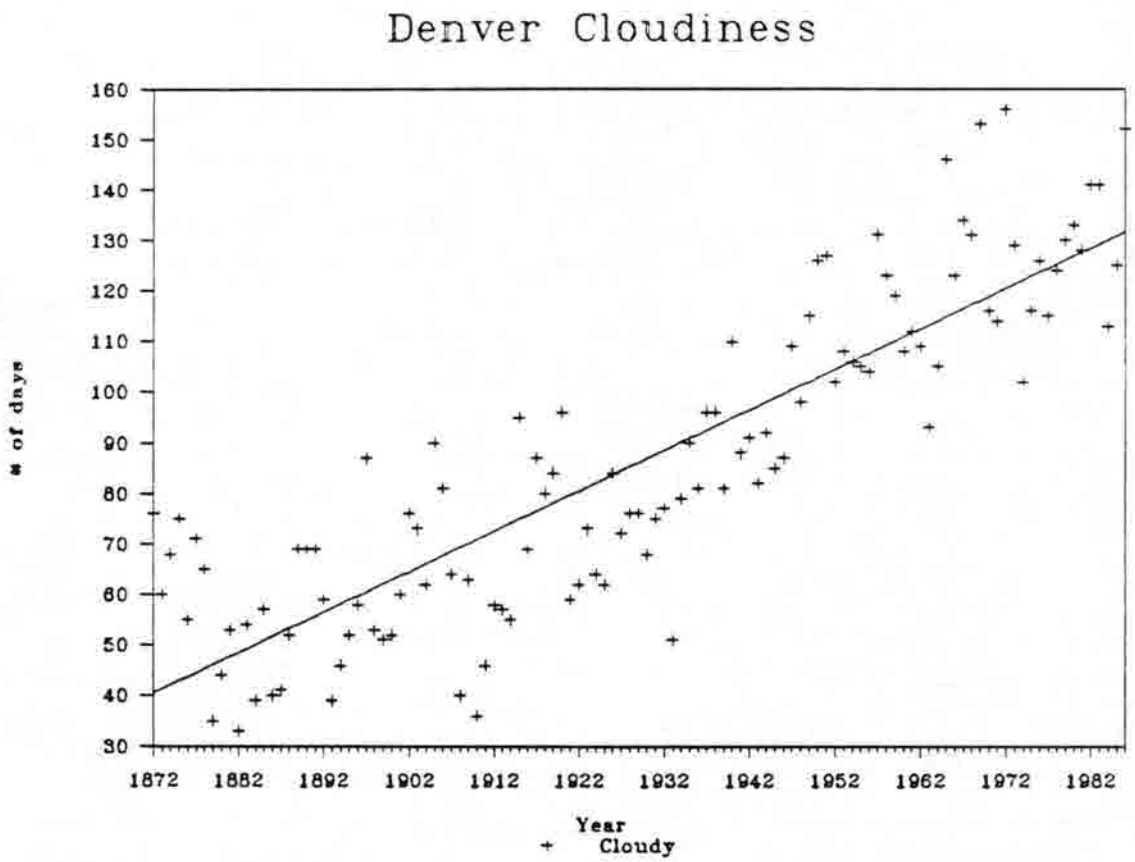

Figure 2. Time series of annual number of cloudy days at Denver, Colorado. Solid line is the computed slope using linear regression.

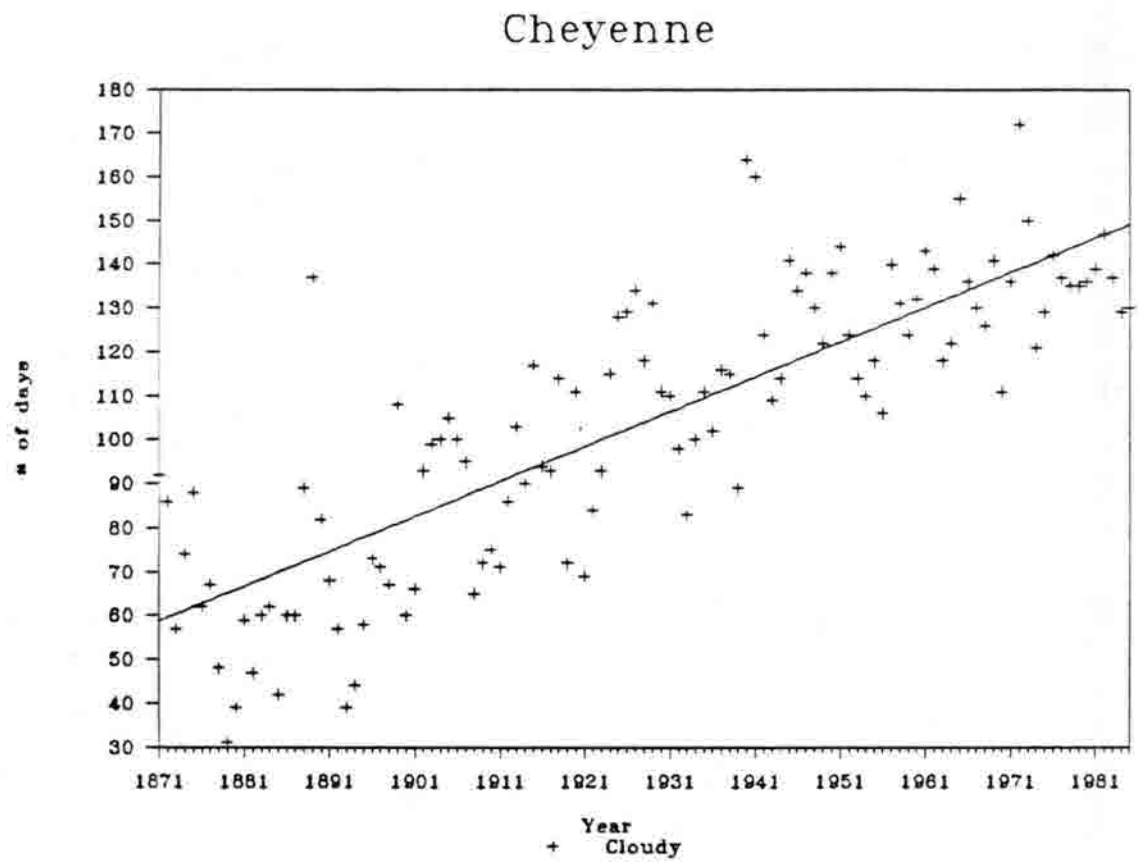

Figure 3. Time series of annual number of cloudy days at Cheyenne, Wyoming. Solid line is the computed slope using linear regression.

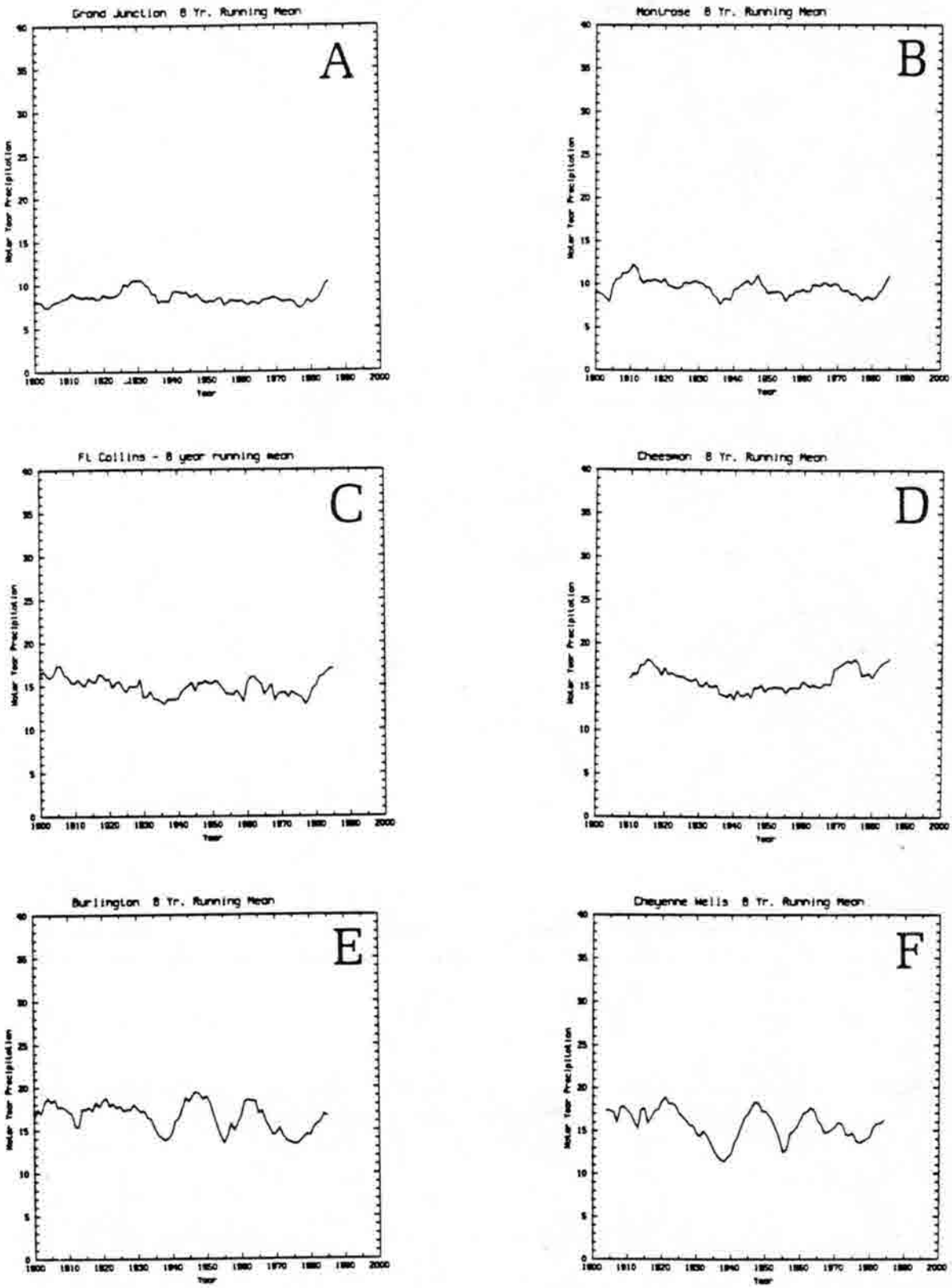

Figure 4. Time series of annual water year precipitation (inches) smoothed with an 8-year running mean for six locations in Colorado. A) Grand Junction, B) Montrose, C) Fort Collins, D) Cheesman, E) Burlington, and F) Cheyenne Wells.

the traditionally noisy precipitation time series using an 8-year running mean. Trends are not apparent in these smoothed time series and correlations with the cloudiness time series are fairly poor. The possible exception is Cheesman where steady increases in precipitation have been observed over the past 40 years. There are a number of interesting features, however, that are worthy of note. For example, the cyclic behavior that prompted theories of the double-sunspot correlation with precipitation (Mitchell, et al., 1979) is very visible in the precipitation records on the Colorado eastern plains. This characteristic is not observed in other portions of Colorado. One feature that has been noted at all six stations has been the sharp upturn in precipitation in the past decade. Doesken and McKee (1987) reported that the 1982-1986 period was the wettest in Colorado for the state as a whole since the 1920's.

The lack of apparent correlation between precipitation and cloudiness at first seems confusing and unlikely. In fact, it is tempting to assume that there may be some sort of a problem in one or both of the data sets. But with a better understanding of the climate of this region it is possible to get comfortable with the idea that precipitation and cloudiness may, in fact, be nearly uncorrelated for the stations used in this analysis. Figure 5 shows average monthly precipitation and average number of cloudy days for Denver. They, in a crude sense, are negatively correlated. Most precipitation east of the mountains in Colorado falls during the growing season. The greatest number of cloudy days occurs during the winter months when precipitation is typically low. Large percentages of the annual precipitation fall in just a few hours of the year from intense local summer thunderstorms. Therefore, there is really no reason to assume that increased cloudiness should cause a significant and detectable increase in precipitation in this part of the country. More comprehensive analyses of the relationships between precipitation and cloudiness on a seasonal basis would be necessary to draw more meaningful conclusions.

While the relationship between cloudiness and precipitation is perhaps obscure, increased cloudiness should have a noticeable effect on temperatures (Schneider, 1972; Stephens and Webster, 1981). Time series of mean annual maximum and minimum temperatures for Burlington, Fort Collins, Montrose, and Durango are assembled in Figure 6. Figure 7 combines information on maximum and minimums for the same four stations to show the mean annual diurnal range. Looking first at maximum temperatures, linear regression suggests that all four stations have experienced at least a slight warming during the past century. But, with the possible exception of Fort Collins, the upward trend has not been consistent. Records from the other three locations all suggest a discernible warming up until the 1930's (at Durango the warming seemed to continue into the early 1950's) followed by a noticeable and consistent cooling of about 2°F over the past three decades. The Fort Collins maximum temperature time series does suggest a warming tendency from the early teens into the 1930's. Little change is apparent since then except for some reduction in variability. Of the four stations shown here, Fort Collins has experienced the greatest urban growth in the past three decades. It appears likely that a developing urban heat island may be responsible for the observed differences in temperature characteristics.

Looking at the minimum temperature time series, three of the four stations have seen an increase in minimum temperatures during the past century, while Durango, until recently, had been on a steady decline. The

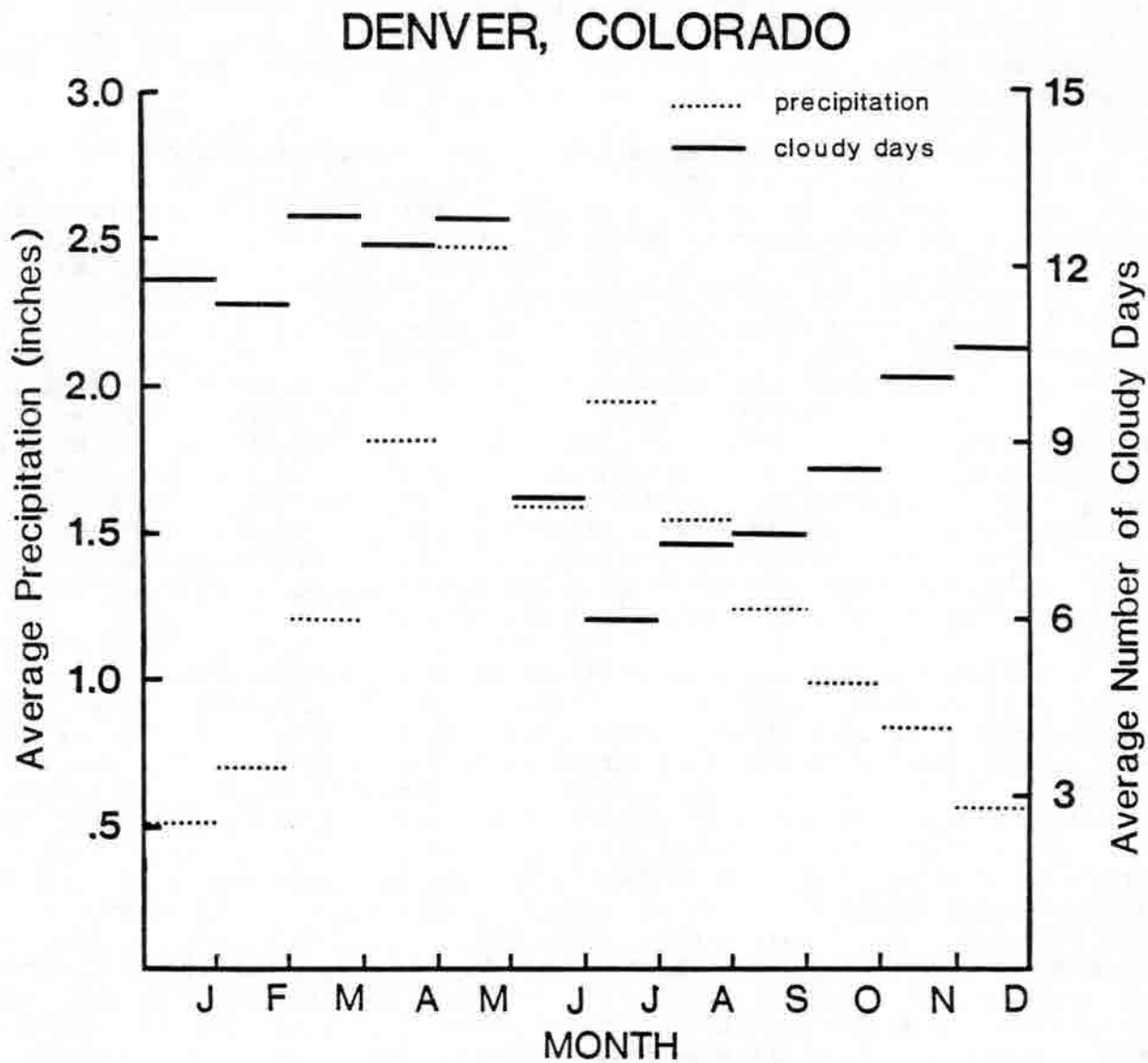

Figure 5. Comparison of average monthly precipitation and average number of cloudy days at Denver, Colorado. Averages are based on 1951-1980 data.

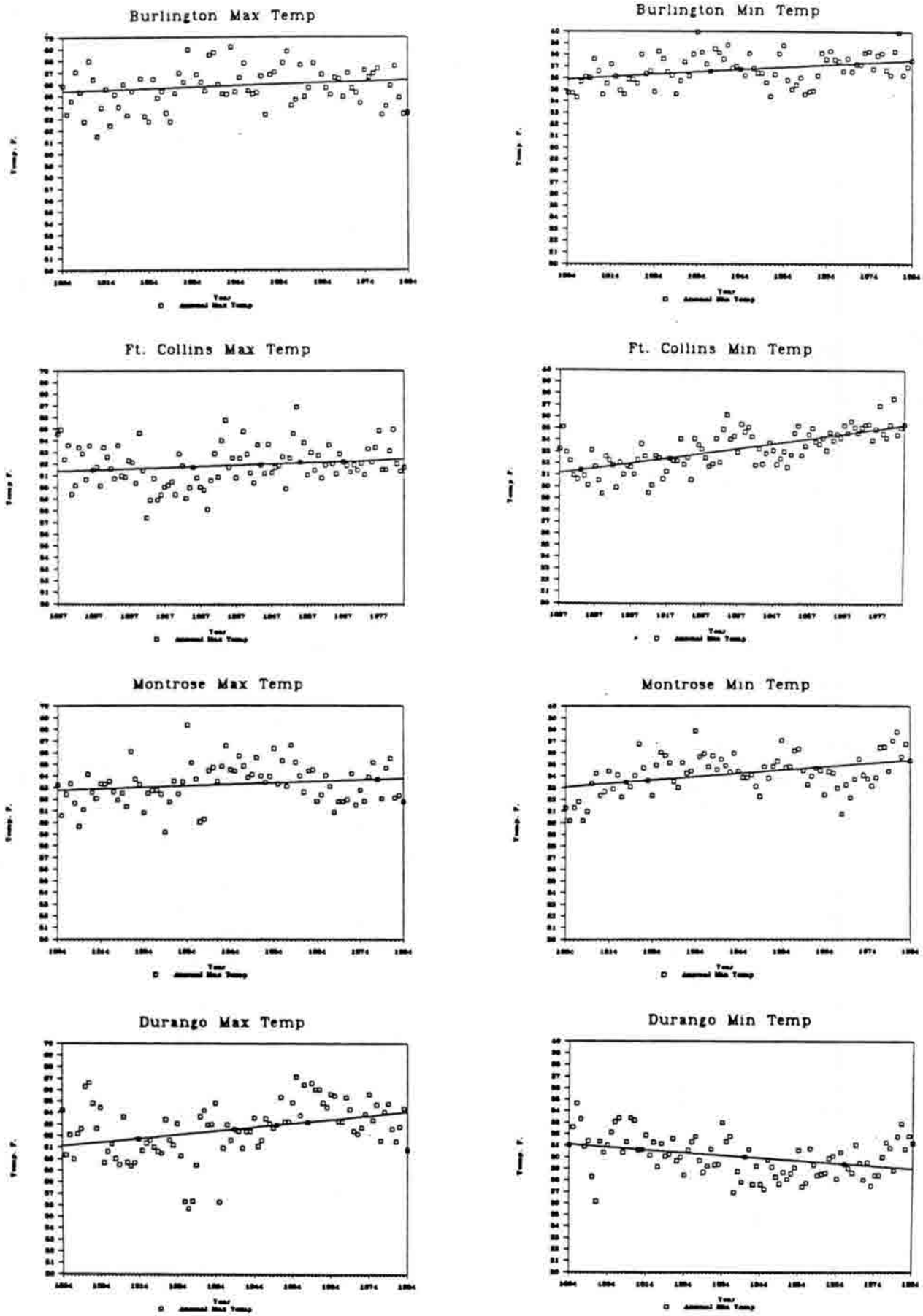

Figure 6. Time series of mean annual maximum and minimum temperatures with best-fit linear regression lines for four locations in Colorado: Burlington, Fort Collins, Montrose, and Durango.

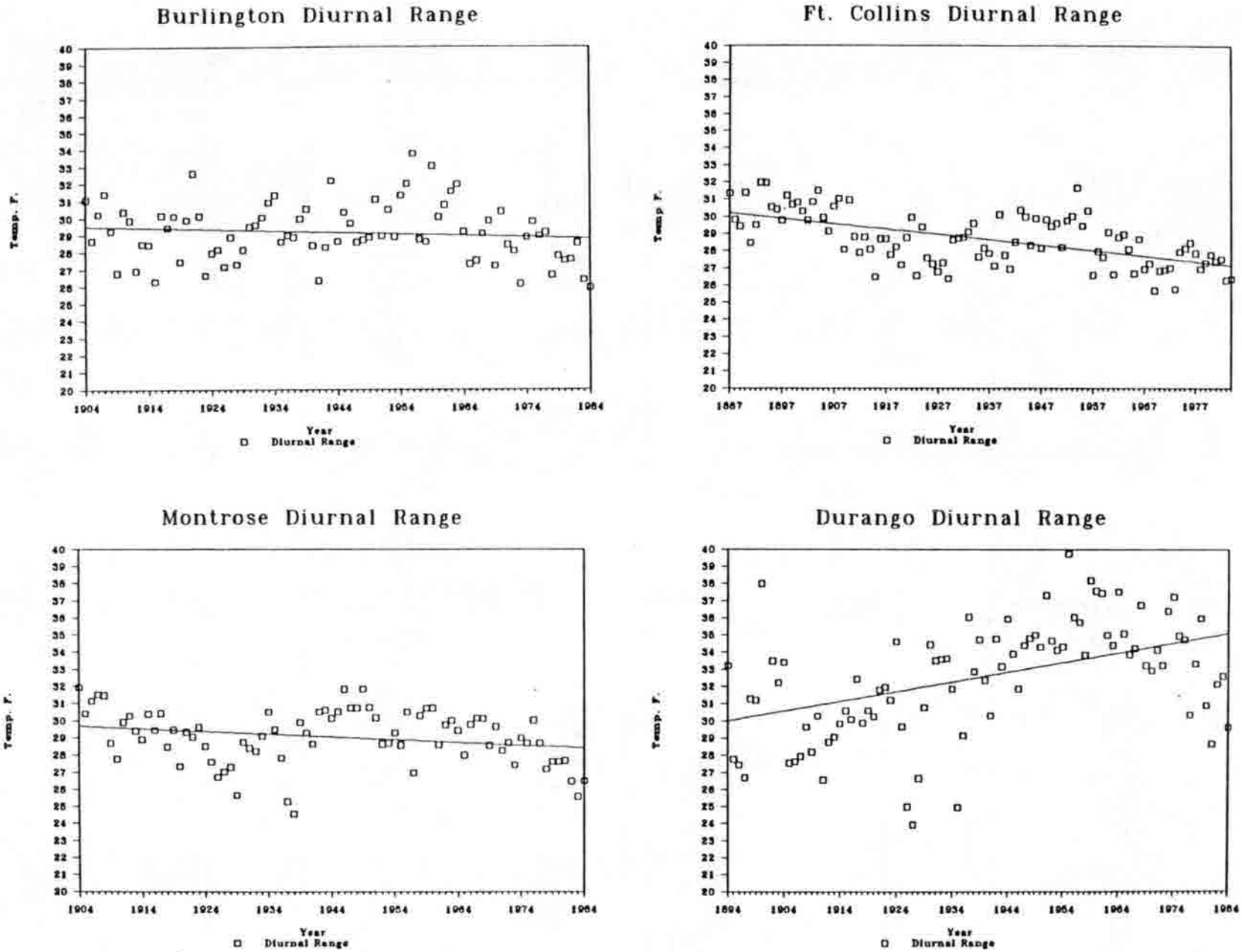

Figure 7. Time series of mean annual diurnal range of temperature with best-fit linear regression lines for four locations in Colorado: Burlington, Fort Collins, Montrose, and Durango.

rate of increase is much more significant at Fort Collins than at any other station. The mean annual minimum temperature has increased by 3°F during the past century. At Burlington and Montrose there is some indication of the same pattern that was observed in the maximum temperatures; a slight increase up until the 1930's followed by a decline up until about 1960. Since the early 1960's all stations except Burlington show a rather obvious increase in minimum temperatures.

The time series of diurnal range (Figure 7) presents a composite approach for examining possible relationships between increased cloudiness and temperature. Considering only radiative processes, increased cloudiness would be expected to produce a decrease in daily high temperatures while also producing an increase in nighttime minimum temperatures. These would combine to produce a decrease in diurnal range which would likely be of a greater magnitude than any changes in either maximums or minimums. Indeed, at three of the four stations analyzed, decreases in diurnal range were observed. Montrose, Fort Collins, and Burlington have all exhibited similar characteristics during the 20th Century although Fort Collins has experienced the greatest decrease. Durango, which has a higher average diurnal range than the other cities, has exhibited different behavior. Substantial increases in the diurnal range occurred up until the 1950's. Since the 1950's all four stations have shown decreases in diurnal range. Durango's unique behavior is not explained at this time. Data from a larger number of stations would be useful in determining if this same characteristic was wider spread or just a local phenomenon. Fairly complex changes in temperatures in mountain valleys could be expected under an assumed increase in cloudiness, since cloudiness greatly alters wind patterns and inversion formation in these regions of complex terrain.

Discussions and Conclusions

Available data on the number of cloudy days each year show that cloudiness has increased dramatically during the past century in Colorado. However, except for just the past few years, there has been no apparent increase in precipitation. Temperature data appear to support the increased cloudiness time series. Stations have generally experienced an increase in mean temperature and a decrease in diurnal range, particularly during the past 30 years.

There are enough uncertainties and local variations in the results shown above to cast some doubt on the results. The increase in apparent cloudiness is so great that, if true, more obvious changes in other climatic elements, particularly temperature, would be expected. There is no evidence that a change in definition of cloudy days occurred during the period of analysis, but some changes in operational procedures are known. Early in the record the assessment of cloudy days was likely based on only three point observations of cloudcover per day. This later increased to hourly observations with the advent of the aviation weather observation program. There is also some question about the interpretation of thin and opaque clouds that is not easily resolvable from available documentation. The lack of obvious discontinuities in the cloudiness time series suggests that no abrupt changes in definition or policy were implemented during the period of record. This does not discount the possibility of a gradual change of interpretation over a period of time. Data do appear to be verifiably consistent during the past 40 years. During this period the slope of the increasing cloudiness trend has continued at about the same rate as in the

earlier years. Related temperature records, which do appear to be consistent over the period of record, have changed enough to add some credence to the cloudy day analysis. However, factors other than clouds, such as the urban effect apparent at Fort Collins, could explain some of the observed variations.

Throughout this climatological analysis we have divorced ourselves from the issue of increased greenhouse gases and potential climate change. We have simply tried to determine what, if any, evidence for climate change we see from basic climate records within our state borders. Since there are some apparent changes, it is appropriate to discuss possible cause-effect relationships.

Cirrus clouds from ever-increasing jet aircraft operations are believed to be on the increase resulting in greater cloudy day frequencies in parts of the United States (Changnon, 1981). This explanation may seem reasonable, as much of Colorado is under a major east-west transportation flyway. But it can not possibly apply to the entire period of record since the observed increase was well underway long before jets had been invented. Any tie to changes in greenhouse gases is also obscure. Many scientists feel climate change from increased carbon dioxide should be a relatively recent phenomenon associated with the increased rate of change of greenhouse gases within the past three decades. However, gradual increases in carbon dioxide have likely been taking place over a longer period. Defining a cause-effect relationship is beyond the scope of this work, but the time scales of these two changes are sufficiently consistent to allow for some possible association.

There is inadequate coherence or consistency in the observed precipitation records analyzed as a part of this study to make any substantive statements about climate change. Temperature records, however, do seem to suggest a possible warming and also a reducing diurnal range consistent with increased cloudiness. Decreased diurnal ranges have also been observed over much broader regions (Karl et al., 1984). More than likely, changes in temperature are a reflection of increased cloudiness as opposed to cloudiness increasing in response to increased local temperatures. But again, such quantification is beyond the intended scope of this review.

The prevailing public perception in Colorado in recent years has been that we are not as sunny as we used to be. This is consistent with the data we have shown. Perceptions concerning temperature and precipitation have been more ambiguous. What we have shown here suggests that there is reason for concern on the local scale about possible climate change in our lifetimes. But cause-effect relationships are weak enough that care should be taken in relating all observed changes in temperature and cloudiness in Colorado to increased greenhouse gases. It is important that organizations like ours, with good public contact, stay well informed of advances in research on the greenhouse-climate change issue on a national and international scale. It would be easy to overreact to observed trends, such as the cloudiness data we have shown, and lead the public into a bold perception of visible and dramatic climate change when, in fact, nothing of the sort is occurring. At the same time, it is folly to give the impression that the climate system is in static equilibrium and can compensate for everything that Man can to do it. The climate has changed in the past and

will change in the future. The closer we observe and monitor its fluctuations, the better equipped we should be for the future.

Acknowledgements

This research was made possible by ongoing support for climate research and data archiving by the Colorado Agricultural Experimentation through the Colorado State University College of Engineering. Partial support was also provided by the Water Resources Research Program of the U.S. Geological Survey, Grant #14-08-0001-G1294.

References

Changnon, S. A., 1981: Midwestern Cloud, Sunshine and Temperature Trends since 1901: Possible Evidence of Jet Contrail Effects. Journal of Applied Meteorology, Vol. 20, 496-508.

Doesken, N. J. and T. B. McKee, 1987: Colorado Climate Summary Water Year Series, October 1985 - September 1986. Climatology Report 87-3. Colorado Climate Center, Department of Atmospheric Science, Colorado State University, Fort Collins, CO. 102 p.

Karl, T. R., G. Kukla and J. Galvin, 1984: Decreasing Diurnal Temperature Range in the United States and Canada from 1941 through 1980. Journal of Climate and Applied Meteorology, Vol. 23, No. 11, 1489-1504.

Mitchell, J. M., Jr., C. W. Stockton and D. M. Meko, 1979: Evidence of a 22-year Rhythm of Drought in the Western U.S. Related to the Hale Solar Cycle since the 17th Century. Solar-Terrestrial Influences on Weather and Climate, B. M. McCormac and T. A. Selga, Eds. D. Reidel, 125-143.

Schneider, S. H., 1972: Cloudiness as a Global Climatic Feedback Mechanism: The Effects on the Radiation Balance and Surface Temperature of Variations in Cloudiness. Journal of the Atmospheric Sciences, Vol. 29, 1413-1422.

Stephens, G. L. and P. J. Webster, 1981: Clouds and Climate: Sensitivity of Simple Systems. Journal of the Atmospheric Sciences, Vol. 39, 235-247.

HYDROCLIMATIC DATA ERRORS AND THEIR EFFECTS ON THE PERCEPTION OF CLIMATE CHANGE

Robert D. Jarrett, Research Hydrologist
U S. Geological Survey
MS415
P.O. Box 25046
Lakewood, Colorado 80225

ABSTRACT

One of the basic premises of hydroclimatic investigations is that the data are accurate and representative. There are some hydroclimatic data that contain significant errors. These errors also may be biased. Extremes of hydroclimatic data commonly contain large and sometimes biased errors; these errors are of great concern because they commonly are a major factor in a hydroclimatic investigation. Before a hydroclimatic investigation is started, it is essential to ascertain that the data or the methods (and equations) to be used are applicable and valid to a study area. It is important to identify erroneous hydroclimatic data because use of these data may result in invalid conclusions in subsequent hydroclimatic investigations, such as investigations of water quality, acid precipitation, precipitation-runoff modeling, geochemistry, sediment transport, availability of streamflow for river compacts and energy development, and climate change. An understanding of the source, types, and magnitude of hydroclimatic-data errors is essential to mitigate the effect on these investigations.

INTRODUCTION

One of the basic premises of hydroclimatic investigations is that the data are accurate and representative. An evaluation of the accuracy of hydroclimatic data is needed before accurate assessment of subsequent hydroclimatic investigations can be made. Certain questions need to be answered before starting a hydroclimatic investigation:

1. Were data-measuring devices and data-collection techniques used properly?

2. How accurate are the data?

3. How representative are the data?

Extreme-value data generally are of greatest concern in subsequent hydroclimatic investigations and interpretations because these data commonly are a major factor in these investigations; however, these extreme data commonly have the greatest errors.

A number of studies have been done on the accuracy of hydroclimatic data. For example, Winter (1981) presented an excellent overview of the uncertainties in estimating water balance in lakes. Generally hydroclimatic data have small errors; however, some data contain significant and biased errors. It is important to identify these erroneous hydroclimatic data and to determine if the data can be corrected and used in subsequent analyses.

Many, if not most, hydroclimatic investigations today are based on the assumption of stationarity (a variable remains relatively constant with time). Climate change is difficult to determine given the natural climatic variability. Natural climatic variations occur throughout an extensive spectrum of time, from days to hundreds of thousands of years; hence, determining that a climate change has occurred rather than natural climatic variability is difficult. Climate-change studies encompass an extensive range of hydroclimatic characteristics, such as changes in temperature, precipitation, mean annual streamflow, and the occurrence of floods for a specified time. Relevant questions about climate change are: (1) Is there a local or global warming or cooling trend? and (2) Are there more floods or droughts today than in the recent past? Detection of climate changes requires accurate data before trend analyses can be made. Analyses of erroneous data may lead to invalid conclusions of hydroclimatic variations. The purposes of this paper are to identify several sources of error in hydroclimatic data, to indicate the importance of reviewing data for errors, and to present methods of data review. This paper focuses attention on errors and their effects on hydroclimatic investigations. Through an understanding of the errors and of the ways erroneous data are collected, future data errors can be minimized.

DETECTING ERRORS IN HYDROCLIMATIC DATA

One of the basic needs of good data collection and interpretation is an understanding of basic hydroclimatic principles. This is important in establishing and operating a data network and in subsequent hydroclimatic investigations. Another source of potential error in hydroclimatic investigations is from the inappropriate transfer of methods or equations beyond the area or range of data from which they were calibrated. For example see Williams' (1983) discussion on improper use of regression equations in earth sciences.

This section presents several examples of identified sources of error in climatic and hydrologic and hydraulic data and investigations of these data. These examples are not all encompassing; rather, they indicate the need for error analyses of hydroclimatic data. These errors, in most, if not all, examples, resulted from collecting data using the then state-of-the-art equipment, collection methods, and analyses. This paper is not a criticism of any study; rather it is to indicate types of errors and the need to review data for their accuracy. Generally, data are collected under the assumption (or philosophy) that some data are better than no data.

Climatic Data

There are several sources of error in climatic data. Because of limited space for this paper, only errors in precipitation data are discussed here. These errors in precipitation data include: (1) Equipment errors, (2) measurement errors, (3) analysis errors, and (4) a combination of these errors.

Precipitation-gage data are subject to various types of errors. These errors generally are small; their tendency is to result in values that are too small. The most serious equipment error is the inaccuracy of precipitation measurement because of wind effects; this is especially true for falling snow. Brooks (1938) reported that an unshielded gage may be 75 percent or more deficient in snow catch, or 5 to 10 percent deficient in rain catch. The earliest documented attempt to decrease the adverse effects

of wind on precipitation gages was by Thomas Stevenson in Scotland in 1842 (Brooks, 1938). Subsequently, many different devices were attached to the gages prior to the adoption of the Alter shield in 1937.

About 1908 (Warnick, 1956), C.F. Marvin, then Chief of the Instrumentation Division of the U.S. Weather Bureau, fabricated a cone-shaped, solid-metal windshield with a top diameter of about 1 meter that could be attached to the top of a precipitation gage (Fig. 1). Unfortunately, this windshield had the effect of "funneling" hail and rainsplash into the precipitation gage. Use of the Marvin windshield resulted in substantially overregistered summer precipitation (when hail is common) in Leadville, Colorado, during 1919-38. Analysis of these precipitation data indicated that the monthly precipitation for these years was overregistered by as much as 157 percent of the long-term monthly precipitation at Leadville (Jarrett and Crow, in press).

The Marvin windshield was used on the official U.S. Weather Bureau gage in Leadville, Colorado from 1919 to 1938 (Jarrett and Crow, in press). It is unknown at this time (1987) how many other precipitation gages were equipped with the experimental Marvin windshield; it is unlikely that it was used only on one gage. Analyses of the precipitation records for the gage at Leadville and four nearby precipitation gages, streamflow records, and paleohydrologic investigations were done by Jarrett and Crow (in press).

The precipitation record at Leadville is an unusual and significant data set because it dates back to 1888 and is from a high elevation (3,100 meters). The precipitation record at Leadville has been used in many hydroclimatic investigations because of this long record. Some investigators have interpreted the "increase" in precipitation regime from 1919 to 1938 as an indicator of a climate change.

The precipitation records at Leadville include the largest (and record breaking) higher elevation (above 2,300 meters) rainstorm (110 millimeters in about 1 hour) recorded in Colorado. However, this storm occurred on July 27, 1937, which was during the period the Marvin windshield was used. There was an extraordinary quantity of hail associated with this storm (Jarrett and Crow, in press); their investigations indicated a more probable storm total of about 43 millimeters. Climatologists and hydrologists have used this storm for the development of design rainfall. Because this storm is the largest and only officially recorded large rainstorm in the mountains of Colorado, it has a large effect on design rainfall. The results of the use of the Leadville data in other hydroclimatic studies are unknown. Because of the importance of the precipitation record at Leadville, a Marvin windshield has been reconstructed, installed on a precipitation gage, and operated next to a standard precipitation gage in Leadville since June 1987.

There are two types of the second category of precipitation error, measurement error and errors associated with unsubstantiated measurements. Curry (1966) reported that 290 millimeters of rain fell in 24 hours in Mayflower Gulch (elevation 3,551 meters) near Frisco, Colorado, on July 31, 1961, and that 245 millimeters of rainfall occurred in 24 hours in the same location on August 18, 1961. He collected these precipitation records in a standard U.S. Weather Bureau nonrecording gage from June through September 1961. Rainstorms of this magnitude (290 and 245 millimeters in 24 hours) are unprecedented at higher elevations of Colorado (even one such storm) and in other areas have resulted in catastrophic flooding.

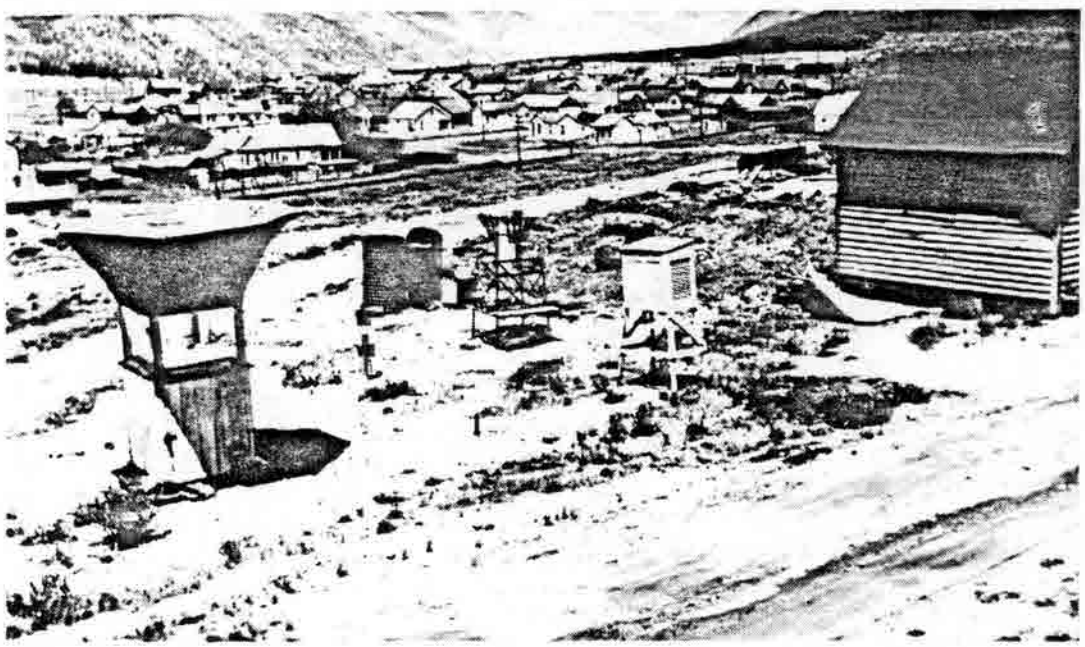

Figure 1.--Northeast view of precipitation gages in Leadville, Colorado, June 1948. Marvin-shielded gage is on the left; Alter-shielded gage is in the center. Photograph courtesy of the Colorado Climate Center, Colorado State University, Fort Collins, Colorado.

Because of these large quantities of reported rainfall, the site was visited to determine the extent of flooding (Jarrett, 1987). Onsite paleohydrologic investigations, analyses of records for nearby precipitation data, and inspection of nearby downstream streamflow-gaging station records did not indicate that large flooding had occurred. Rather, small-magnitude snowmelt runoff accounted for the peak flow for the year on May 31. Streamflow increased slightly above base flow on August 1. This indicated that the precipitation data collected by Curry (1966) were erroneously recorded, probably by an order of magnitude because of misreading the gage (Jarrett and Crow, in press).

The other type of measurement error seems to be attributed to reported, but unsubstantiated, rainfall quantities. A number of these have been reported. For example, Larry Lang (Colorado Water Conservation Board, written commun., 1986) reported that a 254-millimeter rainfall had occurred in about 4 hours during June 1984 on Wolf Creek Pass, Colorado. If this quantity of rain actually fell, it would have been indicated in streamflow records (and as a major flood). The official national Weather Service precipitation gage at Wolf Creek Pass recorded a maximum 24 hour precipitation amount of 43 millimeters for June 1984. Streamflow records of streams that drain Wolf Creek Pass in the San Juan River and Rio Grande basins do not indicate any significant rainfall runoff during June 1984 (Jarrett, 1987). This reported storm is erroneous, yet it has been cited as a major flood-producing storm.

The third type of precipitation error, analysis error, generally is the most difficult to detect because users generally are unfamiliar with the data or the reconstructed data. In mountainous areas or other areas where precipitation records are few, storm data have been reconstructed from streamflow data. Miller and others (1978) reconstructed flood peaks of the Big Thompson River flood in 1976 based on rainfall-runoff analyses to evaluate the storm precipitation. Their objective was to enhance the available, but sparse, precipitation data for the 1976 storm. They determined that it was difficult or impossible to reconcile slope-area peak discharges with rainfall measurements. However, point-rainfall data are not good indicators of basinwide rainfall for localized storms. Reconstructed peak discharges based on rainfall-runoff analyses generally were 25 to 50 percent smaller than the peak discharges determined by the slope-area method. However, they chose to accept that the larger peak discharges were correct (this incorrect assumption is discussed later) and increased the rainfall (intensities and volume) for the storm.

Mears (1979) used rainfall-runoff analyses to reconstruct storm rainfall of a 1977 "flood" in the East River tributary near Crested Butte, Colorado. He reconstructed a world-record-breaking rainfall that ranged from 168 to 207 millimeters in 10 minutes. The 1977 "flood" was a debris flow and the computed peak discharge of 108 to 134 cubic meters per second was erroneous (Costa and Jarrett, 1981). Their geomorphologic and hydraulic investigations of the site indicated that there was no supporting evidence of a large flood. They reconstructed a 1977 waterflood discharge of about 6 cubic meters per second and a 10-minute rainfall amount of about 10 millimeters. Debris flows and waterfloods can be identified from onsite investigations of the channels and the basin (Costa and Jarrett, 1981; Jarrett, 1987).

A further problem with precipitation data may occur with point-precipitation data. Development of regional (storm) estimates from point

precipitation is difficult (Winter, 1981) and can result in large errors. These errors result from insufficiently dense precipitation-gage network and from the methods used to estimate the regional precipitation (such as discussed above). In general, sampling errors tend to increase with increasing areal mean precipitation and to decrease with increasing network density, duration of precipitation, and size of area (Winter, 1981). In one study, an investigator, unaware that an earlier investigator had enhanced (increased) the July 27, 1937 Leadville, precipitation data, enhanced the previously enhanced data so that the magnitude of the original data values was almost doubled.

Erroneous precipitation data, regionalized precipitation estimates, and reconstructed precipitation from flood data have been used in subsequent hydroclimatic investigations, generally without the investigator knowing of these errors or the methods used to obtain the data. This may produce inaccurate estimates of rainfall and flood discharges that are used in hydroclimatic studies.

Hydrologic and Hydraulic Data

There is a great potential for errors in hydrologic and hydraulic data because of the diversity of variables. As with climatic errors, only selected errors are discussed. Changes in the precipitation regime would be detected in streamflow; hence, these changes are interrelated. Streamflow variables investigated in climate-change studies are mean annual flow and flood discharge.

In the discussion of precipitation, errors in peak discharges and their use in reconstructing precipitation were discussed. Peak discharges are computed indirectly after floods for which direct discharge measurements cannot be made because of adverse conditions. The method most commonly used in the United States is the slope-area method. In the slope-area method, discharge is computed on the basis of equations that involve channel characteristics, water-surface profiles, and a roughness coefficient for use in the Manning equation (Chow, 1959). This method requires that certain hydraulic conditions be met. In some streams, not all these conditions can be met and various assumptions are made. For example, are the stream conditions similar to those that were used to verify the Manning's roughness coefficient n?

Most users of the data assume that peak-discharge accuracy is within 25 percent of the true discharge, and many measurements have that accuracy or better. However, because of problems associated with making the slope-area measurements during certain conditions, peak-discharge values may consistently indicate positive bias--values greater than the true discharge. During an evaluation of 70 slope-area measurements in higher gradient streams (stream slopes greater than 0.002 meter per meter) from throughout the United States, peak discharges were determined to be affected by n-values, scour, expansion and contraction losses, viscosity (including debris-flow problems), unsteady flow, number of cross sections, state of flow, and stream slope (Jarrett, 1986). Problems due to measurement error commonly can be as great as or can exceed 100 percent; these can cause overestimation of the actual peak discharge. These problems are most common in higher gradient, small drainage basins; generally the errors become greater as stream slope increases.

Generally, the most erroneous peak-discharge estimates have been used to reconstruct rainfall data. Their use can result in misleading maximum precipitation and flood discharge, erroneous flood-frequency analyses, and misinterpretation of climate change. The use of these overestimated peak-discharge values (generally the cause of a flood being identified as a high outlier in flood-frequency analysis) will result in overestimated discharges for a given frequency.

These large peak-discharge estimates also have been used to revise envelope curves of maximum recorded discharge for various sizes of drainage area. The Committee on Geology and Public Policy (1978) has reported that larger floods have been recorded since 1890, particularly for drainage basins less than 130 square kilometers. Increased maximum peak discharge with time has been interpreted as a climate change or the result of additional data collection. A number of the peak discharges that define the upper or increased envelope curve were overestimated by 50 to 100 percent or more (Jarrett, 1986). These overestimated flood discharges are the reason for much of the increase in the envelope curves and interpretation of possible climate change of increased peak discharges in certain streams.

More and more hydroclimatic investigations, such as investigations of water quality, acid precipitation, precipitation-runoff modeling studies, geochemistry, sediment transport, availability of streamflow for river-basin compacts and energy development, and climate change are being done in mountainous regions. These investigations rely on and require accurate streamflow data. Most of the work done to establish methods to determine streamflow were done in lower gradient stream environments, generally in the eastern United States. Before an investigation is done, it is essential to ascertain that the data or the methods (and equations) used are applicable and valid to a study area.

Streamflow can be measured directly by current meter or indirectly using hydraulic equations such as those of Manning and Bernoulli. When making a current-meter measurement of streamflow, one of the basic conditions is that the velocity profile is approximately logarithmic (Chow, 1959). When the velocity profile is logarithmic, a single-point velocity obtained at 0.6 the depth of flow is the mean flow velocity; hence, this and the cross-sectional area of flow are multiplied to compute streamflow. A logarithmic velocity profile has been met for most streamflow conditions (Chow, 1959). However, in higher gradient mountain streams, the velocity profile is nonlogarithmic or S-shaped (Fig. 2); velocities are less near the streambed and greater near the water surface than for a logarithmic velocity profile (Jarrett, 1985). Mean velocity in the vertical, determined by measuring the velocity at 0.6 the depth, consistently is too small; hence, discharge is too small.

Most indirect determinations of streamflow in open channels require an evaluation of the roughness coefficient, usually Manning's n. The selection of n values for channels is subjective, even though there are a number of guidelines available (Chow, 1959; Barnes, 1967). The U.S. Geological Survey has done many n-verification studies to assist in the selection of n values. Most of this work has been in lower gradient streams. Recent investigations have indicated that n values in higher gradient cobble and boulder bed channels have been underestimated, typically by about 60 percent (Jarrett, 1986). In some streams for normal conditions, n values have been underestimated by several hundred percent. This underestimation primarily is because there are additional energy losses in steeper streams than for

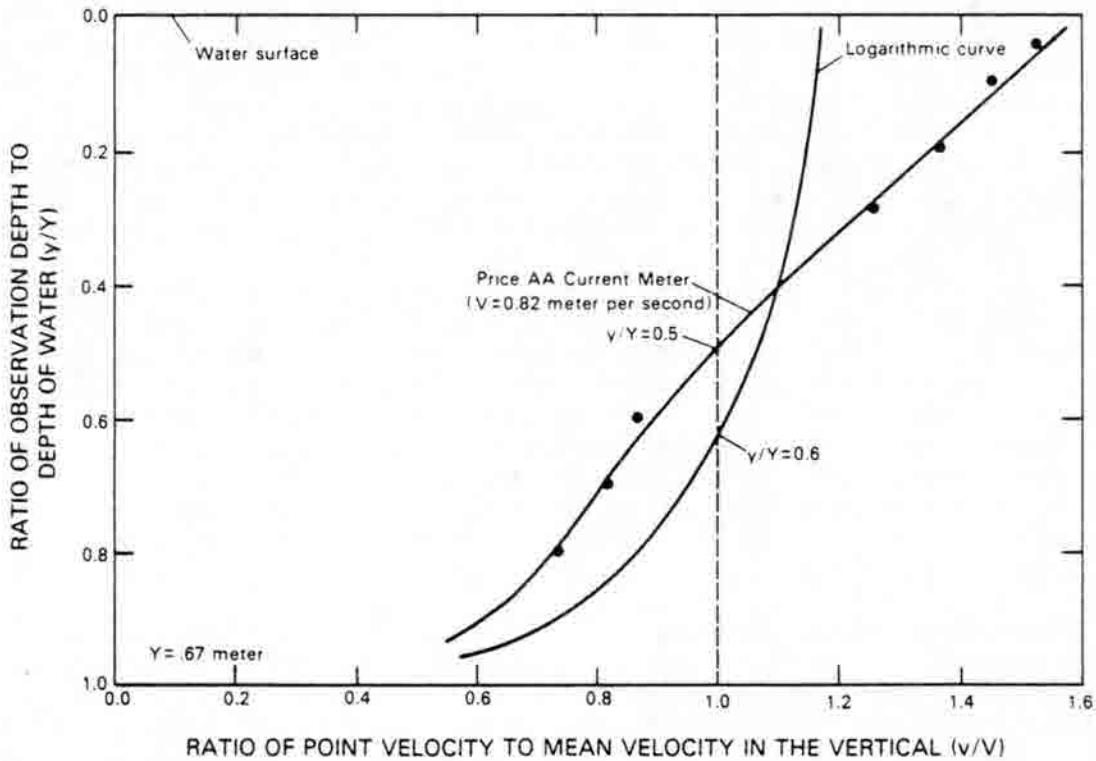

Figure 2.--Velocity profile, Lake Creek above Twin lakes Reservoir at station 7 meters, August 16, 1983 (modified from Marchand and others, 1984).

hydraulically similar lower gradient streams. If n values are too small, then discharges that are computed by using hydraulic equations will be too large.

SUMMARY AND DISCUSSION

There are a number of sources of error in hydroclimatic data. Errors can develop from using methods (or equations) in areas for which the methods were not developed or by using values beyond the range of conditions of the original data. An understanding of these errors and the basic hydroclimatic or physical principles is essential to mitigate the effect on subsequent hydroclimatic investigations. Erroneous data may cause erroneous interpretations and conclusions in numerous hydroclimatic investigations. In most hydroclimatic investigations, it is the extreme-value data that generally are the major factor in the study; hence, these data need to be closely evaluated.

Large errors, though cause for concern, probably are not as important and significant as biased errors. With knowledge of the accuracy of the data, the data can be weighted on the basis of their accuracy and used accordingly in an investigation. Is quality control lacking in the collection of hydroclimatic data? My evaluation of hydroclimatic data would indicate that there is not a lack of adequate quality control in most instances; rather, certain data that are outside the normal range of data collected need to be scrutinized more carefully. For example, the accuracy of the thousands of U.S. Geological Survey peak-discharge measurements generally is within 25 percent. However, when evaluating the largest floods in the United States, errors commonly are greater than 25 percent are are biased (consistently overestimated). Accurate and representative hydroclimatic data are needed for correct interpretations of subsequent hydroclimatic investigations, including the knowledge of the correct streamflow for investigations of water quality, acid precipitation, precipitation-runoff modeling, sediment transport, geochemistry, availability of streamflow for river-basin compacts and energy development, and climate change.

Users of hydroclimatic data first need to review the data for inconsistencies and possible errors. Data can be checked against data for nearby sites. One method of checking data is to compare the data with other sources of data. An example would be if precipitation data indicate a trend, compare against other nearby precipitation-gage and streamflow-gage data. A comparison of the methods and equations based on the data in order to establish the range of applicability will help minimize erroneous results from extrapolation.

Finally, and particularly for extreme-value data, it would be desirable to review the original source of data for qualification statements on the accuracy of the data. In some instances the original source of the data indicate that the data are so erroneous that they should not be used. However these data are in use in the literature. Are significantly erroneous data worth publishing? This question can be used for further discussion.

REFERENCES

Barnes, H.H., Jr., 1967, Roughness characteristics of natural channels: U.S. Geological Survey Water-Supply Paper 1849, 213 p.

Brooks, C.F., 1938, Need for universal standards for measuring precipitation, snowfall, and snowcover: Bulletin 23, International Association of Hydrology, I.U.G.G. Riga, 1938.

Chow, V.T., 1959, Open-channel hydraulics: New York, McGraw Hill Book Company, 680 pp.

Committee on Geology and Public Policy, 1978: Floods and people; a geologic perspective, Geological Society of America Report, 7 pp.

Costa, J.E., and Jarrett, R.D., 1981, Debris flows in small mountain stream channels of Colorado and their hydrologic implications: Bulletin of the Association of Engineering Geologists, vol. 18, no. 3, pp. 309-322.

Curry, R.R., 1966, Observations of alpine mudflows in the Tenmile Range, Central Colorado: Geological Society of America Bulletin, vol. 77, pp. 771-776.

Jarrett, R.D., 1985, Analyses of vertical-velocity profiles in higher gradient streams in Colorado: EOS, vol. 66, no. 46, p. 912.

Jarrett, R.D., 1987, Flood hydrology of foothill and mountain streams in Colorado: Ph.D. Dissertation, Colorado State University, Fort Collins, 238 p.

Jarrett, R.D., 1986, An evaluation of the slope-area method for computing peak discharge: U.S. Geological Survey Water-Supply Paper 2310, pp. 13-24.

Jarrett, R.D., and Crow, L.W., in press, Experimental Marvin windshield effects on precipitation records in Leadville, Colorado, Water Resources Bulletin, American Water Resources Association.

Marchand, J.P., Jarrett, R.D., and Jones, L.L., 1984, Velocity profile, water-surface slope, and bed-material size for selected streams in Colorado: U.S. Geological Survey Open-File Report 84-733, 82 p.

Mears, A.I., 1979, Flooding and sediment transport in a small alpine drainage basin in Colorado: Geology, vol. 7, pp. 53-57.

Miller, D.L., Everson, C.E., Mumford, J.A. and Bertle, F.A., 1978, Peak discharge estimates used in refinement of the Big Thompson storm analysis: Boston, Massachusetts, Conference on Flash Floods, Hydrometeorological Aspects, American Meteorological Society, pp. 135-142.

Warnick, C.C., 1956, Influence of wind on precipitation measurements at high altitudes, Bulletin 10, Engineering Experiment Station, University of Idaho, 61 p.

Williams, G.P., 1983, Improper use of regression equations in earth sciences: Geology, vol. 11, pp. 195-197.

Winter, T.C., 1981, Uncertainties in estimating the water balance of lakes: Water Resources Bulletin, American Water Resources Association, vol. 17, no. 1, pp. 82-115.

III. Extending the Interpretation of Global Climate Simulations

R. Pielke

T. Kittel and M. Coughenour

Evaluation of Climate Change Using Numerical Models

R. A. Pielke
Cooperative Institute for Research in the Atmosphere
and
Department of Atmospheric Science
Colorado State University
Fort Collins, Colorado 80523

1 Abstract

This short paper discusses two approaches to permit the interpolation of GCM model results down to local scales. The first approach uses a synoptic classification of GCM output to construct dominant large scale weather scenarios from which local scale model simulations can be performed. The second approach links the GCM model output to two-way multiple interactive numerical model grids which telescope down to the local scale. The local scale models in both cases include detailed terrain, and vegetation and soil representations of the area. Vegetation changes due to climate change can assist in the estimation as to whether alterations in the biosphere can mitigate climate change perturbations (i.e., the Lovelock Gaia hypothesis).

2 Introduction

Climate global circulation models (GCMs) have been effective at focusing attention on potential long-term changes in global climate (e.g., see the Schlesinger et al., 1985 excellent review). Unfortunately, however, these models have not yet attained sufficient spatial resolution to target specific geographic areas, nor have they included a number of important physical feedback mechanisms.

This short paper discusses two approaches to permit the interpolation of GCM model results down to local scales. The first approach uses a synoptic classification of GCM output to construct dominant large scale weather scenarios from which local scale model simulations can be performed. The second approach links the GCM model output to two-way multiple interactive numerical model grids which telescope down to the local scale. The local scale models in both cases include detailed terrain, and vegetation and soil representations of the area. Vegetation changes due to climate change obtained from ecosystem models can assist in the estimation as to whether alterations in the biosphere can mitigate climate change perturbations (i.e., the Lovelock Gaia hypothesis; Lovelock, 1979).

The final section of the paper lists several physical mechanisms which need to be added to GCM simulations before the model results could be accepted as definitive. Also discussed are additional tests which need to be performed to demonstrate the credibility of the GCMs.

3 Synoptic Classification Using GCM Output

Pielke et al. (1987) discussed a procedure to type synoptic weather using conventional large scale weather analyses. Illustrated in Figure 1[1],

[1]Figure 1 and Tables 1 and 2 are reproduced from Pielke et al. (1987).

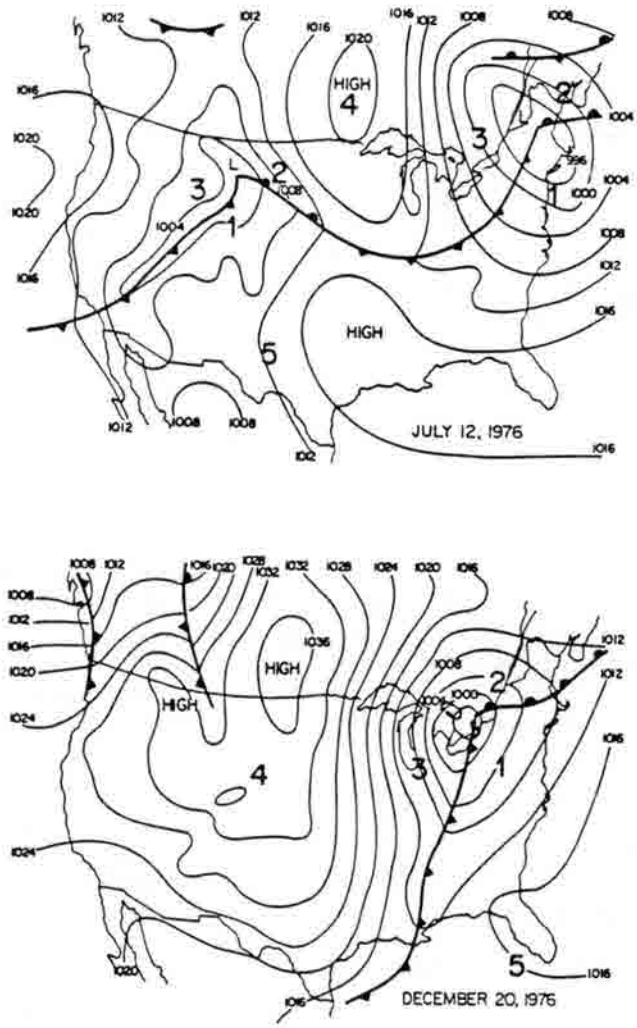

Figure 1. Synoptic classification scheme illustrating typical (a) summer and (b) winter patterns.

the dominant zones within major midlatitude weather systems are identified. Table 1[1] and 2[1] summarize major attributes of each synoptic category. Several investigations have used this synoptic categorization to analyze local climatology. In Yu and Pielke (1986), for example, the frequency and duration of these synoptic classes for a five-year period between October and May in southern Utah were determined as part of an air quality study. Pielke et al. (1986) have used these synoptic categories, and subclasses related to surface synoptic geostrophic wind speed and direction within each category, to estimate worst case air pollution dispersion situations over southern Florida. Garstang et al. (1980), and Lindsey (1980), where this synoptic classification procedure was first introduced, determined the daily frequency of the different synoptic categories for a 10-year period along the Atlantic and Gulf coasts of the United States. Lindsey and Glantz (1984, 1986) used this approach to characterize local meteorology at nuclear facilities. Snow (1981) applied the synoptic classification scheme to determine representative cases to integrate a mesoscale meteorological model in order to estimate wind energy potential for regions along the Gulf of Mexico and Atlantic coasts of the United States. It was found for that study that only three integrations for each site of the mesoscale model were needed to characterize the wind energy available. Recently Stocker and Pielke (1987) have added two categories (corresponding to the monsoon trough and eastern side of the subtropical ridge) for application to the western United States.

Pielke et al. (1987) discussed the application of this synoptic classification scheme to define frequency of occurrence of major weather features as related to the polar front, and to use the frequency of times a location is poleward of the front to meteorologically define seasons. An example of the use of this technique was presented using 10 years of data from the Atlantic and Gulf coasts of the United States. While the frequency of the specific types of major synoptic weather features vary with latitude, the meteorological definitions of season was found to be comparatively invariant with latitude (differing by no more than a month) for this geographic area. Using a meteorological definition, the average winter occurs from late October or early November to late March or early April in the geographic region studied. Summer is from late May to early June until late August or late September. Changes in climatic conditions do not occur as just a gradual change in temperature or in the amount of precipitation but rather in the frequency with which a given region is subjected to the dominant synoptic systems. The net result of the aggregation of synoptic systems yields climate. If the aggregation changes, climate changes. Thus by using GCM model output and typing the weather categories in a climate change scenario, representative cases within each scenario can be used to integrate a numerical mesoscale model in order to assess local long-term weather changes due to GCM simulated large scale climate changes.

With the finest spatial resolution of about 2° x 2° (222 km x 222 km) in GCM models, it is impossible to adequately resolve features with a scale of $4\Delta x$ or smaller (i.e., 888 km x 888 km), as discussed in Pielke (1984, Chapter 10) and elsewhere. Therefore, it will be impossible to properly simulate local climate effects due to only information from a GCM simulation of a change in climate. Using the synoptic classification approach, however, it will be possible to integrate down to local scales using the

[1]Figure 1 and Tables 1 and 2 are reproduced from Pielke et al. (1987).

Table 1. Synoptic classification scheme (from Pielke, 1982; modified from Lindsey, 1980).

Category	Air mass	Reason for categorization*
1	*mT*	*In the warm sector of an extratropical cyclone.* In this region the thickness and vorticity advection is weak with little curvature to the surface isobars. There is limited low level convergence with an upper level ridge tending to produce subsidence. Southerly low-level winds are typical
2	mT/cP, mT/cA, mP/cA	*Ahead of the warm front in the region of cyclonic curvature to the surface isobars.* Warm air advecting upslope over the cold air stabilizes the thermal stratification, while positive vorticity advection and low-level frictional convergence can add to the vertical lifting. Because of the warm advection, the geostrophic winds veer with height. Low-level winds are generally north-easterly through south-easterly
3	*cP; cA*	*Behind the cold front in the region of cyclonic curvature to the surface isobars.* Positive vorticity advection and negative thermal advection dominate, with the resultant cooling causing strong boundary layer mixing. The resulting thermal stratification in the lower troposphere is neutral, or even slightly, superadiabatic. Gusty winds are usually associated with this sector of an extratropical cyclone. Because of the cold advection, the geostrophic winds back with height. Low-level winds are generally from the north-east through south-west
4	*cP; cA*	*Under a polar high in a region of anticyclonic curvature to the surface isobars.* Negative vorticity advection, weak negative thermal advection and low-level frictional divergence usually occur, producing boundary layer subsidence. Because of relatively cool air aloft, the thermal stratification is only slightly stabilized during the day, despite the subsidence. At night, however, the relatively weak surface pressure gradient associated with this category causes very stable layers near the ground on clear nights due to long-wave radiational cooling. The low-level geostrophic winds are usually light to moderate varying slowly from north-westerly to south-easterly as the ridge progresses eastward past a fixed location
5	*mT*	*In the vicinity of a subtropical ridge* where the vorticity and thickness advection, and the horizontal pressure gradient at all levels are weak. The large upper-level ridge, along with the anticyclonically curved low level pressure field, produces weak but persistent subsidence. This sinking causes a stabilization of the atmosphere throughout the troposphere. Low-level winds over the eastern United States associated with these systems tend to blow from the south-east through south-west

* This discussion applies to northern hemisphere.

Table 2. Overview of meteorological aspects of the 5 synoptic categories illustrated in Figure 1 which can be directly obtained from synoptic surface analysis (northern hemisphere) (adapted from Forbes and Pielke, 1985 and Pielke et al., 1986).

Category Characteristics	Category 1	2	3	4	5
Category Class	mT: In the warm sector of an extratropical cyclone	mT/cP, mT/cA, mP/cA: Ahead of the warm front in the region of cyclonic curvature at the surface	cP, cA: Behind the cold front in the region of cyclonic curvature to the surface isobars	cP, cA: Under a polar high in a region of anticyclonic curvature at the surface	mT: In the vicinity and west of a subtropical ridge
Surface winds	Brisk SW surface winds	Light to moderate SE to ENE surface winds	Strong NE to SW surface winds	Light and variable winds	Light SE to SW winds
Vertical motions	Weakening synoptic descent as the cold front approaches	Synoptic ascent due to warm advection and negative vorticity advection aloft becomes positive vorticity advection aloft closer to low center, resulting in enhanced vertical motion	Synoptic ascent due to positive vorticity advection aloft (in this region this ascent more than compensates for the descent due to cold advection)	Synoptic descent (due to warm advection and/or negative vorticity advection aloft)	Synoptic subsidence (descending branch of the Hadley cell). Descent becomes stronger as you approach the ridge axis
Temperature advection	Little temperature advection at the surface	Warm advection above the frontal inversion	Cold advection at the surface	Weak temperature advection at the surface	Weak temperature advection at the surface
Inversion	Weak synoptic subsidence inversion caps planetary boundary layer	Boundary layer capped by frontal inversion	Deep planetary boundary layer	Synoptic subsidence inversion and/or warm advection aloft create an inversion which caps the planetary boundary layer	Synoptic subsidence inversion
Diurnal variation in boundary-layer stability	Moderate diurnal variability in the boundary-layer stability	Little diurnal variability in boundary-layer stability because of cloud cover	Little diurnal variability in the boundary-layer stability because of strong winds and destabilizing of boundary layer by cold advection	In the absence of snow cover, because of clear skies and light winds, there is large diurnal variability in boundary-layer stability	Moderate diurnal variability in boundary-layer stability
Diurnal variation in surface layer stability	Moderately unstable surface layer during the day Moderately stable surface layer during the night	Stably stratified surface layer day and night	Near neutral surface layer day and night	Weakly to moderately unstable surface layer during the day unless snow cover present or low Sun angle, in which case surface layer tends to be stably stratified. Very stable surface layer at night	Moderately to strongly unstable surface layer during the day. Moderately to strongly stable surface layer during the night
Humidity near the surface	Often humid in relative and absolute sense	Often dry in absolute sense, but humid in relative sense	Dry in the absolute sense; usually dry in the relative sense	Dry in the absolute sense, humid in the relative sense at night/dry in relative sense during the day except when ground is snow-covered	Humid in relative and absolute sense
Cloud cover	Clear to partly cloudy skies except near squall lines	Mostly cloudy to cloudy	Clear to scattered or broken shallow to medium depth convective clouds	Clear except tendency for fog at night	Day: scattered fair weather cumulus Night: clear (except near the mesoscale systems listed below)
Dominant mesoscale systems	Squall lines	Embedded lines of convection	Forced airflow over rough terrain systems; lake effect storms	Mountain-valley flows, land-sea breezes, urban circulations (thermally-forced systems)	Mountain-valley flows, land-sea breezes, urban circulations (thermally-forced systems)
Precipitation types	Organized lines of convective precipitation	Often stable cloud types and precipitation. Overcast in general	Medium to shallow depth convective clouds, showery precipitation	No precipitation	Shallow low convective clouds with deeper convective clouds and precipitation organized by thermally forced mesoscale systems such as listed above
Ventilation	Moderate to good ventilation	Poor ventilation of low level (i.e. below frontal inversion) emissions	Excellent ventilation	Night or snow-covered ground: poor ventilation Day: poor to moderate ventilation	Day: moderate to good ventilation Night: moderate to poor ventilation
Deposition	Dry deposition except wet deposition in showers	Dominated by wet deposition	Dry deposition except in showers	Dry deposition	Dry deposition except wet deposition in showers and thunderstorms
Transport	Long range	Long range above inversion	Long range	More local as you approach the centre of the polar high	More local as you approach the centre of the subtropical high

synoptic categories and a physically sophisticated mesoscale meteorological model. Such a modeling approach has the advantage of being able to represent terrain feature which do not currently occur in a region, such as glaciers, snowfields, and different types of vegetation. In addition, GCM predictions of prevailing wind flows different from those found currently could be realistically represented since the model is based on fundamental physical concepts. Greenhouse gas effects could similarly be included.

In summary, GCM model output can be quantitatively evaluated in terms of synoptic categories. Using grid point data from the GCMs the following quantities can be used to define categories (illustrated here for midlatitudes):

- Category 1:
  - cyclonic 1000 mb height curvature; negligible 500 mb vorticity advection; and negligible 700 and 850 mb temperature advection; equatorward of polar front
- Category 2a:
  - cyclonic 1000 mb height curvature; positive 700 and 850 mb temperature advection; negative 500 mb vorticity advection; poleward of polar front
- Category 2b:
  - cyclonic 1000 mb height curvature; positive 700 and 850 mb temperature advection; positive 500 mb vorticity advection; poleward of polar front
- Category 3:
  - cyclonic 1000 mb height curvature; negative 700 and 850 mb temperature advection; positive 500 mb vorticity advection; poleward of polar front
- Category 4a:
  - anticyclonic 1000 mb height curvature; negative 700 and 850 mb temperature advection; negative 500 mb vorticity advection; poleward of polar front
- Category 4b:
  - anticyclonic 1000 mb height curvature; positive 700 mb and 800 mb temperature advection; negative 500 mb vorticity advection; poleward of polar front
- Category 5:
  - anticyclonic 1000 mb height curvature; equatorward of polar front; west side of a subtropical ridge's north-south axis

- Category 6:

  - anticyclonic 1000 mb height curvature; equatorward of polar front; east side of a subtropical ridge's north-south axis

- Category 7:

  - cyclonic 1000 mb height curvature; equatorward of polar front

Within each category, average wind speed and direction, average temperature and moisture soundings, and their standard deviations would be used to set up the initial conditions for the mesoscale meteorological model.

To obtain the synoptic categories, the GCM models must be integrated with seasonal cycles in order to provide the most accurate climate estimates. The integration of GCM models for many days with frozen external forcing in order to obtain "equilibrium conditions" is unrealistic. The real atmosphere is not in equilibrium since the solar input changes continuously throughout the year.

4 Telescoping Nested Grids

The use of GCM model output to provide boundary conditions for a regional-mesoscale nested grid model is an effective technique to link climate changes from a global model to what is expected to occur on a local scale. Such nested models are becoming state-of-the-art. One such example is the Regional Atmosphere Mesoscale Model (RAMS) reported most recently in Cotton et al. (1987) where the nested approach was applied on the large eddy simulation scale. Cram and Pielke (1987) describe a one-way nested version of RAMS used to link National Meteorological Center (NMC) analyses on a large scale to a regional-mesoscale nested grid simulation of a major snowstorm in Colorado.

This approach has the advantage of being able to include detailed terrain, vegetation characteristics, and details of glaciation, if present, which are necessarily lacking in the GCM model because of its lack of resolution. The mesoscale model can even be linked to an ecosystem model in order to investigate the interaction between local climate and the biosphere. Local summer snowfield effects on the surface energy budget can also be included if they develop in the local scale model. Such snowfields will have a major effect on local climate because of changes in albedo that result.

The cost of a nested model simulation for several hundred years is greater than that of the GCM alone but is feasible with state-of-the-art supercomputers. An example of a grid which could be applied to simulate the grassland-forest boundary in the central United States is presented as Figure 2.

A statistical model correlation between GCM output and local weather cannot be applied for general climatic change since a regression model can only be expected to be accurate for the same range of input-output conditions for which it was developed. Even for that case, the model should be tested against an independent data set. When the input parameters fall outside of the data used to construct the regression, nonlinear effects can cause the regression estimate to be in serious error. Thus for future

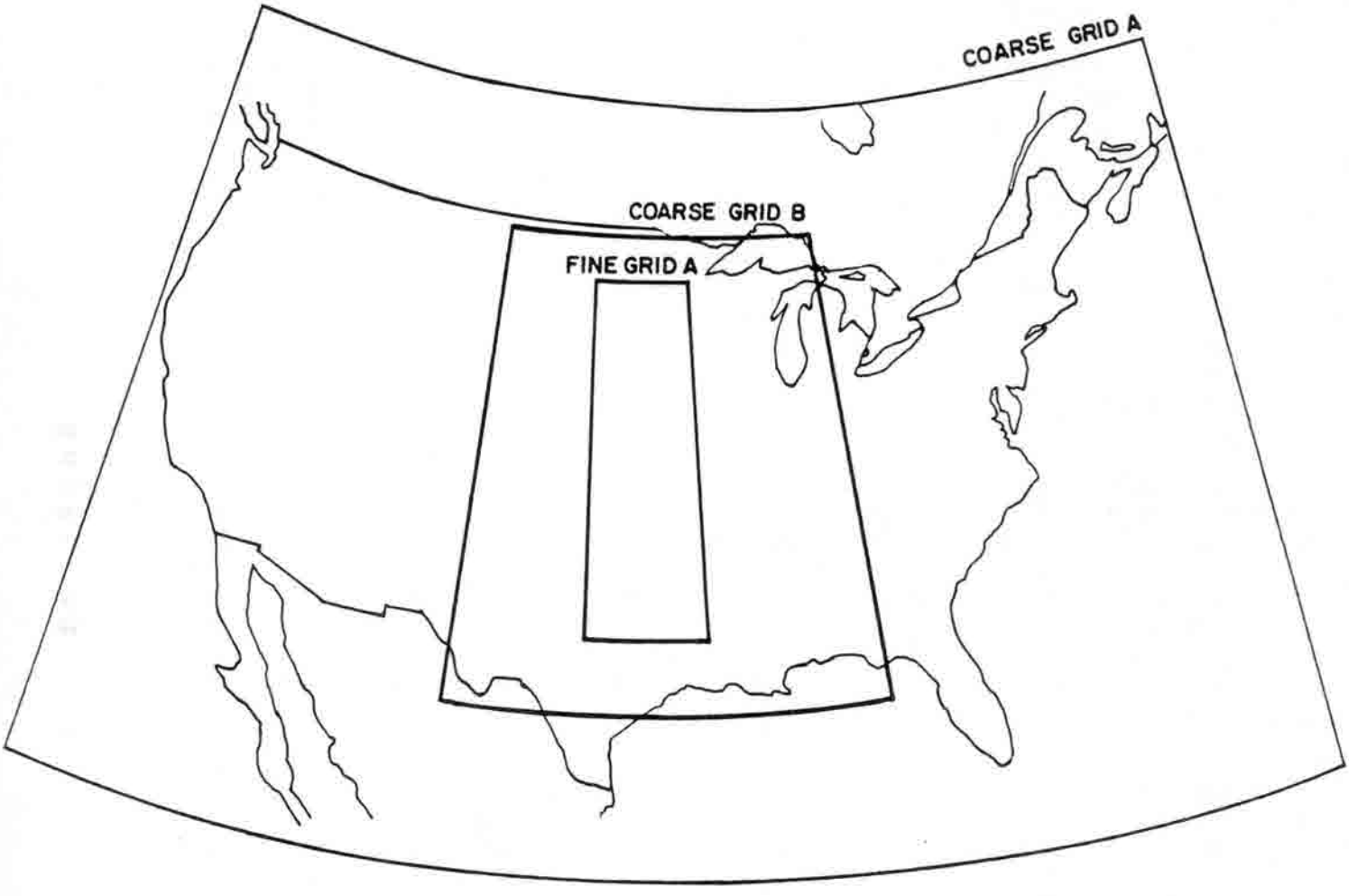

Figure 2. Illustration of telescoping interactive grid nests used to simulate prairie-deciduous forest boundary in the central United States. Boundary conditions for coarse grid A comes from a GCM simulation.

climate scenarios since no data, of course, exists such a model is likely to be insufficient since no analog is available to correctly construct such a tool.

Similarly, objective analysis models which obtain output from a GCM model are able to provide efficient estimates of the effect of complex topography on winds only for very restricted atmospheric conditions (see Pielke, 1985). Only a dynamically complete meteorological model such as RAMS is able to represent the complex interactions between the surface and the overlying atmosphere.

5 Missing Physical Feedback Mechanisms in GCMs

The influence of a number of physical processes in GCMs makes interpretation of their results tentative. Such models, for example, do not represent changes in the average earth's albedo due to anthropogenic aerosol pollution which can alter the albedo of the atmosphere directly, or when the aerosols are entrained into cloud droplets. A greater concentration of aerosols which serve as cloud condensation nuclei can make the clouds colloidally more stable, thereby allowing the clouds to persist longer, thus contributing to a larger planetary albedo for short wave radiation.

The dynamic accuracy of GCM models have not been adequately tested. Such models need to be used to predict short-term weather changes since skill at such forecasts is essential if the models are to demonstrate a numerical fidelity in simulating wave-wave interactions. If GCMs have insufficient spatial resolution or physics to forecast weather as accurately as current operational weather numerical weather prediction models, what confidence should be placed on their skill at predicting long-term climate change? Long-term climate is made up of a cumulation of day-to-day weather.

6 Summary

This short paper discusses two approaches to permit the interpolation of GCM model results down to local scales. The first approach uses a synoptic classification of GCM output to construct dominant large scale weather scenarios from which local scale model simulations can be performed. The second approach links the GCM model output to two-way multiple interactive numerical model grids which telescope down to the local scale. The local scale models in both cases include detailed terrain, and vegetation and soil representations of the area. Vegetation changes due to climate change can assist in the estimation as to whether alterations in the biosphere can mitigate climate change perturbations (i.e., the Lovelock Gaia hypothesis).

7 Acknowledgements

The author acknowledges the support of Doug Wesley in obtaining Figure 2 used in this paper. The opportunity to present these views was facilitated by the goal of CIRA Director Tom Vonder Haar to permit an effective exchange of ideas at annual CIRA workshops. Dallas McDonald is thanked for completing her normal outstanding editorial preparation of the paper. Support for the typing of the paper was provided by NSF grant #ATM-3616662.

8 References

Cotton, W. R., R. A. Pielke, C. Chen, M. G. Hadfield, C. J. Tremback, and R. L. Walko, 1987: Large eddy simulations of plume transport and dispersion over flat and hilly terrain. Final Report, EPRI Contract No. 1630-25, September, Electric Power Research Institute, Inc., Palo Alto, California, 60 pp. + Appendices.

Cram, J. M. and R. A. Pielke, 1987: The importance of synoptic forcing and mesoscale terrain to a numerical simulation of an orographically-induced system. Proceedings of the 3rd AMS Conference on Mesoscale Processes, August 21-26, 1987. Vancouver, British Columbia, Canada, 118-119.

Garstang, M., S. Nnaji, R. A. Pielke, J. Gusdorf, C. Lindsey, J. W. Snow, 1980: Coastal zone wind energy, Part 1. Synoptic and mesoscale controls and distributions of coastal wind energy. DOE Contract DE-AS06-76ET-20274, March 1980.

Lindsey, C. G., 1980: Analysis of coastal wind energy regimes. M.S. Thesis, University of Virginia, June 1980.

Lindsey, C. G. and C. S. Glantz, 1984: A method to characterize local meteorology for air pollution studies and emergency response needs. Reprint, AMS Fourth Joint Conference on Application of Air Pollution Meteorology, 16-19 October 1984, Portland, Oregon, 260-263.

Lindsey, C. G. and C. S. Glantz, 1986: A method to characterize local meteorology at nuclear facilities for application to emergency response needs. Report prepared for the U.S. Nuclear Regulatory Commission, NUREG/CR-3882 PNL-5155, 53 pp.

Lovelock, J. E., 1979: A New Look at Life on Earth, Oxford University Press, 175 pp.

Pielke, R. A., 1984: Mesoscale Meteorological Modeling, Academic Press, New York, NY, 612 pp.

Pielke, R. A., 1985: The use of mesoscale numerical models to assess wind distribution and boundary layer structure in complex terrain. Bound. Layer Meteor., **31**, 217-231.

Pielke, R. A., M. Garstang, C. Lindsey and J. Gusdorf, 1987: Use of a synoptic classification scheme to define seasons. Theor. Appl. Climatol., **38**, 57-68.

Pielke, R. A., R. W. Arritt, M. Segal, M. D. Moran and R. T. McNider, 1987: Mesoscale numerical modeling of pollutant transport in complex terrain. Bound.-Layer Meteor. (in press).

Schlesinger, M. E. and J. F. B. Mitchell, 1987: Model projections of the equilibrium climatic response to increased carbon dioxide. Rev. Geophys., **25**, 760-798.

Snow, J. W., 1981: Coastal zone wind power assessment. Ph.D. Dissertation, Department of Environmental Sciences, University of Virginia, 244 pp.

Stocker, R. A. and R. A. Pielke, 1987: A synoptic classification of air mass, wind direction, and wind speed for the western United States (1980-1984). (In preparation).

Yu, C-H. and R. A. Pielke, 1986: Mesoscale air quality under stagnant synoptic cold season conditions in the Lake Powell area. Atmos. Environ., **20**, 1751-1762.

PREDICTION OF REGIONAL AND LOCAL ECOLOGICAL CHANGE FROM GLOBAL CLIMATE MODEL RESULTS: A HIERARCHIAL MODELING APPROACH

Timothy G.F. Kittel[1,2] and Michael B. Coughenour[2]

1. Introduction

Ecological impacts of increasing levels of greenhouse gases are likely to be far-reaching and multifaceted. Both the climatic effects of rising concentrations of greenhouse gases and the direct physiological effects of elevated CO_2 are anticipated to have plant through ecosystem level consequences (Lemon 1983, Bazzaz 1986, Oechel and Riechers 1986, Solomon 1986, Bolin et al. 1986, Shands and Hoffman 1987, Pastor and Post 1988, Schimel et al. 1988). Such ecological changes are expected in turn to have feedbacks to climate through their effect on biophysical properties of the land surface (Dickinson 1983, 1985) and on biogeochemical processes that generate greenhouse gases (Bolin 1984).

The modeling of ecosystem processes will play a central role in prediction of such ecological change. Simulation of ecological change can identify the response of key ecosystem processes to novel climatic conditions and atmospheric chemistry. Key processes include those with the potential for (1) extra-regional to global ecological impacts (e.g., through changes in drainage basin nutrient effluxes or changes in the distribution of biomes), (2) socio-economic impacts (e.g., through changing forest, range, and crop production), and for (3) feedbacks to climate (e.g., through changes in albedo, transpiration, and trace gas production). Identification of ecological processes with high sensitivity to CO_2 and climate change will aid in designing strategies for change detection.

---

[1]Cooperative Institute for Research in the Atmosphere, Colorado State University, Ft. Collins, CO 80523

[2]Natural Resource Ecology Laboratory, Colorado State University, Ft. Collins, CO 80523

Prediction of ecological response to CO_2 and climate change will require (1) simulation of the interaction of different ecological processes at multiple temporal scales and (2) translation of climatic and ecological responses to finer or coarser spatial scales. The first requirement is dictated by differences in response times of physiological, community, and ecosystem processes. The second requirement arises from the need to both scale down global climate model results to reflect biologically important geographical variation in surface climate and to scale up ecological simulations to assess socio-economic impacts and biological feedbacks to climate on regional and global scales.

In this paper, we present a hierarchial modeling approach for meeting these requirements in which information is passed between models of different spatial and temporal resolutions. A hierarchial approach allows for processes simulated at one scale to be limited by processes modelled at coarser scales while being sensitive to processes modelled at finer scales (Simon 1962, Rosen 1971, Allen and Starr 1982, O'Neill et al. 1986). Figure 1 shows examples of models that can be used in a hierarchial framework to model climatic and ecological dynamics of the North American Central Grasslands. Such a framework can be used to address questions of change over a range of scales, e.g. subcontinental, regional, or site scales and century, annual, or daily response times. We present an overview of this approach in the next section and discuss its application in Sections 3 and 4.

2. Hierarchial Modeling

a. Background

Mechanistic plant physiological models with enough detail to represent plant response through several life cycles, for several biomes, have been

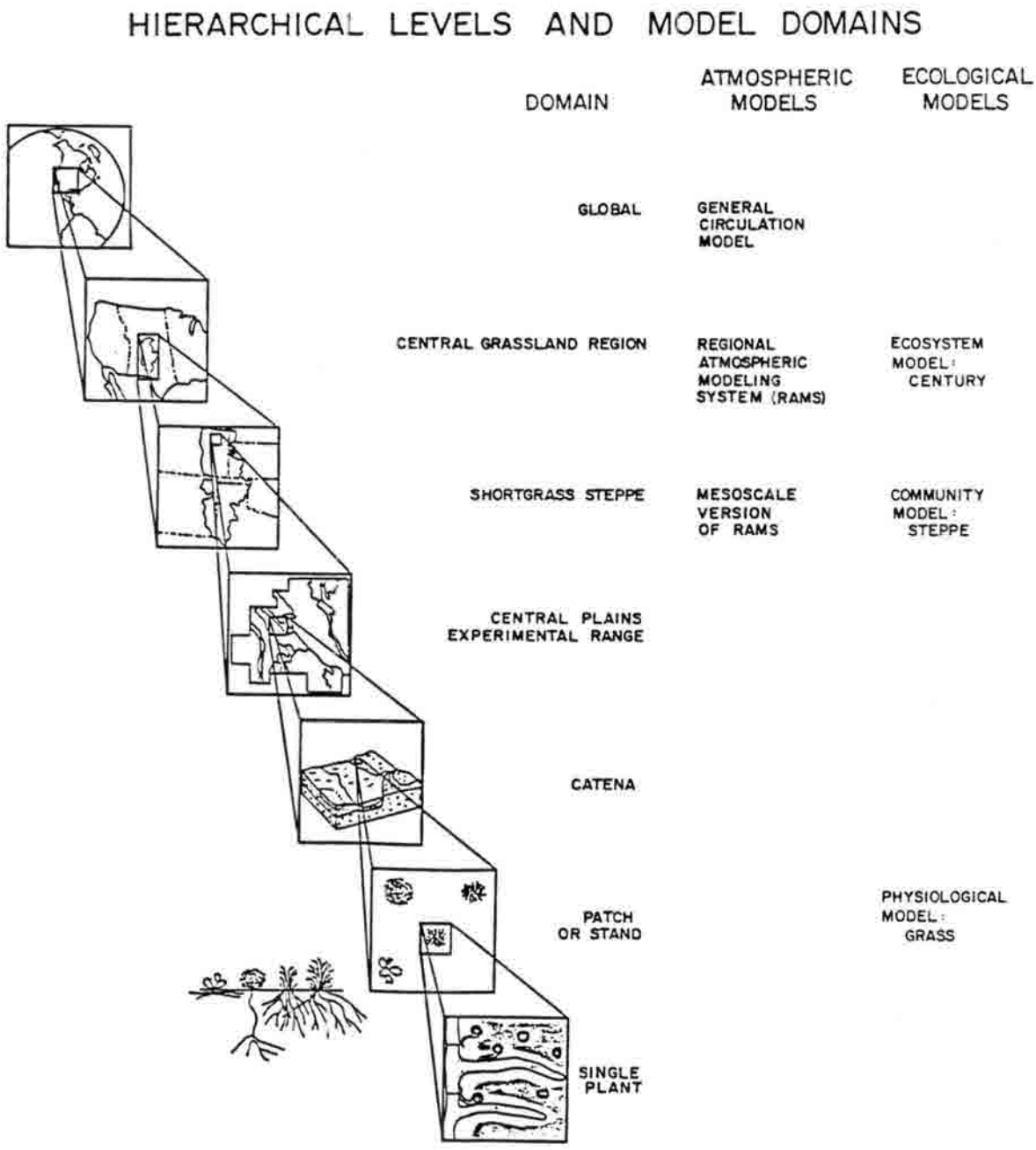

Figure 1. Hierarchial levels and spatial domains of atmospheric and ecological models discussed in the text.

suggested as forming the core of the needed tool for predicting the ecological impacts of CO_2 and climate change (Strain and Bazzaz 1983). Other suggestions include a "generic" or universally applicable model of plant growth (Reynolds and Acock 1985) and a model that starts out with a detailed analysis of the physiological responses of two species, then subsequently becomes a model of a multispecies community through stepwise model extension, validation, and refinement (Bazzaz et al. 1985). However, serious attention needs to be given to problems of scaling up physiological responses at small scales to ecosystem level responses (Shugart and Emanuel 1985).

Existing models can be modified to address the problem of ecosystem CO_2 and climate change responses individually. This fragmented approach would probably provide an inconsistent or confusing set of predictions because individual models are constructed for different purposes and consequently cannot be expected to give comparable predictions for all situations. Individual models are also constructed at widely differing spatial and temporal scales. Failure to consider scale differences sometimes results in different predictions of the same apparent phenomena (e.g., Clark 1985, Jarvis and McNaughton 1986, Belsky 1987).

We know of no modeling systems available at present that explicitly synthesize predictions at scales of leaves, plants, communities, ecosystems, and regions, although paradigms have been proposed (Senft et al. 1987, Urban et al. 1987, French 1986, Clark 1985). Reiners (1986) recently expressed a similar need for multiple complementary models of energy, nutrient, and community level phenomena. Urban et al. (1986) suggested that a hierarchical model is the best vehicle to reconcile traditional bottom-up and top-down approaches to systems analysis. Olson (1986) similarly proposed a nested array of large-scale models which begins with middle-

number systems, scaling upwards by looking at populations of landscape subunits or downwards for finer analysis. The idea of developing a modeling paradigm in systems ecology analogous to the compound or zoom microscope, zooming in and out of different scales, is particularly intriguing (Shugart and Smith 1986).

b. Approach

The time step of a model must be scaled to the turnover rate of its state variables. If, however, a model contains state variables with a wide range of turnover rates, the model might be most appropriately represented as a hierarchy of interacting submodels having different time steps. In such a hierarchial model, coarse and fine scale processes interact: slowly changing variables constrain rapidly changing variables, while filtered variations in rapidly changing variables modify slowly changing variables (Fig. 2a).

For example, in the plant physiological model GRASS (Coughenour et al. 1984a, 1984b, Coughenour 1984), leaf mass is a state variable that changes every day. This slowly changing variable is entered as a constant into hourly calculations of photosynthesis and minutely calculations of transpiration. Thus, leaf mass constrains total photosynthesis and transpiration. Conversely, minute-scale variations in stomatal conductance are averaged (i.e. filtered) to calculate hour-scale variations in photosynthesis. Hourly photosynthetic uptake is in turn summed to calculate daily assimilation, translocation, and growth, affecting leaf mass. In this manner, leaf mass is sensitive to variations in stomatal conductance.

In a model hierarchy, information exchange between models operating at different scales can be facilitated by using a model at a given level to parameterize a coarser scaled model or to drive a finer scaled model. Output from a fine-scale model can be filtered to form parameters used in a

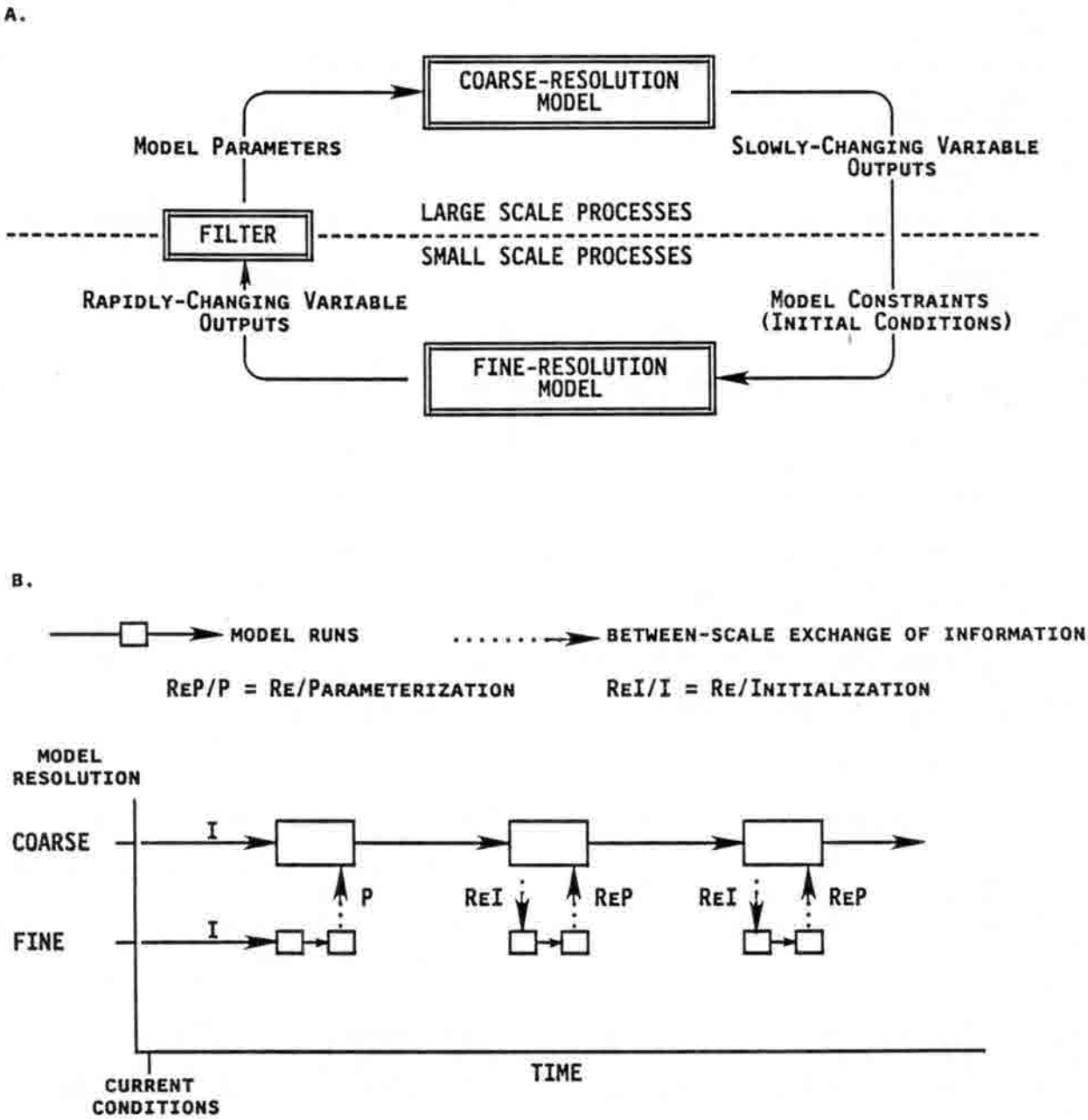

Figure 2. Hierarchial linking of models. **a**, Exchange of information between two differently scaled models: Scaling down is facilitated by using a coarse resolution model to generate conditions to drive a fine resolution model, and scaling up is achieved by filtering output from a fine resolution model to parameterize a coarse resolution model. **b**, Zooming in and zooming out: Periodic invoking of a fine resolution model and reparameterization of a coarse resolution model.

coarse-scale model. Filters can be simple, such as sums or averages, or complex transformations of high resolution data (Allen and Starr 1982). A coarse-scale model can in turn be used to generate an environment or a set of initial conditions for a fine-scale model. For example, a plant community dynamics model with an annual time step can be run for five hundred years to generate a canopy structure that is used as initial conditions for a daily time step model of individual plant photosynthesis. Such downscaling (or zooming in) is apparently a far less common technique than upscaling (zooming out) in systems modeling.

Information exchange between two differently scaled models can be fully interactive, as illustrated in Figure 2a. In simulating a multiscale response over very long time periods, such interactive coupling need only be invoked periodically (i.e. with a long time step) if parameters in the coarse scale model are expected to change slowly (Fig. 2b). For example, in a simulation run of plant community change under changing CO_2 and climate conditions, growth rate modifiers in the community model can be reparameterized every 50 or so years by zooming in to the plant scale, running a plant physiological model to generate new modifiers, and then zoom back out to the community level.

The hierarchial modeling approach can be applied to simulating the ecological impact of global climate change and of atmospheric CO_2 enrichment in two stages: (1) modeling regional climate response to global climate change and (2) modeling ecosystem response to elevated CO_2 and regional climate change.

3. Modeling Regional Climate Response to Global Climate Change

A major problem with using of GCM results as inputs to ecological models is in translating the coarse spatial resolution climate model output (e.g., 3.9° latitude x 5° longitude grid, ~400 km square in the mid-latitudes) to a finer resolution closer to the scales of ecologically significant spatial variation in surface climate. Interpolation (e.g., by kriging) of GCM surface climate results to finer scales is limited by subgrid-scale heterogeneity in topography, vegetation, and other environmental factors that modify regional climate. Alternatively, GCM output fields of upper air circulation, pressure, temperature, and moisture can be used to drive a regional or mesoscale atmospheric model that can generate a higher resolution view of temperature and precipitation distribution (see Figs. 1 and 3). Such models include the Pennsylvania State University/NCAR Mesoscale Model (Anthes and Warner 1978) and the Colorado State University Regional Atmospheric Modeling System (RAMS) (Cotton et al. 1987, Pielke 1974). This method, involving the nesting of GCM and finer scaled atmospheric models, is discussed by Pielke (1988) in this volume.

The higher resolution models have the ability to interpret coarse resolution atmospheric fields at finer spatial scales by accounting for the effects of sub-GCM grid scale atmospheric and land surface processes. These include the effects of subregional topography on synoptic circulation (Cram and Pielke 1987) and on the development of mesoscale circulations (Abbs and Pielke 1986). Surface contrasts in evapotranspiration, albedo, and roughness arising from vegetation distribution patterns also have important effects on mesoscale circulation and are simulated by these models (Segal et al. 1988).

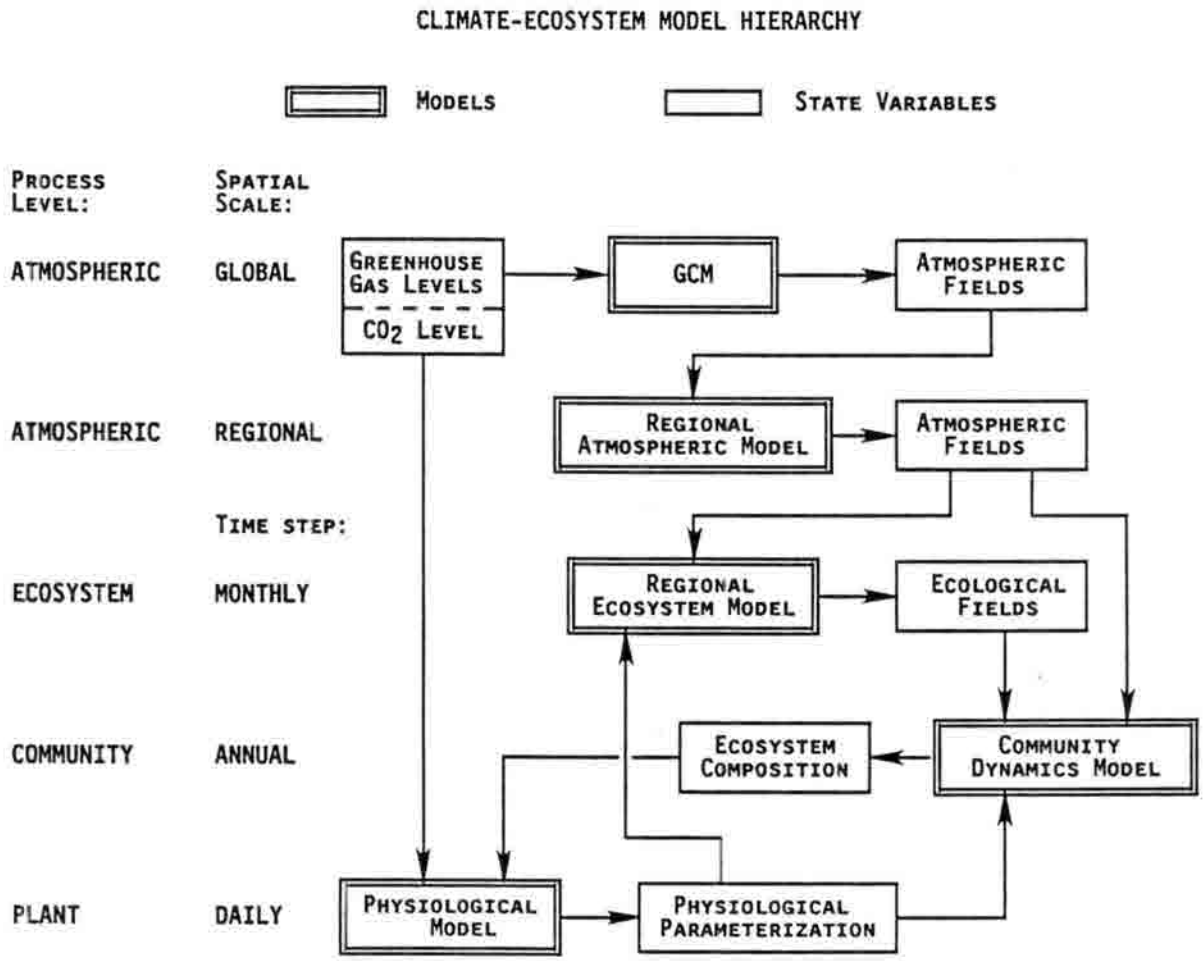

Figure 3. Climate-ecosystem model hierarchy. Interactions between climate and ecological models operating at different spatial or temporal scales needed for the prediction of regional ecological response to climatic effects of rising concentrations of greenhouse gases and to direct physiological effects of elevated atmospheric CO_2.

In the nesting of these models, the GCM data required to drive regional/mesoscale models must have a high temporal resolution (e.g., hourly or twice-daily). This is because longer term data of circulation parameters (e.g., monthly means) do not have the temporal information needed to determine monthly precipitation. High temporal resolution climate data (or derived frequency statistics) are additionally of value because they can be used by some fine-scale ecological models.

Together, GCMs and regional and mesoscale models form a hierarchial framework within which climate change can be examined at a range of scales. Regional (e.g., 50-100 km) through mesoscale (e.g., 5-20 km) resolution climatologies can be developed for GCM $1xCO_2$ and $2xCO_2$ equilibrium climate simulations (e.g., Hansen et al. 1984, Washington and Meehl 1984, Wetherald and Manabe 1986) or for simulations of transient climate change (e.g., Schlesinger 1988, this volume). These high spatial resolution climatologies can be used to drive ecological models for the prediction of the impacts of climate change across regions such as the North American Central Grasslands (see Section 4.b). The hierarchial nesting of atmospheric models is also being used by Dickinson and colleagues (Dickinson et al. 1987) in a study of past, present, and future hydrology of the Intermountain West.

4. Hierarchial Modeling of Ecological Response

a. Overview

A hierarchial ecological modeling system that can simulate response to CO_2 and climate change must have a set of levels (Fig. 3) ranging from those that can utilize regional/mesoscale climate inputs to those that can account for changes in physiological responses. Models of ecosystem nutrient dynamics that focus on the role of climatic and other environmental variables with large scale (e.g. regional) gradients are well suited for the

study of the impacts of regional/mesoscale climate change (Schimel et al. 1988). In such models, physiological and other rapidly changing processes are commonly treated empirically rather than mechanistically. Consequently, major changes in environmental conditions with time, such as ambient CO_2 concentration and community structure, may dictate model reparameterization. Reparameterization can be accomplished by running a plant physiological model and other fine-scale models at periodic intervals. A community dynamics model can be run in parallel to ecosystem model simulations to change community makeup and density used in the ecosystem model and/or the physiological model. The hierarchial linking of a regional ecosystem with the longer time step community and shorter time step physiological models will facilitate the prediction of ecological change over a range of spatial and temporal scales.

b. Example

Figures 1 and 3 show a set of ecological models that can be hierarchically linked to predict the impacts of global atmospheric CO_2 and climate change across the North American Central Grasslands. CENTURY (Parton et al. 1987) is a regional grassland ecosystem model. The model successfully simulates biogeochemical cycling of C, N, and other nutrients through plant, litter, and soil reservoirs (Parton et al. 1987, 1988). These processes are modeled with a monthly time step with inputs of monthly temperature and precipitation. For different soil types and land management practices, CENTURY has the potential ability to make predictions of future regional changes in ecosystem dynamics, including (1) primary production, (2) decomposition and mineralization rates, (3) soil carbon (addressing the question whether the soil becomes a source or sink for C), and (4) biogenic trace gas production (such as NO and other important greenhouse gases) (Schimel et al. 1988). However, the application of CENTURY to CO_2 and

climate change is partially limited by its simplicity. For example, primary production is empirically predicted from monthly rainfall and available nitrogen and is not directly affected by CO_2 or temperature. In addition, model parameters for plant processes are generalized for the plant community.

CENTURY's formulation can be refined and its domain expanded to encompass future environmental conditions (such as elevated CO_2) by basing its parameters on filtered results of multiple simulations of a fine scale plant physiological model, such as GRASS (Coughenour et al. 1984a,b, Coughenour 1984) (Fig. 3). Described in part in Section 2, GRASS is a high resolution plant stand model suitable for examination of short-term, mechanistic plant responses to CO_2 and climate (McNaughton et al. 1986). Simulations with GRASS to parameterize CENTURY can include factorial runs for the effects of varying CO_2, temperature, rainfall, grazing, etc.

GRASS must be initialized for a stand's species and plant density. A community model, such as STEPPE, can be run under changed or changing climate and CO_2 levels and under different grazing intensities to yield initial conditions for the physiological model (Fig. 3). STEPPE is a gap dynamics model developed for the shortgrass steppe by Coffin and Lauenroth (Coffin 1988, Coffin and Lauenroth 1986, 1987). It is analogous to widely used forest gap models (Shugart 1984, Solomon 1986, Pastor and Post 1986) and is being expanded for other grassland types (W. Lauenroth, personal communication). This model simulates recruitment, growth, and mortality of individual plants on small plots through time on an annual time step. Seed germination and establishment are affected by temporal patterns of temperature and moisture, while subsequent growth is dependent on precipitation, temperature, and nutrients.

While STEPPE can generate constraints for the plant physiological model, GRASS can in turn be used to parameterize the community model (Fig. 3). Estimates of annual growth response to precipitation, temperature, grazing, seasonality of moisture, and CO_2 used in STEPPE can be generated from multiple runs of GRASS.

Driven by regional or mesoscale climate change scenarios and operating within a hierarchial framework (Fig. 3), CENTURY can predict the regional response of grassland ecosystems to changing CO_2 and climate. CENTURY's domain in ecosystem response space is expanded, because many of its parameters and constraints, responding to processes at other scales, are able to change with changing CO_2 and climate. In addition to plant physiological processes, other fine-scale processes affecting nutrient cycling can be upscaled and incorporated in CENTURY by using corresponding models, such as those for rapidly changing soil processes (e.g. PHOENIX, McGill et al. 1981) and ruminant nitrogen metabolism (e.g., Swift 1983).

The hierarchial linking of these models can be used to address questions regarding ecological change across many spatial and temporal scales in addition to the ecosystem impacts modeled by CENTURY alone (mentioned above). The linked models can predict (1) short vs. long-term responses of productivity to elevated CO_2, (2) shoot vs. root allocation of biomass, (3) transpiration and water use efficiency, (4) tissue C:N and nutrient use efficiency, (5) plant-plant interactions (e.g., relative competitiveness of plants with C_4 vs. C_3 photosynthetic pathways), (6) community composition and ecosystem distribution, and (7) plant-herbivore interactions (e.g., forage quality).

5. Other Considerations

Predictions of ecological change over large areas are presently limited by a number of conceptual and methodological difficulties in addition to the interaction of processes across scales and the low spatial resolution of GCM simulations. These include: (1) model data requirements, (2) subregional spatial heterogeneity, (3) uncertainty in climate predictions, (4) the nature of equilibrium vs. transient responses, and (5) biospheric feedbacks to climate.

Model data requirements. Parameterization of physiological and community level models for all major species in a region such as the Central Grasslands is unpractical. This problem can be approached in two ways: (i) species can be modeled as plant functional groups (such as C_3 short and tallgrasses), and (ii) model experiments can "zoom in" from larger domains (e.g. subcontinental) to smaller domains where parameterizations are well known (e.g., study sites).

Subregional spatial heterogeneity. Climate and other geographical model inputs, such as soil texture and land use, can have high spatial heterogeneity at the scale of regional/mesoscale atmospheric model grids. Running ecological models for all subareas (e.g., atmospheric model grid points) in a region can be computationally prohibitive. Alternatively, response surfaces of ecological model outputs can be generated over the range of climatic and other model input factors. Interpolation on these response surfaces can then be used to produce maps of ecological change in combination with maps of factor data held in a geographical information system. In this manner, the number of model runs is reduced, while the spatial resolution of the regional response to CO_2 and climate change is preserved.

Uncertainty in climate predictions. Limitations in climate models and the role of currently unpredictable climate forcing mechanisms (such as changes in solar output and volcanic activity) indicate that GCM scenarios of climate change are not likely to be exactly realized. In spite of these uncertainties, studies using such predictions are worthwhile because they can explore the potential for ecological change under plausible climate change scenarios.

Equilibrium vs. transient response. To reveal changes in the next 50-100 years, studies of transient climatic and ecological response to increasing levels of greenhouse gases are more appropriate than equilibrium studies. This is because greenhouse gas levels are likely to continue increasing into the next century (Ramanathan et al. 1985). In addition, lags in climate, nutrient dynamics, and community dynamics will require substantial time periods (on the order of a hundred to a thousand or more years) for new steady states to arise (Cole 1985). However, most GCM simulations to date are for 1x and $2xCO_2$ equilibrium climates (e.g. Hansen et al. 1984, Washington and Meehl 1984, Wetherald and Manabe 1986). The simulation of transient climatic response by GCMs is computationally intensive, requiring representation of lagged oceanic responses (see Schlesinger 1988, this volume) and of biospheric feedbacks to climate (discussed below). Simulations of ecological change will improve as more transient climate experiment results become available.

Biospheric feedbacks to climate. Dickinson and Henderson-Sellers (1987), Meehl and Washington (1987), Sud and Molod (1986), Rind (1984), and others have demonstrated the sensitivity of GCMs to land surface processes. However, at present, most GCM climate simulations do not include climate-induced changes in land surface properties which can in turn influence climate. Some schemes currently exist to model changes in biophysical

properties within GCMs, e.g., the Simple Biosphere Model (SiB) (Sellers et al. 1986) and the Biosphere-Atmosphere Transfer Scheme (BATS) (Dickinson et al. 1986). However, simulation of long-term changes in ecosystem and community dynamics that will affect land surface-climate interactions are not included (Schimel and Kittel 1988). A hierarchial modeling approach may facilitate the incorporation of ecological processes by providing a means to synthesize at GCM scales the multiscaled interactions of climate and the biosphere.

6. Summary

Prediction of ecological response to global climate change and elevated atmospheric CO_2 requires translation of global climate model results to finer spatial scales and simulation of the interaction of different ecological processes at multiple scales. To solve these scaling problems, a hierarchial modeling approach permits information to be passed between models of different spatial and temporal scales. Using this approach, regional and mesoscale atmospheric models can be driven by GCM simulation output to generate a higher spatial resolution view of climate change. The hierarchial linking of community, ecosystem, and physiological models enables simulations of ecosystem change to account for long-term changes in community structure while being sensitive to filtered changes in rapidly varying physiological processes. Such a hierarchial approach will permit us to address questions regarding the regional response of community structure, biogeochemical cycles, and biophysical processes to the direct physiological effects of elevated CO_2 and the effects of greenhouse gas-induced global climate change as predicted by GCMs.

7. Acknowledgements

W. Lauenroth, W. Parton, R. Pielke, and D. Schimel contributed to the formulation of ideas presented here. Thanks are also due to I. Burke, W. Lauenroth, J. Moore, R. Pielke, and D. Schimel for their comments on the manuscript.

8. References

Abbs, D.J., and R.A. Pielke. 1986. Thermally forced surface flow and convergence patterns over northeast Colorado. Mon. Wea. Rev. 114:2281-2296.

Allen, T.F.H., and T.B. Starr. 1982. Hierarchy: Perspectives for Ecological Complexity. University of Chicago Press, Chicago.

Anthes, R.A., and T.T. Warner. 1978. Development of hydrodynamic models suitable for air pollution and other mesometeorological studies. Mon. Wea. Rev. 106:1045-1078.

Bazzaz, F.A. 1986. Global CO_2 levels and the response of plants at the population and community levels. pp. 31-35. In: Climate-Vegetation Interactions. C. Rosenzweig and R. Dickinson, eds. University Corporation for Atmospheric Research, Boulder, Colorado. Report OIES-2.

Bazzaz, F.A., K. Garbut, and W.E. Williams. 1985. Effect of increased atmospheric carbon dioxide concentration on plant communities. Ch. 7 In: Direct Effects of Increasing Carbon Dioxide on Vegetation. B.R. Strain and J.D. Cure, eds. Dept. of Energy, Washington, D.C.

Belsky, A.J. 1987. The effects of grazing: Confounding ecosystem, community and organismal scales. Amer. Nat. 129: 777-783.

Bolin, B. 1984. Biogeochemical processes and climate modeling. pp. 213-224. In: The Global Climate. F.T. Houghton, ed. Cambridge University Press.

Bolin, B., B.R. Döös, J. Jäger, and R.A. Warrick (eds.). 1986. The Greenhouse Effect, Climatic Change, and Ecosystems. Wiley, Chichester. 541 pp.

Clark, W.C. 1985. Scales of climate impacts. Climatic Change 7:5-27.

Coffin, D.P. 1988. Gap-phase dynamics and succession in the shortgrass steppe. Ph.D. Dissertation. Colorado State University.

Coffin, D.P., and W.K. Lauenroth. 1986. The role of gap-phase dynamics in a short-grass community. Program of the IV International Congress of Ecology, Syracuse, N.Y. (abstract).

Coffin, D.P., and W.K. Lauenroth. 1987. Small-scale disturbances and gap dynamics in a shortgrass prairie community. Program of the 72nd Annual Meeting of the Ecological Society of America, Aug. 1987, Columbus, Ohio. (abstract)

Cole, K. 1985. Past rates of change, species richness, and a model of vegetative inertia in the Grand Canyon, Arizona. Amer. Nat. 125:289-303.

Cotton, W.R., R.A. Pielke, C. Chen, M.G. Hadfield, C.J. Tremback, and R.L. Walko. 1987. Large eddy simulations of plume transport and dispersion over flat and hilly terrain. Final Report, EPRI Contract No. 1630-25, September, Electric Power Research Institute, Inc., Palo Alto, California, 60 pp. + Appendices.

Coughenour, M.B. 1984. A mechanistic simulation analysis of water use, leaf angles, and grazing in East African grasslands. Ecol. Modelling 26:203-230.

Coughenour, M.B., S.J. McNaughton, and L.L. Wallace. 1984a. Modelling primary production of perennial graminoids - Uniting physiological processes and morphometric traits. Ecol. Modelling 23:101-134.

Coughenour, M.B., S.J. McNaughton, and L.L. Wallace. 1984b. Simulation study of East-African perennial graminoid responses to defoliation. Ecol. Modelling 26:177-201.

Cram, J.M., and R.A. Pielke. 1987. The importance of synoptic forcing and mesoscale terrain to a numerical simulation of an orographically-induced system. Proceedings of the 3rd American Meteorological Society Conference on Mesoscale Processes, August 21-26, 1987, Vancouver, British Columbia. pp. 118-119.

Dickinson, R.E. 1983. Land surface processes and climate-surface albedos and energy balance. Advances in Geophysics 25:305-353.

Dickinson, R.E. 1985. Climatic sensitivity. Adv. Geophys. 28A:99-129.

Dickinson, R.E., and A. Henderson-Sellers. 1987. Modelling tropical deforestation: A study of GCM land-surface parameterizations. Quart. J. Royal Met. Soc. (in revision).

Dickinson, R.E., A. Henderson-Sellers, P.J. Kennedy, and M.F. Wilson. 1986. Biosphere-Atmosphere Transfer Scheme (BATS) for the NCAR Community Climate Model. National Center for Atmospheric Research, Boulder, Colorado. Tech. Note/TN-275+str. 69 pp.

Dickinson, R.E., R.M. Errico, F. Giorgi, and G.T. Bates. 1987. Modeling of Historic, Prehistoric, and Future Climates of the Great Basin. Progress Report to USGS/NNWSI. 27 pp.

French, N.R. 1986. Hierarchical conceptual model of the alpine geosystem. Arc. Alp. Res. 18:133-146.

Hansen, J., A. Lacis, D. Rind, G. Russell, P. Stone, I. Fung, R. Ruedy, and J. Lerner. 1984. Climate sensitivity: Analysis of feedback mechanisms. pp. 130-163. In: Climate Processes and Climate Sensitivity. J.E. Hansen and T. Takahashi, eds. American Geophysical Union, Washington, DC.

Jarvis, P.G., and K.G. McNaughton. 1986. Stomatal control of transpiration: Scaling up from leaf to region. Adv. Ecol. Res. 15:1-49.

Lemon, E.D. (ed.). 1983. CO_2 and Plants. The Response of Plants to Rising Levels of Atmospheric Carbon Dioxide. AAAS Selected Symposium #84. Westview Press, Boulder, Colorado.

McGill, W.B., H.W. Hunt, R.G. Woodmansee, and J.O. Ruess. 1981. PHOENIX, a model of the dynamics of carbon and nitrogen in grassland soils. Ecol. Bull. (Stockholm) 33:49-115.

McNaughton, S.J., R.W. Ruess, and M.B. Coughenour. 1986. Ecological consequences of nuclear war: Grassland ecosystem simulations. Nature 321:483-487.

Meehl, G.A., and W.M. Washington. 1987. A comparison of soil moisture sensitivity in two global climate models. J. Atmos. Sci. (submitted).

Oechel, W.C., and G.H. Riechers. 1986. Impacts of increasing CO_2 on natural vegetation, particulary the tundra. pp. 36-42. In: Climate-Vegetation Interactions. C. Rosenzweig and R. Dickinson, eds. University Corporation for Atmospheric Research, Boulder, Colorado. Report OIES-2.

Olson, J.S. 1986. Global and regional synthesis: Needs and opportunities for a hierarchy of scales of remote sensing and modeling. pp. 9-22. In: Coupling of Ecological Studies with Remote Sensing. M.I. Dyer and D.A. Crossley, Jr., eds. U.S. Department of State Publ. 9504, Man and the Biosphere Program. Washington, D.C.

O'Neill, R.V., D.L. DeAngelis, J.B. Waide, and T.F.H. Allen. 1986. A Hierarchical Concept of Ecosystems. Princeton University Press. Princeton. 253 pp.

Parton, W.J., D.S. Schimel, C.V. Cole, and D.S. Ojima. 1987. Analysis of factors controlling soil organic matter in the Great Plains. Soil Sci. Soc. Amer. J. 51:1173-1179.

Parton, W.J., J.W.B. Stewart, and C.B. Cole. 1988. Dynamics of C, N, P and S in grassland soils: A model. Biogeochemistry 5:109-131.

Pastor, J., and W.M. Post. 1986. Influence of climate, soil moisture and succession on forest carbon and nitrogen cycles. Biogeochemistry 2:3-27.

Pastor, J., and W.M. Post. 1988. Response of northern forests to CO_2-induced climatic change: Dependence on soil water and nitrogen availabilities. Science (submitted).

Pielke, R.A. 1974. A three-dimensional numerical model of the sea breezes over south Florida. Mon. Wea. Rev. 102:115-139.

Pielke, R.A. 1988. Evaluation of climate change using numerical models. In: Monitoring Climate for the Effects of Increasing Greenhouse Gas Concentrations. R.A. Pielke and T.G.F. Kittel, eds. Colorado State Univ., Ft. Collins.

Ramanathan, V., R.J. Cicerone, H.B. Singh, and J.T. Kiehl. 1985. Trace gas trends and their potential role in climate change. J. Geophysical Res. 90:5547-5566.

Reiners, W.A. 1986. Complementary models for ecosystems. Amer. Nat. 127:59-73.

Reynolds, J.F., and B. Acock. 1985. Predicting the response of plants to increasing carbon dioxide: A critique of plant growth models. Ecol. Modelling 29:107-129.

Rind, D. 1984. The influence of vegetation on the hydrological cycle in a global climate model. pp. 73-91. In: Climate Processes and Climate Sensitivity. J.E. Hansen and T. Takahashi (eds.). American Geophysical Union, Washington, DC.

Schimel, D.S., and T.G.F. Kittel. 1988. Biogeochemical constraints on biosphere/atmosphere exchange: Modeling framework and data from FIFE. J. Geophys. Res. (Atmospheres) (in preparation).

Schimel, D.S., W.J. Parton, C.V. Cole, D.S. Ojima, and T.G.F. Kittel. 1988. Grassland biogeochemistry: Links to atmospheric processes. Clim. Change (submitted).

Schlesinger, M.E. 1988. Equilibrium and transient climatic effects of increased atmospheric CO_2. In: Monitoring Climate for the Effects of Increasing Greenhouse Gas Concentrations. R.A. Pielke and T.G.F. Kittel, eds. Colorado State Univ., Ft. Collins.

Segal, M., R. Avissar, M. McCumber, and R.A. Pielke. 1988. Evaluation of vegetation effects on the generation and modification of mesoscale circulations. J. Atmos. Sci. (in press).

Sellers, P.J., Y. Mintz, Y.C. Sud, and A. Dalcher. 1986. A simple biosphere (SiB) model for use within general circulation models. J. Atmos. Sci. 43:505-531.

Senft, R.L., M.B. Coughenour, D.W. Bailey, L.R. Rittenhouse, O.E. Sala, and D.M. Swift. 1987. Large herbivore foraging and ecological hierarchies. Bioscience 37: 789-799.

Shands, W.E., and J.S. Hoffman. 1987. The Greenhouse Effect, Climate Change, and U.S. Forests. The Conservation Foundation, Washington, D.C. 304 pp.

Shugart, H.H. 1984. A Theory of Forest Dynamics. Springer-Verlag. New York.

Shugart, H.H., and T.M. Smith. 1986. Computer models of terrestrial ecosystems. pp. 71-81. In: Coupling of Ecological Studies with Remote Sensing. M.I. Dyer and D.A. Crossley, Jr., eds. U.S. Department of State Publ. 9504, Man and the Biosphere Program. Washington, D.C.

Shugart, H.H., and W.R. Emanuel. 1985. Carbon dioxide increase: The implications at the ecosystem level. Plant Cell and Environ. 8:381-386.

Solomon, A.M. 1986. Transient response of forests to CO_2-induced climate change: Simulation modeling experiments in eastern North America. Oecologia 68:567-579.

Strain, B.R., and F.A. Bazzaz. 1983. Terrestrial plant communities. pp. 177-222. In: CO_2 and Plants. The Response of Plants to Rising Levels of Atmospheric Carbon Dioxide. E.R. Lemon, ed. AAAS Selected Symposium #84. Westview Press, Boulder, Colorado.

Sud, Y.C., and A. Molod. 1986. Sensitivity of atmospheric circulation and rainfall to land surface fluxes -- GCM simulation studies at GLA. pp. 91-94. In: Climate-Vegetation Interactions. C. Rosenzweig and R. Dickinson, eds. University Corporation for Atmospheric Research, Boulder, Colorado. Report OIES-2.

Swift, D.M. 1983. A simulation model of energy and nitrogen balance for free-ranging ruminants. J. Wildl. Manage. 47:620-645.

Urban, D.L., R.V. O'Neill, and H.H. Shugart. 1986. Linkages in hierarchical models. In: M.I. Dyer and D.A. Crossley Jr., (eds.), Coupling of Ecological Studies with Remote Sensing. U.S. Department of State Publ. 9504, Man and the Biosphere Program. Washington, D.C. pp. 116-124.

Urban, D.L., R.V. O'Neill, and H.H. Shugart. 1987. Landscape Ecology. Bioscience 37:119-127.

Washington, W.M., and G.A. Meehl. 1984. Seasonal cycle experiment on the climate sensitivity due to a doubling of CO_2 with an atmospheric general circulation model coupled to a simple mixed-layer ocean model. J. Geophysical Res. 89:9475-9503.

Wetherald, R.T., and S. Manabe. 1986. An investigation of cloud cover change in response to thermal forcing. Clim. Change 8:5-23.

LIST OF PARTICIPANTS

Henry F. Diaz
NOAA/ERL
325 Broadway
Boulder, Colorado 80303

Nolan J. Doesken
Colorado Climate Center
Department of Atmospheric Science
Colorado State University
Fort Collins, Colorado 80523

Jon Eischeid
Cooperative Institute for Research
in the Environmental Sciences
Campus Box 449
University of Colorado
Boulder, Colorado 80309

Hugh W. Ellsaesser
Atmospheric and Geophysical
Sciences Division
Lawrence Livermore National Laboratory
P.O. Box 808
Livermore, California 94550

Robert D. Jarrett
U.S. Geological Survey
MS415
P.O. box 25046
Lakewood, Colorado 80225

Thomas R. Karl
National Climatic Data Center
NOAA/NESDIS
Federal Building
Asheville, North Carolina 28801

Timothy G.F. Kittel
Cooperative Institute for Research
in the Atmosphere, and Natural
Resource Ecology Laboratory
Colorado State University
Fort Collins, Colorado 80523

Sergej Lebedeff
Goddard Institute for Space Studies
2880 Broadway
New York, New York 10025

Patrick J. Michaels
Center for Study of Global
Environmental Change, and
Department of Environmental Sciences
University of Virginia
Charlottesville, Virginia 22903

Roger A. Pielke
Cooperative Institute for Research
in the Atmosphere, and
Department of Atmospheric Science
Colorado State University
Fort Collins, Colorado 80523

Michael E. Schlesinger
Department of Atmospheric Sciences
and Climatic Research Institute
Oregon State University
Corvallis, Oregon 97331

Thomas H. Vonder Haar
Cooperative Institute for Research
in the Atmosphere, and
Department of Atmospheric Science
Colorado State University
Fort Collins, Colorado 80523